From the Institute of Experimental Dermatology
Of University of Lübeck

Director: Prof. Dr. Dr. Enno Schmidt

Role of mitochondria in the development of airway remodeling in severe asthma

Dissertation

for Fulfillment of Requirements

for the Doctoral Degree of the University of Lübeck

from the Department of Medicine

Submitted by

Rakhee Kizhuvappat Ramakrishnan

from Sharjah, United Arab Emirates

Lübeck 2020

First referee:

Second referee:

Additional referee:

Chairman:

Date of oral examination:

Approved for printing:

Table of Contents

1. Introduction

Asthma is an age-old disease which continues to puzzle and confuse physicians, back from the time of Hippocrates to this day and age. The very first account of an asthma attack dates back to the second century of the Common Era by the Greek physician Aretaeus of Cappadocia (1). The word “asthma” is derived from the Greek word “aazein” which means “panting or noisy breathing” (1, 2). Nonetheless, the ancient Egyptian, Hebrew and Indian medical writings also contain references to asthma. Today, asthma is widely accepted as a chronic respiratory disease of the conducting airways of the lungs that affects children and adults of all ages alike.

1.1 Definition of asthma

The definition of asthma has steadily evolved with evolution in our overall understanding of this disease. Asthma was originally described as an allergic disease because patients developed an exaggerated immune response to normally innocuous environmental allergens or irritants. In 1959, airway hyperreactivity and reversible airflow obstruction were proposed as the cardinal clinical features of asthma (3, 4). Asthma was then largely considered a disease of bronchial muscle spasm and treated with bronchodilators (5). Thereafter, in 1992, the status “chronic inflammatory disease of the airways associated with reversible airflow obstruction and enhanced airway hyperresponsiveness” was conferred by the International Consensus Report on the Diagnosis and Treatment of Asthma (3, 6). Chronic airway inflammation, reversible airflow obstruction and enhanced bronchial reactivity are thus, the three key components used to define asthma. The definition of asthma has also progressed from mere clinical characterization to integration of the underlying physiological and pathological characteristics of the disease.

According to the Global Initiative for Asthma (GINA) 2019 update on the Global Strategy for Asthma Management and Prevention, asthma is presently defined as:

"Asthma is a heterogeneous disease, usually characterized by chronic airway inflammation. It is defined by the history of respiratory symptoms such as wheeze, shortness of breath, chest tightness and cough that vary over time and in intensity, together with variable expiratory airflow limitation. (7)"

This definition captures the essential clinical symptoms associated with asthma before commencement of controller treatment and aims to distinguish asthma from other respiratory ailments. Nevertheless, the definition and accurate classification of asthma continue to remain an ongoing challenge.

1.2 Epidemiology of asthma

Asthma is slowly but steadily emerging as a global health problem. Asthma remains one of the most common non-communicable diseases that is estimated to affect nearly 339.4 million people worldwide (1). This number is likely to increase by another 100 million by 2025. In the United States alone, the Centers for Disease Control and Prevention (CDC) estimated that 1 in every 13 people has asthma (8). Despite the advancements made in the field, the global epidemic of asthma continues to rise especially in low-to-middle income countries.

The International Study of Asthma and Allergies in Childhood (ISAAC) serves as the milestone survey depicting the global prevalence of asthma in children, but the last surveys were conducted 15 years ago (1, 9). Nearly 798,685 adolescents aged 13-14 years in 233 centers in 97 countries were surveyed by questionnaires between 2002 and 2003. Wide geographical variability existed in the prevalence and severity of asthma, not only between countries but also

between centers within a country. The highest prevalence of asthma (≥20%) was observed in Australasia, Europe and North America, and also in parts of Latin America (Fig. 1.1A). The lowest prevalence (<5%) was seen in the Indian subcontinent, Asia-Pacific, Eastern Mediterranean, and Northern and Eastern Europe.

Around the same time as ISAAC, the World Health Survey conducted by the World Health Organization (WHO) estimated the prevalence of asthma in young adults, using data from 177,496 adults aged 18-45 years in 70 countries (10). As in children, the observed prevalence of asthma varied substantially in young adults. The highest prevalence was reported in Australia, Northern and Western Europe, and Brazil (Fig. 1.1B). Despite the prevalence being higher in the high-income countries, asthma-related mortality was higher in the low-to-middle income countries. There is, however, a paucity of survey data from the middle-aged and older adults, particularly the elderly, to predict the prevalence of asthma in these age groups.

There is a substantial global burden of disease and disability associated with asthma, including nearly 1000 preventable deaths each day from asthma and reduced quality of life, in people from all age groups and from across the world. In 2016, asthma was ranked 16th among the leading causes of years lived with disability and 28th among the leading causes of burden of disease globally (1). Deaths due to asthma pose a matter of serious concern because of their preventable nature. Asthma deaths are largely attributed to inappropriate asthma management. The essential medications for asthma continue to remain unaffordable, unavailable or of unreliable quality, in many countries. This could explain the increasing prevalence of the disease along with the burden and mortality associated with asthma. At the same time, asthma also constitutes a serious global economic burden in both developing and developed countries (1). Global attention and

commitment towards asthma are crucial to lessen the substantial burden associated with this disease.

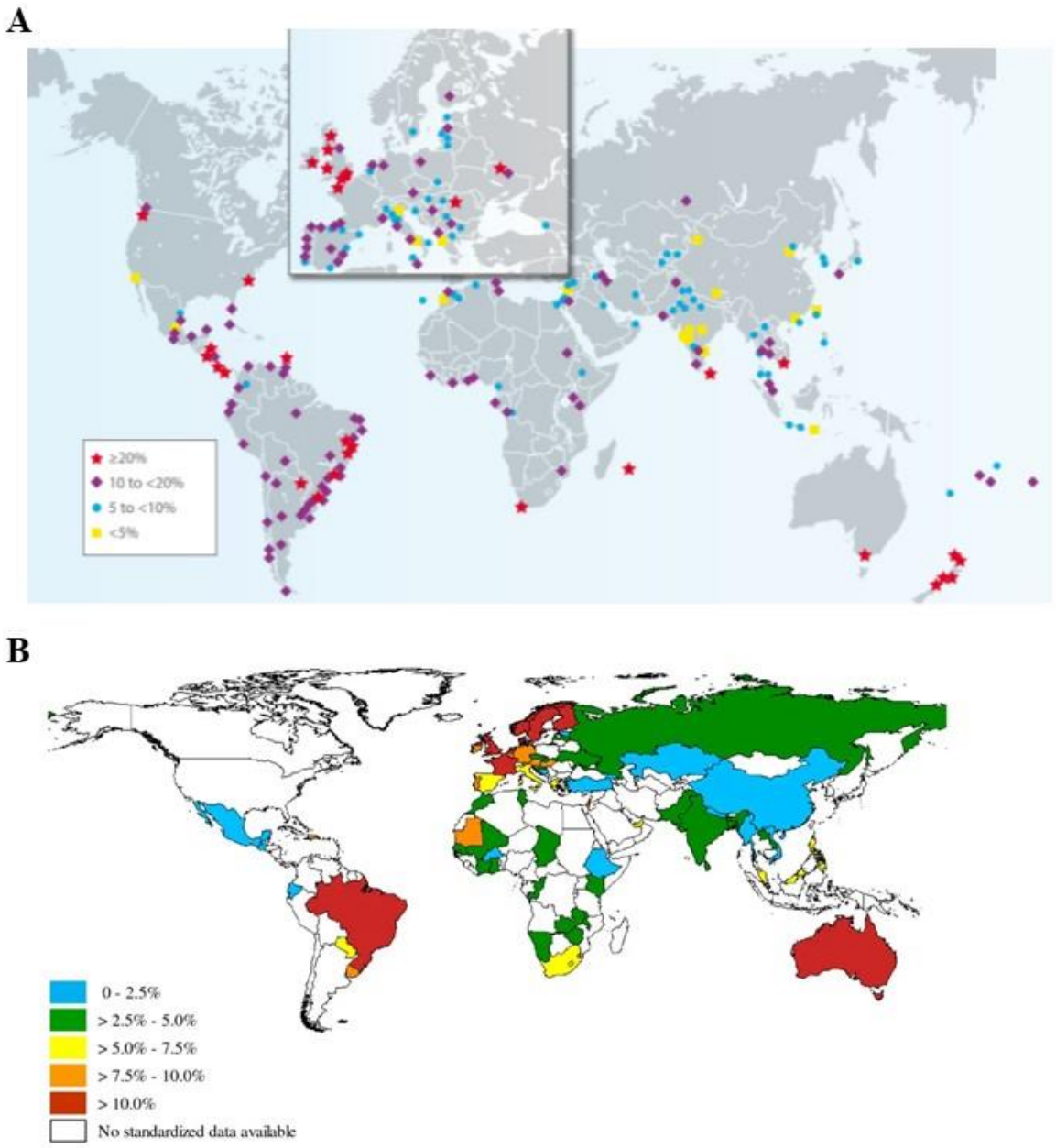

Figure 1.1. The global prevalence of asthma in children and adults.

(A) The prevalence of asthma in children projected by the International Study of Asthma and Allergies in Childhood (ISAAC) study in 2002-2003. (9) **(B)** The prevalence of clinical asthma

in adults projected by the World Health Survey (WHS) implemented by the World Health Organization (WHO) in 2002-2003. (10)

There exist differences in the patterns in incidence and prevalence of asthma between children and adults (11). Although asthma symptoms are most commonly reported in early childhood, asthma can develop at any stage in life, with some developing new-onset asthma in adulthood. Asthma is more common in children when compared to adults, however, asthma-related healthcare use and mortality are greater in adults. Interestingly, sex also influences the incidence and prevalence of asthma. In childhood, increased incidence, prevalence and hospitalization are observed in pre-pubertal boys when compared to girls of the same age-group (12). This trend however, reverses upon progressing into adolescence and adulthood, with a higher asthma burden in women than men (12). The reversal of trend during adolescence suggests the involvement of sex hormones in the etiology of asthma.

In the United Arab Emirates (U.A.E.), relatively few studies have looked into the incidence and severity of asthma across the seven Emirates of U.A.E. In one study, 3002 primary school children aged 6-13 years from the seven Emirates were surveyed between 1997 and 1998 (13). Physician-diagnosed asthma had an overall prevalence of 13% in UAE primary school children. The asthma distribution between the sexes indicated an approximate ratio of 1:1. The highest prevalence was observed in Dubai while the least occurred in Fujairah. In another study, surveying 1220 individuals of varying ages (mean age of 32.9) from the seven Emirates, prevalence of respiratory symptoms was higher in the age bands younger than 20 years and older than 44 years (14). The asthma prevalence was 12.1% in the overall study population and 9.8% in young adults aged 20-44 years.

1.3 Severe asthma – a distinct phenotype of asthma

Vast heterogeneity has been identified in the pathogenesis, pathophysiology, treatment response and severity of asthma. Asthma is now increasingly appreciated as a heterogenous syndrome of disorders and not a singular disease, which can be stratified into different asthma phenotypes and endotypes with varying clinical response to asthma therapies (15). Phenotypes represent the observable characteristics of the disease and does not necessarily portray the disease mechanisms in action. Therefore, although some success may be achieved by treating asthma based on phenotypes, this mode of therapy is sub-optimal considering the variability in treatment response. Alternatively, endotypes signify the molecular mechanisms in action which serve as a better determinant of treatment response. Therefore, treating asthma by taking into consideration both the phenotype and endotype associated with the disease will elicit more effective response to treatment (16). Phenotyping the airways provide cues for precise diagnosis and targeted treatment, however, the endotypes are particularly crucial in this era of biologicals.

There are two major classes of asthma treatments: i) bronchodilators, that target the airway smooth muscle and reverse airway narrowing, and ii) corticosteroids (CS), that target the underlying airway inflammation. These constitute the “asthma essential medicines” as majority of patients diagnosed with asthma respond well to these medications. Despite the longstanding history of asthma and developments in our understanding of the disease, the fact still remains that there is no cure for asthma.

The National Asthma Education and Prevention Program outlined four levels of asthma severity on the basis of the underlying pathophysiological changes in the airways and responses to treatment: intermittent, mild persistent, moderate persistent, and severe persistent (17). To classify asthma severity, GINA also defined five levels on the basis of asthma treatment schemes

that help attain good asthma control (18). The terms ‘severe asthma’, ‘refractory asthma’, or ‘difficult-to-treat asthma’, often used interchangeably, all represent asthmatic individuals in whom good asthma control could not be attained despite high medication dosage, excluding cases with poor treatment compliance.

The European Respiratory Society (ERS)/American Thoracic Society (ATS) Task Force on severe asthma proposed an updated definition of severe asthma, which described severe asthma as:

“Asthma which requires treatment with guidelines suggested medications for GINA steps 4–5 asthma (high dose inhaled corticosteroids (ICS) and long-acting beta agonists (LABA) or leukotriene modifier/theophylline) for the previous year or systemic CS for ≥50% of the previous year to prevent it from becoming “uncontrolled” or which remains “uncontrolled“ despite this therapy (19).”

Thus, according to the above definition, severe asthma includes those patients who show refractoriness or insensitivity to current asthma medications, and also those in whom asthma is complicated by comorbidities.

Severe asthma constitutes a disease entity different from mild and moderate asthma. Patients with severe asthma present with persistent asthma symptoms requiring high dosage of asthma medications and continue to experience frequent asthma exacerbations despite aggressive therapy (20). Alternative to the traditional paradigm of a T-helper type 2 (Th2) inflammation with an eosinophilic response in asthma, the pathogenesis of severe asthma is usually characterized by a non-Th2 inflammation. Additionally, considerable heterogeneity also exists within severe asthma. Airway remodeling is amplified in patients with severe asthma, with highly thickened airway wall (21), increased fibroblasts, airway smooth muscle and larger

mucus glands (22), significant epithelial damage (23) and increased vascularity (24) commonly encountered in severe asthma. The airway segments are integrated into a complex branching system and the degree of inflammation and remodeling are likely to be heterogeneously distributed across the airway tree in severe asthmatic patients (25). Furthermore, both the large and small airways contribute to lung function mechanics in severe asthma (26). As seen in Fig. 1.2, severe asthma is characterized by marked thickening of the airway wall and widespread infiltration of inflammatory cells in contrast to similar sized normal airway (27). These changes contribute to severe narrowing of the airways and reduced baseline lung function (28).

1.4 Pathophysiology of asthma

Over the past 3 decades, there has been remarkable improvement in our understanding of the pathophysiology of asthma and increased appreciation that asthma is a clinical syndrome of immunologically mediated disorders associated with an abnormal airway repair mechanism resulting in inflammatory and structural remodeling changes to the airways (29). Asthma is a multi-faceted disease associated with a myriad of relevant pathobiological pathways. The pathophysiology of asthma is thus, a complex phenomenon, with complex interplay of multiple inflammatory cells, stromal cells and mediators triggering an acute and chronic inflammatory and remodeling response in the airways. Asthma, that manifests usually as airway inflammation and airway hyperresponsiveness (AHR), is often accompanied by structural modifications of the bronchial airway, termed as airway remodeling. The current pathophysiological paradigm of asthma is thus characterized by its hallmark features, including airway inflammation, reversible airflow obstruction, airway hyperresponsiveness and airway remodeling, which manifest as clinical symptoms of wheeze, chest tightness, cough and dyspnea.

Asthma is believed to develop as a result of interactions between the genetic predisposition of an individual and environmental factors (30). There is no single gene as such responsible for asthma, but multiple genetic variants have been associated with asthma (31). Atopic individuals, in particular, are predisposed to developing an exaggerated allergic reaction upon exposure to environmental factors including pollen, air pollutants, respiratory viruses, tobacco smoke, perfumes, antibiotics and diet. These individuals are likely to possess single nucleotide polymorphisms (SNPs) in asthma susceptibility genes encoding pattern recognition receptors, mast cell chymase, T cell receptor α, β-adrenergic receptor, IL-4 receptor α, RANTES, FcϵRIβ and/or class II MHC, rendering them at a higher risk of developing hypersensitivity (32). These asthma susceptibility genes, some of which include *ADAM33, IL4, IL4RA, IL5, IL5RA, TLR4, DPP10, PHF11, TIM-1, GPRA, OPN3, ORMDL3*, and *PDE4D*, were identified through association studies and positional cloning, and have been extensively reviewed previously (30, 33, 34). The complex interplay of these gene polymorphisms with environmental factors contribute to asthma, and may help explain the heterogeneity witnessed in the disease (32). Asthma is a classic example of a T cell-mediated disease with a largely T-helper type 2 (Th2) bias, as Th2 cells and their cytokines are responsible for majority of the pathological changes observed in asthma. IL-4, IL-5 and IL-13 cytokines secreted by Th2 cells are central mediators of asthma owing to their pivotal role in different facets of the disease, right from differentiation of naïve T cells into Th2 cells, IgE class switching and eosinophil recruitment to mucus hypersecretion, AHR and airway remodeling. However, the Th2 paradigm falls short in interpreting the full spectrum of asthma severity.

Although Th2 inflammation is considered the principal pathophysiological pathway underlying asthma, a recent study reported the identification of Th2-high and Th2-low distinct molecular

phenotypes in asthma based on the degree of Th2-driven airway inflammation (35). The mild and moderate asthmatics show signs of a Th2-dominated immune response. Asthma patients exhibiting Th2-high clinical features are an easier sub-group to target in terms of their clinical management because they respond well to classical asthma therapy. Even patients with more severe manifestation of the disease display better asthma control with the recent Th2-targeted biological therapies, including monoclonal antibodies targeting IgE, IL-4, IL-5, IL-13 or their receptors (35-37). On the contrary, patients with a Th2-low phenotype represent a sub-group with severely limited options as currently available and developing therapies are inadequate to meet their clinical demands (35, 38). The scarcity of data available on the underlying disease mechanisms in the Th2-low phenotype further adds to their disease burden. This sub-group of patients is considered to have a severe or refractory form of asthma.

Interestingly, patients with Th2-low phenotype were noticed to display predominantly neutrophilic airway inflammation (35). Since IL-17 is a key mediator in neutrophilic inflammation, a direct connecting link between IL-17 and chronic airway inflammation and remodeling processes has been established in severe asthma (39, 40). These data further suggest that the mechanisms driving the development of mild and severe forms of asthma are fundamentally different. Therefore, better characterization of the disease in asthmatic patients is necessary to improve their clinical management and care (41). While there has been drastic improvement over the years in our understanding of asthma and its underlying pathophysiology, significant gaps in knowledge still exist, particularly in the context of more severe forms of the disease.

Airway hyperresponsiveness is another important pathophysiological feature of asthma. AHR is defined as a blown-up airway response to normally harmless non-specific stimuli such as cold

air, resulting in airway obstruction and subsequent airway narrowing (42). The presence of AHR in individuals presenting with asthma symptoms is detected using bronchial provocation tests in order to arrive at a clinical diagnosis of asthma. Therefore, AHR is now widely used as a tool in the diagnosis, severity classification and management of asthma (43, 44). AHR is often associated with increased risk of asthma (45), increased risk of exacerbation (46), increased lung function decline (45), increased asthma severity (47) and increased level of treatment (48). There is little consensus on the mechanisms underlying AHR, however, genetic predisposition, airway inflammation and structural airway remodeling are expected to contribute to the development and severity of AHR (49).

The nature of the relationship between airway inflammation and airway remodeling have progressed over time. Traditionally, airway inflammation was thought to trigger remodeling leading to fixed airflow obstruction and AHR (50). As an alternative to causal and effect, the relationship between these mechanisms may be complementary in nature. The observation that airway remodeling occurred early in the onset of asthma as illustrated in young children with asthma (51), suggest a parallel occurrence for inflammation and remodeling (52). Airway remodeling being the focus of this thesis is described in depth in the next section.

1.5 Airway remodeling

One of the first reports of airway remodeling in asthma came from post-mortem examinations in 1922 by Huber and Koessler (53). Airway remodeling refers to the pathological re-structuring of the large and small airways in asthma. These structural changes encompass subepithelial fibrosis, airway smooth muscle (ASM) mass, goblet cell and mucus gland enlargement, neovascularization and loss of epithelial integrity, as shown in Fig. 1.2. These pathophysiological modifications render changes in the composition and structural organization

of the cellular and molecular components that make up the airways. The resident structural cells of the airways as well as the infiltrating inflammatory cells promote airway remodeling and inflammation through the dysregulated secretion of extracellular matrix proteins, cytokines and chemokines. As a result, thickened airway walls, airway narrowing and hyperresponsiveness, edema and mucus hypersecretion clinically manifests in asthmatic patients. In addition to thickening of the airway walls and subsequent narrowing of the airway lumen, remodeled airways contribute to poor clinical outcomes in asthmatic patients (54). Clinically, airway remodeling is defined as persistent airflow obstruction which does not respond well to anti-inflammatory therapy (54). Taking into consideration the association of airway remodeling with loss in pulmonary function, it is imperative for clinicians to take measures for early detection and intervention.

Airway remodeling is partially reversible in the milder forms of the disease, but with disease progression, it takes up an irreversible nature in chronic severe asthma. Airway remodeling is initiated as a repair response to the repeated tissue injury from the underlying chronic inflammatory processes and mechanical stretch. Aberrations in the injury-repair response in asthmatic airways lead to persistent structural changes in the airway wall. Asthma progression can thus, pave way to irreversible manifestation of airway remodeling and consequently, irreversible airflow obstruction and thickened airway wall are observed in more severe forms of asthma (55). Although inhaled corticosteroids (ICS) are effective anti-inflammatory drugs, their effects on chronic structural changes and airway remodeling remain a subject of controversy.

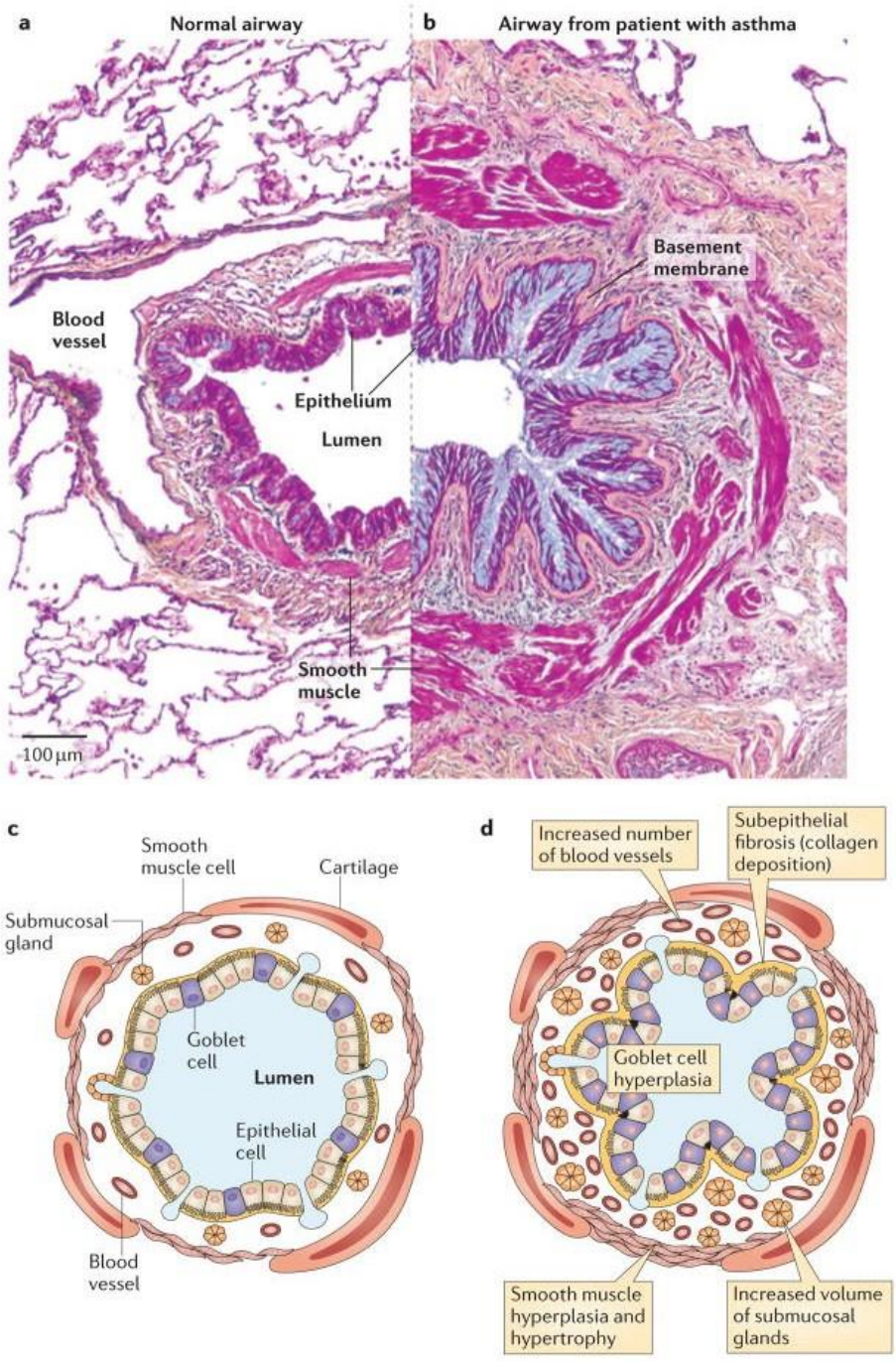

Figure 1.2 Airway remodeling in asthma.

Micrographs of medium-sized airways from **(a)** a non-asthmatic individual and **(b)** a patient with severe asthma stained with Movat's pentachrome stain. The asthmatic airways show significant airway remodelling with mucus hyperplasia and hypersecretion (blue), significant thickening of basement membrane and increased smooth muscle volume. Scale bar=100 µm.

Figure panels (c) and (d) show the schematic representation of airway pathology in **(d)** an asthmatic airway as compared to **(c)** a normal healthy airway. (56, 57)

1.5.1 Subepithelial fibrosis

Subepithelial fibrosis is an important characteristic of airway remodeling documented across all degrees of asthma severity (58, 59) as well as in children with difficult-to-treat asthma (60, 61). Subepithelial fibrosis affects the lamina reticularis underlying the reticular basement membrane that holds together the airway epithelial cells. Fibroblasts, the effector cells of fibrosis, exhibit a bio-synthetic, contractile, adhesive and pro-inflammatory phenotype to orchestrate a self-limited and tightly regulated repair process in response to tissue injury. Under pathological conditions, persistent activation of these fibroblasts paves way to extracellular matrix (ECM) accumulation and remodeling along with their differentiation into apoptosis-resistant myofibroblasts. In addition to being the prime source of ECM proteins (62), they are also important in maintaining a state of chronic pulmonary inflammation through the production of a variety of cytokines, chemokines, proteases and lipid mediators (63).

The intricate network of ECM proteins constitutes the scaffolding of the airways. ECM proteins govern the mechanical properties of the airway as its composition regulates airway tissue elasticity (64). Besides acting as a mechanical support crucial for maintaining airway structure and function, the scaffold is a complex and dynamic network with the potential to affect cellular function, including proliferation, differentiation and migration of several cell types (65, 66). The profile of ECM proteins is altered in asthmatic airways with increased deposition of collagen types I, III, V, fibronectin, tenascin and different proteoglycans (66, 67).

Asthmatic airway fibroblasts exhibit intrinsic differences in their pro-fibrotic response when compared to their healthy counterparts (68). Increased airway fibroblast population, increased collagen deposition, airway smooth muscle hyperplasia and hypertrophy are characteristic airway structural changes that selectively differentiate severe persistent asthma from milder forms of the disease (69). In addition to the central airways, higher myofibroblast numbers were reported in the alveolar/lung parenchyma of asthmatics (70, 71). Other chronic lung diseases, including chronic obstructive pulmonary disease (COPD), and idiopathic pulmonary fibrosis (IPF), also exhibit phenotypically different fibroblasts that are responsible for the loss of the typical airway architecture and known to impair airway function (72). Nonetheless, fibroblasts and their role in asthma pathogenesis have been relatively undervalued and understudied.

Clinically, the subepithelial layer thickness positively correlated with asthma severity score and negatively correlated with lung function (73). This thickening was also associated with increased number of submucosal fibroblasts, increased deposition of subepithelial collagen and AHR (74). The fibroblast numbers and collagen deposition also negatively correlated with the extent of airflow limitation in patients with asthma (69). In addition to collagen, increased proteoglycan deposition is also observed predominantly in the subepithelial layer and correlated with AHR (75). Asthmatic airways are characterized by an imbalance in *de novo* ECM synthesis and degradation, such that the relative levels of proteases and anti-proteases promote a pro-fibrotic phenotype. The interstitial cells, neutrophils, mast cells and macrophages residing in the airway wall are important sources of these proteases and anti-proteases, such as matrix metalloproteinases (MMPs) and tissue inhibitor of metalloproteinases (TIMPs) (54). MMPs are implicated in neutrophilic airway inflammation (76) and in airway remodeling, through their effects on matrix reorganization (77), angiogenic vascularization (78) and ASM hyperplasia and

invasion (77). MMP-9, in particular, is increased with asthma severity and inversely corelated with pulmonary function (76). The MMP and TIMP balance also correlated with airflow obstruction (79) and asthma exacerbation (80). Thus, subepithelial fibrosis is characterized by excessive ECM deposition and a corresponding decrease in ECM degradation (81, 82).

Amongst the remodeling changes, subepithelial fibrosis and ASM hypertrophy are the most challenging to treat, and often show progression despite therapy, contributing to fixed airflow obstruction and severe asthma (83).

1.5.2 Airway smooth muscle mass

Airway smooth muscle cells are critical effector cells in regulating the airway tone. Their pathological and physiological contribution is key to the progression of airway tissue remodeling. Asthmatic airways are associated with an increased ASM mass owing to an increase in the number (hyperplasia) as well as size (hypertrophy) of ASM cells. In addition to their proliferative and secretory phenotype, the asthmatic ASM cells are characterized by their migratory capacity towards the subepithelium and consequently, decreasing the distance between the epithelium and smooth muscle layer (84). Reduced apoptosis of ASM cells may also account for the increase in ASM mass (85). In addition to their self-remodeling properties, ASM contribute to the pathogenesis of asthma by actively participating in immunomodulatory as well as remodeling processes. ASM secrete pro-inflammatory cytokines and chemokines (86), and produce ECM proteins, MMP and TIMP (66). These chemokines in turn direct ASM migration and increase their contractile function *in vitro* (84). Augmented ASM area and hypertrophy are some of the structural changes that distinguish severe persistent asthma from milder forms of the disease (69). Thus, ASM correlated with asthma severity and negatively correlated with forced expiratory volume in 1 second (FEV1).

1.5.3 Epithelial alterations

The airway epithelium is at the forefront to the pathogenesis of asthma. The bronchial epithelium constitutes the first cellular layer in direct contact with the environment and typically provides a protective physical barrier against inhaled pathogens, allergens, cigarette smoke and pollutants. Damage to this protective barrier increases the susceptibility of the airways to insult and is thus, critical to the development and progression of asthma. The epithelial alterations commonly encountered in asthma include destruction of ciliated cells, denudation of epithelial cells, hyperplasia of goblet cells, upregulated release of growth factors and overexpression of growth factor receptors (23, 87, 88).

Epithelial susceptibility to injury during asthma together with impairment in its repair results in loose epithelial cell attachment to the basement membrane (89). This makes the underlying submucosa vulnerable to inflammatory and remodeling processes (90). The damaged epithelium in asthmatic airways in turn release a range of growth factors, which include epidermal growth factor (EGF), transforming growth factor beta (TGF-β), vascular endothelial growth factor (VEGF) and platelet-derived growth factor (PDGF), that through their effects on cell proliferation, ECM deposition and angiogenesis, promote airway remodeling (89, 91). Having said that, blocking the nuclear factor-kappa B (NF-κB) regulated genes in airway epithelium was found to significantly hinder allergen-induced airway remodeling, including peribronchial fibrosis, mucus production and TGF-β levels (92). Th2 cytokines, IL-4 and IL-13, are believed to exert a greater effect on bronchial epithelium as it was found to be the predominant site of signal transducer and activator of transcription 6 (STAT-6) expression and activation (93). Cytokine stimulation of bronchial epithelial cells induced the secretion of various chemokines,

including IL-8, eotaxin and regulated on activation, normal T cell expressed and secreted (RANTES) that cause chemotactic migration of both inflammatory and structural cells (93, 94). Clinically, the degree of epithelial loss correlated with the degree of AHR (95). The extent of epithelial injury thus, plays a crucial role in asthma severity. The epithelium is now increasingly recognized to orchestrate the inflammatory and remodeling responses in the airways of asthmatics.

1.5.4 Goblet and mucus gland enlargement

Mucus secretion is an inherent defense mechanism of the airways. Asthmatic airways are characterized by marked goblet cell hyperplasia, submucosal gland hyperplasia and intraluminal mucus, especially in those asthmatics who died of severe acute asthma attack (61, 96). In the diseased state, the goblet cell population in the airway epithelium expands, mostly in response to epithelial adaptation to injury (97). These abnormalities cause increased mucus secretion leading to occlusion and narrowing of the airways and increased airway wall thickness, thereby impairing lung function (97).

1.5.5 Angiogenesis

Vascular alterations are also commonly encountered in asthmatic airways. Increased airway vascularity with vasodilation and angiogenesis are some of the airway wall changes characteristic of asthma (98). Vessel length density as well as vessel area density were significantly enhanced in the subepithelium (99) together with increased expression of angiogenic factors, such as vascular endothelial growth factor (VEGF), basic fibroblast growth factor (FGF) and angiogenin (100). Moreover, the degree of vascularity negatively correlated with AHR and airway caliber (100). Clinically, these changes in the microvasculature can result in airway wall edema, reduced airway caliber, increased delivery of inflammatory and

remodeling mediators to the airway wall, subsequently having an impact on the inflammatory and structural cells in the vicinity.

1.6 Role of cytokines in airway remodeling

The inflammatory cellular recruit into the airway wall, including but not limited to eosinophils, neutrophils, mast cells, macrophages, Th2 and Th17 lymphocytes, release pro-inflammatory and pro-fibrotic mediators that trigger mucus hypersecretion, bronchoconstriction, AHR and airway remodeling. Some of these mediators include IL-4, IL-5, IL-9, IL-13, IL-17, TGF-β, granulocyte/macrophage colony-stimulating factor (GM-CSF), VEGF, lipid mediators and histamine. These cytokines have largely been studied from an inflammatory perspective. However, they also exert potent remodeling properties.

The close association of T cells with airway structural cells raises the possibility of crosstalk between the cells through cytokines. For instance, IL-4 exerts its pro-fibrotic effect by positively regulating procollagen I (alpha1) transcription by direct promoter activation and by increasing the ratio of TIMP-2 to MMP-2 (68). Th2 cytokines, IL-4, IL-9 and IL-13, induce several mucus-related genes, including MUCI, II and V, leading to dysregulated mucus production (97). Increased IL-11 expression in the epithelium and subepithelium with increasing asthma severity suggests their association with chronic remodeling in asthmatic airways (101). TGF-β, IL-11, and IL-17 are important pro-fibrotic cytokines that are increased in asthmatic airways and contribute to its pathology by promoting subepithelial fibrosis. The increased levels of these cytokines correlated with the deposition of collages types I and III with increasing severity of asthma (102). Furthermore, treatment with corticosteroids failed to decrease collagen deposition and this may be attributed to the persistently high TGF-β expression.

Th17 cells and their canonical cytokines, IL-17A and IL-17F, are key players in the pathogenesis of asthma and are closely associated with the more severe phenotypes (103). Airway tissues from patients with severe asthma demonstrated increased expression of Th17-associated cytokines, IL-17A and IL-17F (39) together with increased expression of IL-8 and excess neutrophilia (104). IL-17 induced the secretion of pro-fibrotic cytokines and pro-inflammatory mediators, including IL-6, IL-11, IL-8 and GROα/CXCL1, by bronchial fibroblasts exerting their importance in regulating fibrotic and inflammatory responses in the airways (105). Furthermore, bronchial fibroblasts when co-cultured with CD4+ T cells promoted a Th17 profile in asthma (106). It was also reported that anti-IL-17 therapy in a murine asthma model exacerbated with lipopolysaccharide (LPS) led to decreased oxidative stress and ECM remodeling (107) further implicating IL-17 in airway remodeling in asthma.

TGF-β1 is another well-known regulator of airway inflammation and remodeling (108). TGFβ1 is the most abundant isoform of the TGF-β family of cytokines. It is secreted by both immune cells and structural cells, including airway epithelial, fibroblast, smooth muscle and endothelial cells. TGF-β regulates multiple features of airway remodeling. TGF-β can exert either an apoptotic or anti-apoptotic effect on airway epithelial cells depending on the signaling pathway involved (109), induce mucin expression in airway epithelial cells (110), facilitate the differentiation of fibroblasts to myofibroblasts activating a proliferative phenotype (111), induce the release of growth factors, such as FGF-2 and connective tissue growth factor (CTGF), that enhances fibroblast proliferation, chemotaxis and ECM synthesis (112, 113), enhance ASM proliferation and migration (114, 115) and enhance production of VEGF (116). This multifunctional role of TGF-β makes it a key player in airway remodeling.

IL-13 is another key stimulator of airway remodeling that regulates subepithelial fibrosis and mucus cell metaplasia. IL-13 increased the invasive properties of asthmatic airway fibroblasts via TGF-β1 and MMPs (117). IL-13 induced collagen type I expression in airway fibroblasts in a TGF-β1 and MMP2-dependent manner (118). IL-13 also initiated a proliferative response in human bronchial epithelial cells (119). There are multiple evidences indicating that IL-13, and not IL-4, is the primary regulator of goblet cell metaplasia and mucus hypersecretion in asthma (120-123). Pro-angiogenic cytokine VEGF also regulates airway remodeling through its influence on angiogenesis (124) and mediating vascular as well as extravascular remodeling and inflammation (125).

Despite our improved understanding of the various mediators and associated signaling pathways involved in airway remodeling, the current treatment options against asthma have limited impact on airway remodeling and in particular, subepithelial fibrosis. Hence, there is a pressing need to identify novel therapeutic targets to alleviate symptoms particularly in severe asthma. Excessive collagen deposition by fibroblasts in the airways of individuals with severe asthma may play a part in the refractory nature of the disease considering the inability of current therapy in alleviating collagen deposition in the airways. Thus, the identification of novel fibrotic mechanisms would aid in generating unique therapeutic targets capable of interfering with the airway remodeling process.

1.7 Role of autophagy in asthma pathogenesis

The term autophagy, meaning “to eat one’s self”, was coined by Christian de Duve to describe the phenomenon of cellular double-membraned vesicles engulfing its own cytosolic proteins and organelles, and ultimately degrading them (126). Autophagy is a highly conserved cellular pathway that sequesters cytoplasmic cargo, including long-lived proteins, defective organelles

and intracellular pathogens, for delivery to the lysosomes where the intracellular cargo gets digested and nutrients get recycled back to the cell (127). Autophagy is critical to maintain cellular homeostasis as the cytosolic substrates that threaten cell viability are the ones that are generally sequestered within autophagosomes for degradation. Membrane lipids and proteins are digested within the autolysosome to generate free fatty acids and amino acids which could be recycled for mitochondrial ATP production and other synthetic activities. Under normal conditions, autophagy is exhibited at basal levels in most cell types for nutrient turnover. However, it can also be induced by changes in environmental conditions, such as nutrient and growth factor depletion, oxidative stress, heat and infection, or upon high bioenergetic and nutrient demands. Upregulation of autophagy is also seen when cells undergo structural remodeling (128).

Autophagy is now emerging as a critical pathway that plays a crucial role in health and disease and helps promote longevity. Autophagy has been demonstrated to play roles in biological processes ranging from immune function and development to diseases such as neurodegeneration, pathogen infections, muscular disorders, cancer and aging (129).

1.7.1 Mechanism of autophagy

There are three major types of autophagy in eukaryotic cells – macroautophagy, microautophagy and chaperone-mediated autophagy. Macroautophagy, herein referred to as autophagy, is the most common type of autophagy and it involves a characteristic double-membrane vesicle, termed autophagosome. Autophagy is a complex pathway with numerous molecular players having distinct roles. Three key protein complexes and their sequential activities are critical for autophagosome biogenesis, namely the ULK1 complex (consisting of ULK1, FIP200, ATG13

and ATG101), the phosphoinositide 3-kinase catalytic subunit type III (PI3KC3) complex (consisting of beclin 1, vacuolar protein sorting 34 (VPS34), VPS15 and ATG14L), and the ATG16L1 complex (consisting of ATG16L1, ATG5 and ATG12) (Fig. 1.3A). The mammalian target of rapamycin complex 1 (mTORC1) phosphorylates and inhibits the activity of ULK1 complex. When the cells are under nutrient deprivation, autophagy is induced by the inhibition of mTORC1, which frees the ULK1 complex to phosphorylate beclin 1 and in turn activate the PI3KC3 complex (130). The PI3KC3 complex creates phosphatidylinositol-3-phosphate (PI3P)-rich subdomains at select endoplasmic reticulum (ER) regions, which constitute the autophagosome precursor structure, also referred to as the phagophore or isolation membrane (131). The PI3P-binding proteins (such as WIPI2) then recruit the ATG16L1 complex, which conjugates ubiquitin-like microtubule-associated protein 1A/1B-light chain 3 (LC3) or LC3-I with phosphatidylethanolamine (PE) and anchors the LC3-PE complex, also called LC3-II, to the lipid bilayer. The isolation membrane is extended by LC3-II-mediated membrane tethering and fusion, and by recruiting lipids, originating from multiple membrane sources, including ATG9L1-bearing endosomal vesicles. The growing membrane expands around the cytoplasmic cargo and then fuses with itself to form the double-membrane bound autophagosome. The autophagosome upon maturation fuses with a lysosome to form an autolysosome, within which the sequestered cytoplasmic material along with the inner membrane is degraded with the help of lysosomal enzymes. Lysosomal proteins, such as class C vacuolar protein sorting (VPS) and SNARE-like proteins, facilitate the autophagosomal fusion with lysosomal vesicles culminating in the degradation and recycling of the sequestered cargo.

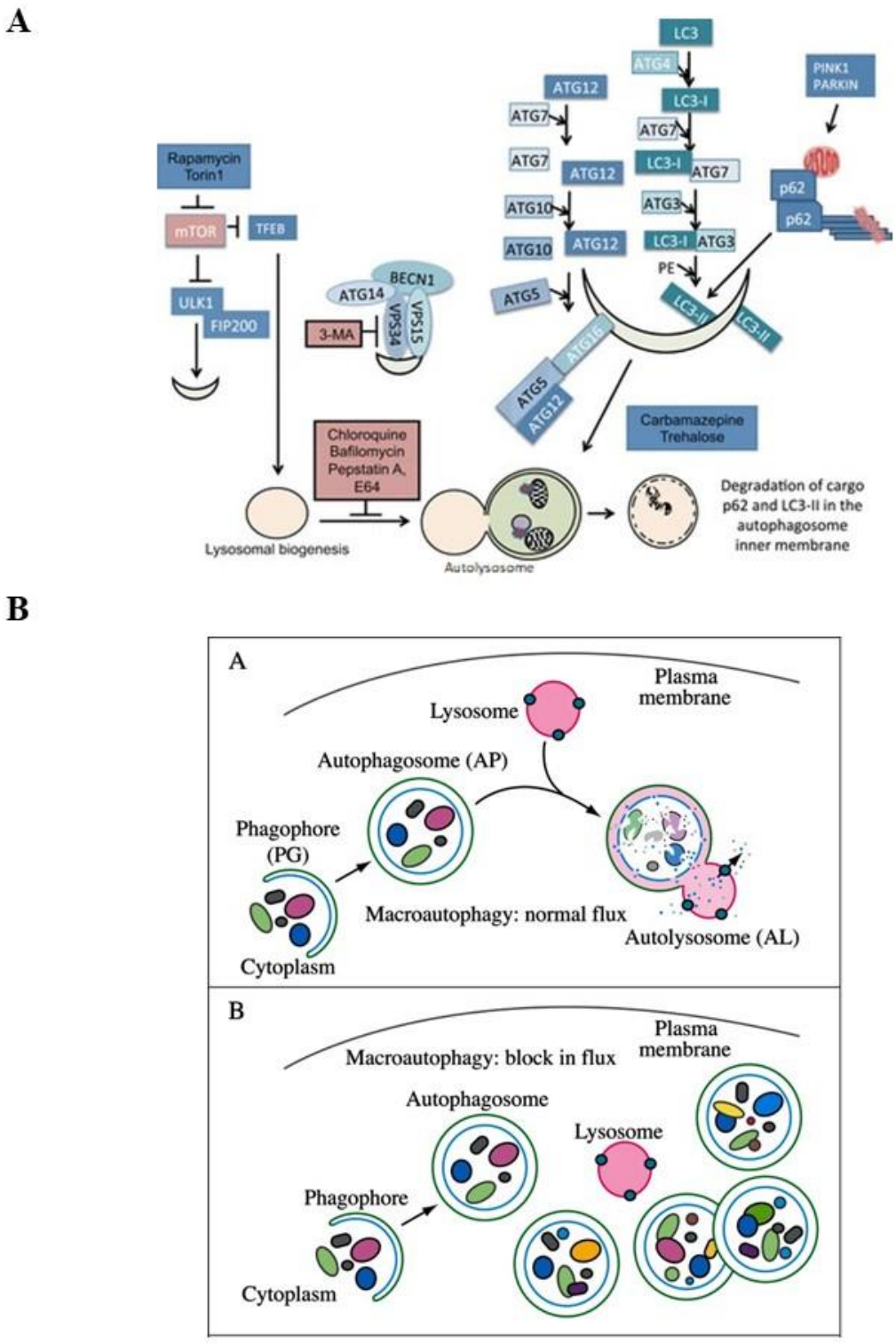

Figure 1.3 Regulation of autophagy.

(A) A schematic representation depicting the initiation of autophagy upon mTOR inhibition during starvation which enables the activation of ULK1 complex and subsequent initiation of

autophagosomal formation. Rapamycin and Torin1 are mTOR inhibitors that in turn activate autophagy. The The PI3KC3 complex comprising Beclin 1, is involved in phagophore formation and is inhibited by 3-MA. The ATG5-ATG12-ATG16 complex then extends the autophagosomal membrane through LC3B lipidation. The interaction between SQSTM1/p62 and LC3B helps sequester the ubiquitinated cargo within the growing autophagosomal membrane. The autophagosomal cargo is subsequently degraded upon fusion with lysosomes leading to autophagy flux. Chloroquine, bafilomycin, E64 and pepstatin A, inhibit lysosomal function and thereby, inhibit autophagic flux. Pink1 and Parkin localization to the mitochondria further tags the mitochondria for clearance by the mitophagy pathway that uses the autophagy machinery. (132) **(B)** A schematic model depicting normal autophagy flux (top panel A) in comparison to a block in autophagy flux (bottom panel B). During normal autophagy flux, there is continuous recycling of the autophagosomal cargo. However, a block in autolysosome formation or lysosomal defect causes a defect in autophagosome turnover leading to accumulation of autophagosomes and reduced autophagy flux. (133) Abbreviations: mTOR = mammalian target of rapamycin; ULK1 = unc-51 like autophagy activating kinase 1; PI3KC3 = phosphoinositide 3 kinase catalytic subunit type III ; 3-MA = 3-methyl adenine; ATG = autophagy-related; LC3B = microtubule-associated protein 1A/1B-light chain 3 B; SQSTM1 = sequestosome 1.

The process of autophagy can be further classified as selective and non-selective. While selective autophagy includes the specific removal of particular cytoplasmic components, non-selective autophagy is a random process eliminating multiple components. Intracellular pathogens, such as protozoa, virus and bacteria, and damaged organelles are usually eliminated through selective autophagy.

Autophagy is involved in the regulation of numerous biological processes. Autophagy is an adaptive process that is activated in response to and provides defense against metabolic stress. Autophagy is also involved in intracellular protein and organelle quality control, and routinely

performs a range of housekeeping functions such as removal of damaged macromolecules and organelles, prevent accumulation of misfolded proteins and abnormal protein aggregates, and elimination of intracellular pathogens. Studies on autophagy-deficient cells indicate a possible role of autophagy in limiting DNA damage and genomic instability (134). On one hand, autophagy is an adaptive mechanism essential for cell survival, with cells undergoing cell death upon defects in their autophagy genes (135, 136). The cytoprotective role of autophagy is best demonstrated under conditions of nutrient deprivation. At the same time, autophagy also constitutes a form of non-apoptotic programmed cell death, called "autophagic cell death". The autophagy genes, Atg7 and beclin1, were shown to be involved in non-apoptotic cell death, which was mediated by caspase-8 inhibition (137). Additionally, calpain-mediated cleavage of Atg5 switched the mode of cell death from autophagy to apoptosis, suggesting that autophagy is closely linked to apoptosis (138). Therefore, autophagy impacts cellular decision on life and death by mediating a pro-survival or pro-death role (139). While the lack of autophagy can be deleterious to a cell, excessive autophagy can be detrimental at the same time, necessitating tight regulation of this subcellular process (135, 140).

Exploring the various roles of autophagy in health and disease may present with opportunities to optimally target this pathway. Autophagy is frequently monitored at both the gene and protein levels. Multiple genes are involved in regulating the autophagy machinery at various levels, including the 32 autophagy-related (*ATG*) genes identified to date (140). LC3B lipidation, which signifies the conversion of LC3 from the free form LC3I to the PE-conjugated form LC3II, is one of the fundamental steps in mammalian autophagy (141). Since LC3, the mammalian orthologue of Atg8, forms a part of the early isolation membrane, autophagic vacuoles and autophagic bodies (142), it is a good marker for studying membrane dynamics during autophagy

in mammalian cells. However, monitoring gene expression and LC3B levels alone do not necessarily correlate with an increase in autophagy flux. Increased accumulation of autophagosomes in cells may possibly reflect a disparity in the rate of autophagic sequestration and autolysosomal degradation, leaving the cells in a state of autophagic stress (143) (Fig. 1.3B). Therefore, maintenance of lysosomal function and its effective fusion with autophagosomes are decisive for the completion of autophagic flux. Mounting evidence suggests that lysosome-associated membrane protein 2 A (LAMP2A) is important for autophagosome-lysosome fusion (144, 145).

Pharmacologically targeting autophagy, that involves inducing or suppressing autophagy using chemical drugs, is another method to develop a clear understanding of the autophagy mechanism involved in disease processes. There are several pharmacological agents currently available to modulate autophagy. As shown in Fig. 1.3A, some of the most commonly used agents include rapamycin, 3-methyladenine (3-MA), bafilomycin-A1 (Baf-A1), chloroquine, and lysosomal protease inhibitors (146, 147). Rapamycin, an inhibitor of the kinase activity of mTOR (148), induces autophagy by negatively regulating mTOR (149). Baf-A1 is a potent inhibitor of the late phase of autophagy. Its mechanism of action includes inhibition of vacuolar type H+-ATPase present in lysosomes leading to an inhibition of lysosome acidification. Baf-A1 thus, prevents maturation of autophagic vacuoles by inhibiting autolysosome formation (150). E64d and pepstatin A are two lysosomal protease inhibitors that block autophagy by inhibiting various lysosomal cathepsins (147). 3-MA suppresses autophagy via inhibition of class III PI3K (151) and thus, interferes with the formation of autophagosomes (152). Therefore, there are several autophagy inhibitors currently available that are capable of impeding different stages of the autophagy process.

1.7.2 Autophagy in asthma

Autophagy has been implicated in various lung diseases, including asthma, COPD, cystic fibrosis (CF), pulmonary hypertension (PH) and acute lung injury (ALI). Studies linking autophagy to the pathogenesis of asthma are emerging rapidly. Genetic association studies have identified a SNP of the *ATG5* gene in two distinct asthma populations (153). This SNP was found to be positively associated with asthma and negatively associated with pre-bronchodilator FEV1, which indicated a role for autophagy in reduced lung function observed in asthmatic patients. This was further validated qualitatively in this study by demonstrating higher number of double-membraned autophagosomes in fibroblasts and epithelial cells from bronchial biopsy tissue of a moderately severe asthma subject by electron microscopy. These genetic and histological observations provide one of the earliest evidences of autophagy in asthma pathogenesis. Other SNPs in the *ATG5* gene were also found to be associated with childhood asthma (154).

In addition to the genetic profile, an understanding of autophagic responses in inflammatory and resident structural cells is essential to develop a comprehensive interpretation of autophagy in asthma. Autophagy regulates immune activity at multiple levels. Ranging from antigen processing and presentation to lymphocyte development to immune tolerance, autophagic regulation of the immune system is multifold. Various studies have linked the MHC class II-restricted presentation of cytosolic and nuclear antigens to autophagy (155-157). Autophagy also plays a critical role in regulating the development and survival of B and T lymphocytes. T lymphocytes deficient in Atg5 exhibited reduced proliferation upon TCR stimulation and enhanced apoptotic rates (158). Another study on Atg7-deficient T lymphocytes revealed that autophagy is critical for normal T lymphocyte homeostasis as defective autophagy in these cells

led to accumulation of superfluous organelles such as mitochondria resulting in accrual of reactive oxygen species (ROS) and imbalance in expression of pro- and anti-apoptotic proteins (159). Moreover, selective degradation of adaptor protein Bcl10 by autophagy modulates TCR-mediated activation of NF-κB and thus keeps in check the hyperactivation of effector T cells (160). Autophagy also enforces the functional integrity of Treg cells as Treg cells were found to undergo apoptosis and lineage instability due to abnormal metabolism in the absence of autophagy (161). Similar to T lymphocytes, B lymphocyte development is hindered in the absence of Atg5. B lymphocytes lacking Atg5 were found to have a defective pro- to pre-B cell transition and reduced number of B1-B cells in the peritoneum (162). IL-4 induction of autophagy in B cells supported B cell survival and enhanced antigen presentation by B cells (163). This was also found to exacerbate immunopathological symptoms in experimental asthma through the activation of multiple pathways.

Studies have also linked autophagy to airway remodeling. A recent study demonstrated elevated autophagy and hallmark features of remodeling in human asthmatic airways and targeting autophagy in murine models of varying asthma severity was found to reduce all key features of allergic asthma and ameliorate airway remodeling (164). In one study, autophagy was shown to regulate TGF-β1-induced fibrotic response in primary human ASM cells (165), indicating autophagy as a critical pathway for ECM secretion in ASM cells. The positive correlation between the gene expression of *ATG5* and collagen, type V, alpha 1 (*COL5A1*) in the airways of refractory asthmatic subjects further suggests that dysregulation of autophagy may contribute to fibrosis in asthmatic airways, particularly in difficult-to-treat refractory asthmatic individuals (166). Using an allergic asthma model, autophagy was also shown to regulate mucus secretion in an IL-13 dependent manner in airway epithelial cells (167). The airway epithelium is also a

significant source of ROS and IL-13 and IL-4 cytokines increased both autophagy and superoxide levels in airway epithelium (167). In turn, ROS exposure can also induce autophagy as a cellular defense mechanism for timely degradation of oxidized proteins and damaged organelles such as mitochondria (168).

Autophagy and airway fibrosis may thus, occur in parallel and autophagy may be a key driver for airway remodeling in asthma. The mechanism of fibrosis requires massive biosynthesis of ECM proteins necessitating substantial energy reserves within the cell. Autophagy flux may thus, serve as the energy source and pathway for cellular survival under diseased condition. It is also important to note that autophagy can take up differential and potentially opposite roles depending on cell types, tissue microenvironment, cell signaling and energy requirements (146).

Additionally, autophagy also plays an important role in respiratory tract viral infections, including influenza A virus, adenovirus, coronavirus, respiratory syncytial virus and rhinovirus, which are major exacerbation risk factors for asthma. In general, viruses appear to use the autophagy machinery to promote viral replication (169-171). They also block autophagosomal fusion with lysosomes in order to evade presentation of viral antigens (172, 173).

Relatively few studies have examined the role of autophagy in severe asthma. The sputum and peripheral blood cells from patients with severe asthma displayed high levels of autophagy than healthy controls and non-severe asthmatics (174). Emerging evidence suggests a role for autophagy in both eosinophilic (175) and neutrophilic inflammation (176) in severe forms of asthma, further connecting autophagy to the severity of asthma. These evidences indicate higher levels of basal autophagy in asthma. Current literature thus, suggests a clear link between autophagy and asthma pathogenesis, particularly in severe asthma, however, the underlying mechanism appears to be cell-context dependent and requires further elucidation.

Mitophagy represents the selective elimination of damaged mitochondria within a cell using the autophagy machinery. Similar to autophagy, dysregulation of mitophagy is emerging as a key player in the pathogenesis of pulmonary fibrosis and COPD (177, 178); however, literature is scarce in the context of asthma. We, therefore, reviewed the available literature on the role of mitochondria in the pathogenesis of asthma.

1.8 Role of mitochondria in asthma pathogenesis

Mitochondria are dynamic cytoplasmic organelles that dictate the balance between life and death (179). These double membraned organelles are separated into four compartments – outer mitochondrial membrane (OMM), intermembrane space (IMS), inner mitochondrial membrane (IMM) and mitochondrial matrix. Being the cellular powerhouse, mitochondrial machinery is designed to generate NADH and ATP through tricarboxylic acid cycle (TCA) and oxidative phosphorylation (OXPHOS). Mitochondrial respiratory chain, commonly called the electron transport chain (ETC), is made up of five large protein complexes, namely Complex I (NADH-Coenzyme Q oxidoreductase); Complex II (succinate-Coenzyme Q oxidoreductase); Complex III (Q-cytochrome c oxidoreductase); Complex IV (Cytochrome c oxidase); Complex V (ATP synthase) respectively. These complexes embedded within the IMM is responsible for OXPHOS respiration (180). The pumping of protons from the matrix into the IMS results in an electrochemical proton gradient across the mitochondrial membranes, with a prominent negative charge in the matrix. This constitutes the mitochondrial membrane potential ($\Delta\Psi m$). A healthy mitochondrial pool is characterized by a high and polarized $\Delta\Psi m$, and a damaged mitochondrial pool by a low and depolarized $\Delta\Psi m$ (181).

Mitochondrial superoxide radicals (O_2^{*-}) are generated within the mitochondria during OXPHOS. Manganese superoxide dismutase (MnSOD) catalyze the conversion of these

superoxide anions into hydrogen peroxide (H_2O_2) in the matrix. In addition to being a major source of ROS production, mitochondria themselves are a target to ROS (182) (Fig. 1.4A). Disturbances in the normal redox balance arising from disruption in the oxidant and antioxidant levels within a cell manifest as oxidative stress. Mammalian cells are equipped with endogenous antioxidant defense systems to tackle this oxidative stress, which include antioxidant enzymes such as superoxide dismutases (SOD), catalase and glutathione peroxidase (183). However, an imbalance between the oxidants and antioxidants trigger apoptotic cell death. Accumulation of ROS causes oxidative damage that has been linked to several pathologies, including pulmonary, cardiovascular and gastro-intestinal diseases. However, low concentrations of ROS are physiologically relevant and critical for healthy cell function (184, 185). The $\Delta\Psi m$ and mitochondrial dynamics further regulate the redox status of a cell.

The exposure of the airway to allergens and oxidants activates airway inflammation in asthmatic individuals, resulting in the release of pro-inflammatory mediators, including leukotrienes and histamines. These mediators in turn recruit the different inflammatory cells relevant to asthma, such as lymphocytes, eosinophils, neutrophils and macrophages (186). The infiltrating inflammatory cells upon activation promote ROS generation, which includes superoxide anions, hydrogen peroxide, hydroxyl radicals, and nitric oxide, in the epithelium and submucosa that overwhelms the antioxidant defenses leading to increased oxidative stress and oxidative damage. The asthmatic epithelium in particular is susceptible to oxidant-induced apoptosis (187).

A

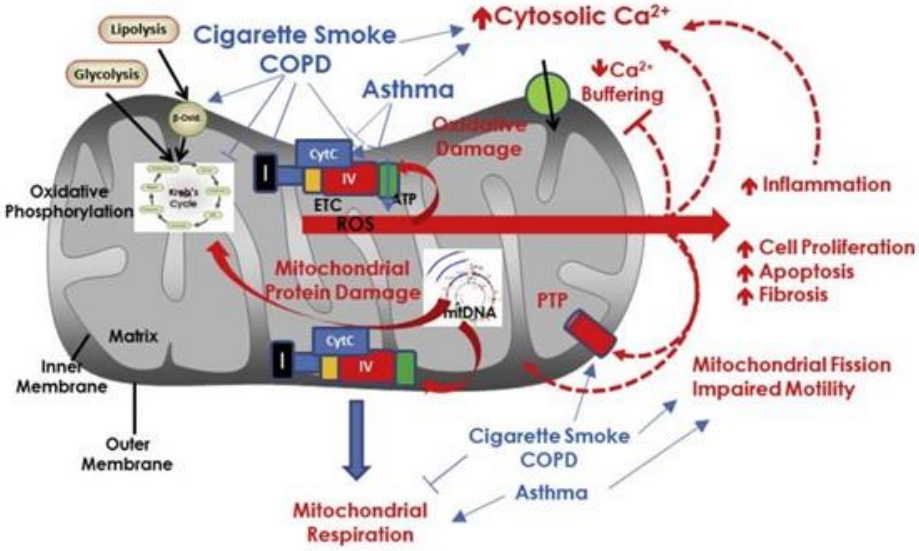
Lipolysis
Glycolysis
Cigarette Smoke
COPD
Asthma
↑Cytosolic Ca2+
↓Ca2+ Buffering
Oxidative Damage
CytC
IV
ETC
ATP
ROS
Oxidative Phosphorylation
↑Inflammation
↑Cell Proliferation
↑Apoptosis
↑Fibrosis
Mitochondrial Protein Damage
mtDNA
PTP
Matrix
Inner Membrane
Outer Membrane
Mitochondrial Fission
Impaired Motility
Cigarette Smoke
COPD
Asthma
Mitochondrial Respiration

B

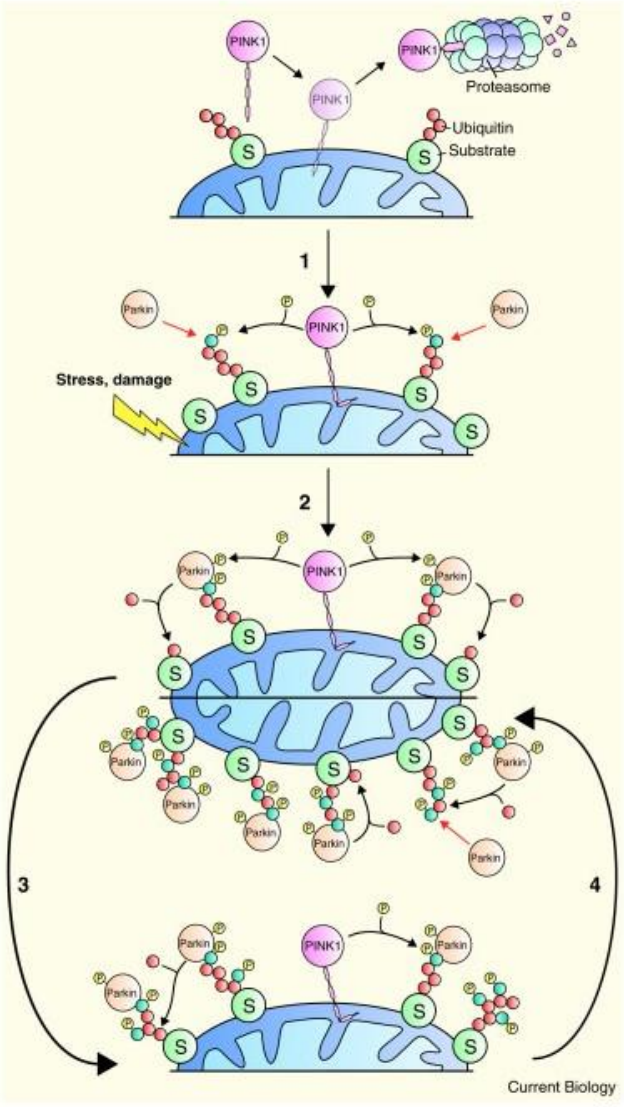
PINK1
Proteasome
Ubiquitin
Substrate
1
Parkin
Stress, damage
2
3
4
Current Biology

Figure 1.4 Mitochondrial dysfunction in airway diseases.

(A) Although ROS is a normal byproduct of mitochondrial respiration, exposure to insults such as inflammation and cigarette smoke in diseases such as asthma and COPD, results in increased mitochondrial ROS production which in turn has downstream effects on inflammation, proliferation, apoptosis, fibrosis, cytosolic calcium ($[Ca^{2+}]_{cyt}$) regulation and mtDNA integrity, which in turn impacts the mitochondria. ROS, thus, in a feedback fashion, influences mitochondrial structure and function. (188) **(B)** Mitochondrial degradation via mitophagy involves (1) stabilization of PINK1 on the OMM under mitochondrial stress and subsequent recruitment of Parkin from the cytosol to the mitochondrial surface. (2) PINK1 phosphorylates Parkin activating its E3 ubiquitin ligase activity. (3 and 4) Activated Parkin ubiquitinates mitochondrial substrates on the OMM and PINK1 further phosphorylates ubiquitin (Ub) triggering the translocation of more Parkin, resulting in a feedback loop that amplifies phospho-Ub moieties on the mitochondrial OMM. (189) Abbreviations: β-Oxid = β-oxidation; CytC = cytochrome C; ETC = electron transport chain; IV = complex IV of the ETC; mtDNA = mitochondrial DNA; PTP = permeability transition pore; ROS = reactive oxygen species; OMM = outer mitochondrial membrane.

Mitochondrial function within a cell is not restricted to its classical role of ATP production via OXPHOS. Mitochondria within a cell form interconnected networks serving multiple functionalities, including metabolic signaling, programmed cell death, biosynthetic pathways, heme and Fe-S cluster synthesis, and Ca^{2+} regulation and homeostasis (181, 188). This is reinforced by the fact that mitochondrial defects can cause diverse and complex diseases, including neurodegenerative diseases, metabolic syndrome, cardiomyopathies, obesity and cancer (181).

1.8.1 Mitochondrial quality control

Mitochondria possesses a multitude of mechanisms to help coordinate stress response and re-establish mitochondrial homeostasis in the face of diseases, including pulmonary pathologies.

Mitochondrial homeostasis is ensured by the coordinated operations of mechanisms including mitophagy, mitochondrial dynamics and mitochondrial biogenesis. PTEN-induced putative kinase 1 (PINK1) and E3 ubiquitin ligase Parkin are well known regulators of mitophagy in cultured cell models, where their coordinated activities are capable of sensing and triggering the removal of damaged mitochondria respectively (190). PINK1 is continuously degraded and recycled in the presence of an intact mitochondria (Fig. 1.4B). Hence, low levels of PINK1 are found in cells with intact mitochondria. However, in the event of mitochondrial depolarization, PINK1 degradation is inhibited leading to its accumulation on the mitochondrial surface and subsequent recruitment of Parkin (190-192) (Fig. 1.4B). The selective recruitment of Parkin from the cytosol to depolarized mitochondria triggers the autophagic degradation of damaged mitochondria. PINK1/Parkin-mediated mitophagy is intimately linked with mitochondrial dynamics and mitochondrial motility as ubiquitination of OMM proteins mitofusin-1, -2, voltage dependent anion channel (VDAC) and Miro by Parkin, tags the mitochondria for autophagic degradation and thereby, modifies mitochondrial behavior (193, 194). Generally, mitophagy is initiated within a cell when the $\Delta\Psi m$ is compromised (195). Mitophagy also regulates mitochondrial quantity depending on the energy requirement of the cell. While the defective mitochondria are selectively recycled via mitophagy, new functional mitochondria are replenished into the pool via biogenesis in order to maintain a functional mitochondrial network under stressful environments. Sirtuin 1 (SIRT1) is a NAD-dependent deacetylase which serves as a cellular sensor of metabolic status. Upon starvation, elevation in NAD^+ levels activates SIRT1 that in coordination with AMP-activated protein kinase (AMPK) regulates mitochondrial mass, ATP production and nutrient oxidation, with the help of the transcription co-factor, peroxisome proliferator-activated receptor gamma coactivator 1 alpha (PGC1α) (196, 197).

In order to mitigate stress, cells activate a number of mechanisms in an effort to re-establish homeostasis. Mitophagy is one such mechanism that is usually enhanced as an early protective response to promote cell survival and stress adaptation by selective elimination of damaged mitochondria. Persistence of stress beyond recovery drives the dysfunctional mitochondria to ignite cell death. Mitophagy is thus involved in cellular homeostasis, stress adaptation and redox balance (198).

Mitochondrial structure undergoes constant change in size, shape, number and distribution through constitutive cycles of fusion and fission (199). These processes are collectively called mitochondrial dynamics and are essential for mitochondrial inheritance as well as to regulate mitochondrial morphology, mitophagy, apoptosis and other biological functions of mitochondria (198). The mechanics of mitochondrial dynamics are not completely understood. Fission events are responsible for segregating the dysfunctional mitochondria from the mitochondrial pool. Dynamin-related protein 1 (DRP1), mitochondrial fission factor (MFF) and fission protein 1 homolog (FIS1) are some of the proteins that coordinate mitochondrial fission. Mitochondrial fusion is coordinated by mitofusins, MFN1 and MFN2 (OMM proteins), together with optic atrophy protein 1 (OPA1; an IMM protein) (200). Fusion events are intended to retain intact mtDNA, matrix metabolites and membrane components, as well as to dilute mitochondrial impairment within a cell (201, 202). Depolarization of $\Delta\Psi m$ triggers mitochondrial fission in order to segregate the damaged portion of the mitochondria. The daughter mitochondria is then prone to clearance by mitophagy. Mitochondrial fission also prevails in diseased cells as a pro-survival mechanism by stimulating mitophagy (195). Mitochondrial fusion, however, is involved in the inhibition of apoptotic cell death (199). The quality control mechanisms are thus intricately connected with cell death.

Emerging evidence suggests that autophagy and mitophagy can play both protective as well as detrimental roles in human pulmonary diseases albeit in a cell type-specific manner (203, 204). Disrupted mitochondrial quality control (QC) mechanisms and mitochondrial dysfunction have been extensively studied in the pathogenesis of other chronic lung diseases, including COPD and IPF (177, 205), but comparatively less explored in asthma, and severe asthma per se.

1.8.2 Mitochondrial dysfunction in asthma

Mitochondrial dysfunction is suggested to have downstream consequences on key aspects of asthma pathophysiology, including fibrosis, proliferation, apoptosis, response to oxidative stress, calcium regulation and airway contractility (188) (Fig. 1.4A). Mitochondrial dysfunction in the different airway cell populations, including alveolar epithelial cells (AECs), fibroblasts and immune cells, contribute towards fibrosis in the lung (206) by stimulating AEC-derived cytokines leading to the activation of myofibroblasts (207).

The importance of mitochondria in the pathogenesis of asthma is gaining momentum. Increasing evidence suggests that mitochondrial dysfunction is key to the pathogenesis of asthma (208-210). However, our understanding of precise connection between mitochondria and asthma is largely incomplete. Oxidative stress and mitochondrial dysfunction are reported to play an important role in the development and progression of asthma (209, 210). Microscopic analysis of bronchial epithelium from asthmatic children revealed abnormal ultrastructural changes in the mitochondria providing one of the early evidences of mitochondrial abnormality in asthma (211). Studies also suggest that mitochondrial structural changes and dysfunction are features associated with experimental allergic asthma (209). Mechanistically, oxidative damage-induced mitochondrial dysfunction drives the molecular processes responsible for the exacerbation of

allergic airway inflammation implying that mitochondrial defects could pose as risk factors for severe allergic disorders in atopic individuals (210).

Exposure to environmental pollutants and oxidants such as tobacco smoke, diesel exhaust particles and ozone caused an increase in cellular ROS levels which subsequently induced mitochondrial dysfunction in the lung (187). Furthermore, asthmatic response is associated with the rapid loss of antioxidant activity (212) and severe asthmatic children showed decreased airway gluthathione and increased oxidative stress biomarkers in their bronchoalveolar lavage (213). Defects in the mitochondrial DNA (mtDNA) have also been implicated in the etiology of asthma (208, 214, 215). That said, this may be a strong indication that beyond its canonical function of ATP production, the non-canonical roles of mitochondria can also influence airway structure and function.

As mentioned earlier in Section 1.7.2, selective autophagy of Bcl10 is critical in regulating NF-κB signaling (160), which is a key player in airway inflammation in asthma (216). However, not much is known regarding the role of Bcl0 and its associated signaling in the context of asthma pathogenesis.

1.9 Role of Bcl10 in immune signaling

B-cell lymphoma/leukemia 10 (Bcl10) was originally described in 1999 when it was found to be associated with the constitutive activation of canonical nuclear factor-κB (NF-κB) in mucosa-associated lymphoid tissue (MALT) B cell lymphoma (217). Bcl10 was identified to undergo oncogenic chromosomal translocation in MALT lymphoma and exhibit a mutated truncated form that strongly induced NF-κB activation. Bcl10 also contains a caspase recruitment domain (CARD) homologous to apoptotic molecules. However, the truncated form of Bcl10 activated NF-κB without induction of apoptosis, implicating Bcl10 in the pathogenesis of tumors.

Interestingly, MALT lymphoma was associated with the nuclear localization of Bcl10 (218). Bcl10 has been largely studied in antigen receptor-mediated lymphocyte activation where it was found to interact with CARMA/ CARD-containing scaffold proteins and MALT1 paracaspase to form the three-component CBM signalosome that sets in motion a cascade of events that eventually lead to NF-κB induction (219, 220). CBM signaling is essential for host defense and tissue homeostasis. However, alterations in the signaling components, including Bcl10, have been implicated in diseases, such as autoinflammatory diseases, lymphoproliferative disorders and immunodeficiencies, as well as cancers (221).

CBM signaling is a highly regulated process and CBM-1 signaling in T and B cells is the most studied. In response to antigen stimulation of T and B cell receptors (TCR and BCR), the CBM-1 signaling complex is assembled by recruiting lymphocyte-specific CARMA1/CARD11, BCL10, and MALT1 (222) (Fig. 1.5A). The signalosome recruits the IκB kinase (IKK) complex, made of the IKKα, β, γ units, resulting in its catalytic activation, which subsequently phosphorylates inhibitor of nuclear factor κB (IκBα) to induce its proteasomal degradation, releasing NF-κB dimers that translocate to the nucleus to activate the canonical NF-κB signaling pathways (223, 224). In addition to NF-κB signaling, the CBM-1 signalosome also activates the stress-activated mitogen-activated protein kinase (MAPK) and c-Jun NH(2)-terminal kinase (JNK) cascades (225). Depending on the cell-specific chromatin landscape accessible to NF-κB or other transcription factors, the activation of these pathways through the CBM complex signaling results in the inducible expression of numerous inflammatory cytokines, chemokines, and factors that control other cellular functions including survival, proliferation and differentiation (226). The NF-κB-mediated transcriptional programs are thus cell-specific, depending on the chromatin landscape established during cell differentiation

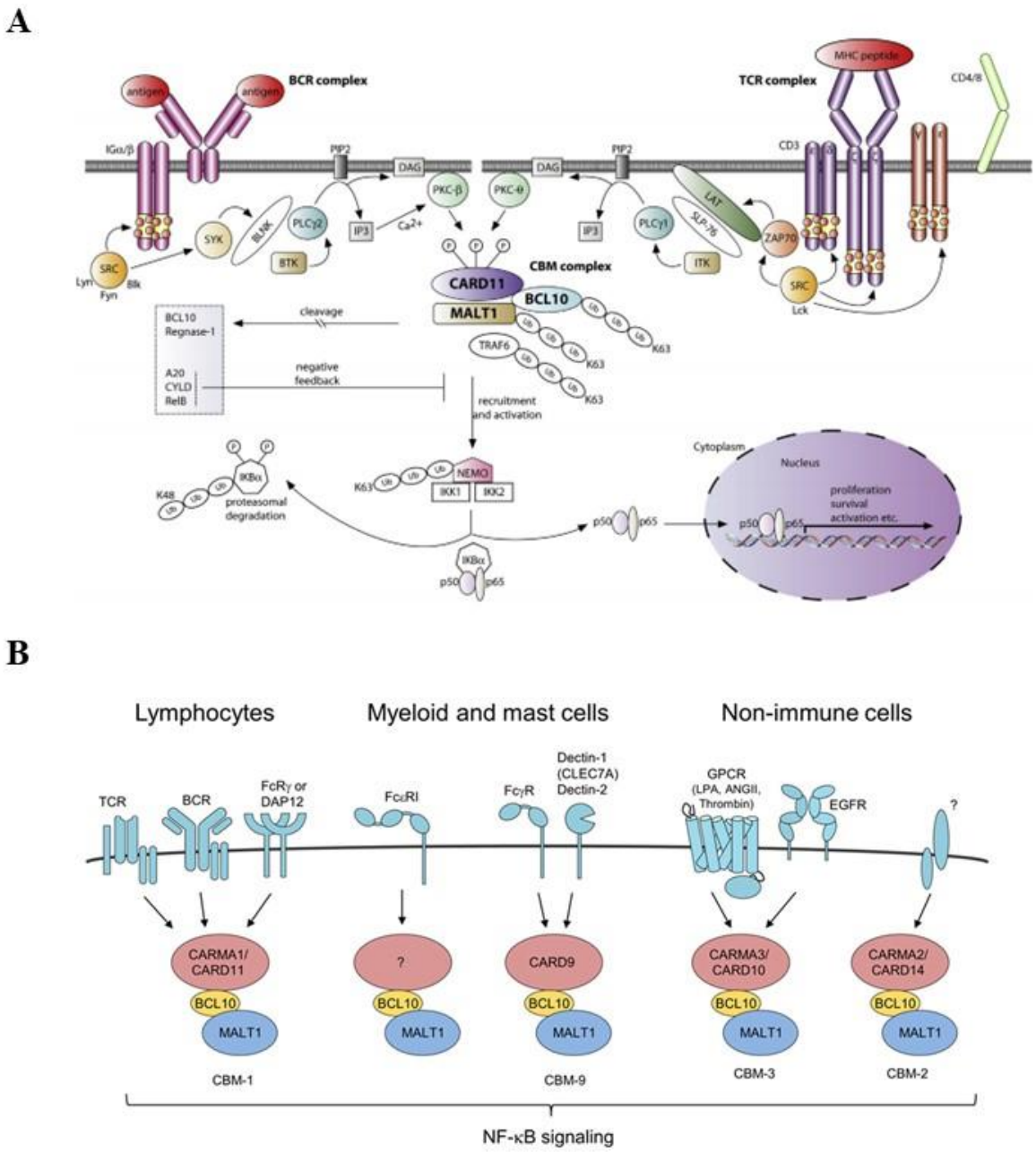

Figure 1.5 The CARMA-BCL10-MALT1 (CBM) signalosome complex.

(A) A schematic overview of the signaling cascade triggered by proximal antigen-receptor cross-linking of BCR and TCR leading to the assembly and activation of the CBM complex culminating in NF-κB activation. (227) **(B)** Distinct upstream stimuli lead to the recruitment of BCL10/MALT1 complex to different CARMA/CARD proteins. The activation of specific receptor types orchestrates the formation of distinct CBM complexes. Irrespective of the

CARMA component, all pathways converge upon the formation of CBM complex and its downstream activation of NF-κB. (228)

The CBM-1 complex is vital for the development of immune cells, including T lymphocytes, B lymphocytes, Treg cells, natural killer (NK), NKT cells, and mature B cell subsets (229, 230). *BCL10* deficiency in T and B cells led to defective NF-κB signaling, failure to upregulate IL-2 and proliferate in response to TCR and BCR stimulation, all of which contributed to blunted antigen-mediated immune response (230). Therefore, Bcl10 together with CARMA1/CARD11 and MALT1 orchestrate antigen signaling in activated lymphocytes to mount an effective adaptive immune response. CBM-1 complex, however, is exclusive to immune cells as CARMA1 is expressed predominantly in lymphocytes (220).

Alternative CBM complexes with a different CARMA/CARD scaffold are involved in other cell types, such as myeloid cells, mast cells and non-immune cells, eliciting cell type-dependent and context-dependent inflammatory responses (Fig. 1.5B). Bcl10 is involved in FcεRI-mediated NF-κB activation, pro-inflammatory cytokine release and degranulation in mast cells (231). IgE-mediated allergic inflammatory response was found to be impaired in Bcl10-deficient mast cells (231, 232), indicating Bcl10 as a key regulator of immune signaling in mast cells. Furthermore, Bcl10 also complexes with CARMA3/ CARD10 and MALT1 to form the CBM-3 signalosome as a result of G-protein-coupled receptor (GPCR) activation to induce pro-inflammatory gene expression in non-immune cells, such as fibroblasts and endothelial cells (233).

Interestingly, studies also indicate Bcl10 to be an important mediator of fibrotic remodeling. Angiotensin II (Ang II)-induced fibrotic signaling, such as ECM synthesis and myofibroblast

proliferation, was mediated by Bcl10 via the CBM-3 signalosome (234, 235). Deletion of Bcl10 severely reduced Ang II-induced cardiac fibrosis, inflammation and improved electrical remodeling, thereby reducing susceptibility to ventricular arrhythmias (235). Bcl10 also regulated LPS-induced activation of NF-κB and IL-8 in human intestinal epithelial cells (236), suggesting a role for Bcl10 in epithelial inflammation. Moreover, NF-κB-regulated genes in the airway epithelium contributed to allergen-induced peribronchial fibrosis and mucus production (92).

Bcl10 is a critical regulator that positively as well as negatively regulates immune cell signaling (228). Degradation of Bcl10 via the proteasomal or autophagy-mediated lysosomal pathway helps terminate NF-κB signaling (237). In response to antigen stimulation of TCR, the IKK complex phosphorylates Bcl10 at multiple sites signaling its proteolysis via the ubiquitin/proteasomal pathway (238). TCR engagement also promotes K63 polyubiquitination of Bcl10, causing enhanced selective autophagy of Bcl10 and ultimately its lysosomal degradation (160, 237). Although Bcl10 degradation negatively regulates NF-κB signaling, more clarity is needed on the precise mechanisms and regulations involved.

NF-κB signaling has been primarily investigated in airway tissues and inflammatory cells in asthma (216). NF-κB activation is increasingly recognized in the pathogenesis of asthma, yet its role in airway remodeling remains unclear. A greater understanding of this pathway, particularly in airway structural cells, is thus required.

1.10 Rationale and hypothesis

Asthma is a complex disease of varying phenotypes and endotypes. Severe asthma, in particular, is characterized by high dosage of asthma medications which entails the disproportionate use of

medical resources. The incomplete understanding of the pathophysiology associated with severe asthma makes it one of the most challenging to treat.

Subepithelial fibrosis, particularly the excessive deposition of collagen in the submucosa, which correlates with disease severity, is a challenging pathological feature to treat, as none of the currently available asthma therapies can remove the excessive collagen deposition in asthmatic airways. The identification of novel pathways that contribute to collagen deposition can thus, help generate therapeutic targets to interfere with airway remodeling.

The literature review above provides evidence of increased autophagy and mitochondrial dysfunction in asthma. Both autophagy and mitochondria influence cellular decision of life and death, however, the interplay between the two is largely unknown in asthma. Previous work by our group had demonstrated the association of autophagy with subepithelial fibrosis in asthma pathogenesis, particularly in the more severe forms of the disease (166). Since very little information is available on mitochondrial behavior in bronchial fibroblasts, that are known to show alterations in their remodeling and inflammatory characteristics during diseased states, we sought to analyze any abnormalities in the mitochondrial behavior by assessing the mitochondrial QC mechanisms of mitophagy and mitochondrial biogenesis in bronchial fibroblasts from severe asthma patients. We, therefore, hypothesized the disruption of mitochondrial homeostasis in severe asthmatic bronchial fibroblasts through alterations in their execution of mitophagy and biogenesis, that contribute to their increased persistence and thereby, drive subepithelial fibrosis associated with airway remodeling in severe asthma.

Furthermore, the increased presence of cytokines in the airway milieu stimulate the activation of fibroblasts to myofibroblasts, which is a key event in fibrosis. This is often accompanied by phenotypic changes in fibroblasts, such as increase in their secretory and contractile properties

which often relies on increased energy utilization yet changes in the energetic profile of these bronchial fibroblasts are not well-documented. There exists a gap in knowledge regarding the role of asthma-related cytokines in mitochondrial dysfunction in asthma, and more importantly in whether this affects airway remodeling in severe asthma. We, therefore, hypothesized that cytokine-mediated activation of fibroblasts is associated with the induction of autophagy and mitochondrial dysfunction, and the blockade of autophagy in bronchial fibroblasts may potentially ameliorate subepithelial fibrosis in severe asthma. Since airway remodeling is an obstinate problem in severe asthma, studying autophagy and its effect on these adverse structural changes presents an important research avenue which could have a positive impact on a disease as complex as human asthma.

Bcl10-mediated NF-κB signaling has widely been studied as an inflammatory pathway in immune cells. It is yet to be explored in the context of airway remodeling in asthma. Since Bcl10 is an important mediator of fibrotic remodeling, we also investigated Bcl10 signaling as an alternative fibrotic mechanism contributing to fibrosis in severe asthma. We hypothesized that Bcl10-mediated NF-κB pathway promotes fibrotic signaling in severe asthmatic fibroblasts. We further postulated that CBM-3 signalosome regulates LPS-induced NF-κB activation and IL-8 production in bronchial fibroblasts.

2. Aims of the thesis

The specific aims and objectives for this study are:

Aim I: To determine the mitochondrial health at baseline in bronchial fibroblasts from remodeled airways of severe asthma patients in comparison to fibroblasts from unaffected airways in healthy subjects. To achieve this aim, we postulated the below three objectives.

Objective 1: To establish the alterations in mitophagy and mitochondrial biogenesis by evaluating mitophagy and biogenesis markers.

Objective 2: To investigate the mitochondrial bioenergetics by evaluating mitochondrial membrane potential, mitochondrial metabolic activity, and mitochondrial ROS production.

Objective 3: To assess the effect of mitochondrial alterations on fibroblast function by evaluating ECM and cytokine production.

Aim II: To examine the effect of asthma-related cytokines on mitochondrial health in bronchial fibroblasts from severe asthma patients in comparison to their healthy counterparts. To achieve this aim, we postulated the below four objectives.

Objective 1: To assess the effect of cytokines on mitophagy and mitochondrial biogenesis in bronchial fibroblasts.

Objective 2: To assess the effect of cytokines on mitochondrial bioenergetics in bronchial fibroblasts.

Objective 3: To assess the effect of cytokines on ECM production in bronchial fibroblasts.

Objective 4: To study the role of autophagy in the above cytokine-mediated functions by using autophagy regulators.

Aim III: To investigate Bcl10 signaling in the presence of mitochondrial alterations in bronchial fibroblasts from severe asthmatic patients and non-asthmatic healthy controls. To achieve this aim, we postulated the below three objectives.

Objective 1: To establish the levels of Bcl10 and NF-κB pathway members at baseline in both group of fibroblasts

Objective 2: To examine the subcellular localization of Bcl10 in bronchial fibroblasts

Objective 3: To evaluate the effect of LPS stimulation on Bcl10 signaling in bronchial fibroblasts.

3. Materials and Methods

3.1 Patient Cohort

Asthma patients were recruited at the Severe Asthma Clinic in the Pulmonary Medicine department at Rashid Hospital, Dubai, U.A.E. Healthy volunteers with no prior history of allergy or asthma, and no recent respiratory infections were enrolled from Rashid Hospital as well as Sharjah Institute for Medical Research, Sharjah, U.A.E. Patients with mild, moderate and severe asthma, who fulfilled the American Thoracic Society (ATS) guidelines and were taking treatments based on GINA guidelines, were recruited by the treating physician and nurse, and the healthy controls by the researcher and nurse. Written informed consent was obtained from all study participants after a detailed explanation of the study. 10 non-asthmatic controls and 22 asthmatics, including 11 non-severe asthmatics (with mild-to-moderate asthma) and 11 severe asthmatics were included in this study. Blood sample collection and endobronchial biopsies were performed in accordance with a study protocol approved by the Dubai Scientific Research Ethics Committee with approval number DSREC-11/2017_04. The clinical characteristics of these subjects are summarized in Table 1.

Table 1. Clinical characteristics of the subjects whose PBMCs were used in this study

Characteristics	**Healthy (n = 10)**	**Non-Severe Asthmatic (n = 11)**	**Severe Asthmatic (n = 11)**
Age (years) Mean (SD, range)	35.6 (13, 32)	35.5 (15, 41)	51.7 (19, 47)
Gender (M%: F %)	25:75	18.2:81.8	36.4:63.6
BMI (Kg/m^2) Mean (SD, range)	23.8 (3, 6)	26.8 (7, 24)	28.2 (7, 22)
Smoking Status (Non-smoker%, Ex-smoker%, Smoker%)	62.5%, 12.5%, 25.0%	90.9%, 9.1%,0%	90.9%, 0%, 9.1%
Allergic Rhinitis (Yes%)	12.5%	72.7%	81.8%
Eczema (Yes%)	0%	18.2%	27.3%
Asthma Control Test Mean (SD, range)	N/A	20.5 (5, 14)	19 (6, 19)
FEV1/FVC (%) Mean (SD, range)	N/A	83.3 (10, 34)	69.7 (11, 31)
Total serum IgE (IU/ml) Mean (SD, range)	N/A	367.2 (389, 1035)	1128.5 (1506, 4862)
Blood eosinophil count (number/µl) Mean (SD, range)	N/A	3.8 (2, 6)	5.6 (6, 18)
Blood neutrophil count (number/µl) Mean (SD, range)	N/A	57.4 (14, 49)	60.6 (14, 47)
Peak Flow (L/min) Mean (SD, range)	453.8 (101, 300)	287.8 (76, 250)	293.6 (150, 410)

3.2 Culture of primary human bronchial fibroblasts

The primary bronchial fibroblasts were isolated from endobronchial tissue biopsies obtained from non-smoking patients with severe asthma or non-smoking healthy volunteers. These fibroblasts were archived at Quebec Respiratory Health Research Network Tissue Bank (McGill

University Health Centre/ Meakins-Christie Laboratories Tissue Bank, Montreal, Canada), as previously described (239). These fibroblasts were shipped to our facility at the University of Sharjah. Bronchial fibroblasts from three non-asthmatic and three severe asthmatic subjects were used in this study. The clinical characteristics of these subjects are summarized in Table 2.

Table 2. Clinical characteristics of the subjects whose fibroblasts were used in this study

Characteristics	**Healthy (n = 3)**	**Severe Asthmatic (n = 3)**
Age (years) Mean (SD, range)	43.7 (12.5, 23)	43.3 (8.3, 16)
Ethnicity, Caucasian (%)	100%	100%
Gender (M%: F %)	67:33	33: 67
BMI (Kg/m^2) Mean (SD, range)	31.6 (2.3, 4.4)	30.3 (2.6, 3.7)

The cells were revived in Dulbecco's modified Eagle's medium (DMEM) – high glucose supplemented with 10% fetal bovine serum (FBS), 2 mM L-glutamine, 100 units/ml of penicillin, and 100 ng/ml streptomycin in 75-cm^2 flasks. The cells were maintained at 37°C in 5% CO_2 with medium change performed every 2-3 days. They were harvested when 80-90% confluent using 0.1% trypsin-ethylenediaminetetraacetic acid (EDTA) and seeded into multiwell tissue culture plates for experiments. Cells isolated from the airways have been reported to maintain the disease phenotype through several passages in culture (240). Accordingly, the fibroblasts were passaged a maximum of 8 times and experiments were conducted using fibroblasts at matched passages. All cell culture reagents were purchased from Sigma-Aldrich.

The cells were seeded into 6-, 12- or 96-well plates at approximate cell density/well of $10x10^4$, $5x10^4$ and $2x10^3$, respectively. At ~50-70% confluency, they were serum-starved in FBS-free DMEM complete medium for baseline measurements or 1% FBS-supplemented medium for cytokine stimulation experiments for a period of 24 hours before experiments. For baseline measurements, the cells were cultured in DMEM complete medium thereafter for the specified amount of time. In order to investigate the lysosomal turnover of mitophagy markers, the fibroblasts were co-incubated with 10µg/ml of E64d (Santa Cruz, Cat. No. sc-201280A) and 10µg/ml of Pepstatin A (Santa Cruz, Cat. No. sc-45036). For cytokine stimulation experiments, the cells were stimulated with 25ng/ml of recombinant human IL-17A (Sigma-Aldrich, Cat. No. SRP3080), 10ng/ml IL-13 (Prospec, Cat. No. CYT-446-b) or 10ng/ml TGF-β1 (Sigma-Aldrich, Cat. No. T7039) for 48 hours (for mRNA) or 96 hours (for protein). Considering the prolonged culture conditions, the treatments were refreshed after 48 hours. Autophagy modulation was achieved by pre-treating cells with 10nM bafilomycin-A1 (Baf-A1) (Santa Cruz, Cat. No. sc-201550), 1000nM rapamycin (Santa Cruz, Cat. No. sc-3504) or 1mM 3-methyl adenine (3-MA) (R&D Systems, Cat. No. 3977) for 4 hours prior to stimulation with cytokines. Co-treatment with 10µM carbonyl cyanide-4-(trifluoromethoxy) phenylhydrazone (FCCP) (Tocris, Cat. No. 0453-10) for 2 hours was used as a positive control to induce mitochondrial dysfunction.

3.3 Isolation of human peripheral blood mononuclear cells

Approximately 12ml of peripheral blood was drawn from the study participants into EDTA-containing blood collection tubes and mixed well. The tubes were kept on ice and processed by the Histopaque method of blood separation within 4 hours. Briefly, the undiluted blood sample was carefully layered onto equal volume of Histopaque-1077 (Sigma-Aldrich, Cat. No. 10771) in a 50ml centrifuge tube and centrifuged at 400rcf for 30 minutes at room temperature (RT) to

separate out the layers. The opaque interface containing peripheral blood mononuclear cells (PBMCs) were transferred into a 15ml centrifuge tube and washed three times with phosphate-buffered saline (PBS) solution before pelleting and then stored at -80°C until RNA extraction.

3.4 Quantitative real-time polymerase chain reaction (qRT-PCR)

In order to investigate the mRNA expression of the genes of interest in the bronchial fibroblasts and PBMCs, qRT-PCR was performed. Total RNA was extracted from cell pellets using the RNeasy Mini Kit (Qiagen, Cat. No. 74106) or Trizol Reagent (Invitrogen, Cat. No. 15596018), according to manufacturer instructions. RNA quality and yield were determined by Nanodrop (Thermo Scientific) spectrophotometric measurements. cDNA synthesis was performed from 100-500ng of total RNA using the FIREScript RT cDNA Synthesis Kit (Solis Biodyne, Cat. No. 06-15-00050) or the High-Capacity cDNA Reverse Transcription Kit (Applied Biosystems, Cat. No. 4368814) in the Veriti Thermal Cycler (Applied Biosystems). qRT-PCR reactions were set up using the 5x Hot FirePol EvaGreen qRT-PCR SuperMix (Solis Biodyne, Cat. No. 08-36-00001) in QuantStudio 3 Real-Time PCR System (Applied Biosystems). The primers used are listed in Table 3. Gene expression was analyzed using the Comparative C_T ($\Delta\Delta C_T$) method after normalization to the housekeeping gene 18s RNA. All results are presented as fold expression change compared to non-asthmatic healthy controls or untreated controls.

Table 3. Primer sequences used for qRT-PCR

Genes	Forward Primer Sequence (5'-3')	Reverse Primer Sequence (5'-3')
BECN1	ATGCAGGTGAGCTTCGTGTG	CTGGGCTGTGGTAAGTAATGGA
ATG5	GACCAGTTTTGGGCCATCAATC	GTGCAACTGTCCATCTGCAGC
LC3B	GAACGGACACAGCATGGTCAGC	ACGTCTCCTGGGAGGCATAG
SQSTM1	TTGTACCCACATCTCCCGCCA	TACTGGATGGTGTCCAGAGCCG
LAMP2	AACTTCAACAGTGGCACCCACC	AGTGATGTTCAGCTGCAGCCCC
PINK1	CCTGCGCCAGTACCTTTGTGT	TGGGTCCAGCTCCACAAGGATG
PRKN	CTCCAGCCATGGTTTCCCAGTG	CCAGGTCACAATTCTGCACAGTC
COL1A1	GATTGACCCCAACCAAGGCTG	GCCGAACCAGACATGCCTC
COL3A1	GATCAGGCCAGTGGAAATG	GTGTGTTTCGTGCAACCATC
COL5A1	GTCGATCCTAACCAAGGATGC	GAACCAGGAGCCCGGGTTTTC
FN1	CTGGGAACACTTACCGAGTGGG	CCACCAGTCTCATGTGGTCTCC
ACTA2	CTTCGTGTTGCCCCTGAAGAG	GCATAGAGAGACAGCACCGC
IL6	GAAAGCAGCAAAGAGGCAC	GCACAGCTCTGGCTTGTTCC
IL11	GTGGCCAGATACAGCTGTCGC	GGTAGGACAGTAGGTCCGCTC
IL8	CCACACTGCGCCAACACAG	CTTCTCCACAACCCTCTGC
GROα	CTGCAGGGAATTCACCCCAAG	GATGCAGGATTGAGGCAAGC
18s	TGACTCAACACGGGAAACC	TCGCTCCACCAACTAAGAAC

3.5 Western blotting

In order to investigate the expression of proteins in the mitochondrial and NF-κB pathways, western blotting was performed. The cell pellets were lysed in either RIPA lysis buffer prepared in the lab (Tris, NaCl, 1% sodium deoxycholate, 0.1% sodium-dodecyl-sulfate (SDS), 1% Triton X-100, pH 7.5) or readymade 10X RIPA buffer (abcam, Cat. No. ab156034) diluted to 1X, and supplemented with 1x Protease Inhibitor Cocktail (Sigma-Aldrich, Cat. No. P2714) and 1mM PMSF (Sigma-Aldrich, Cat. No. P7626). The protein lysates were quantified using the Protein Assay Kit II (Bio-Rad, Cat. No. 5000002) with bovine serum albumin (BSA) as standard. The lysates were boiled in 10x Laemmli Sample Buffer and 20-50μg of total protein was separated using varying percentages of gels depending on the molecular weight of the protein of interest. Alternatively, 4-20% Mini-PROTEAN TGX Precast Protein Gels (Biorad, Cat. No. 4561095-6) were used for some experiments. Post electrophoresis, the proteins were transferred onto a 0.2μm nitrocellulose membrane (Bio-Rad, Cat. No. 1620112) and blocked in 5% non-fat dry milk for at least an hour at RT before incubating the membrane overnight at 4°C with the primary antibody. The membrane was subsequently incubated for 1 hour at RT with the respective horshradish peroxidase (HRP)-linked secondary antibody. The blots were developed using the Clarity™ Western ECL Substrate (Bio-Rad, Cat. No. 170-5060) in the ChemiDoc™ Touch Gel and Western Blot Imaging System (Bio-Rad). The anti-human antibodies used in this study are listed in Table 4. Anti-β-actin or anti-GAPDH were used as the loading control. The membranes were washed in TBS-T buffer, three times for 10 minutes each between all incubation steps. Image Lab software (Bio-Rad) was used to detect and quantify the protein bands. Protein levels were normalized to β-actin or GAPDH in the respective experiments. For cytokine stimulation experiments, they were thereafter normalized to the untreated controls.

Table 4. Antibodies used for western blotting

Genes	Description
LC3B	Rabbit polyclonal; abcam, Cat. No. ab51520
Mitophagy Antibody Sampler Kit	Cell Signaling Technology, Cat. No. 43110T
LAMP2A	Rabbit monoclonal; abcam, Cat. No. ab125068
SIRT1	Mouse monoclonal; Cell Signaling Technology, Cat. No. 8469s
PGC1α	Rabbit polyclonal; Novus Biologicals, Cat. No. NBP1-04676
AMPKα2	Rabbit polyclonal; abcam, Cat. No. ab3760
Phospho-AMPKα (Thr172)	Rabbit monoclonal; Cell Signaling Technology, Cat. No. 2535T
Survivin	Rabbit monoclonal; abcam, Cat. No. ab134170
Bcl10	Mouse monoclonal; Santa Cruz, Cat. No. sc-5273
IKBα	Rabbit monoclonal; Cell Signaling Technology, Cat. No. 4812s
Phospho-IKBα	Rabbit monoclonal; Cell Signaling Technology, Cat. No. 2859s
Cell Fractionation Antibody Sampler Kit	Cell Signaling Technology, Cat. No. 11843
TLR4	Rabbit polyclonal; abcam, Cat. No. ab13556
Mitochondrial Dynamics Antibody Sampler Kit	Cell Signaling Technology, Cat. No. 48799T

β-actin	Mouse monoclonal; Sigma-Aldrich, Cat. No. A5441
GAPDH	Rabbit monoclonal; Cell Signaling Technology, Cat. No. 2118S
Anti-Rabbit IgG, HRP-linked	Cell Signaling Technology, Cat. No. 7074S
Anti-Mouse IgG, HRP-Linked	Cell Signaling Technology, Cat. No. 7076S

3.6 Autophagy Assays

3.6.1 Autophagosome Detection

Autophagosomal levels were assessed in the bronchial fibroblasts using the Autophagy Assay Kit (Sigma-Aldrich, Cat. No. MAK138). Autophagy detection was performed as per kit instructions. Briefly, the fibroblasts were stained with the Autophagosome Detection Reagent for 30 minutes at 37°C in the dark. The fluorescence intensity was measured at an excitation of 360nm and emission of 520nm in Synergy HTX fluorescence reader (BioTek) and imaged using Olympus BX51 fluorescence microscope.

3.6.2 Autophagy Sensor LC3B-GFP

Premo Autophagy Sensor LC3B-GFP (BacMam 2.0) (Invitrogen, Cat. No. P36235) was used to transduce the fibroblasts as per manufacturer instructions, so as enable the visualization of LC3B protein and thereby visualize autophagy. Briefly, the BacMam LC3B-GFP reagent was added directly to the plated cells in DMEM complete medium and incubated for 24 hours at 37°C for LC3B protein expression. The cells were then fixed and processed using the immunofluorescence protocol for dual staining.

3.6.3 LysoTracker lysosomal staining

LysoTracker Deep Red (Invitrogen, Cat. No. L12492) fluorescent probe was used to label and visualize the lysosomes. Cells were stained with 50nM Lyostracker Deep Red while protected from light for 30 minutes at 37°C in an atmosphere of 5% CO_2 and imaged using the Nikon Eclipse Ti confocal microscope.

3.7 Mitochondrial Functional Assays

3.7.1 Determination of mitochondrial mass using MitoTracker Green

The mitochondrial mass was tagged using MitoTracker Green (Invitrogen, Cat. No. M7514) that stains the lipid membrane of the mitochondria independent of mitochondrial membrane potential. The cells were stained with 50nM MitoTracker Green while protected from light for 30 minutes at 37°C in an atmosphere of 5% CO_2. After staining, the cells were washed with PBS for immunofluorescence processing or flow cytometry staining buffer (FACS Buffer) (PBS, 2% FBS, 1mM EDTA) for flow cytometry processing in order to remove the excess stain. For fluorescence microscopy, the cells were imaged using the Nikon Eclipse Ti confocal microscope. For flow cytometry, the cells were then analyzed using the BD FACSAria III flow cytometer and the acquired data analyzed using FlowJo v10 software.

3.7.2 Determination of mitochondrial membrane potential and associated apoptosis

Mitochondrial membrane potential ($\Delta\Psi m$) in the control and asthmatic fibroblasts was measured using the cationic dye tetraethylbenzimidazolylcarbocyanine iodide (JC-1; abcam, Cat. No. ab113850) that aggregates in energized mitochondria, in accordance with

manufacturer's instructions. For microplate readouts, non-asthmatic and severe asthmatic fibroblasts were seeded in the same dark 96-well microplate at a density of $2x10^3$ cells/well. The cells were allowed to attach overnight and serum-starved for 24 hours. Briefly, the cells were stained with 10μM JC-1 solution for 10 minutes at 37°C in the dark, washed and incubated in 1x supplemented dilution buffer. The microplate was read in the presence of buffer in the Varioskan Flash multi-mode plate reader (Thermo Scientific) at an excitation wavelength of 475nm, and emission wavelength of 590nm so as to measure the JC-1 aggregate signal and 530nm to measure the JC-1 monomer fluorescence. A decrease in the JC-1 aggregate fluorescence is indicative of depolarization. For each independent experiment, each condition was performed in triplicate.

For flow cytometry readouts, the harvested cells were stained with 10μM JC-1 solution for 15 minutes at 37°C in the dark. The cells were washed twice with FACS buffer thereafter and analyzed using the BD FACSAria III flow cytometer and the acquired data analyzed using FlowJo v10 software. A decrease in JC-1 ratio (Aggregate/Monomer) is also indicative of depolarization.

The mitochondrial membrane potential-associated apoptosis was measured using the Mitochondrial Membrane Potential Apoptosis Kit, with Mitotracker Red & Annexin V Alexa Fluor 488 (Invitrogen, Cat. No. V35116). The cells were stained with 50nM MitoTracker Red while protected from light for 30 minutes at 37°C in an atmosphere of 5% CO_2. The stained cells were thereafter washed with FACS buffer and labelled with Annexin V-AF488 for 15 minutes at RT in the dark. Alternatively, apoptosis was also measured in fibroblasts using the PE Annexin V Apoptosis Detection Kit with 7-AAD (Biolegend, Cat. No. 640934), according to manufacturer instructions. Briefly, the cells were labelled with Annexin V-PE and 7-AAD

for 20 minutes at RT in the dark. The cells were then analyzed using the BD FACSAria III flow cytometer and the acquired data analyzed using FlowJo v10 software.

3.7.3 MitoSOX Superoxide Indicator Assay

MitoSOX Red Mitochondrial Superoxide Indicator (Invitrogen, Cat. No. M36008) was used to measure levels of mitochondrial superoxide production specifically in live fibroblasts, as mitochondrial superoxide alone and none of the other reactive oxygen species (ROS) or reactive nitrogen species (RNS) is capable of oxidizing MitoSOX Red dye to emit red fluorescence. The harvested cells were stained with 5µM MitoSOX solution in Hank's Balanced Salt Solution (HBSS) for 15 minutes at 37°C in the dark. The cells were washed twice with FACS buffer thereafter and analyzed using the BD FACSAria III flow cytometer and the acquired data analyzed using FlowJo v10 software.

3.7.4 MTT Metabolic Activity Assay

Non-asthmatic and severe asthmatic fibroblasts were seeded in the same 96-well plate at a density of $2x10^3$ cells/well. The cells were allowed to attach, and serum-starvation performed the same day so as to not give cells the time to start proliferation. After overnight serum-starvation, the cells were cultured in DMEM complete medium for up to 96 hours. The primary bronchial fibroblasts exhibited doubling times of 30-48 hours, therefore, the formazan conversion within a period of 48 hours can be considered to be due to the intrinsic metabolic activity of the seeded cells without the interference of increase in cell number due to proliferation. After the desired incubation period, 10µl of MTT (3-(4,5-dimethylthiazol-2-yl)-2,5-diphenyltetrazolium bromide) solution (5mg/ml in PBS; Sigma-Aldrich, Cat. No. M5655) was added and incubated for 3 hours at 37°C. The medium was completely discarded before adding 100µl of dimethylsulfoxide (DMSO; Sigma-Aldrich, Cat. No. D8418) to solubilize the

formazan crystals. The absorbance was read at 570nm on a Synergy H1 multi-mode microplate reader (BioTek). For each independent experiment, each condition was performed in triplicate.

3.7.5 ROS-Glo H2O2 Assay

Another ROS species, namely hydrogen peroxide, and its levels in the control and diseased fibroblasts was also measured using the ROS-Glo H_2O_2 Assay (Promega, Cat. No. G8820), in accordance with manufacturer's instructions. The non-asthmatic and severe asthmatic fibroblasts were seeded in the same white 96-well microplate at a density of $2x10^3$ cells/well. The cells were allowed to attach overnight and serum-starved for 24 hours. For cytokine stimulation experiments, the cells were stimulated with 25ng/ml IL-17A, 10ng/ml IL-13 or 10ng/ml TGF-β1 for 96 hours. Considering the long-term culture conditions, the treatments were refreshed after 48 hours. The cells were incubated with the H_2O_2 Substrate solution in the final 6 hours of treatment. The ROS-Glo Detection Solution was added thereafter and incubated for 20 minutes at RT. The luminescence was read in the Varioskan Flash multi-mode plate reader (Thermo Scientific). The luminescent signal is proportional to the H_2O_2 levels in the cells. For each independent experiment, each condition was performed in triplicate.

3.7.6 CellTiter-Glo Viability Assay

The cellular viability of bronchial fibroblasts in response to exposure to asthma-related cytokines was measured using the CellTiter-Glo Luminescent Cell Viability Assay (Promega, Cat. No. G7572), in accordance with manufacturer's instructions. The non-asthmatic and severe asthmatic fibroblasts were seeded in the same white 96-well microplate at a density of $2x10^3$ cells/well. The cells were allowed to attach overnight and serum-starved for 24 hours. For cytokine stimulation experiments, the cells were stimulated with 25ng/ml IL-17A, 10ng/ml IL-13 or 10ng/ml TGF-β1 for 96 hours. Considering the long-term culture conditions, the

treatments were refreshed after 48 hours. Post 96 hours of cytokine treatments, the cells were incubated with the CellTiter-Glo Reagent for 2 minutes on an orbital shaker at RT. The plate was then incubated for another 10 minutes at RT to stabilize the luminescent signal, which was then recorded in the Varioskan Flash multi-mode plate reader (Thermo Scientific). The luminescent signal is proportional to the number of viable cells. For each independent experiment, each condition was performed in triplicate.

3.8 β-galactosidase Senescence Assay

Cellular senescence was measured in fibroblasts using the β-galactosidase staining kit (abcam, Cat. No. ab102534) as per kit protocol. In brief, the cells were fixed and incubated in X-gal staining solution overnight at 37°C inside a sealable bag. Images were taken using a bright-field microscope (Olympus BX51). The total number of cells positive for β-galactosidase staining in 5 separate fields of view was counted for each fibroblast.

3.9 Immunofluorescence microscopy

Mitophagy tracking was performed using fibroblasts transduced with Premo Autophagy Sensor LC3B-GFP, cultured for 24 hours and stained thereafter for PINK1. The fibroblasts were grown on sterile coverslips and rinsed with PBS before fixing the cells in 4% paraformaldehyde (PFA) for 15 minutes at RT. The cells were then washed thrice with PBS and permeabilized with 0.1% Triton X-100 for 15 minutes. The cells were blocked in 1% BSA for at least an hour at RT before incubating the cells overnight at 4°C with anti-PINK1 (Novus Biologicals, Cat. No. BC100-494) primary antibody. The cells were subsequently incubated for 1 hour at RT with the respective fluorochrome-conjugated secondary antibody. The coverslips with cells were washed and mounted on slides using ProLong Gold Antifade Mountant with DAPI (Invitrogen, Cat. No.

P36935). The fibroblasts were thereafter imaged using the Nikon Eclipse Ti confocal microscope.

3.10 Bronchoscopy

Fiberoptic bronchoscopy was performed on severe asthmatic patients in three stages - 1) administration of premedication with a mild sedative (Versed 1-3 mg intravenously); 2) nose, throat, vocal cords and windpipe were anaesthetized locally with lidocaine spray; 3) the bronchoscope was passed through the mouth into the windpipe. 6 biopsies were taken from the carina of the subsegments in the upper, middle and lower lobes (1-2 mm or 1/12-1/24 inch per biopsy) of the right lung of each subject. The biopsies were immediately transferred into tubes containing 4% PFA in PBS. The biopsies were collected and embedded as previously described (241). Briefly, the biopsies were transferred into another tube containing sterile PBS and stored overnight at 4°C. They were then embedded into paraffin blocks using routine procedure.

3.11 Immunohistochemistry

Paraffin slides of bronchial biopsy tissues obtained by fiberoptic bronchoscopy from non-asthmatic control, mild asthma, moderate asthma and severe asthma subjects that were archived at the Biobank of the Quebec Respiratory Health Research Network Canada with MUHC REB number BMB-02-039-t (166), were obtained. Formalin-fixed paraffin-embedded (FFPE) biopsy samples from severe asthma patients recruited from the Severe Asthma Clinic at Rashid Hospital were also used.

Immunohistochemical staining of FFPE biopsy tissue was performed to determine the protein expression levels and distribution of PINK1 and Bcl10 as previously described (241). Briefly, 3μm thick sections were cut from the paraffin blocks and routine deparaffinization in xylene

and rehydration steps in decreasing concentrations of ethanol were performed. Heat-activated antigen retrieval was carried out using sodium citrate buffer at pH 6.0 for PINK1 and Tris EDTA buffer at pH 9.0 for Bcl10, as per manufacturer recommendations. The sections were incubated in hydrogen peroxidase blocking solution for 30 minutes to block the endogenous peroxidase activity. The slides were blocked in 1% BSA for 20 minutes at RT and immunostained with rabbit anti-PINK1 (Novus Biologicals, Cat. No. BC100-494) or mouse anti-Bcl10 (Santa Cruz, Cat. No. sc-5273) antibody overnight at 4°C. The slides were developed using HRP/DAB (ABC) Detection IHC kit (abcam, Cat. No. ab64264), according to manufacturer recommendations. The primary antibody was omitted to serve as technical negative control and appropriate positive control tissue was used. Nuclei were counterstained blue with hematoxylin (Thermo Scientific Shandon). The slides were washed in PBS, three times for 3 minutes each between all incubation steps and mounted with cover slips for viewing. The stained slides were then examined and analyzed by a histopathologist.

3.12 Cellular Fractionation

Cellular fractionation of the bronchial fibroblasts was performed using the Cell Fractionation Kit (Cell Signaling Technology, Cat. No. 9038S), as per kit instructions. Briefly, the cell pellets were sequentially lysed in the provided cytoplasm isolation buffer, membrane isolation buffer and cytoskeleton/nucleus isolation buffer to separate out the cytoplasmic, membrane/organelle, and nuclear/cytoskeletal distinct fractions respectively. The Cell Fractionation Antibody Sampler Kit (Cell Signaling Technology, Cat. No. 11843T) was then used to determine the purity of the separated subcellular fractions.

3.13 Cellular clot preparation for immunocytochemistry

Similar to preparing paraffin block of biopsy tissues, the fibroblast cells were clotted to process them as done for immunohistochemistry. Briefly, $5x10^5$ cells were centrifuged at 1200rpm for 5 minutes and placed on ice immediately after centrifugation. 120µl of plasma was then added dropwise to the cell pellet followed by gentle vortexing for 10 seconds. 80µl of thrombin (Sigma-Aldrich, Cat. No. T4393) was then added and mixed so as to clot the cells together. The clotted cells were then transferred to a sheet of Speci-wrap paper, which was folded and secured inside a formalin cassette. The cassette was then placed inside a formalin jar for 4 hours. The clotted cells were then processed thereafter in the Excelsior AS Tissue Processor (Thermo Fisher Scientific) to generate FFPE blocks of clotted cells.

3.14 Statistical Analysis

All data are presented as mean ± standard error of the mean (SEM) of 2–4 independent experiments using GraphPad Prism 6.0 software (GraphPad, San Diego, CA, USA). Data analyses were performed using unpaired Student's t-test while comparing NHBF and DHBF, one-way ANOVA followed by Tukey's multiple comparison tests or two-way ANOVA followed by Sidak's multiple comparison tests for statistical analysis of the data. A p value < 0.05 was considered statistically significant.

4. Results

In order to investigate the role of mitochondria in subepithelial fibrosis associated with airway remodeling in severe asthma, we used bronchial fibroblasts derived from airway biopsies of severe asthmatic and non-asthmatic healthy subjects. Thus, two groups of fibroblasts were used in this study – normal human bronchial fibroblasts (NHBF) and diseased human bronchial fibroblasts (DHBF). The latter signifying the severe asthmatic (S-As) fibroblasts. These fibroblasts were characterized in-house in Canada after isolation from bronchial biopsies by visual confirmation as well as by their immunoreactivity to vimentin, desmin and pan-keratin antibodies through immunocytochemistry. In addition, we tested these cells for mycoplasma contamination upon receiving them at our facility, and further characterized their gene expression where they were found to serve as a good *ex vivo* model to study the pathology associated with severe asthma.

In order to characterize the mitochondrial phenotype in bronchial fibroblasts, we first investigated the mitochondrial QC machinery in these cells at baseline.

4.1 Augmentation of mitochondrial quality control machinery to overcome the manifestation of mitochondrial dysfunction in bronchial fibroblasts from severe asthmatic patients

Previously, our group showed the increased presence of autophagosomes in fibroblasts from moderately severe asthmatics (153). In addition, we demonstrated a positive correlation between increased *ATG5* gene expression and collagen deposition in the airways of refractory asthmatics (166). Since these studies suggested the dysregulation of autophagy to promote subepithelial

fibrosis in severe asthmatic airways, we first examined basal autophagy on a molecular level in human primary bronchial fibroblasts from severe asthmatics and healthy controls.

4.1.1 Increased basal autophagy in severe asthmatic fibroblasts

In order to assess basal expression, the bronchial fibroblasts were serum-starved for 24 hours and then cultured in DMEM complete growth medium for 4 hours. We used the Autophagy Assay kit to detect autophagosomes by fluorometry. Fluorescence microscopy showed brighter blue staining of autophagic vacuoles in DHBF than in NHBF (Fig. 4.1.1A, left panel). The fluorescence intensity when quantified using a fluorescent plate reader also showed a 1.35-fold increase in DHBF when compared to NHBF ($p=0.0314$) (Fig. 4.1.1A, right panel), which suggested the increased presence of autophagosomes at basal levels in S-As fibroblasts.

We next determined whether the autophagy-related genes are differentially expressed between NHBF and DHBF, by evaluating the expression of *ATG5*, *LC3B*, *SQSTM1/p62* and *LAMP2* genes by qRT-PCR. Although no differences were detected in the mRNA expression of *ATG5*, *LC3B* and *SQSTM1* genes between NHBF and DHBF, the *LAMP2* gene, encoding a lysosomal protein, was significantly upregulated in DHBF ($p=0.0327$) (Fig. 4.1.1B).

Western blot analysis was then used to determine the protein levels of these autophagy markers. Upon activation, the cytosolic LC3BI is converted to the autophagosomal membrane-bound LC3BII, which serves as an early indicator of autophagosomal formation. LC3B existed predominantly in the membrane-bound functional form (LC3BII) in DHBF. LC3B lipidation, i.e. conversion of LC3BI to LC3BII (LC3BII/LC3BI ratio), as well as LC3BII levels were increased in DHBF when compared to NHBF (Fig. 4.1.1C). Interestingly, DHBF also demonstrated an increase in p62 levels (Fig. 4.1.1C).

Accumulation of LC3BII and p62 can be indicative of either increased autophagosome formation or decreased autophagosomal clearance by lysosomes (143) (Fig. 1.3B). In order to distinguish whether the observed increase in autophagosomes in S-As fibroblasts was due to an increase in basal autophagy or due to a lysosomal defect, we determined the protein levels of LAMP2A using western blot analysis and labelled the lysosomes using the LysoTracker probe. Western blot analysis indicated significant overexpression of LAMP2A protein in DHBF compared to NHBF (Fig. 4.1.1C). This agrees with the observed increase in *LAMP2* gene expression in DHBF (Fig. 4.1.1B). In concordance, intense LysoTracker fluorescence was also detected in DHBF (Fig. 4.1.1D), confirming the presence of active lysosomes in S-As fibroblasts and thus, excluding the possibility of a block in lysosomal delivery of autophagic vacuoles. Furthermore, we transduced the fibroblasts with LC3B-GFP to assess the co-localization of LC3B with lysosomes. Increased co-localization of autophagosomes with lysosomes was indicated in DHBF as compared to NHBF (Fig. 4.1.1E).

Autophagy being a dynamic process necessitates the use of multiple assays to monitor autophagy as well to appropriately interpret the process (133). The growing literature on autophagy have improved our understanding of some of the common misconceptions in interpreting LC3B data. Autophagy being a catabolic process, intra-autophagosomal contents including LC3BII and p62 get degraded by the lysosomal hydrolases following the fusion of autophagosomes with lysosomes. Since significant degradation of these endogenous markers occurs during the process, the lysosomal turnover of these markers provides a more accurate account of autophagic activity than its cellular baseline levels (242).

Therefore, to further confirm the observed increase in basal autophagy in S-As fibroblasts, we co-incubated the fibroblasts with two lysosomal protease inhibitors, namely E64d and pepstatin

A, for a period of 6 hours to monitor the kinetics of autophagy flux. The membrane-bound LC3BII was the predominant form in DHBF (Fig. 4.1.1F). The kinetics of LC3B lipidation was found to vary in a cell-line dependent manner. In the presence of E64d and pepstatin A, accumulation of LC3BII was observed in both group of fibroblasts, albeit to a more significant extent in DHBF. A corresponding increase in p62 levels was also noted in DHBF upon treatment with E64d and pepstatin A (Fig. 4.1.1F), indicating their lysosomal turnover through autophagy. Taken together, these results so far suggest that at baseline, the S-As fibroblasts exhibit increased formation of autophagosomes that is accompanied by enhanced autophagy flux, in comparison to their healthy counterparts.

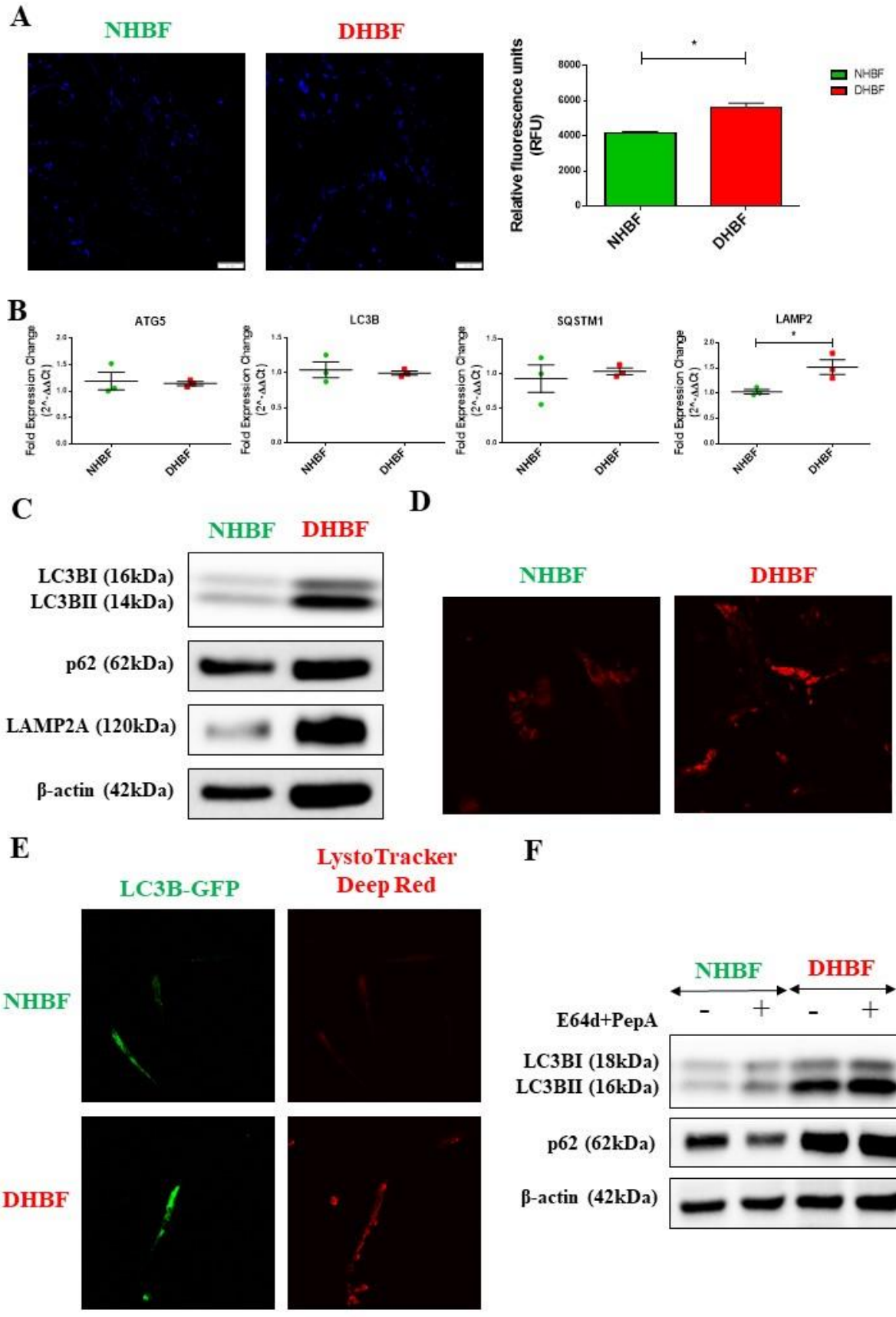
A
NHBF
DHBF
Relative fluorescence units (RFU)
8000
6000
4000
2000
0
*
NHBF
DHBF
B
ATG5
LC3B
SQSTM1
LAMP2
Fold Expression Change (2^-ΔΔCt)
NHBF
DHBF
C
NHBF
DHBF
LC3BI (16kDa)
LC3BII (14kDa)
p62 (62kDa)
LAMP2A (120kDa)
β-actin (42kDa)
D
NHBF
DHBF
E
LC3B-GFP
LysoTracker Deep Red
NHBF
DHBF
F
NHBF
DHBF
E64d+PepA
- + - +
LC3BI (18kDa)
LC3BII (16kDa)
p62 (62kDa)
β-actin (42kDa)

Figure 4.1.1 Increased levels of basal autophagy in severe asthmatic fibroblasts.

The control (NHBF) and severe asthmatic (DHBF) fibroblasts were cultured in DMEM complete medium for 4 hours post serum-starvation to measure autophagy at baseline. **(A)** To measure autophagosomal levels, the fibroblasts were stained with Autophagosome Detection Reagent for 30 minutes at 37°C in the dark and fluorescent readings were taken using a fluorescence microscope and plate reader. Representative images showing fluorescent staining of autophagosomal vacuoles (blue) in NHBF and DHBF. Scale Bar=200μm (left panel). Quantitative representation of autophagosomal levels in relative fluorescence units (RFU). $*p < 0.05$, determined by unpaired two-tailed Student t-test (right panel). **(B)** Under basal conditions, mRNA expression of autophagy markers, ATG5, LC3B, SQSTM1/p62 and LAMP2, in NHBF and DHBF was analyzed by qRT-PCR and expressed as fold expression change relative to NHBF post normalization to housekeeping gene 18s rRNA. $*p < 0.05$, determined by unpaired two-tailed Student t-test. **(C)** Representative immunoblots depicting protein levels of LC3B, p62 and LAMP2A in NHBF and DHBF. β-actin was used as loading control. **(D)** NHBF and DHBF were cultured in DMEM complete medium for 48 hours post serum-starvation for immunofluorescence measurements at baseline. Representative images of LysoTracker Deep Red fluorescence of lysosomes in NHBF and DHBF. **(E)** Representative images depicting fluorescent staining of autophagosomes using LC3B-GFP (green) and lysosomes using 50nM LysoTracker Deep Red (red). **(F)** NHBF and DHBF were cultured in the presence of lysosomal protease inhibitors, E64d and pepstatin A, for 6 hours post serum-starvation. Cell lysates were subjected to immunoblot analysis of autophagy proteins LC3B and p62. β-actin was used as loading control. Graphical data are represented as mean ± SEM from at least 3 unique donors in each group.

4.1.2 Accumulation of full-length PINK1 in severe asthmatic fibroblasts

We next aimed to investigate if the increase in autophagy displayed by S-As fibroblasts was associated with their mitochondrial health by studying the mitochondrial QC mechanisms. Mitochondrial health is under constant scrutiny by the mitochondrial QC machinery comprising of mitophagy, mitochondrial dynamics and mitochondrial biogenesis. We first investigated the mechanism of mitophagy by evaluating the gene expression of mitophagy markers, *PINK1* and *PRKN*, in NHBF and DHBF by qRT-PCR. At baseline, a mild increase in the mRNA transcripts of *PINK1* and *PRKN* was observed in DHBF compared to NHBF (Fig. 4.1.2A), however, they did not reach statistical significance. This suggested a trend of enhanced Pink1/Parkin-mediated mitophagy in S-As fibroblasts.

PINK1 protein is a reliable sensor of mitochondrial damage as its processing depends on the state of mitochondrial membrane potential ($\Delta\Psi m$). Rapid and constitutive voltage-dependent degradation of PINK1 occurs in healthy cells whereas a loss in $\Delta\Psi m$ stabilizes the mitochondrial accumulation of full-length PINK1 (192) (Fig. 1.4B). In order to assess PINK1 processing and its stability in severe asthma, the fibroblasts were cultured for 12 and 24 hours in DMEM complete medium post serum-starvation, after which they were harvested and assayed for PINK1 protein levels using western blot analysis. PINK1 protein has a short half-life. Therefore, due to the low endogenous levels of PINK1 in these bronchial fibroblasts, the blots had to be over-exposed to detect the various PINK1 bands. Interestingly, PINK1 showed increased stabilization in DHBF with the full-length (FL) precursor of PINK1 (~60kDa) being the predominant form at both 12 and 24 hours, with faint bands of their ~30-50kDa cleaved fragments (Fig. 4.1.2B). In contrast, FL PINK1 as well as its cleaved isoforms were detected in NHBF at 12 and 24 hours. While the FL PINK1 in NHBF decreased with time, a corresponding

increase in the cleaved isoforms at ~50kDa and ~30kDa was noted at 24 hours in comparison to 12 hours, which suggested increased degradation of PINK1 with time in control fibroblasts. Since mitochondrial integrity is critical in PINK1 processing, stabilization of endogenous FL PINK1 in the steady state indicates dissipation of $\Delta\Psi m$ in the S-As fibroblasts.

Explicit mitochondrial damage stabilizes PINK1 on the OMM, which selectively recruits Parkin to the damaged mitochondria. PINK1-dependent Parkin activation promotes the synthesis of ubiquitin chain linkages (243), which subsequently conjugates to various mitochondrial substrates (244). Autophagy receptor proteins then sequester the ubiquitinated cargo within the growing autophagosomal membrane to promote their clearance through autophagy (245). Multiple adaptor proteins serve as mitophagy receptors to facilitate PINK1/Parkin-mediated mitophagy, including BCL2/adenovirus E1B-interacting protein 3-like (BNIP3L)/Nix, BNIP3, p62, Optineurin and NDP52 (189). We next assessed the expression of these receptor proteins by western blot analysis. Besides PINK1, Parkin and LC3B, the autophagy and mitophagy receptor proteins, including p62, Optineurin, NDP52, BNIP3 and BNIP3L showed increased expression in DHBF when compared to NHBF (Fig. 4.1.2C), which suggested the activation of the PINK1/Parkin-mediated mitophagy machinery that delivers the damaged mitochondria to autophagosomes.

Next, we assessed the lysosomal turnover of intra-autophagosomal PINK1 by culturing the fibroblasts in the presence of E64d and pepstatin A for 4 hours. Western blot analysis showed significant accumulation of PINK1 in DHBF (Fig. 4.1.2D), indicating their lysosomal turnover through autophagy. To confirm the observed increase in mitophagy flux, we employed fluorescence microscopy to assess the co-localization of mitochondria with autophagosomes and mitochondria with lysosomes. To determine mitochondria-autophagosome co-localization,

the fibroblasts were transduced with LC3B-GFP and immunostained using an antibody against PINK1. The fluorescence intensity of LC3B as well as PINK1 staining was brighter in DHBF when compared to NHBF (Fig. 4.1.2E). Additionally, greater co-localization of LC3B and PINK1 puncta was detected in DHBF. These results suggest increased PINK1 accumulation in S-As fibroblasts that trigger their sequestration within autophagosomes. Since autophagosomal cargo is eventually delivered to the lysosomes, we monitored mitochondria-lysosome co-localization by co-labeling the fibroblasts with MitoTracker Green and LysoTracker Deep Red probes, that stains the mitochondria and lysosomes respectively. DHBF demonstrated increased MitoTracker and LysoTracker fluorescence in comparison to NHBF (Fig. 4.1.2F). Furthermore, a large proportion of the mitochondria in DHBF co-localized with lysosomes, indicating their degradation via the lysosomal pathway.

The above findings reflect the enhanced presence of depolarized mitochondria in S-As fibroblasts that upon being sensed by the mitophagy machinery within the cell led to the stabilization of PINK1 on the damaged mitochondria and activation of PINK1/Parkin-mediated mitophagy. The PINK1-tagged mitochondria were shown to be subsequently cleared through increased autolysosomal degradation.

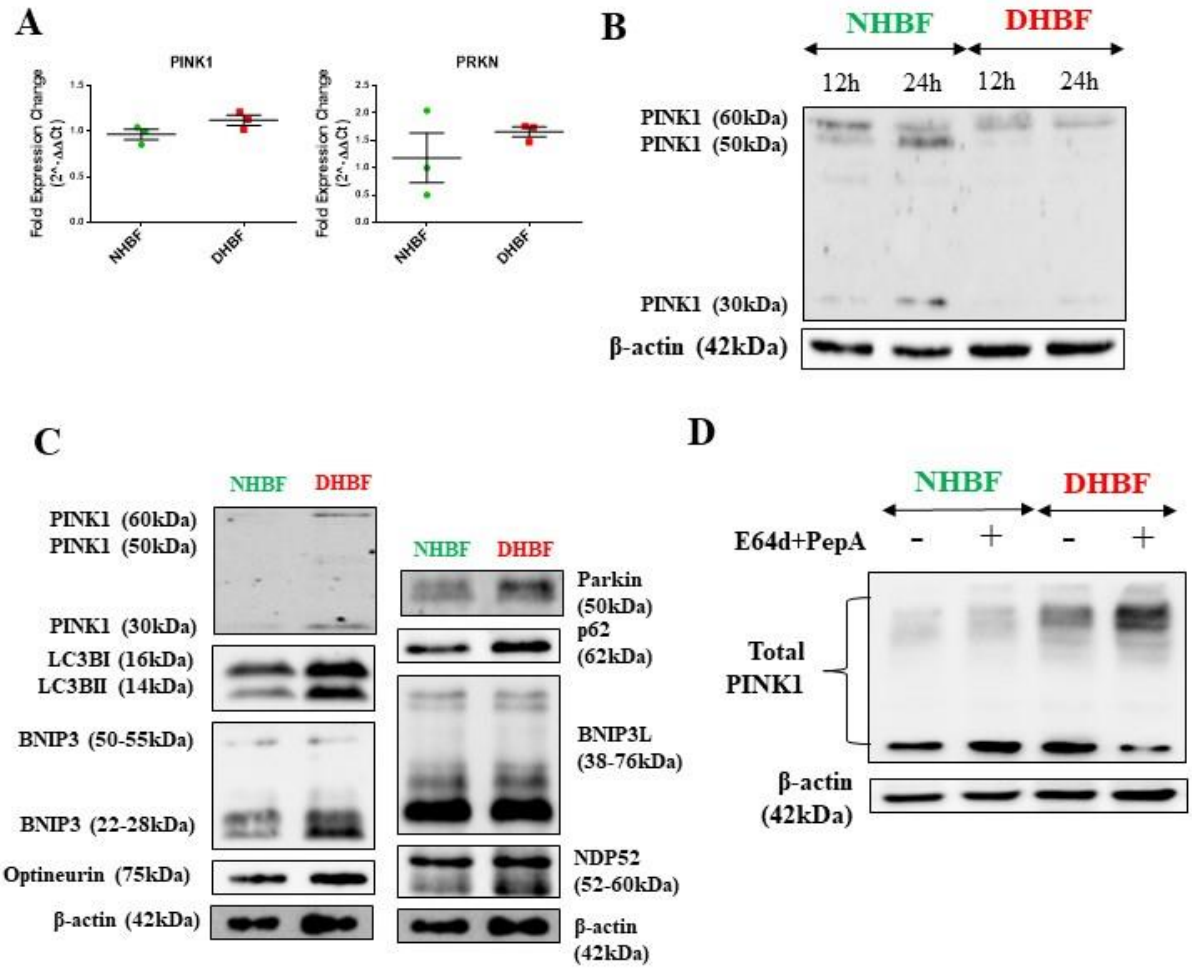
A
PINK1
PRKN
Fold Expression Change (2^-ΔΔCt)
NHBF
DHBF
B
NHBF
DHBF
12h
24h
12h
24h
PINK1 (60kDa)
PINK1 (50kDa)
PINK1 (30kDa)
β-actin (42kDa)
C
NHBF
DHBF
PINK1 (60kDa)
PINK1 (50kDa)
PINK1 (30kDa)
LC3BI (16kDa)
LC3BII (14kDa)
BNIP3 (50-55kDa)
BNIP3 (22-28kDa)
Optineurin (75kDa)
β-actin (42kDa)
Parkin (50kDa)
p62 (62kDa)
BNIP3L (38-76kDa)
NDP52 (52-60kDa)
β-actin (42kDa)
D
NHBF
DHBF
E64d+PepA
-
+
-
+
Total PINK1
β-actin (42kDa)
E
LC3B-GFP
PINK1-PE
NHBF
DHBF
F
MitoTracker Green
LysoTracker Deep Red

Figure 4.1.2 Stabilization of PINK1 in severe asthmatic fibroblasts.

(A) NHBF and DHBF were cultured in DMEM complete medium for 4 hours post serum-starvation. Under basal conditions, mRNA expression of mitophagy markers, PINK1 and PRKN, in NHBF and DHBF was analyzed by qRT-PCR and expressed as fold expression change relative to NHBF post normalization to housekeeping gene 18s rRNA. Data are represented as mean ± SEM from at least 3 unique donors in each group. $*p < 0.05$, determined by unpaired two-tailed Student t-test. **(B)** NHBF and DHBF were cultured in complete medium for the indicated time points post serum-starvation. Whole cell lysates were subjected to immunoblot analysis of PINK1 protein. β-actin was used as loading control. **(C)** Representative immunoblots depicting mitophagy related proteins, PINK1, Parkin, LC3B, p62, BNIP3, BNIP3L, NDP52, and optineurin in NHBF and DHBF. β-actin was used as loading control. **(D)** NHBF and DHBF were cultured in the presence of lysosomal protease inhibitors, E64d and pepstatin A, for 6 hours post serum-starvation. Cell lysates were subjected to immunoblot analysis of PINK1. β-actin was used as loading control. **(E)** NHBF and DHBF were cultured in DMEM complete medium for 48 hours post serum-starvation for immunofluorescence measurements at baseline. Representative images depicting NHBF and DHBF transduced with LC3B-GFP (green) and immunostained with PINK1-PE (red). **(F)** Representative images depicting fluorescent staining of mitochondria using 50nM MitoTracker Green (green) and lysosomes using 50nM LysoTracker Deep Red (red).

4.1.3 Reduced mitochondrial function in severe asthmatic fibroblasts

In order to confirm the presence of depolarized mitochondria in severe asthmatic fibroblasts, we evaluated the ΔΨm in these cells using JC-1 assay and also examined the mitochondrial metabolic activity using MTT assay.

The state of mitochondrial polarization in bronchial fibroblasts was determined using the fluorescent JC-1 probe that accumulates in healthy mitochondria yielding a red to orange colored aggregate emission at 590nm. Accordingly, a decrease in the aggregate fluorescence is indicative of mitochondrial depolarization. We detected a statistically significant drop in JC-1

aggregate fluorescence by 25% in DHBF when compared to NHBF (p=0.0248) (Fig. 4.1.3A), indicating that the mitochondria are partially depolarized in these fibroblasts. This depolarization of mitochondria in S-As fibroblasts, thus, explains the increased mitophagy flux observed in these cells.

The ability of mitochondrial dehydrogenases in metabolically active cells to convert MTT to a colored formazan product may be used as an index of mitochondrial activity (246, 247). Since the bronchial fibroblasts displayed doubling times of 30-48 hours, the fibroblasts were seeded at the same cell densities in 96-well plates, serum-starved the same day after cellular adhesion and cultured thereafter for up to 96 hours in order to assess their intrinsic mitochondrial metabolic activity ahead of proliferation. As expected, across both 24 and 48 hours, DHBF displayed significantly reduced mitochondrial metabolic activity compared to NHBF (Fig. 4.1.3B). The metabolic activity dropped by 50% at 24 hours and by 40% at 48 hours. It was however interesting to note that with progression of time, the difference in metabolic activity between NHBF and DHBF kept reducing. This could perhaps be explained by the difference in proliferation rates between the fibroblasts. Taken together, the reduced $\Delta\Psi m$ and mitochondrial metabolic activity suggest compromised OXPHOS metabolism in the severe asthmatic fibroblasts.

In addition to decreased $\Delta\Psi m$, damaged mitochondria display the release of stress signals such as reactive oxygen species (ROS). We, therefore, measured the levels of different ROS species, including superoxide and H_2O_2, using the MitoSOX fluorescent assay and ROS-Glo bioluminescent assay. Reduced ROS levels were detected at baseline in DHBF when compared to NHBF (Fig. 4.1.3C). MitoSOX Red directly measures the superoxide generated in the mitochondria and ~1.5-fold reduction in mitochondrial superoxide production was indicated in

DHBF as compared to NHBF (Fig. 4.1.3C, left panel). The amount of total H_2O_2 (including intracellular and extracellular) in DHBF sample wells was also drastically reduced ($p<0.0001$) in comparison to NHBF (Fig. 4.1.3C, right panel). This could be a result of increased scavenging of ROS by the cellular antioxidant defense systems in S-As fibroblasts to avoid ROS-induced cell death.

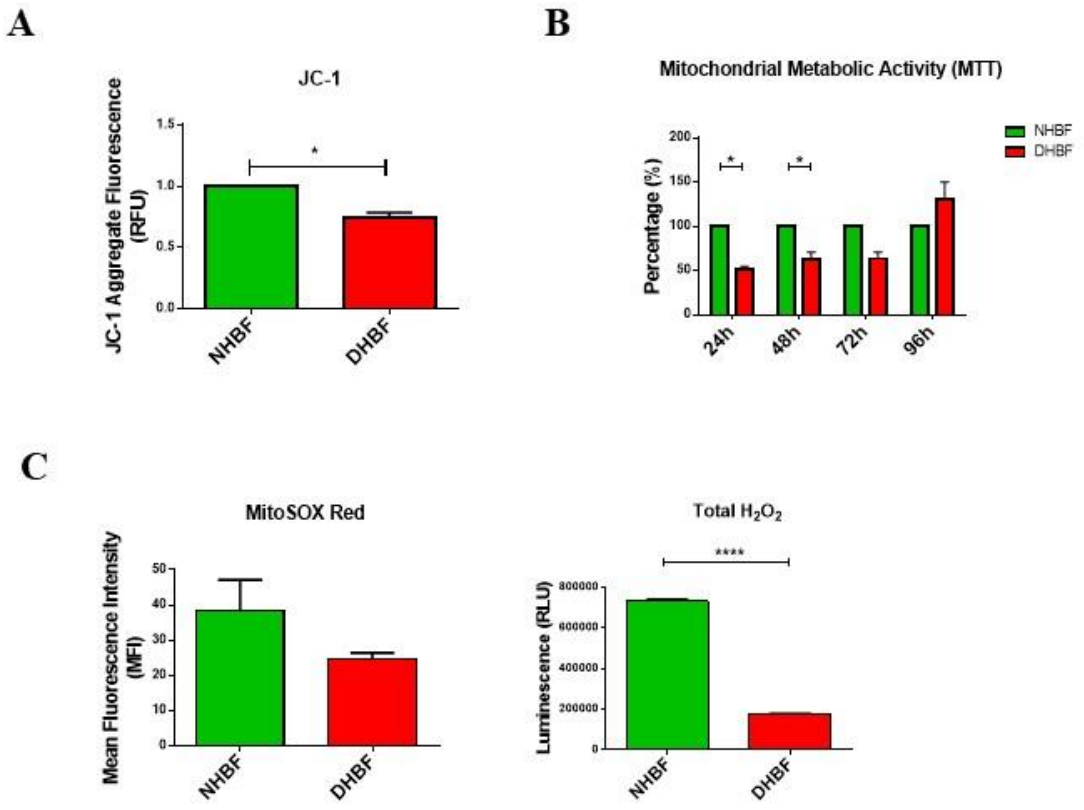

Figure 4.1.3 Altered mitochondrial function in severe asthmatic fibroblasts.
(A) NHBF and DHBF were labelled with JC-1 dye for 10 minutes and cultured thereafter for 4 hours. Quantitative representation of JC-1 aggregate fluorescence in relative fluorescence units (RFU) normalized to NHBF and representative of two independent experiments with each condition performed in triplicate. *$p < 0.05$, determined using unpaired two-tailed Student t-test. **(B)** NHBF and DHBF were cultured in complete medium for up to 96 hours post serum-starvation. MTT reagent was added at the indicated time points and

spectrophotometric readings were taken after 3 hours of incubation. Quantitative representation of mitochondrial metabolic activity represented as percentage (%) of NHBF and representative of two independent experiments with each condition performed in triplicate. *$p < 0.05$, determined using unpaired two-tailed Student t-test. **(C)** NHBF and DHBF were cultured in complete medium for 96 hours post serum-starvation. To measure the mitochondrial superoxide production, the fibroblasts were stained with 5μM MitoSOX Red for 15 minutes and analyzed by flow cytometry. Quantitative representation of mitochondrial superoxide levels in mean fluorescence intensity (MFI) in NHBF and DHBF (left panel). The total hydrogen peroxide levels were also measured using the ROS-Glo H_2O_2 Assay. Quantitative representation of H_2O_2 levels in relative luminescence units (RLU) in NHBF and DHBF. (right panel). ****$p < 0.0001$, determined using unpaired two-tailed Student t-test. Graphical data are represented as mean ± SEM from at least 3 replicates.

4.1.4 Adaptive fibroblast persistence through increased AMPKα phosphorylation, SIRT1 and PGC1α expression in severe asthmatic fibroblasts

Since the S-As fibroblasts demonstrated enhanced mitophagy flux as a consequence of mitochondrial depolarization, we then sought to investigate the other mitochondrial QC mechanisms of mitochondrial dynamics and mitochondrial biogenesis. In the event of mitochondrial depolarization, the cellular ATP production is impeded resulting in lower cellular ATP levels. AMPK is an important energy sensor involved in cellular response to mitochondrial insult and energetic stress by regulating autophagy and promoting mitochondrial homeostasis (248). Therefore, we assessed the phosphorylation of AMPKα in S-As fibroblasts. Western blot analysis showed a notable amplification in AMPKα phosphorylation (p=0.08) in DHBF (Fig. 4.1.4A, left panel), which paralleled with a significant decrease in AMPKα levels in these cells when compared to NHBF (p=0.0031) (Fig. 4.1.4A, right panel).

AMPK activation functions to maintain cellular energy stores by enhancing mitochondrial biogenesis (249). Moreover, fibroblasts with mitochondrial defects are known to adapt to metabolic stress by altering their mitochondrial dynamics and biogenesis (250). The mitochondrial dynamics showed no remarkable differences between NHBF and DHBF (data shown in Appendix 9.4.2). However, mitochondrial biogenesis was significantly upregulated in DHBF as assessed by the expression of mitochondrial biogenesis markers, SIRT1 and PGC1α (Fig. 4.1.4B). This suggests that upon elimination of the defective mitochondria in S-As fibroblasts by mitophagy, the mitochondrial pool is replenished with new mitochondria through biogenesis (251). Therefore, we next measured the mitochondrial mass in these fibroblasts using ΔΨm-independent MitoTracker Green. MitoTracker Green staining quantifies the total mitochondrial content irrespective of ΔΨm. MitoTracker Green fluorescence was comparable between the two group of fibroblasts (Fig. 4.1.4C), which suggested efficient turnover of depolarized mitochondria in S-As fibroblasts.

In order to ensure turnover of defective mitochondria in S-As fibroblasts, we further measured cellular apoptosis and senescence in these fibroblasts by Annexin V and β-galactosidase staining, respectively. No induction of cellular apoptosis or senescence was detected in DHBF when compared to NHBF (Fig. 4.1.4D&E), indicating an adaptive survival mechanism in S-As fibroblasts through increased AMPKα phosphorylation, and SIRT1 and PGC1α activation. This adaptive response to mitochondrial depolarization restores the energy metabolism in S-As fibroblasts, thereby rescuing them from mitochondrial dysfunction and mitochondrial damage-induced cellular death and cellular senescence.

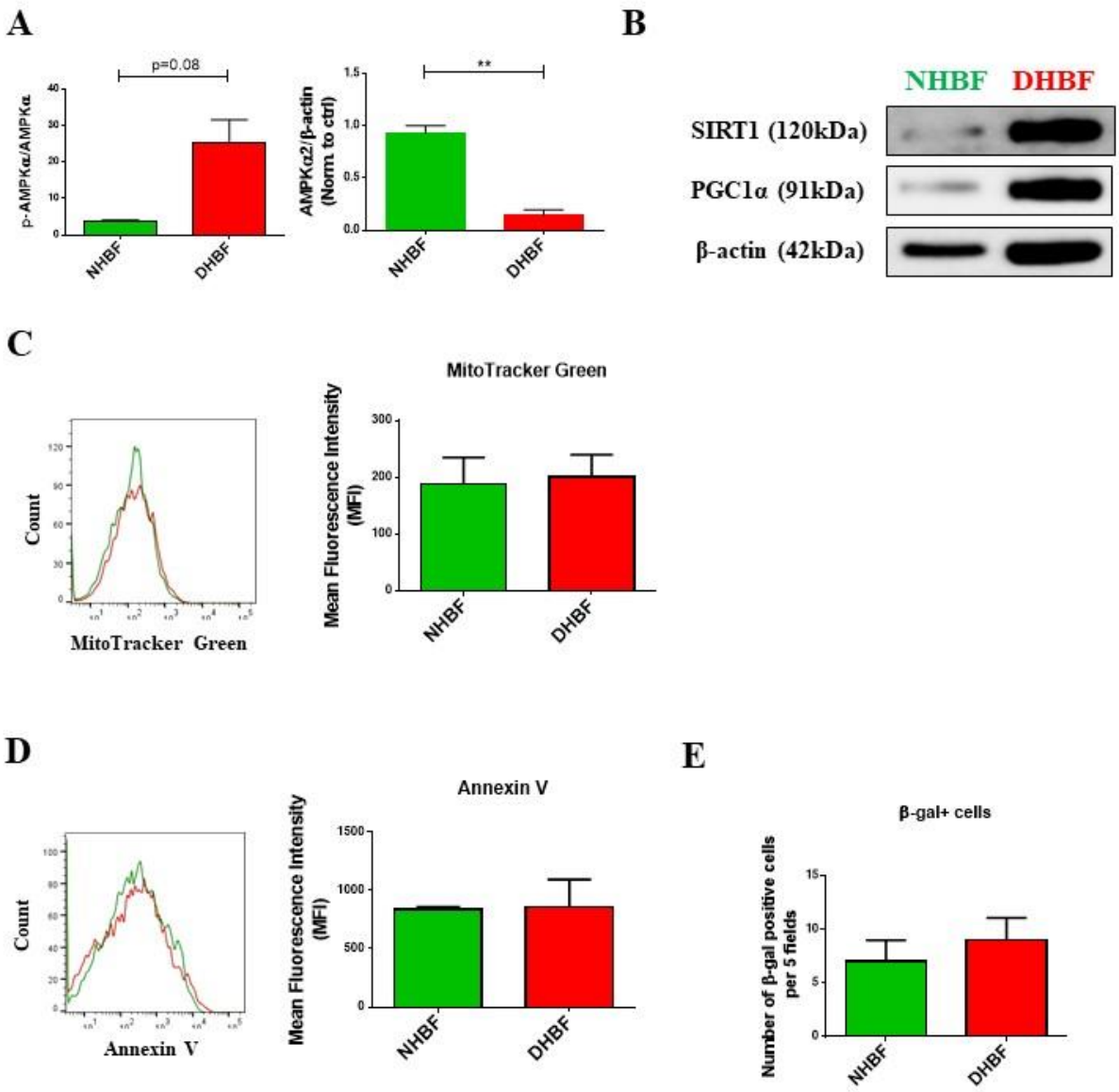

Figure 4.1.4 Adaptive fibroblast persistence through increased AMPKα phosphorylation, SIRT1 and PGC1α expression in severe asthmatic fibroblasts.

(A) NHBF and DHBF were cultured in DMEM complete medium for 24 hours post serum-starvation. Whole cell lysates were subjected to immunoblot analysis of AMPKα and p-AMPKα with β-actin used as loading control. Densitometric analysis of AMPKα phosphorylation in NHBF and DHBF represented as the ratio of p-AMPKα to AMPKα (left panel) and AMPKα levels normalized to NHBF (right panel). $^{**}p < 0.01$, determined by unpaired two-tailed Student t-test. (B) Representative immunoblots depicting protein levels of

SIRT1 and PGC1α with β-actin used as loading control. (C) NHBF and DHBF were cultured in DMEM complete medium for 96 hours post serum-starvation. The fibroblasts were then stained with 50nM MitoTracker Green for 30 minutes and analyzed by flow cytometry. Representative histogram and bar chart of MitoTracker Green fluorescence in NHBF and DHBF showing mitochondrial mass in mean fluorescence intensity (MFI). (D) NHBF and DHBF were cultured in DMEM complete medium for 48 hours post serum-starvation. Representative histogram and bar chart of the levels of Annexin-V positive fluorescence in MFI, and (E) the levels of β-galactosidase (β-gal) positive cells in a total of 5 microscopic fields in NHBF and DHBF. Graphical data are represented as mean ± SEM from at least 3 replicates.

4.1.5 Increased pro-fibrotic and pro-inflammatory signaling in severe asthmatic fibroblasts

In the presence of these mitochondrial alterations, we next wanted to determine the functional phenotype of these bronchial fibroblasts. Asthmatic airways are known to exhibit phenotypically different fibroblasts with a pro-fibrotic and pro-inflammatory profile depicted by the excessive secretion of ECM proteins, cytokines and chemokines when compared to non-asthmatics (81, 82, 105). We therefore, characterized their baseline expression of ECM proteins, including collagen types I, III and V (*COL1A1*, *COL3A1* and *COL5A1*) and fibronectin (*FN1*), cytokines, including *TGF-β1*, *IL-6* and *IL-11*, and chemokines, including *IL-8* and *GROα* (*CXCL1*), by qRT-PCR. The ECM proteins and pro-inflammatory chemokines were differentially expressed between NHBF and DHBF. At baseline, DHBF exhibited increased gene expression of *COL1A1* (p=0.0328), *COL3A1*, *COL5A1*, and *FN1*, albeit to a lesser extent, when compared to NHBF (Fig. 4.1.5A). Although the expression of cytokines *TGF-β1*, *IL-6* and *IL-11*, showed no differences between NHBF and DHBF (Fig. 4.1.5B), the chemokine expression of *IL-8* and *GROα* was higher in DHBF in comparison to NHBF, but they did not

reach statistical significance (Fig. 4.1.5C). Consistent with previous reports (82, 105), the S-As fibroblasts demonstrated a pro-fibrotic and pro-inflammatory profile. These fibroblasts were thus, observed to maintain the disease phenotype through several passages in culture as reported previously (240) providing a good *ex vivo* model to study severe asthma. Taken together, our results suggest that the heightened mitochondrial QC mechanisms of mitophagy and biogenesis promote a pro-fibrotic and pro-inflammatory phenotype in S-As fibroblasts.

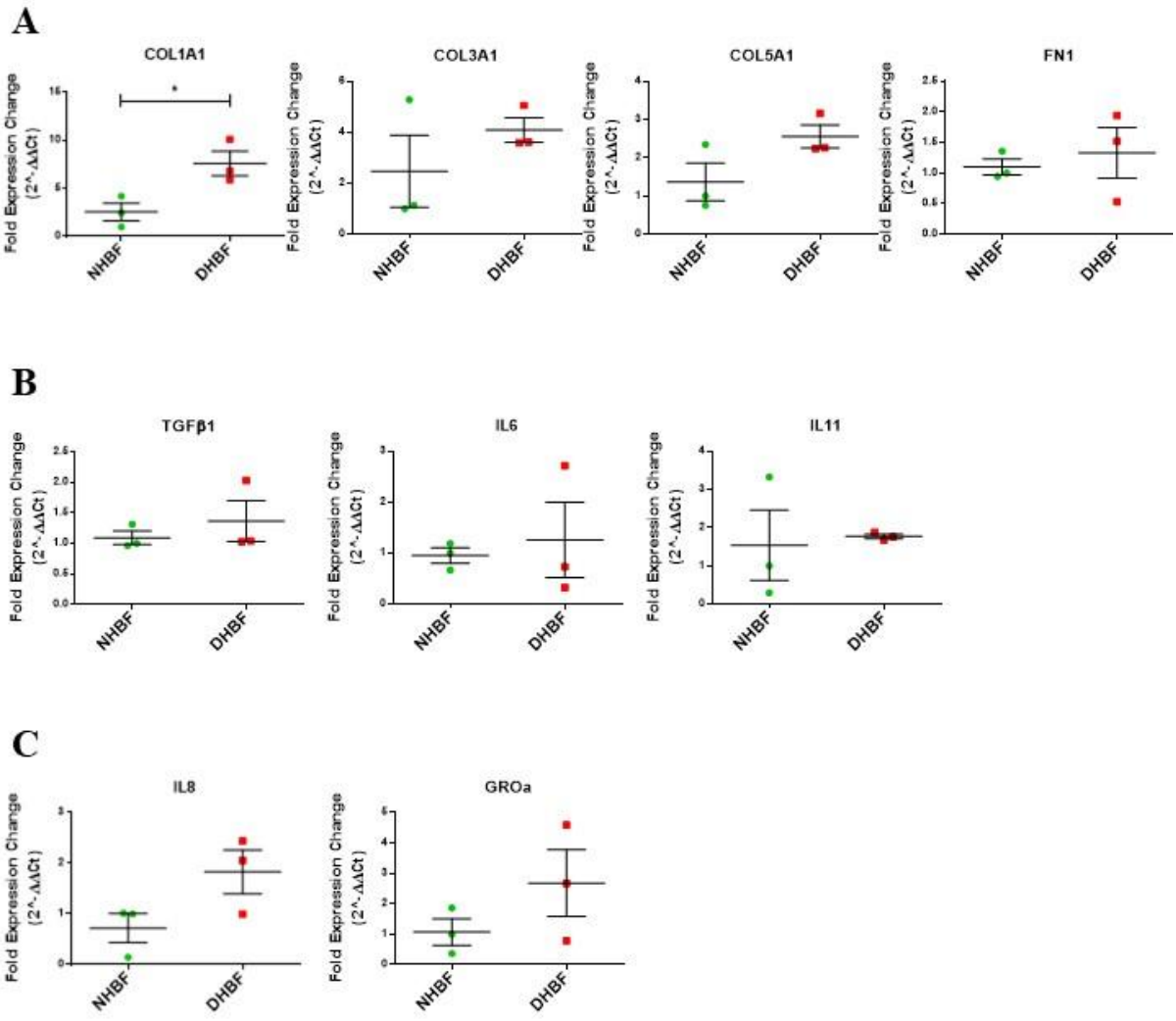

Figure 4.1.5 Increased pro-fibrotic and pro-inflammatory signaling in severe asthmatic fibroblasts.

NHBF and DHBF were cultured in DMEM complete medium for 2 hours post serum-starvation. Under basal conditions, mRNA expression of (A) ECM components COL1A1, COL3A1, COL5A1 and FN1, (B) cytokines TGF-β1, IL-6 and IL-11, and (C) chemokines IL-8 and GROα, in NHBF and DHBF was analyzed by qRT-PCR and expressed as fold expression change relative to NHBF post normalization to housekeeping gene 18s rRNA. Data are represented as mean ± SEM from at least 3 unique donors in each group. $*p < 0.05$, determined by unpaired two-tailed Student t-test.

4.2 Effects of asthma-related cytokines on mitochondrial phenotype in bronchial fibroblasts from severe asthma patients and non-asthmatic subjects

Severe asthmatic airways are characterized by the increased expression of several mediators of remodeling (252), including IL-17 (39), TGF-β1 (253) and IL-13 (254). Significant crosstalk exists between the T cells and airway structural cells through these cytokines linking the increased activity of these cytokines to the pathogenesis of severe asthma. We, therefore, aimed to determine the effects of these implicated cytokines on mitochondrial phenotype and subepithelial fibrosis.

4.2.1 IL-17 induced autophagy regulates mitochondrial dysfunction and fibrosis in non-asthmatic and severe asthmatic fibroblasts

Since IL-17 is strongly implicated in the pathogenesis of severe asthma (103), we first investigated the effects of IL-17 on mitochondrial function, and more importantly whether this axis affects fibrosis in severe asthma. Here, we inspected the putative link between autophagy and IL-17A induced mitochondrial dysfunction and fibrosis in non-asthmatic and S-As fibroblasts. IL-17A will henceforth be referred to as IL-17 in the rest of this study.

4.2.1.1 IL-17 stimulation induced mitochondrial dysfunction in bronchial fibroblasts

In order to investigate the effects of IL-17 on mitochondrial mass and function, we stimulated the bronchial fibroblasts with IL-17 at a concentration of 25ng/ml, that was previously reported to activate inflammatory and remodeling responses in bronchial fibroblasts (255). NHBF and DHBF were cultured either in DMEM complete medium or DMEM supplemented with IL-17 for a duration of 96 hours in order to assess the long-term effect of IL-17 on these fibroblasts.

Since IL-17 induced mitochondrial dysfunction was found to be associated with mitochondrial depolarization and dysfunctional mitochondrial respiration in rheumatoid arthritis synovial fibroblasts (256), we assessed whether IL-17 altered the mitochondrial quantity and quality in bronchial fibroblasts using ΔΨm-independent MitoTracker Green and ΔΨm-dependent MitoTracker Red, respectively. MitoTracker Green and Red staining showed a trend of declining fluorescence in NHBF with IL-17 treatment (Fig. 4.2.1.1A&B), where their normalized fluorescence to untreated controls decreased from 1 to 0.85 and 0.77, respectively. However, IL-17 significantly attenuated mitochondrial mass and ΔΨm in DHBF when compared to untreated cells (Fig. 4.2.1.1A&B). In DHBF, IL-17 treatment resulted in a drop in MitoTracker Green and MitoTracker Red fluorescence normalized to untreated controls from 1 to 0.79 and 0.63 respectively, indicating a reduction in the number and functionality of mitochondria in these cells. IL-17 thus, alters the mitochondrial network in both NHBF and DHBF, with an overall loss of mitochondrial mass and increasing the fraction of dysfunctional mitochondria. These data suggest that IL-17 is a key pathological cytokine that induces mitochondrial dysfunction in healthy bronchial fibroblasts and intensifies pre-existing mitochondrial damage in S-As fibroblasts, as was shown in Fig. 4.1.3.

Given that mitochondrial damage is closely related to cell death (257, 258), we next studied mitochondrial damage-mediated cell apoptosis by using Annexin V staining to detect apoptotic cells. Flow cytometric analysis showed a significant decline in Annexin V staining with IL-17 treatment in both NHBF and DHBF (Fig. 4.2.1.1C), which suggested that IL-17 protected these fibroblasts from mitochondrial damage-mediated apoptosis. Western blot analysis further indicated that IL-17 increased the expression of survivin, an anti-apoptotic protein, in both

NHBF and DHBF (Fig. 4.2.1.1D). Taken together, these findings suggest that IL-17 induced mitochondrial dysfunction may be associated with increased survival of bronchial fibroblasts.

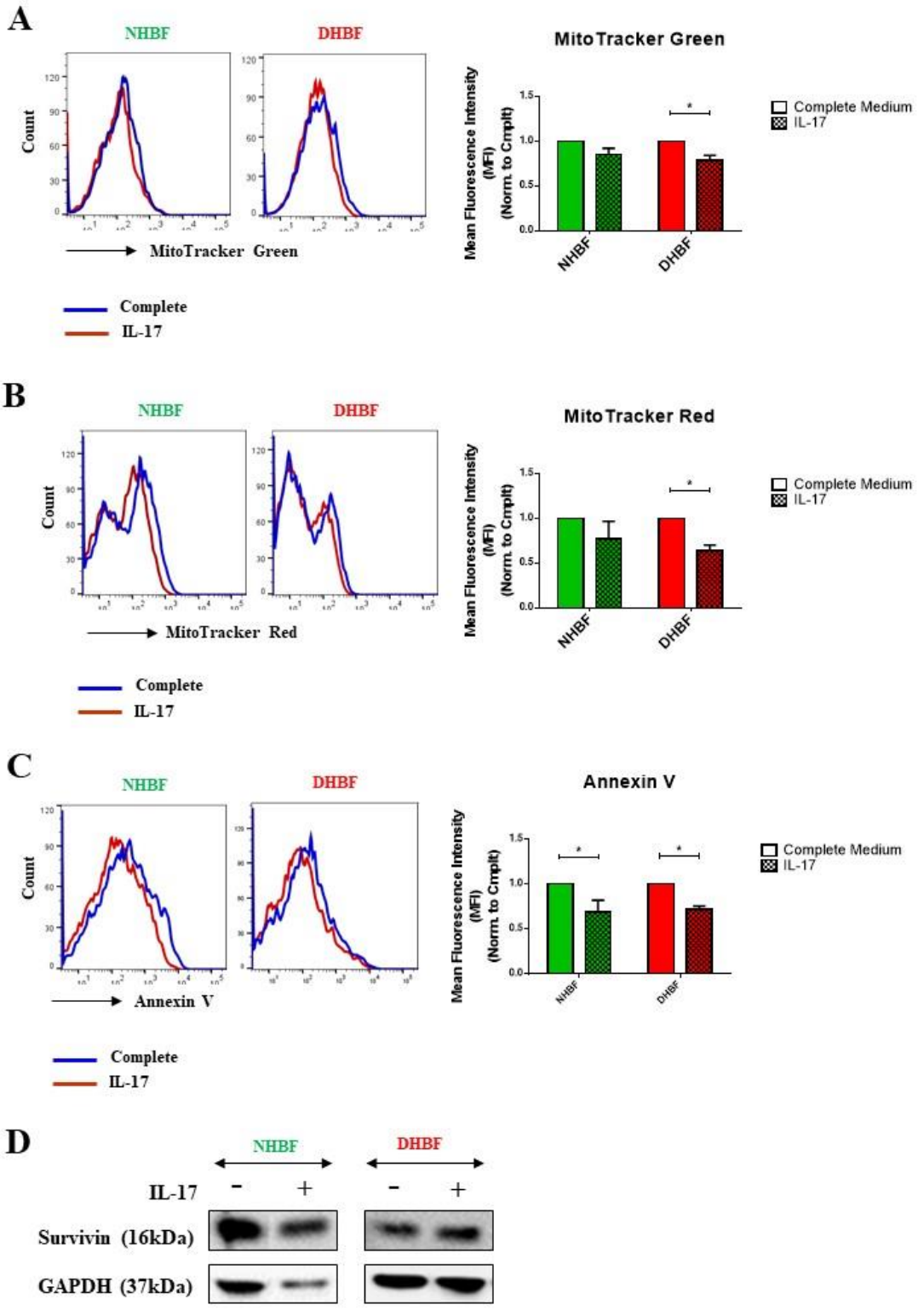

Figure 4.2.1.1 IL-17 stimulation induced mitochondrial dysfunction in non-asthmatic and severe asthmatic fibroblasts.

NHBF and DHBF were serum-starved for 24 hours and thereafter, cultured in DMEM complete medium without or with IL-17 (25ng/ml) for 96 hours. **(A)** Representative histogram and bar chart of fibroblasts stained with 50nM MitoTracker Green, **(B)** 50nM MitoTracker Red, and **(C)** Annexin V followed by flow cytometric analysis. 10,000 events were analyzed in each flow cytometry experiment. Data representative of n=3 repeats. **(D)** Representative immunoblots depicting the effect of IL-17 on the expression of anti-apoptotic protein, Survivin, in NHBF (left panel) and DHBF (right panel). GAPDH was used as loading control. Data presented as mean ± SEM after normalization to the respective untreated control (Complete Medium). * $p<0.05$, statistical significance assessed by 2-way ANOVA with Sidak's multiple comparison tests.

4.2.1.2 IL-17 impaired the balance of mitochondrial quality control mechanisms in bronchial fibroblasts

To study the effects of IL-17 on the mitochondrial QC mechanisms in bronchial fibroblasts, we cultured NHBF and DHBF in the absence or presence of IL-17 for a duration of 48 and 96 hours for mRNA and protein analyses, respectively. We then assessed the mRNA expression of key autophagy genes, including *BECN1*, *ATG5*, *LC3B, SQSTM1* and *LAMP2* by qRT-PCR. Although NHBF exhibited no difference in their autophagy gene signature upon IL-17 treatment, IL-17 increased *SQSTM1* expression alone in NHBF (Fig. 4.2.1.2A). However, the autophagy gene signature was significantly upregulated by IL-17 in DHBF (Fig. 4.2.1.2A). Western blot analysis further showed that IL-17 boosted LC3B lipidation and p62 levels in both NHBF and DHBF (Fig. 4.2.1.2B). LC3BII/LC3BI ratio was increased from 1.14 to 1.45 in NHBF, and from 1.76 to 2.21 in DHBF. Taking into consideration that autophagy levels were elevated at baseline in S-As fibroblasts (Fig. 4.1.1), the increase in autophagy markers, both at

the mRNA and protein levels, suggest that IL-17 further upregulated autophagy in these fibroblasts.

We next determined the direct effects of IL-17 on mitophagy and biogenesis markers in bronchial fibroblasts. In NHBF, the expression of PINK1 and Parkin appeared to be increased by IL-17 (Fig. 4.2.1.2C). However, this was not accompanied by a corresponding increase in SIRT1 and PGC1α expression. In contrast, a decline in SIRT1 and PGC1α expression was noted in NHBF (Fig. 4.2.1.2D). IL-17 thus, contributed to increased mitophagy and decreased biogenesis in non-asthmatic fibroblasts. Surprisingly, IL-17 stimulation led to a reduction in PINK1 and Parkin expression (Fig. 4.2.1.2C) together with a significant drop in SIRT1 and PGC1α levels in DHBF (Fig. 4.2.1.2D). Considering the intrinsic mitochondrial damage in S-As fibroblasts, the IL-17 induced simultaneous reduction in mitophagy, and biogenesis reinforces the manifestation of mitochondrial dysfunction in S-As fibroblasts. These results suggest that chronic exposure to IL-17 leads to an increase in autophagy particularly in S-As fibroblasts but disrupts the balance between mitophagy and mitochondrial biogenesis leading to impairment in the mitochondrial QC machinery in bronchial fibroblasts. This failure in the QC machinery can further amplify the mitochondrial dysfunction induced by IL-17.

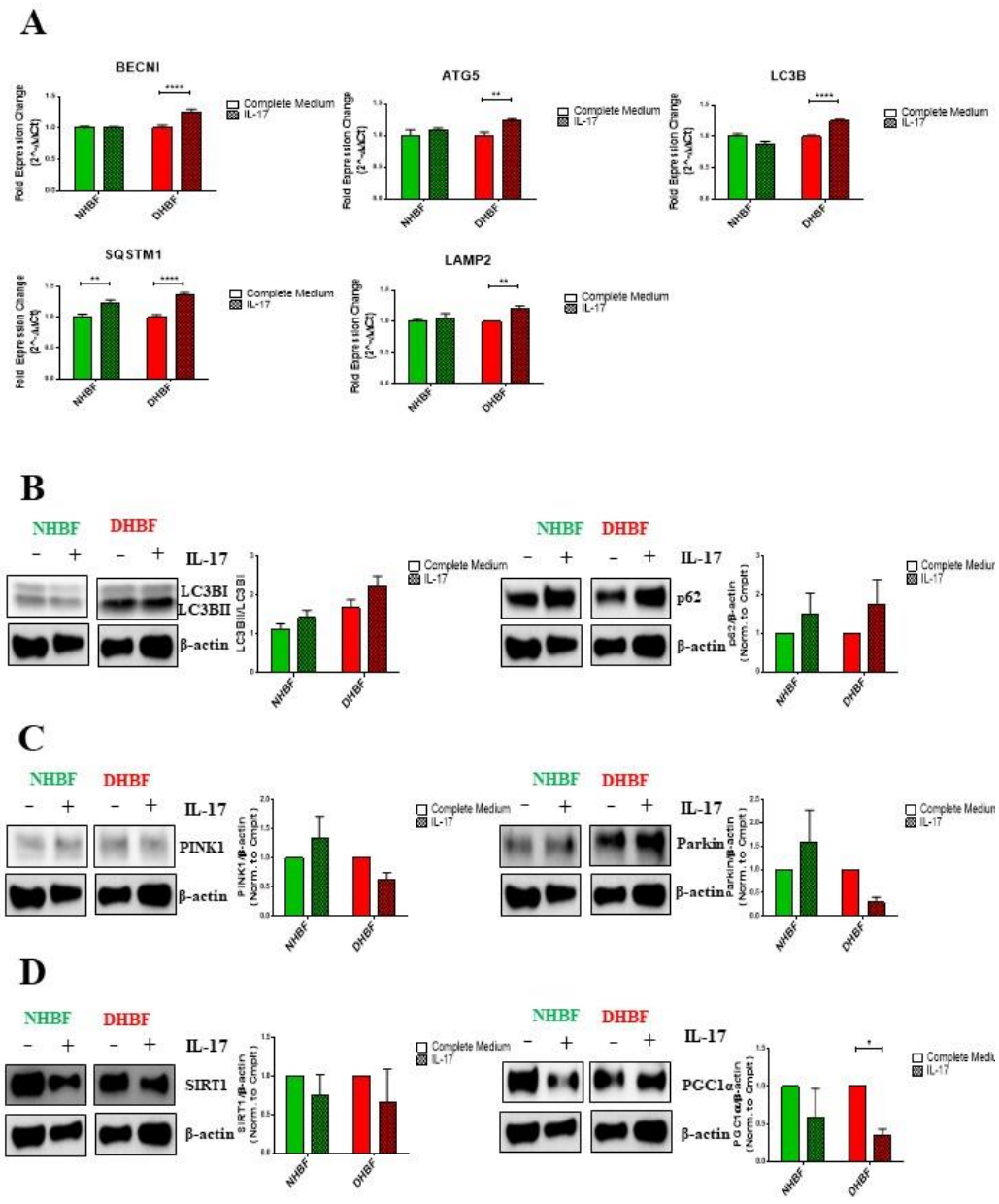

Figure 4.2.1.2 IL-17 impaired the balance of mitochondrial quality control mechanisms in bronchial fibroblasts.

NHBF and DHBF were serum-starved for 24 hours and thereafter, cultured in DMEM complete medium without or with IL-17 (25ng/ml) for 48 hours for mRNA analysis and 96 hours for protein analysis. **(A)** Effect of IL-17 on mRNA expression of autophagy genes, BECN1, ATG5, LC3B, SQSTM1 and LAMP2 in NHBF and DHBF was analyzed by qPCR and expressed as fold expression change relative to the respective untreated control post

normalization to housekeeping gene 18s rRNA. Data representative of n=3. **(B)** Representative immunoblots and densitometric analysis of autophagy markers, LC3B lipidation represented as the ratio of LC3BII to LC3BI (left panel) and p62 expression (right panel), **(C)** mitophagy markers, PINK1 (left panel) and Parkin (right panel), and **(D)** mitochondrial biogenesis markers, SIRT1 (left panel) and PGC1α (right panel), in NHBF and DHBF in response to IL-17. Data representative of two independent experiments with n=3 subjects in each group. β-actin was used as loading control. Data presented as mean ± SEM after normalization to the respective untreated control (Complete Medium). * $p<0.05$, ** $p<0.01$, **** $p<0.0001$, statistical significance assessed by 2-way ANOVA with Sidak's multiple comparison tests.

4.2.1.3 IL-17 induced mitochondrial dysfunction triggered by autophagy in bronchial fibroblasts

The enhanced levels of autophagy in S-As fibroblasts was further elevated in response to IL-17. In order to study further the role of autophagy in IL-17 induced mitochondrial dysfunction, we pharmacologically targeted autophagy in bronchial fibroblasts. We used the following pharmacological agents to modulate autophagy – rapamycin to induce autophagy, 3-MA to block autophagosomal formation, and Baf-A1 to block autophagosomal fusion with lysosomes. The effects of rapamycin and 3-MA on these bronchial fibroblasts are addressed in Appendix 9.4.3.

Since Baf-A1 blocks autolysosomal formation, it causes the accumulation of autophagosomal vacuoles, which can be confirmed by the increased abundance of LC3BII and p62 in cells treated with Baf-A1. After serum-starvation, the bronchial fibroblasts were pre-treated with Baf-A1 at 10nM for 4 hours and then stimulated with IL-17 for up to 48 hours for mRNA and up to 96 hours for protein analyses. NHBF and DHBF were further incubated with 10μM of FCCP in the final 2 hours of treatment to induce mitochondrial uncoupling and to serve as a positive control for mitophagy (259). FCCP treatment resulted in increased *BECNI* gene expression (Fig.

4.2.1.3A) and increased levels of LC3BII and p62 proteins (Fig. 4.2.1.3B) in NHBF, indicating activation of the autophagy machinery upon mitochondrial uncoupling. Increased *PINK1* and *PRKN* gene expression was induced by FCCP in NHBF (Fig. 4.2.1.3C&D), in agreement with the fact that FCCP induced mitochondrial uncoupling signals the removal of damaged mitochondria by increasing mitophagy. NHBF demonstrated a quick response to FCCP treatment within 2 hours. Baf-A1 significantly decreased *BECN1* gene expression (Fig. 4.2.1.3A) and increased LC3B and p62 accumulation (Fig. 4.2.1.3B) in NHBF, indicating successful inhibition of autophagy flux in NHBF. Baf-A1 treatment also suppressed mitophagy in NHBF as reduced *PINK1* and *PRKN* gene expression was observed (Fig. 4.2.1.3C&D). Stimulation with IL-17 marginally increased the abundance of LC3BII and p62 in NHBF compared to time-matched untreated controls (Fig. 4.2.1.3B). However, *PINK1* and *PRKN* gene expression was not affected by IL-17 in NHBF (Fig. 4.2.1.3C&D). Co-treatment with IL-17 and Baf-A1 reduced the *PINK1* and *PRKN* gene expression to the lowest levels when compared to untreated controls (Fig. 4.2.1.3C&D). Thus, blocking autophagy using Baf-A1 appears to reduce the trigger for mitophagy in non-asthmatic fibroblasts and more significantly in the presence of IL-17.

In DHBF, FCCP induced LC3BII and p62 expression (Fig. 4.2.1.3B). However, *PINK1* and *PRKN* gene expression was not affected by FCCP (Fig. 4.2.1.3C&D), possibly due to the presence of depolarized mitochondria at baseline in DHBF. Baf-A1 increased LC3B and p62 accumulation (Fig. 4.2.1.3B) in DHBF, indicating successful inhibition of autophagy flux in DHBF as well. IL-17 induced activation of autophagy in DHBF as observed by elevated *BECN1* gene expression (Fig. 4.2.1.3A) and buildup of LC3BII and p62 proteins (Fig. 4.2.1.3B) upon IL-17 treatment. A significant increase in *PINK1* (1.3-fold) and *PRKN* (1.28-fold) gene

expression (Fig. 4.2.1.3C&D) by IL-17 was also noted in these fibroblasts, which suggested that IL-17 induced mitochondrial damage in DHBF signaling their detection and increased tagging by PINK1 and Parkin. Interestingly, co-treatment with IL-17 and Baf-A1 reversed the IL-17 mediated changes in *PINK1* and *PRKN* mRNA levels (Fig. 4.2.1.3C&D) in DHBF, indicating that IL-17 induced mitochondrial dysfunction in S-As fibroblasts is regulated by autophagy. Blocking autophagy reduced the expression of *PINK1* and *PRKN*, indirectly suggesting an improvement in mitochondrial health resulting in a reduced demand for PINK1/Parkin-mediated mitophagy.

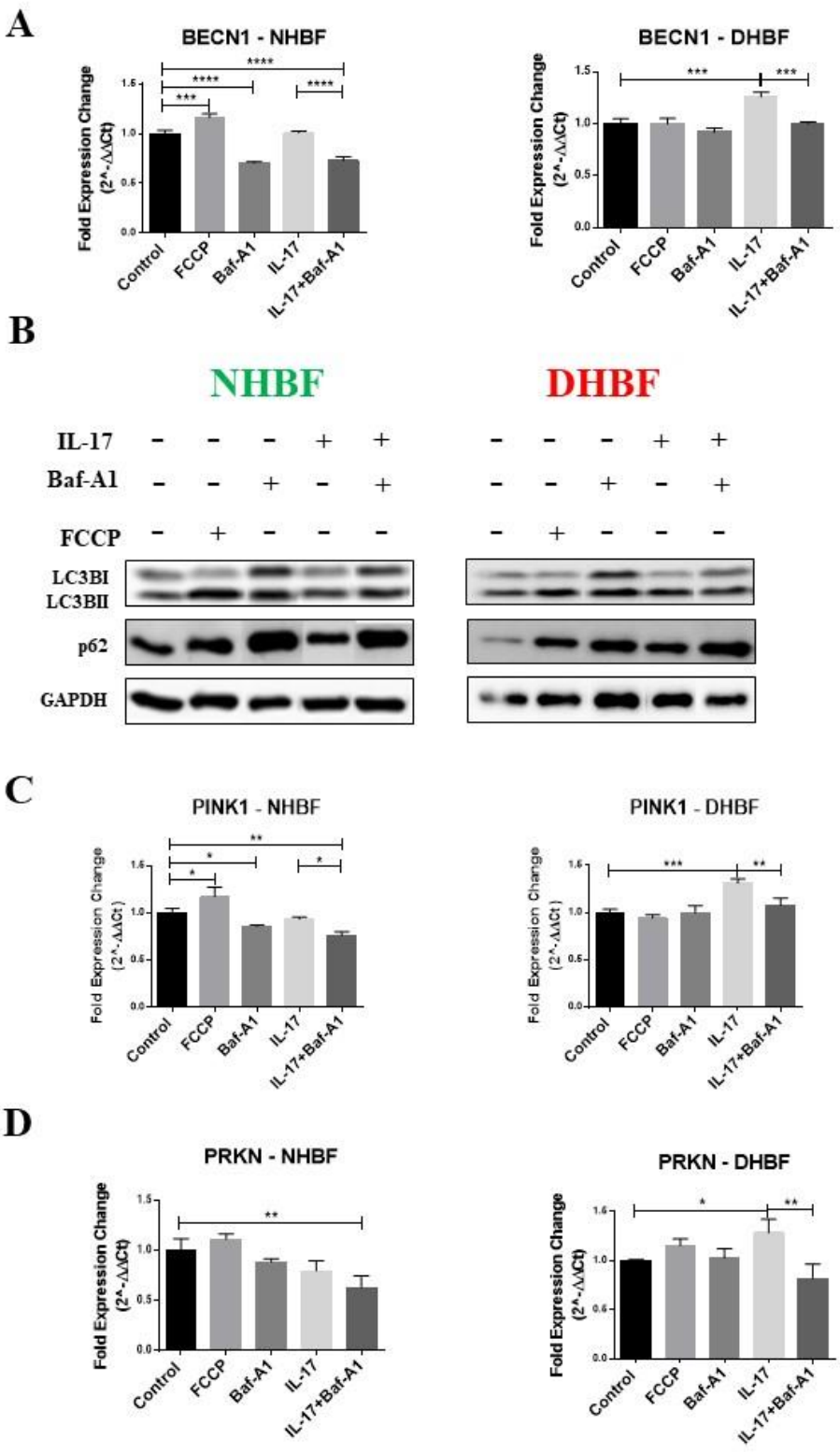
A
BECN1 - NHBF
Fold Expression Change (2^-ΔΔCt)
Control
FCCP
Baf-A1
IL-17
IL-17+Baf-A1
BECN1 - DHBF
B
NHBF
DHBF
IL-17
Baf-A1
FCCP
LC3BI
LC3BII
p62
GAPDH
C
PINK1 - NHBF
PINK1 - DHBF
D
PRKN - NHBF
PRKN - DHBF

Figure 4.2.1.3 IL-17 induced mitochondrial dysfunction triggered by autophagy in bronchial fibroblasts.

NHBF and DHBF were serum-starved for 24 hours, pre-treated with Bafilomycin-A1 (Baf-A1) (10nM) for 4 hours and thereafter, cultured in DMEM complete medium without or with IL-17 (25ng/ml) for 48 hours for mRNA analysis and 96 hours for protein analysis. The cells were co-incubated with FCCP (10μM) in the final 2 hours of treatment. **(A)** mRNA expression of autophagy gene, BECN1, in NHBF (left panel) and DHBF (right panel) was analyzed by qPCR and expressed as fold expression change relative to the respective untreated control post normalization to housekeeping gene 18s rRNA. Data representative of n=3. **(B)** Representative immunoblots depicting expression of autophagy markers, LC3B and p62 in NHBF (left panel) and DHBF (right panel) with the indicated treatments. GAPDH was used as loading control. **(C)** mRNA expression of PINK1 and **(D)** Parkin in NHBF (left panel) and DHBF (right panel) was analyzed by qPCR and expressed as fold expression change relative to the respective untreated control post normalization to housekeeping gene 18s rRNA. Data representative of n=3. Data presented as mean ± SEM after normalization to untreated control. * $p<0.05$, ** $p<0.01$, *** $p<0.001$, **** $p<0.0001$, statistical significance assessed by 1-way ANOVA with Tukey's multiple comparison tests.

4.2.1.4 IL-17 induced pro-fibrotic phenotype triggered by autophagy in bronchial fibroblasts

To ascertain the impact of IL-17 on the progression of subepithelial fibrosis, NHBF and DHBF were stimulated with IL-17 for 48 hours. Asthmatic airways are characterized by the increased deposition of collagen fibers of types I, III and V as well as fibronectin, in addition to myofibroblast differentiation of airway fibroblasts (102, 260, 261). We, therefore, determined the effect of IL-17 on the expression of key fibrotic genes, including *COL1A1*, *COL3A1*, *COL5A1*, *FN1* and *ACTA2* (α-SMA), by qRT-PCR.

IL-17 stimulation enabled a strong induction of fibrogenic signals in both non-asthmatic and S-As fibroblasts but with a greater impact on S-As fibroblasts. In NHBF, IL-17 significantly

upregulated the expression of *COL1A1*, *COL3A1* and *FN1* as compared to untreated time-matched controls (Fig. 4.2.1.4A). IL-17 demonstrated a stronger effect on DHBF, where IL-17 increased the transcriptional levels of *COL1A1* (1.3-fold), *COL3A1* (1.6-fold), *COL5A1* (1.3-fold) and *FN1* (1.2-fold). The gene expression of *ACTA2* was also induced by IL-17 in DHBF when compared to NHBF (Fig. 4.2.1.4A) but it did not reach statistical significance. The significant increase in pro-fibrotic gene expression observed at mRNA levels in NHBF and DHBF, suggests that IL-17 induced a potent fibrotic response in non-asthmatic and S-As bronchial fibroblasts. Chronic exposure to IL-17 thus, promotes the development of subepithelial fibrosis in normal airways and intensifies the fibrotic damage in S-As airways.

Next, we aimed to investigate whether there was an association between autophagy and IL-17 induced fibrogenesis in bronchial fibroblasts. We evaluated whether the expression of fibrotic genes, *COL1A1*, *COL3A1*, *COL5A1*, *FN1* and *ACTA2* (α-SMA), in bronchial fibroblasts is affected by autophagy by inhibiting autophagy flux using Baf-A1. As shown in Figs. 4.2.1.4B-F, blocking basal autophagy levels using Baf-A1 significantly decreased the expression of *COL1A1*, *COL3A1*, *FN1* and *ACTA2* in NHBF, and *COL1A1*, *COL3A1* and *ACTA2* in DHBF. Interestingly, co-treatment with IL-17 and Baf-A1 reversed the IL-17 induced increase in *COL1A1*, *COL3A1*, *COL5A1*, *FN1* and *ACTA2* in NHBF, and *COL1A1*, *COL3A1* and *ACTA2* in DHBF compared to their respective untreated controls. Together, these findings suggest that IL-17 is a potent inducer of pro-fibrotic phenotype through autophagy induction in bronchial fibroblasts.

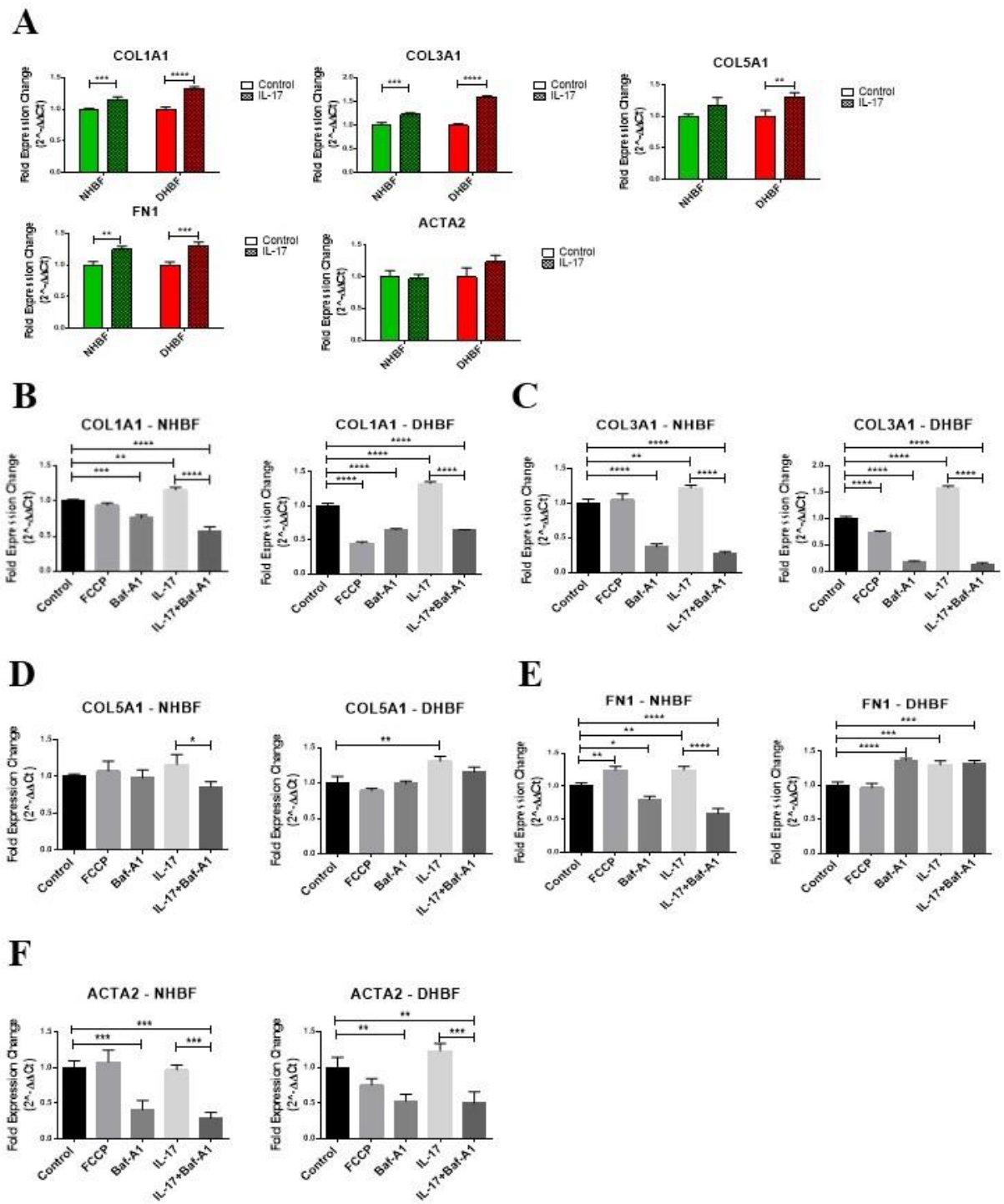
A
COL1A1
COL3A1
COL5A1
FN1
ACTA2
Control
IL-17
NHBF
DHBF
B
COL1A1 - NHBF
COL1A1 - DHBF
C
COL3A1 - NHBF
COL3A1 - DHBF
D
COL5A1 - NHBF
COL5A1 - DHBF
E
FN1 - NHBF
FN1 - DHBF
F
ACTA2 - NHBF
ACTA2 - DHBF
Control
FCCP
Baf-A1
IL-17
IL-17+Baf-A1

Figure 4.2.1.4 IL-17 induced pro-fibrotic phenotype triggered by autophagy in bronchial fibroblasts.

NHBF and DHBF were serum-starved for 24 hours, pre-treated with Bafilomycin-A1 (10nM) for 4 hours and thereafter, cultured in DMEM complete medium without or with IL-17 (25ng/ml) for 48 hours. **(A)** Effect of IL-17 on mRNA expression of fibrotic genes, COL1A1, COL3A1, COL5A1, FN1 and ACTA2 in NHBF and DHBF was analyzed by qPCR and expressed as fold expression change relative to the respective untreated control post normalization to housekeeping gene 18s rRNA. Data representative of n=3. mRNA expression of fibrotic genes, **(B)** COL1A1, **(C)** COL3A1, **(D)** COL5A1, **(E)** FN1, and **(F)** ACTA2, in NHBF (left panel) and DHBF (right panel) in response to Baf-A1 and IL-17 was analyzed by qPCR and expressed as fold expression change relative to the untreated control post normalization to housekeeping gene 18s rRNA. Data representative of n=3. Data presented as mean ± SEM after normalization to untreated control. * $p<0.05$, ** $p<0.01$, *** $p<0.001$, **** $p<0.0001$, statistical significance assessed by 1-way ANOVA with Tukey's multiple comparison tests.

4.2.2 Asthma-related cytokines alter mitochondrial bioenergetics in non-asthmatic and severe asthmatic fibroblasts

In severe asthma, the chronic exposure of airway fibroblasts to the various pleiotropic cytokines in the airway microenvironment induces phenotypic changes and activation of these fibroblasts, that is also accompanied by increased energy utilization. Since asthma-related cytokines, IL-17, TGF-β1 and IL-13, have been implicated in mitochondrial dysfunction (256, 262), we next investigated their effects on the regulation of mitochondrial bioenergetics in bronchial fibroblasts as their energetic profile is not very well described. Post serum-starvation, NHBF and DHBF were cultured separately in the presence of cytokines TGF-β1, IL-17 and IL-13, at concentrations of 10ng/ml, 25ng/ml and 10ng/ml respectively, for 96 hours. Considering the long-term culture conditions, the treatments were refreshed after 48 hours and overnight

treatment with 10μM FCCP at 72 hours was used as positive control. FCCP accelerated the decay of ΔΨm and as a result, decreased the JC-1 ratio in both NHBF and DHBF (Fig. 4.2.2A). Mitochondrial depolarization was also detected in both groups of fibroblasts with exposure to TGF-β1, IL-17 and IL-13, when compared to their respective time-matched untreated controls, but it did not reach statistical significance (Fig. 4.2.2A). These results suggest that cytokine-dependent activation of bronchial fibroblasts may be accompanied by mitochondrial depolarization which may lead to the manifestation of mitochondrial dysfunction, especially in S-As fibroblasts with pre-existing mitochondrial damage.

Since mitochondrial ROS and depolarization are functionally coupled, we next measured the ROS levels using the ROS-Glo H_2O_2 bioluminescent assay. TGF-β1, IL-17 and IL-13 significantly altered the ROS levels in both NHBF and DHBF by producing a significant drop in the bioluminescent signal (Fig. 4.2.2B). IL-17 and IL-13 treatments appeared to reduce the ROS levels to a greater extent than TGF-β1 treatment across both group of fibroblasts. Interestingly, similar ROS profiles were observed in NHBF and DHBF with exposure to these cytokines.

The crosstalk between mitochondrial depolarization and ROS potentiates apoptosis and thus, regulates cell viability (263). While ROS accumulation is known to potentiate cell death (264), we hypothesized that the drastic reduction in ROS levels when exposed to cytokines maintains ROS at optimal levels to boost redox signaling and thus, improve cell viability. We, therefore, assessed cell viability using the CellTiter-Glo bioluminescent assay. Mitochondrial uncoupler FCCP that depolarized ΔΨm enhanced cell viability, although to a significantly greater extent in DHBF (Fig. 4.2.2C). This suggested that mitochondrial depolarization and subsequent dysfunction favors persistence of these fibroblasts, a typical feature of subepithelial fibrosis in

severe asthma. Additionally, TGF-β1, IL-17 and IL-13, boosted cell viability in both group of fibroblasts but to varying extents (Fig. 4.2.2C). TGF-β1, IL-17 and IL-13 stimulation induced a 3.8-fold, 3.3-fold and 1.9-fold increase respectively in NHBF, while a 5.6-fold, 5-fold and 3.1-fold respective increase was detected in DHBF, indicating these cytokines to have a more profound effect on S-As fibroblasts when compared to their healthy counterparts. Taken together, these results suggest that pro-fibrotic, Th17 and Th2 cytokines in the airway microenvironment significantly regulate the mitochondrial bioenergetics in bronchial fibroblasts.

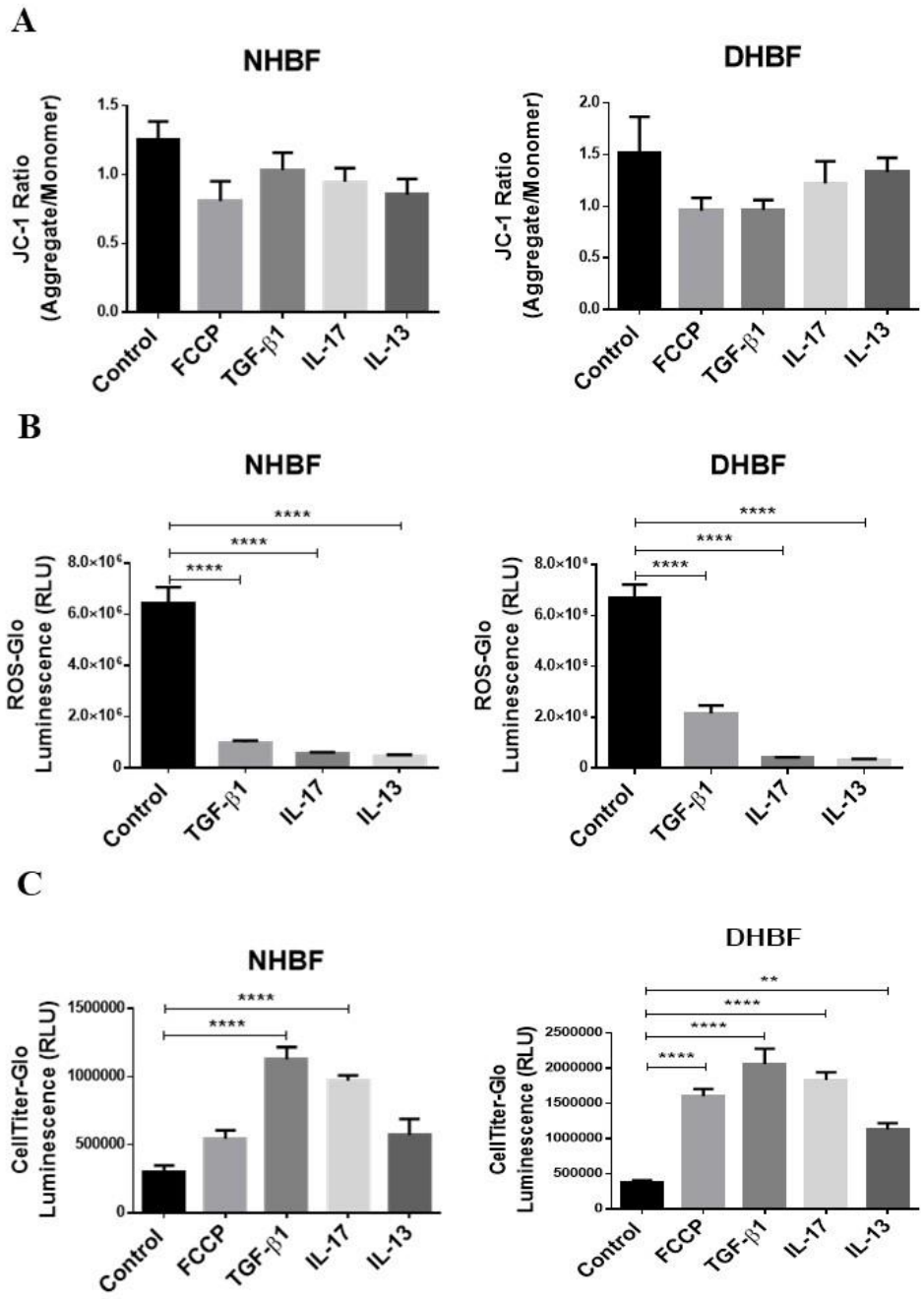

Figure 4.2.2 Asthma-related cytokines alter mitochondrial bioenergetics in non-asthmatic and severe asthmatic fibroblasts.

NHBF and DHBF were serum-starved for 24 hours and thereafter, cultured in DMEM complete medium without or with TGF-β1 (10ng/ml), IL-17 (25ng/ml) or IL-13 (10ng/ml) for 96 hours. The cells were co-incubated with FCCP (10μM) in the final 2 hours of treatment. **(A)** To measure mitochondrial membrane potential, the fibroblasts were thereafter, labelled with JC-1

dye for 10 minutes at 37°C . JC-1 aggregate and monomer fluorescence was then measured using a fluorescence plate reader. Data presented as JC-1 ratio of aggregate to monomer fluorescence. Data representative of two independent experiments with each condition performed in triplicate. **(B)** The ROS levels were measured using the ROS-Glo H_2O_2 Assay and **(C)** the cellular viability using CellTiter-Glo Luminescent Cell Viability Assay. The measurements were taken using a luminescence plate reader. Data presented as relative luminescence units (RLU) and representative of n=3 readings. Data presented as mean ± SEM after subtracting the background. ** $p<0.01$, **** $p<0.0001$, statistical significance assessed by 1-way ANOVA with Tukey's multiple comparison tests.

4.2.3 Assessment of mitochondrial health in bronchial biopsy tissues and PBMCs from severe asthma patients and non-asthmatic subjects

PINK1 is fundamental to mitochondrial homeostasis and serves as a sensor of mitochondrial damage (265). In order to validate our findings so far on mitochondrial health in bronchial fibroblasts, we next assessed PINK1 immunoreactivity within bronchial mucosa from a cohort of 6 patients with severe asthma and 2 non-asthmatic control subjects using immunohistochemistry. While the control group showed low PINK1 expression levels (negative or weak staining) in the mucosal and submucosal layers, high PINK1 immunoreactivity (moderate to strong staining) was detected in the bronchial epithelium as well as in fibroblasts of four out of the six (66.67%) severe asthmatic patient biopsies (Fig. 4.2.3A). PINK1 immunoreactivity in the airway submucosa was higher in severe asthma when compared to control, further confirming our observations of mitochondrial dysfunction in S-As fibroblasts.

Since the autophagy and mitochondrial QC markers were differentially expressed in airway structural fibroblasts, we questioned if this characteristic profile was reflected in the blood immune cells. We, therefore, analyzed their gene expression in peripheral blood mononuclear

cells (PBMCs) from 10 healthy subjects, and 11 asthmatics each with non-severe (mild and moderate asthma) and severe disease. The PBMCs were isolated from these study subjects and qRT-PCR was performed to analyze the mRNA levels of autophagy markers, *ATG5*, *LC3B*, *SQSTM1* and *LAMP2*, mitophagy markers, *PINK1* and *PRKN*, and biogenesis markers, *SIRT1* and *PGC1α*.

Interestingly, all selected markers showed the same pattern of expression in non-severe and severe asthma cases relative to the control. The autophagy, mitophagy and biogenesis gene signatures in PBMCs from S-As patients were significantly downregulated when compared to that in non-severe asthma and also lower than the expression in control (Fig. 4.2.3B). The PBMCs from non-severe asthma showed an increased trend in expression of these markers relative to control but was not statistically significant. However, those from severe asthma exhibited a significant drop in expression. Thus, the gene expression data clearly suggested that the gene expression of these markers increased in the early stages of asthma (mild-to-moderate asthma). However, their expression drastically reduced with disease severity. The mRNA expression of these markers in S-As PBMCs contrasted with their expression in S-As fibroblasts. Taken together, these findings suggest that the autophagy and mitochondrial QC profiles in peripheral blood cells are distinct from the structural lung cells, emphasizing the cell-specific behavior of autophagy and mitochondrial pathways depending on the varying cellular contribution to airway structure and function.

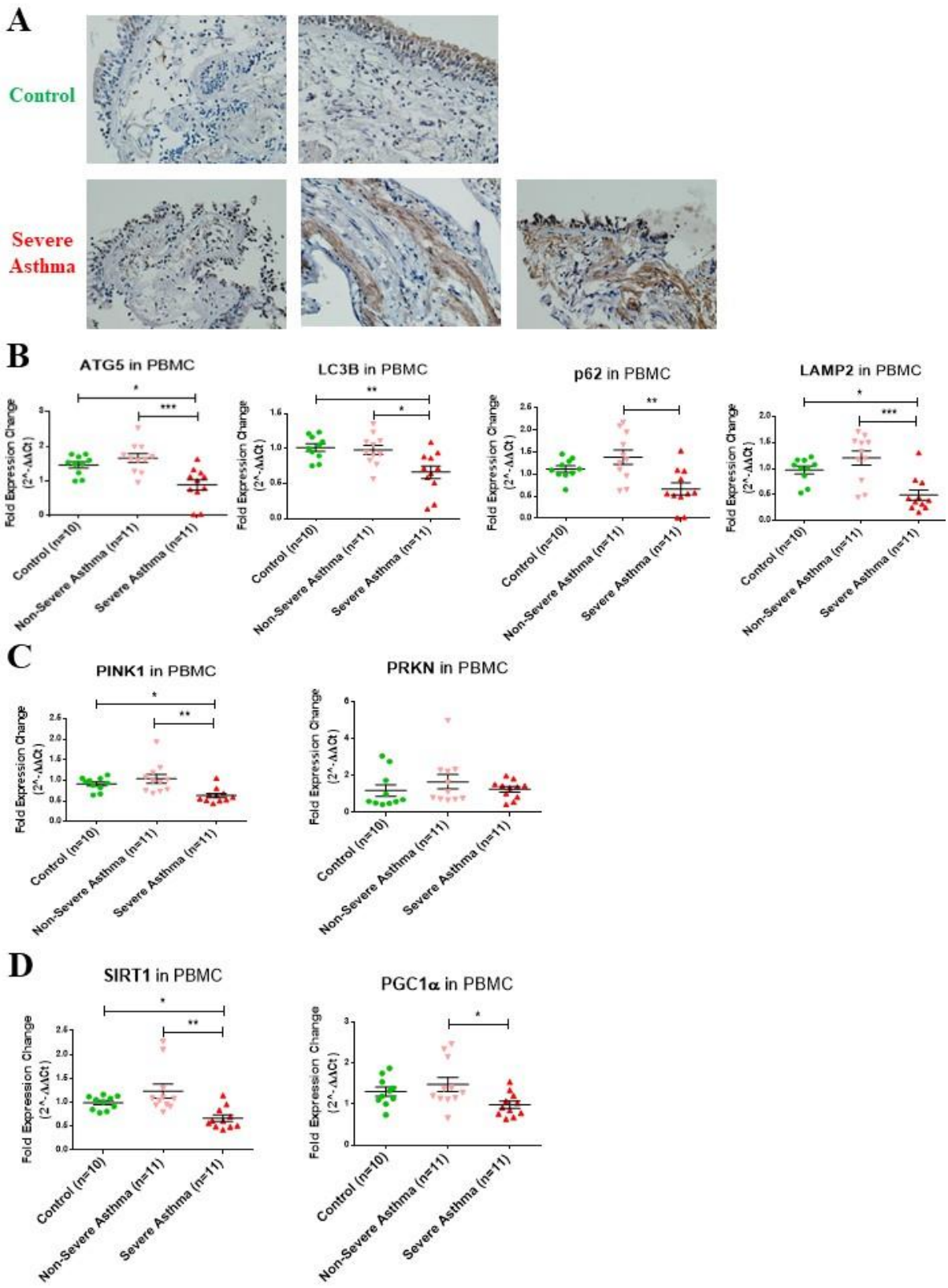
A
Control
Severe Asthma
B
ATG5 in PBMC
LC3B in PBMC
p62 in PBMC
LAMP2 in PBMC
Fold Expression Change (2^-ΔΔCt)
Control (n=10)
Non-Severe Asthma (n=11)
Severe Asthma (n=11)
C
PINK1 in PBMC
PRKN in PBMC
D
SIRT1 in PBMC
PGC1α in PBMC

Figure 4.2.3 Assessment of mitochondrial health in bronchial biopsy tissues and PBMCs from severe asthma patients and non-asthmatic subjects.

(A) Representative images taken at 40X magnification showing PINK1 immunostaining developed with 3,3′-diaminobenzidine diaminobenzidine (brown). Nuclei were counterstained with hematoxylin (blue). Representative bronchial biopsy sections from healthy control showing weak, and severe asthmatic showing moderate to strong PINK1 protein expression. **(B)** Peripheral blood mononuclear cells (PBMCs) were isolated from 10 healthy control, 11 non-severe asthmatics (with mild to moderate disease) and 11 severe asthmatics. mRNA expression of autophagy markers ATG5, LC3B, p62 and LAMP2, **(C)** mitophagy markers PINK1 and PRKN, and **(D)** mitochondrial biogenesis markers SIRT1 and PGC1α, in PBMCS was analyzed by qRT-PCR and expressed as fold expression change relative to the healthy control post normalization to housekeeping gene 18s rRNA. Data are represented as mean ± SEM from indicated donors in each group. *$p < 0.05$, **$p<0.01$, ***$p<0.001$, determined by 1-way ANOVA with Tukey's multiple comparison tests.

4.3 Innate Bcl10 response in the presence of mitochondrial perturbations in severe asthmatic fibroblasts

Nuclear factor (NF)-kappaB (NF-κB) is a key component of the inflammatory network that controls cytokine production in airway pathology (216). Persistent NF-κB activation is also known to characterize severe uncontrolled asthma (266). Bcl10 being a critical mediator of NF-κB signaling as well as fibrotic remodeling, we next investigated Bcl10 signaling as an alternative mechanism contributing to fibrotic remodeling in severe asthma.

4.3.1 Constitutive activation of NF-κB in severe asthmatic fibroblasts

To characterize the pattern of NF-κB activation in structural cells of severe asthma, we first examined the expression of various components of this pathway in bronchial fibroblasts from severe asthmatics and healthy subjects. To compare the basal expression levels, NHBF and DHBF cells in culture were pelleted and lysed for western blot and qRT-PCR analysis. Considering the absence of any information on Bcl10 activity in asthma, it was interesting to note a 3-fold increase in the relative protein expression of Bcl10 in DHBF in comparison to NHBF ($p=0.0524$) (Fig. 4.3.1A). We then looked into the phosphorylation status of IKBα, a downstream target of Bcl10. DHBF also demonstrated increased expression of the phosphorylated form of IKBα when compared to NHBF (Fig. 4.3.1B), suggesting constitutive activation of Bcl10 signaling in S-As fibroblasts.

To further confirm the persistent activation of NF-κB in S-As fibroblasts, we investigated the NF-κB gene signature in these fibroblasts at basal levels. Despite no difference in the mRNA expression of *BCL10*, the gene expression of *TLR4* ($p<0.01$) and *MALT1* ($p<0.001$) was significantly upregulated in DHBF relative to NHBF (Fig. 4.3.1C). While *IKBα* gene expression

was significantly downregulated in DHBF ($p<0.05$), *A20* deubiquitinase, another negative regulator of NF-κB that terminates downstream signaling events (267), was also lowered in DHBF as compared to NHBF (Fig. 4.3.1C). Increased mRNA levels of *RELA* subunit were also found in DHBF compared to NHBF, although it did not reach significance ($p=0.09$). This characteristic gene expression pattern in S-As fibroblasts in comparison to their healthy counterparts indicates NF-κB activation in S-As fibroblasts.

Here, we show that the expression of Bcl10 is elevated in bronchial fibroblasts from severe asthmatic subjects in addition to an increased signature of key NF-κB genes at baseline, which suggest constitutive activation of the Bcl10-mediated NF-κB pathway in S-As fibroblasts.

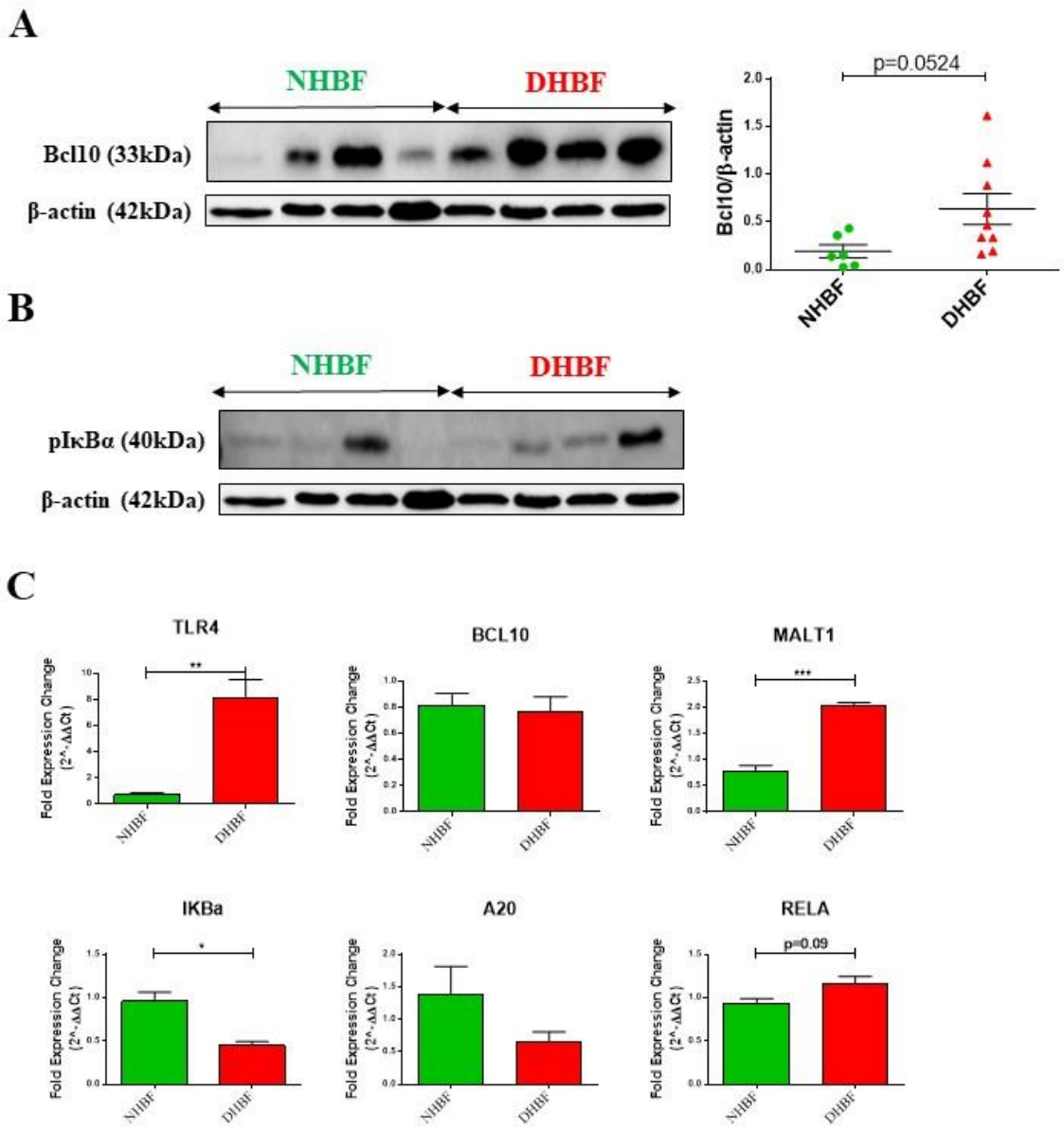

Figure 4.3.1 Constitutive activation of NF-κB in severe asthmatic fibroblasts.

NHBF and DHBF were cultured in DMEM complete medium post serum-starvation. Whole cell lysates were subjected to immunoblot analysis of **(A)** Bcl10 and **(B)** IκBα protein levels. β-actin was used as loading control. **(C)** Under basal conditions, mRNA expression of NF-κB pathway members, TLR4, BCL10, MALT1, IκBα, A20 and RELA, in NHBF and DHBF was analyzed by qRT-PCR and expressed as fold expression change relative to NHBF post normalization to housekeeping gene 18s rRNA. Data are represented as mean ± SEM from at least 3 unique donors in each group. *$p < 0.05$, **$p<0.01$, ***$p<0.001$ determined by unpaired two-tailed Student t-test.

4.3.2 Subcellular localization of Bcl10 in bronchial fibroblasts and epithelial cells

Subcellular localization of Bcl10 correlated with the development of MALT lymphoma, with strong nuclear Bcl10 expression seen in MALT lymphomas with t(1;14)(p22;q32) translocation (218). To study the potential role of Bcl10 in fibroblast function, we next assessed their subcellular localization in bronchial fibroblasts from severe asthmatic and healthy subjects. We used the Cell Fractionation Kit to isolate the cytoplasmic, membrane/organelle and nuclear cell fractions. The Cell Fractionation Antibody Kit was used to determine the purity of the separated subcellular fractions, where MEK1/2 is used as a marker of the cytoplasmic fraction (268), apoptosis-inducing factor (AIF) as a marker of the mitochondrial fraction (269), and core histone protein, H3, as a marker of the nuclear fraction (270).

Bcl10 expression was predominantly detected in DHBF with very faint expression in NHBF (Fig. 4.3.2A). Interestingly, Bcl10 expression was observed in both the cytoplasmic and membrane/organelle fractions in DHBF with no expression detected in the nuclear/cytoskeletal fraction (Fig. 4.3.2A). Strong Bcl10 expression was noted in the membrane/organelle compartment of DHBF.IKBα primarily resides in the cytoplasm. However, its localization to the mitochondria (271) and nucleus (272) exhibited functions separate from NF-κB inhibition. Therefore, we examined the subcellular localization of IKBα in bronchial fibroblasts and noticed IKBα to localize predominantly to the membrane/organelle and nuclear/cytoskeletal fractions (Fig. 4.3.2A). It is noteworthy that we also detected a higher molecular weight isoform in the organelle fraction.

We also studied the cellular localization pattern of Bcl10 and IKBα in bronchial epithelial cells from asthmatic and healthy subjects. While Bcl10 was detected only in the cytoplasmic fraction

in both NHBE and DHBE, IKBα localized predominantly to the membrane/organelle compartment in addition to the cytoplasm (Fig. 4.3.2B). These results indicate that Bcl10 and IKBα actively shuttles through the cellular compartments and their localization is also cell type-dependent.

In order to visualize the cellular localization of Bcl10, we further clotted the bronchial fibroblasts and bronchial epithelial cells, and performed immunocytochemistry. In bronchial fibroblasts, Bcl10 expression was highly intense in DHBF when compared to NHBF (Fig. 4.3.2C). While NHBF showed both nuclear as well as cytoplasmic Bcl10 expression, strong cytoplasmic Bcl10 expression was noted in DHBF. In bronchial epithelial cells as well, a greater number of Bcl10 positive cells were detected in DHBE relative to NHBE (Fig. 4.3.2D). Both NHBE and DHBE showed cytoplasmic expression of Bcl10. Taken together, these findings confirm constitutively high Bcl10 expression in asthma, particularly in severe asthma, and its localization predominantly in the cellular cytoplasmic compartment in bronchial fibroblasts.

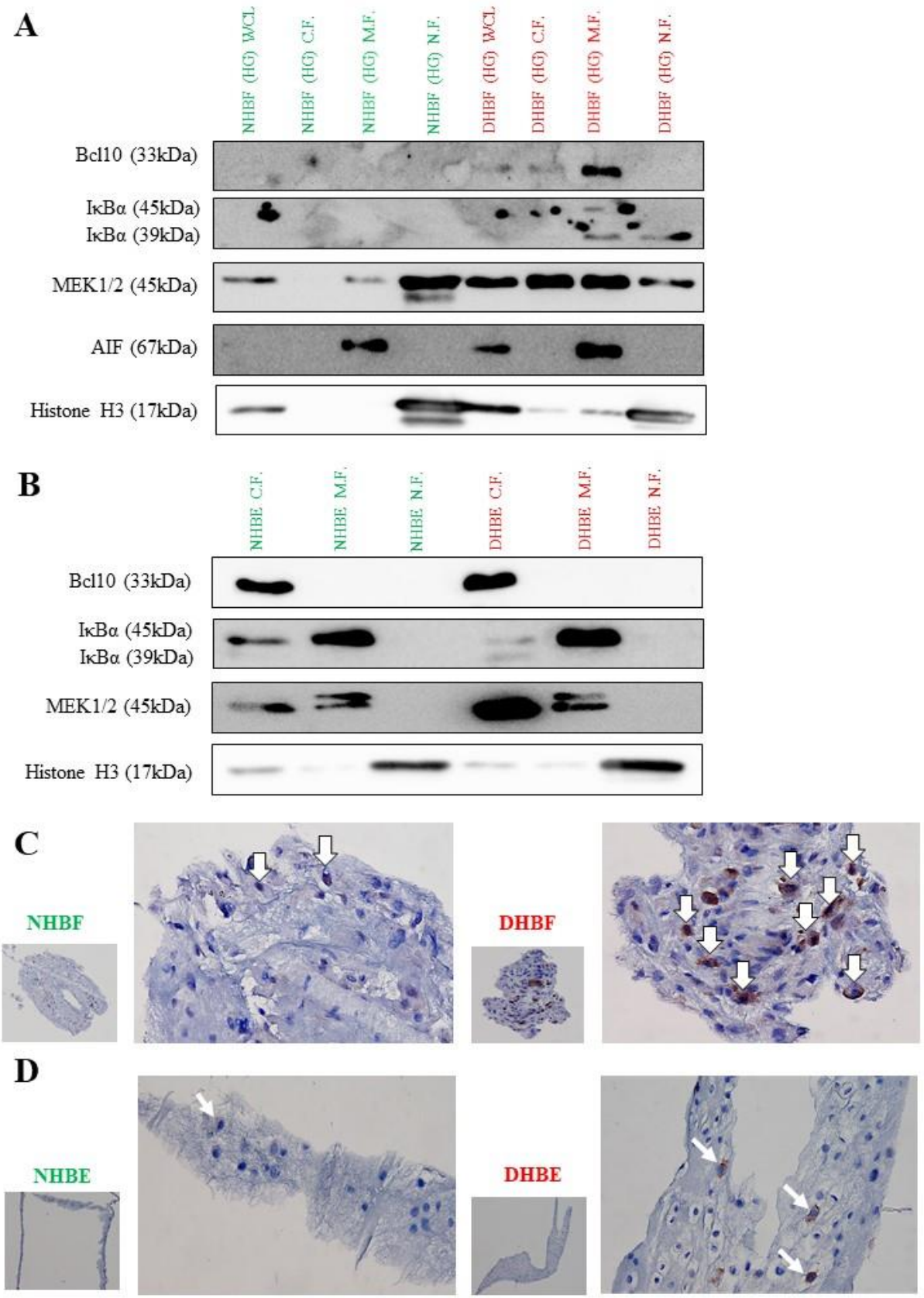
A
NHBF (HG) WCL
NHBF (HG) C.F.
NHBF (HG) M.F.
NHBF (HG) N.F.
DHBF (HG) WCL
DHBF (HG) C.F.
DHBF (HG) M.F.
DHBF (HG) N.F.
Bcl10 (33kDa)
IκBα (45kDa)
IκBα (39kDa)
MEK1/2 (45kDa)
AIF (67kDa)
Histone H3 (17kDa)
B
NHBE C.F.
NHBE M.F.
NHBE N.F.
DHBE C.F.
DHBE M.F.
DHBE N.F.
Bcl10 (33kDa)
IκBα (45kDa)
IκBα (39kDa)
MEK1/2 (45kDa)
Histone H3 (17kDa)
C
NHBF
DHBF
D
NHBE
DHBE

Figure 4.3.2 Subcellular localization of Bcl10 in bronchial fibroblasts and epithelial cells. **(A)** NHBF and DHBF were cultured in DMEM complete medium, and **(B)** NHBE and DHBE were cultured in Pneumacult complete medium. Whole cell lysates (WCL) were fractionated into cytoplasmic (C.F.), membrane/organelle (M.F.) and nuclear cell fractions (N.F.) and subjected to immunoblot analysis of Bcl10 and IκBα protein levels. MEK1/2, AIF and H3 were used as positive controls for the cytoplasmic, mitochondrial and nuclear compartments, respectively. **(C)** Cellular clots of NHBF and DHBF, and (D) NHBE and DHBE were stained for Bcl10 and the white arrows indicate Bcl10-positive cells.

4.3.3 Increased cytoplasmic Bcl10 expression in subepithelial fibroblasts of bronchial biopsy tissues

In order to authenticate the increased Bcl10 expression in severe asthma, we examined its protein expression and distribution in normal airway tissues and asthmatic airways of varying severities by immunohistochemistry of formalin-fixed and paraffin-embedded tissues. Bcl10 protein was expressed in both normal and asthmatic airways. In the airways, the protein was expressed abundantly in severe asthmatic airway cells, moderately in mild-moderate cases and weakly in the non-asthmatic healthy airways (Fig. 4.3.3A-D). The epithelium showed stronger Bcl10 expression when compared to the submucosa. The epithelium showed Bcl10 immunoreactivity in both the cytoplasm and nuclear compartments while the fibroblasts showed more of a cytoplasmic localization. The strong nuclear expression of Bcl10 in the epithelial cells distinguished them from the rest of the airway tissue which showed more cytoplasmic Bcl10 expression.

In the control biopsies, the epithelium showed positive Bcl10 expression in both the cytoplasm and the nucleus while the subepithelial fibroblasts were mostly negative for Bcl10 (Fig. 4.3.3A). Biopsies from mild and moderate cases of asthma displayed moderate Bcl10 expression in the

epithelium and submucosa with a few subepithelial fibroblasts staining positively for Bcl10 (Fig. 4.3.3B-C). Biopsies from severe asthmatic subjects showed intense Bcl10 expression in the epithelium as well as the sub-epithelium (Fig. 4.3.3D). Numerous subepithelial fibroblasts showed positive cytoplasmic expression of Bcl10. These findings suggest that the intensity as well as extent of positive Bcl10 staining increased with increasing severity of asthma.

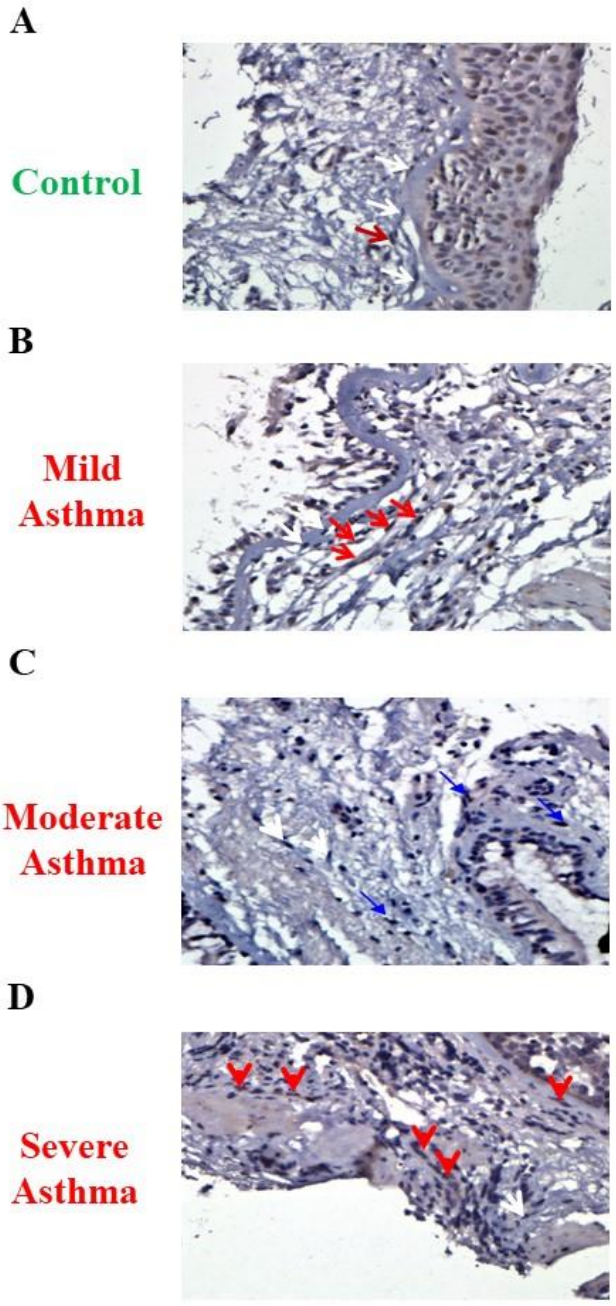

Figure 4.3.3 Increased cytoplasmic Bcl10 expression in subepithelial fibroblasts of bronchial biopsy tissues.

Representative images taken at 40X magnification showing Bcl10 immunostaining developed with 3,3′-diaminobenzidine diaminobenzidine (brown). Nuclei were counterstained with hematoxylin (blue). Representative bronchial biopsy sections from **(A)** healthy control showing weak, **(B)** mild and **(C)** moderate asthmatic showing moderate and **(D)** severe asthmatic showing strong Bcl10 protein expression. Red and blue arrows indicate Bcl10-positive fibroblasts and white arrows indicate Bcl10-negative fibroblasts.

4.3.4 LPS-induced IL-8 signaling mediated by Bcl10-dependent NF-κB activation in bronchial fibroblasts

In epithelial cells, TLR4 response is known to be mediated by Bcl10 (236, 273). TLR4 responses in human primary fibroblasts were found to be dependent on Bcl10 and Bcl10 deficiency in turn abolished TLR4 signaling (274). Since a 11-fold increase in *TLR4* mRNA expression was detected in DHBF relative to NHBF at baseline (Fig. 4.3.1C), we aimed to investigate the TLR4-Bcl10-NF-κB inflammatory axis in bronchial fibroblasts by stimulating these cells with LPS to understand better the relevance of this increase. Therefore, the fibroblasts were serum-starved for 24 hours and then exposed to 10 µg/ml of LPS from 30 minutes to 6 hours. We then studied the effect of LPS stimulation on the gene expression of different components along the TLR4-Bcl10-NF-κB inflammatory axis, including *TLR4*, *CARMA3*, *BCL10*, *MALT1*, *IKBα*, *A20* and *RELA* by qRT-PCR. While LPS stimulated the maximal gene expression of *TLR4* at 6h in NHBF compared to the unexposed control at 0h, an opposite pattern was detected in DHBF, where the mRNA expression significantly dropped with time (Fig. 4.3.4A). LPS also significantly induced the expression of *CARMA3* ($p<0.0001$), *BCL10* ($p<0.0001$) and *MALT1* ($p<0.01$) at 6h in both NHBF as well as DHBF in comparison to their respective unexposed controls. Interestingly,

with increased duration of exposure to LPS, the mRNA transcript levels of *TLR4, CARMA3, BCL10* and *MALT1* exhibited an oscillatory pattern in NHBF, which suggested the capability of these non-asthmatic fibroblasts to restrain their NF-κB activation depending on the antigen presence in the environment. However, despite the decrease in *TLR4* mRNA expression with increased exposure to LPS in DHBF, the mRNA transcript levels of *CARMA3*, *BCL10* and *MALT1* dramatically increased by 2h but appeared to plateau by 6h in DHBF.

The negative regulators of NF-κB activation were also induced by LPS in both NHBF and DHBF. Interestingly, LPS stimulated an initial increase in *IKBα* gene expression which was found to reduce thereafter with time in both NHBF and DHBF (Fig. 4.3.4A). However, the *A20* expression levels continually increased with time upon exposure to LPS in NHBF and DHBF, when compared to their respective unexposed controls. However, a prominent increase in *A20* levels was noted in NHBF when compared to DHBF. Intriguingly, LPS induced a far more significant increase in *RELA* gene expression in NHBF in comparison to DHBF.

The effects of LPS on TLR4, Bcl10 and IKBα expression were also determined by western blot analysis. With exposure to LPS over increasing time periods, TLR4 protein expression spiked as early as 30 minutes but then reduced thereafter in both NHBF and DHBF (Fig. 4.3.4B). Similarly, cellular Bcl10 and IKBα protein levels increased at 30-minute exposure and progressively reduced thereafter in NHBF and DHBF. Nonetheless, higher Bcl10 and IKBα expression was observed in DHBF when compared to NHBF. An exaggerated response to LPS was also noted in DHBF relative to NHBF.

Cross-linking of TLR4 with LPS induces the synthesis and secretion of pro-inflammatory and pro-fibrotic cytokines, including IL-8 (275). We, therefore, examined IL-8 expression in NHBF and DHBF upon LPS stimulation. Interestingly, LPS strongly induced *IL-8* gene expression in

both NHBF and DHBF, which was found to increase with time to a dramatically greater extent in NHBF when compared to their unexposed control (Fig. 4.3.4C). However, LPS-induced *IL-8* mRNA transcript levels were considerable higher in DHBF relative to NHBF. Therefore, these results suggest that LPS-induced IL-8 expression is mediated by Bcl10 in bronchial fibroblasts. While the non-asthmatic healthy fibroblasts are more sensitive to LPS stimulation, they appear to be able to restrain NF-κB activation. However, the constitutive activation of NF-κB pathway in S-As fibroblasts leads to an exaggerated response to LPS causing a greater extent of inflammatory damage.

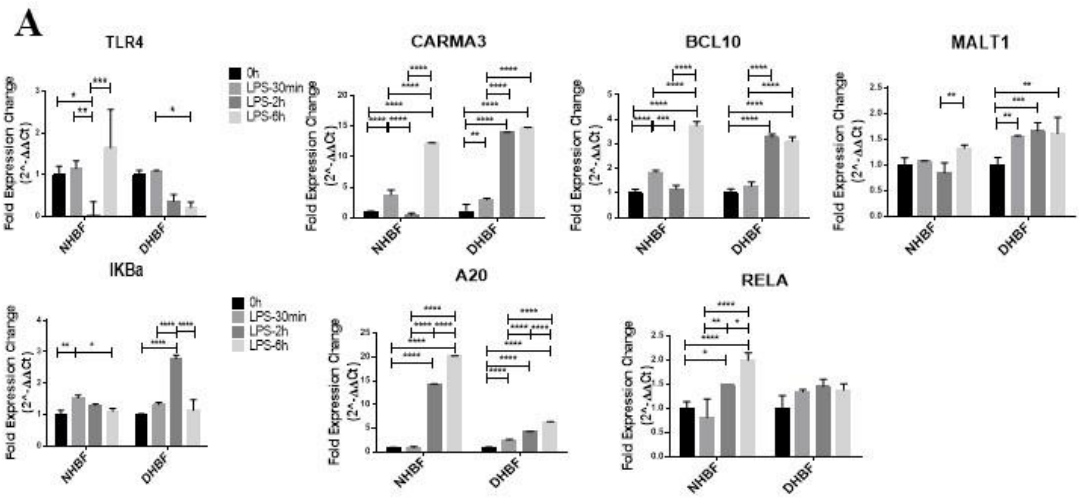
A
TLR4
CARMA3
BCL10
MALT1
IKBa
A20
RELA
0h
LPS-30min
LPS-2h
LPS-6h
Fold Expression Change (2^-ΔΔCt)
NHBF
DHBF

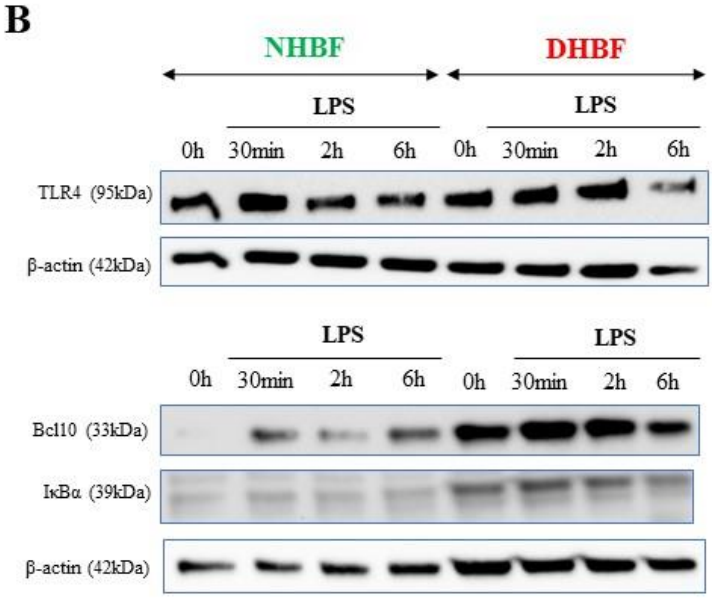
B
NHBF
DHBF
LPS
0h
30min
2h
6h
TLR4 (95kDa)
β-actin (42kDa)
Bcl10 (33kDa)
IκBα (39kDa)

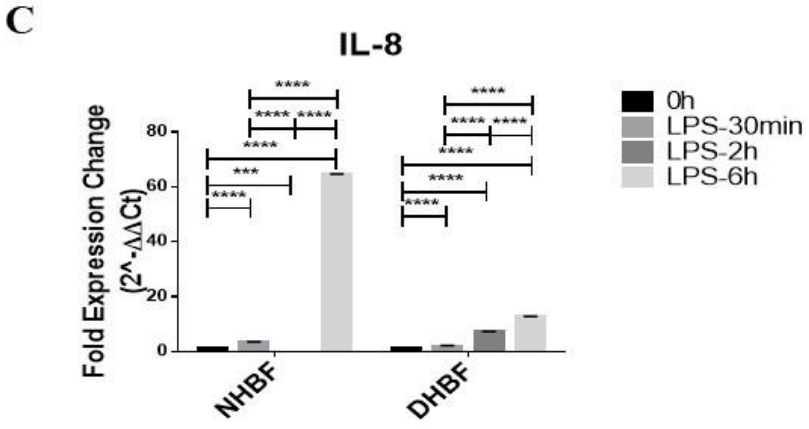
C
IL-8
Fold Expression Change (2^-ΔΔCt)
0h
LPS-30min
LPS-2h
LPS-6h
NHBF
DHBF

Figure 4.3.4 LPS-induced IL-8 signaling mediated by Bcl10-dependent NF-κB activation in bronchial fibroblasts.

NHBF and DHBF were serum-starved for 24 hours, and thereafter, exposed to LPS (10μg/ml) for the indicated time points up to 6 hours for mRNA analysis and protein analysis. (A) The effect of LPS on the mRNA expression of NF-κB pathway members, TLR4, CARMA3, BCL10, MALT1, IκBα, A20 and RELA, was analyzed by qPCR and expressed as fold expression change relative to the respective untreated control at 0-hour post normalization to housekeeping gene 18s rRNA. Data representative of n=3. (B) Representative immunoblots depicting expression of TLR4, BCL10 and IκBα, in NHBF and DHBF in response to LPS. β-actin was used as loading control. (C) The effect of LPS on the mRNA expression of IL-8 in NHBF and DHBF was analyzed by qPCR and expressed as fold expression change relative to the respective untreated control at 0-hour post normalization to housekeeping gene 18s rRNA. Data representative of n=3. Data presented as mean ± SEM after normalization to untreated control. * $p<0.05$, ** $p<0.01$, *** $p<0.001$, **** $p<0.0001$, statistical significance assessed by 2-way ANOVA with Tukey's multiple comparison tests.

4.3.5 Assessment of Bcl10 in PBMCs from asthma patients and non-asthmatic subjects

Since Bcl10 was differentially expressed in airway structural fibroblasts, we were interested to explore if Bcl10 could serve as a potential biomarker to characterize patient phenotype. We therefore analyzed its gene expression in PBMCs from healthy subjects, and asthmatics with non-severe (mild and moderate asthma) and severe disease. The PBMCs were isolated from these study subjects and qRT-PCR was performed to analyze the mRNA levels of *BCL10*.

BCL10 expression in PBMCs from S-As patients was significantly lower than that in non-severe asthma and also lower than the expression in control (Fig. 4.3.5A). The PBMCs from non-severe asthma showed increased expression of these markers relative to control. However, those from severe asthma exhibited a significant drop in expression relative to non-severe asthma. Thus,

the gene expression data clearly suggested that the gene expression of this marker increased in the early stages of asthma (mild-to-moderate asthma). However, its expression markedly decreased with disease severity.

To explore the association of Bcl10 with the clinical characteristics of non-severe and severe asthma patients, we further performed correlation analysis of their mRNA levels with FEV1/FVC and total serum IgE levels. In severe asthmatics, the mRNA expression of *BCL10* positively correlated with FEV1/FVC ratio (Fig. 4.3.5B). Taking the asthmatics as a whole, including patients with non-severe and severe asthma, this correlation was reiterated in the case of non-severe asthma as well (Fig. 4.3.5C). In addition, Bcl10 expression was found to negatively correlate with total serum IgE levels in asthmatics. These results suggested that clinical improvement in asthma patients was associated with an increase in the mRNA expression of *Bcl10* in PBMCs. As shown in Fig. 4.3.5A, the expression of these markers in S-As were significantly lower than that in non-severe asthma and healthy control groups. It is equally important to note that the mRNA expression of *BCL10* in S-As PBMCs contrasted with its expression in S-As fibroblasts further stressing the cell-specific nature of NF-κB pathway. Furthermore, it also highlights the importance of Bcl10 in phenotyping asthma severity and staging.

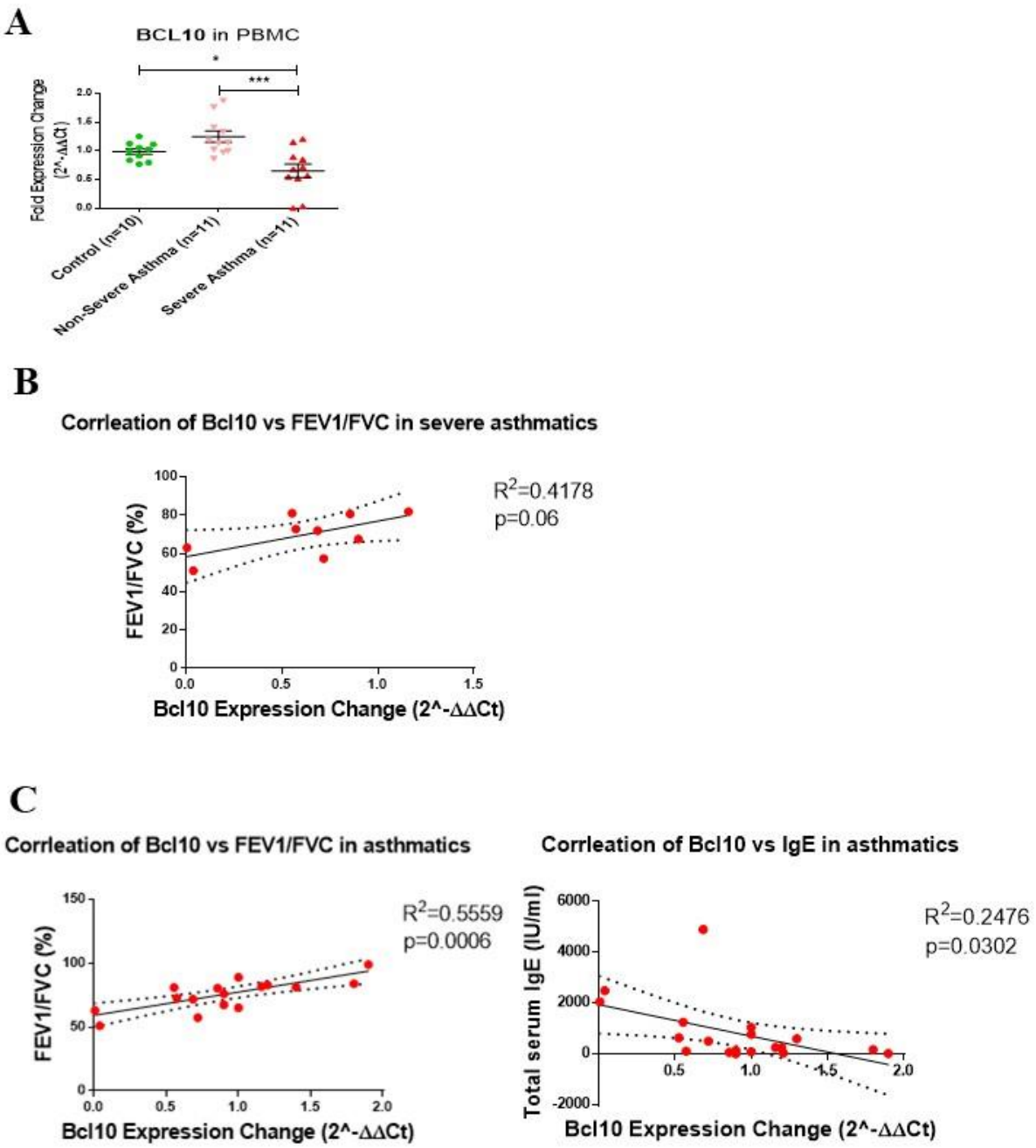

Figure 4.3.5 Assessment of Bcl10 in PBMCs from asthma patients and non-asthmatic subjects.

(A) Peripheral blood mononuclear cells (PBMCs) were isolated from 10 healthy control, 11 non-severe asthmatics (with mild to moderate disease) and 11 severe asthmatics. mRNA

expression of BCL10 in PBMCS was analyzed by qRT-PCR and expressed as fold expression change relative to the healthy control post normalization to housekeeping gene 18s rRNA. **(B)** Correlation analysis of Bcl10 with FEV1/FVC ratio in severe asthmatics. **(C)** Correlation analysis of Bcl10 with FEV1/FVC ratio (left panel) and total serum IgE levels (right panel) in asthmatics (non-severe and severe). Data are represented as mean ± SEM from indicated donors in each group. *$p < 0.05$, ***$p<0.001$, determined by 1-way ANOVA with Tukey's multiple comparison tests.

5. Discussion

The ability of fibroblasts to produce ECM proteins as well as pro-inflammatory cytokines have implicated them in remodeling and inflammation, two key processes involved in the pathogenesis of asthma. Although there are several reports indicating differences in ECM and cytokine profiles between healthy and asthmatic fibroblasts, the mitochondrial role in these pathological changes is not well established. Previously, our group demonstrated the involvement of autophagy in asthma pathogenesis and asthma severity (153). We also reported a positive correlation between *ATG5* gene expression and collagen deposition in the airways of refractory moderate-to-severe asthmatics suggesting that dysregulation of autophagy may promote subepithelial fibrosis in severe asthmatic airways (166). In light of the increasing evidence of mitochondrial dysfunction and autophagy in asthma, and the relative scarcity of information on severe asthma, the role of mitochondria and autophagy in the pathogenesis of fibrosis in severe asthma was investigated in our study.

5.1 Increased significance of mitochondrial quality control machinery in severe asthmatic fibroblasts

Currently, very little is known about the state of mitochondrial health in patients with severe asthma. Here, by using an *ex vivo* cell culture approach, we provide evidence of increased activation of mitophagy at baseline as a result of mitochondrial depolarization in severe asthmatic fibroblasts. Nevertheless, these fibroblasts demonstrated cellular adaptation to mitochondrial defects by upregulating AMPKα phosphorylation and mitochondrial biogenesis which prevented cellular apoptosis or senescence. Furthermore, the severe asthmatic fibroblasts

exhibited a pro-fibrotic and pro-inflammatory phenotype despite their intrinsic mitochondrial alterations. These results have important implications in understanding the role of mitochondrial QC in increased fibroblast persistence associated with airway remodeling.

Mitochondrial homeostasis is maintained by balancing the QC mechanisms of mitophagy and mitochondrial biogenesis that are responsible for maintaining a functional pool of mitochondria by continuous mitochondrial turnover, in which damaged and dysfunctional mitochondria are selectively eliminated from the mitochondrial pool through mitophagy and the pool is replenished with healthy and functional mitochondria through biogenesis (251). Therefore, in order to understand better the state of mitochondria health in severe asthmatic fibroblasts, we first investigated the mechanism of mitophagy. We as well as others have previously reported on the enrichment of the autophagy pathway in asthma as well as severe asthma (164, 175, 276). Consistent with published data, we demonstrated in this study an upregulation of basal autophagy at the protein level through increased LC3B lipidation and autophagosomal formation in S-As fibroblasts when compared to their healthy counterparts (Fig. 4.1.1A&C). It is also worth noting that transcriptional regulation of autophagy may not closely correlate with functional autophagy flux, whereby stable mRNA levels may be shown even in the presence of active autophagic flux and vice versa (277), as was corroborated in our study (Fig. 4.1.1B). Moreover, mRNA upregulation is usually a part of the long-term autophagic response and autophagy-related gene expression was assessed at 4 hours in our study.

Autophagosome is an intermediary structure in the dynamic process of autophagy. Therefore, the number of autophagosomes in a cell at a specific point in time is dependent on the rate of its formation and the rate of its degradation by lysosomes. Since endogenous LC3BII is degraded by lysosomal hydrolases after formation of autolysosomes, the cellular levels of LC3B alone is

not a reliable marker of autophagy. We, therefore, examined the expression of lysosomal protein, LAMP2A, that is essential for the fusion between autophagic vacuoles and lysosomes (278). The S-As fibroblasts exhibited increased gene and protein expression of LAMP2 (Fig. 4.1.1B&C) as well as increased lysosomal activity (Fig. 4.1.1D). The enhanced co-localization of LC3B-GFP with lysosomes in these fibroblasts (Fig. 4.1.1E) further reflected effective fusion between autophagosomes and lysosomes, and active degradation of autophagosomal cargo.

Furthermore, static levels of LC3B provide an incomplete assessment of autophagy without the evaluation of autophagy flux, either directly through lysosomal blockade or indirectly inferring from p62/SQSTM1 levels. Increased cellular levels of endogenous LC3BII reflect either increased autophagy induction or reduced autophagy turnover. To further distinguish between the two, we studied endogenous LC3B and p62 levels in the presence of E64d and pepstatin A, which inhibit lysosomal proteolytic activity and by this means, inhibit lysosomal turnover of LC3BII and p62 during autophagy (133). Although LC3B lipidation increased across both group of fibroblasts, the accumulation of LC3BII in the presence of E64d and pepstatin A was more prominent in the S-As fibroblasts when compared to the healthy controls (Fig. 4.1.1F). It was thus confirmed that basal autophagic activity in severe asthmatic fibroblasts is higher than in control fibroblasts.

Adaptor protein p62 is also an indicator of autophagosomal turnover because they recruit ubiquitinated proteins into the autophagosome and get degraded post lysosomal fusion (133). Generally, p62 levels are inversely correlated to the activation of autophagy (133). Interestingly, increased p62 protein expression was noted in S-As fibroblasts in comparison to control fibroblasts (Fig. 4.1.1C). This, however, aligns with some studies where upregulation of p62 levels was observed with an increase in autophagy flux (279-281). The p62 levels further

accumulated in S-As fibroblasts in the presence of E64d and pepstatin A, confirming the lysosomal turnover of p62 (Fig. 4.1.1F), and thereby, an increase in autophagy flux in severe asthmatic fibroblasts.

Mitophagy genes, *PINK1* and *PRKN*, were differentially expressed to some extent between the two groups of fibroblasts indicating an activation of the PINK1/Parkin-mediated mitophagy in S-As fibroblasts (Fig. 4.1.2A). We, therefore, probed the protein expression of various mitophagy-related proteins. Mitochondrial stress or damage stabilizes PINK1 on the OMM, which subsequently triggers mitophagy. PINK1 processing is a very rapid process and involves tight regulation of the cleaved PINK1 isoforms. We investigated the mitochondrial processing of the PINK1 precursor and the cleaved isoforms of PINK1. PINK1 is known to have multiple cleavage sites, however, in our experiments, we observed primarily two post-translationally cleaved forms of PINK1, at ~50kDa and ~30kDa, on western blot analysis. Endogenous PINK1 was detected in the full length and cleaved forms in the control fibroblasts while the full-length precursor predominated in the S-As fibroblasts (Fig. 4.1.2B). Interestingly, the increased accumulation of PINK1, Parkin, LC3B and p62 proteins was accompanied by the increased expression of various other autophagy and mitophagy adaptor proteins, including BNIP3, BNIP3L/Nix, Optineurin and NDP52 (Fig. 4.1.2C). This further highlighted the increase in mitophagy levels at baseline in S-As fibroblasts. Additionally, treatment with E64d and pepstatin A also led to increased accumulation of the full-length precursor form of PINK1 in the S-As fibroblasts (Fig. 4.1.2D) confirming its active turnover through mitophagy. Furthermore, the increased co-localizations of mitochondria with autophagosomes and lysosomes substantiated the increase in mitophagy flux in S-As fibroblasts (Fig. 4.1.2E&F).

Using cultured primary bronchial fibroblasts, we demonstrated mitochondrial defects associated with a reduction in mitochondrial membrane potential and mitochondrial metabolic activity in S-As fibroblasts. Dissipation of ΔΨm, as observed in the S-As fibroblasts (Fig. 4.1.3A), is a sign of mitochondrial damage that explains the accumulation of PINK1 (Fig. 4.1.2B). MTT assay is a popular colorimetric assay used to assess metabolic viability of cultured cells. MTT assay is based on the activity of intracellular NAD(P)-dependent oxidoreductases, predominantly dehydrogenases, in reducing the tetrazolium salt MTT into the strongly light-absorbing water-insoluble formazan. These NAD-dependent dehydrogenases are one of the main indicators of the mitochondrial functional state (282). It is, however, important to keep in mind that the reduction of tetrazolium salts can also be caused by enzymes of the endoplasmic reticulum, cytosol, endosomal/lysosomal vesicles and plasma membrane (282). Although with its set of limitations, MTT assay may be used as an indicator of mitochondrial function to evaluate mitochondrial activity and here, we showed reduced mitochondrial metabolic activity in S-As fibroblasts (Fig. 4.1.3B).

While the loss of PINK1 is known to promote mitochondrial ROS production (283), we observed that the ROS levels were significantly lower in S-As fibroblasts when compared to healthy (Fig. 4.1.3C). This could be explained by the continuous turnover of damaged mitochondria in severe asthmatic fibroblasts preventing their accumulation and thereby, ROS buildup. Reduced mtROS production may also be a mechanism of chronic adaptation to oxidative stress as this was shown to impair mitochondrial metabolism and microbicidal response in COPD alveolar macrophages (284).

Previous reports have showed increased mitochondrial ROS, disruption of ΔΨm and increased mitochondrial activity in ASM cells of asthmatics (285). ASM from asthmatic subjects were

characterized by increased mitochondrial mass and enhanced calcium-dependent mitochondrial biogenesis contributing to increased cell proliferation associated with airway remodeling (286). ASM from COPD patients were associated with mitochondrial dysfunction reflected by increased mitochondrial ROS, reduced $\Delta\Psi m$ and mitochondrial respiration compared with those from healthy control subjects (240). This oxidative stress-induced mitochondrial dysfunction triggered inflammation and airway smooth muscle remodeling in COPD patients. In COPD, exposure to cigarette smoke led to mitophagy and mitochondrial dysfunction in epithelial cells (287). Abnormal mitochondrial structural and functional changes were induced by prolonged cigarette smoke exposure (CSE) which persisted upon CSE cessation (288). Moreover, epithelial cells in the lungs of IPF patients were also characterized by the accumulation of dysfunctional mitochondria making them vulnerable to apoptosis and activation of pro-fibrotic responses thereby promoting the development of pulmonary fibrosis (289). Thus, mitochondrial dysfunction is a characteristic feature of lung diseases, including severe asthma; however, the associated mitochondrial changes are cell type-dependent and based on the functional phenotype of the cell.

AMPK is a key nutrient and energy sensor that is central to the regulation of cellular energy homeostasis (290). In the event of mitochondrial depolarization, the cellular ATP production is impeded resulting in lower cellular ATP levels. AMPK is usually activated as a rescue mechanism when the intracellular AMP to ATP ratio is high (290). AMPK impacts metabolism and growth by regulating a number of pathways including glucose and lipid metabolism, autophagy and cell polarity. In a study by Distelmaier *et al*., primary human fibroblasts exhibiting Complex I-associated mitochondrial dysfunction were found to heavily rely on extracellular glucose and AMPKα phosphorylation to initiate an adaptive cell survival response

(291). Despite the mitochondrial depolarization exhibited by the S-As fibroblasts, these cells demonstrated cell cycling comparable to the control fibroblasts (data shown in Appendix 9.4.1). This could be explained by the increased phosphorylation of AMPKα (Fig. 4.1.4A) which enabled the cells to metabolically adapt to the innate mitochondrial damage without any induction of cellular apoptosis or senescence (Fig. 4.1.4D&E). Furthermore, elevation in NAD+ levels also activate SIRT1 that in coordination with AMPK regulates mitochondrial mass, ATP production and nutrient oxidation, with the help of transcription co-factor, PGC1α (196, 197). Accordingly, increased SIRT1 and PGC1α expression was noted in the fibroblasts from severe asthmatics (Fig. 4.1.4B). The absence of any significant difference in the mitochondrial mass between the severe asthmatic and control fibroblasts (Fig. 4.1.4C) further reflected the effective turnover of depolarized mitochondria in S-As fibroblasts.

Persistent stress triggers excessive ROS generation and release of mitochondrial pro-apoptotic proteins. This disrupts ATP synthesis and activates the cell death pathways. Cells have developed a defense mechanism against allowing abnormal mitochondria to harm the cell. Here, the aberrant mitochondria are selectively sequestered by double membraned autophagosomes and subsequently degraded by lysosomes before it activates the cell death pathways (195). Autophagy, therefore, acts as a sentinel responsible for organelle quality control (292). Therefore, autophagy is elevated so that the membrane lipids and proteins are digested within the autolysosome to generate free fatty acids and amino acids which could be recycled for mitochondrial ATP production and other synthetic activities. Autophagy may thus, be a key driving force behind airway remodeling in asthma. Since fibrosis entails a massive synthetic drive of ECM proteins and other fibrotic mediators that requires substantial energy, elevated autophagy flux may serve this energy need under diseased condition.

At the cellular level, mitochondrial dysfunction is also known to trigger adaptive changes to overcome unfavorable cellular consequences and escape cell death (248, 250). These adaptive mechanisms include induction of mitophagy and mitochondrial biogenesis, alterations in mitochondrial dynamics and morphology, upregulation of glycolysis and alterations in antioxidant responses (293). Constant turnover of damaged mitochondria is a prerequisite for the establishment of functional mitochondrial network. Exposure of alveolar macrophages in pulmonary fibrosis to mitochondrial oxidative stress induces mitophagy in these cells which orchestrated TGF-β1 expression and fibroblast differentiation (294). Furthermore, the increased mitophagy also contributed to apoptosis resistance and development of pulmonary fibrosis. Since the mitochondria in severe asthma are constantly exposed to oxidative damage (295, 296), enhanced mitophagy levels may serve as a stress adaptation mechanism to avoid cell death. Taking into consideration the increased mitophagy and biogenesis in S-As fibroblasts, the comparable mitochondrial content within the two group of fibroblasts reflect unimpeded mitochondrial turnover in the diseased fibroblasts. Despite their intrinsic mitochondrial defects, the severe asthmatic fibroblasts demonstrated increased pro-fibrotic ECM (Fig. 4.1.5A) and chemokine (Fig. 4.1.5C) gene expression implicating dysregulation of mitophagy and biogenesis in the pathogenesis of severe asthma. The ability of these severe asthmatic fibroblasts to increasingly produce ECM proteins as well as pro-inflammatory cytokines support their active role in promoting remodeling and inflammation, two key processes involved in the pathogenesis of asthma.

Although the precise mechanism and role of the observed mitophagy and biogenesis levels remain elusive, it is plausible that in the presence of depolarized mitochondria in S-As fibroblasts, mitochondrial QC is elevated as a rescue mechanism against mitochondrial

oxidative stress to prevent apoptosis and senescence in bronchial fibroblasts. This, in turn, may exacerbate the pathophysiology of severe asthma through the persistence of these fibroblasts. Further studies are paramount to elucidate the molecular events driven by these mitochondrial defects in severe asthmatic fibroblasts that lead to their persistent activation and fibrotic behavior.

Oxidative stress-induced mitochondrial dysfunction was shown to promote ASM remodeling in COPD patients (240). Mitochondria evidently plays a crucial role in airway remodeling, not only in COPD but in asthma as well. Mitochondrial oxidative stress was shown to contribute to the pathogenesis of asthma as well as disease severity (276, 297). Therefore, it is not surprising that with increasing severity of asthma, the airways are prone to excessive mitochondrial damage. The increased activity of the mitochondrial QC machinery in S-As fibroblasts sheds light on the increased susceptibility of their mitochondria to insult. Thus, with increased mitochondrial stress, the mitochondrial QC mechanisms of mitophagy and biogenesis are enriched in S-As fibroblasts. In fact, an intact and functional mitochondrial QC machinery rescues these fibroblasts from the manifestation of mitochondrial dysfunction. This in turn could help maintain a chronic but non-lethal level of oxidative stress which in turn promotes airway remodeling.

In summary, we show that increased mitophagy flux is associated with increased mitochondrial biogenesis and improved survival in S-As fibroblasts. As shown in Fig. 5.1, in the increased presence of stressors such as allergens, pollutants or cigarette smoke, the mitochondria are increasingly prone to damage in S-As fibroblasts. These damaged mitochondria are effectively cleared by increased mitophagy. To compensate for the mitochondrial loss, new functional mitochondria are generated which eventually fall prey to the mitochondrial stressors. This

reflects a vicious pathological cycle ensuring the increased persistence of S-As fibroblasts.

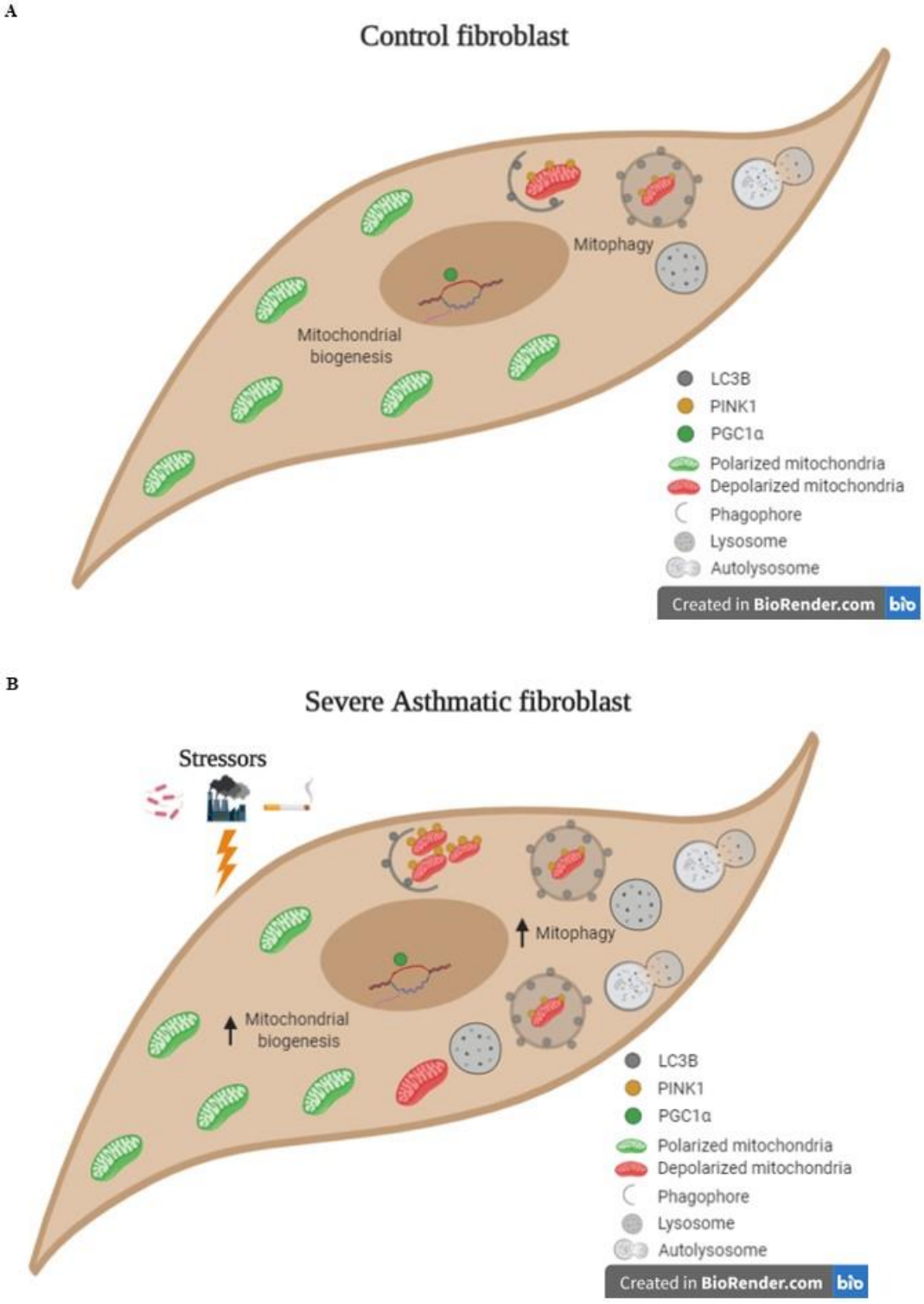

Figure 5.1 Schematic representation of mitochondrial homeostasis in severe asthmatic and control bronchial fibroblasts.

In control fibroblasts, mitochondrial homeostasis is ensured by basal levels of mitophagy and mitochondrial biogenesis. With exposure of hyperresponsive airways in severe asthma to stressors such as allergens, pollutants or cigarette smoke, the mitochondria are increasingly prone to damage in S-As fibroblasts. The damaged mitochondria are effectively recycled by increased mitophagy and biogenesis. The new mitochondria eventually fall prey to the mitochondrial stressors reflecting a vicious pathological cycle ensuring the increased persistence of S-As fibroblasts.

5.2 Asthma-related cytokines impair mitochondrial function in non-asthmatic and severe asthmatic fibroblasts

The state of mitochondrial health and mitochondrial QC was differential at baseline in the non-asthmatic and S-As fibroblasts with increased mitochondrial depolarization and mitochondrial turnover displayed by the S-As fibroblasts. Therefore, we next aimed to study these mechanisms in the presence of cytokines relevant to asthma considering the elevated expression of several mediators of remodeling in airway tissues (252). Th17 cytokine IL-17, pro-fibrotic cytokine TGF-β1 and Th2 cytokine IL-13, and their regulation of mitochondrial function and fibrosis was investigated in bronchial fibroblasts from non-asthmatic and S-As subjects.

To our knowledge, this is the first study to demonstrate that IL-17 accelerated mitochondrial dysfunction and fibrosis in bronchial fibroblasts, but to a greater extent in S-As fibroblasts when compared to non-asthmatic controls. This induction was further shown to be associated with the activation of autophagy in these fibroblasts. Our data suggests that the pre-existing mitochondrial damage and fibrotic phenotype in S-As fibroblasts is amplified by IL-17. On a

similar note, TGF-β1 and IL-13 also impaired mitochondrial function in bronchial fibroblasts, with a more profound effect on S-As fibroblasts, reinforcing the pathological behavior of these cytokines in the pathogenesis of severe asthma.

Because of the increasing implications of the pro-inflammatory and pro-fibrotic roles of IL-17 in severe asthma, we started by testing the impact of IL-17 on mitochondrial dysfunction indicated in S-As fibroblasts. The effects of IL-17 were more evident in S-As fibroblasts than in their healthy counterparts. One of the hallmarks of mitochondrial dysfunction is decreased mitochondrial membrane potential. In agreement, IL-17 significantly decreased the ΔΨm and mitochondrial mass in S-As fibroblasts (Fig. 4.2.1.1A&B). At the same time, a tendency towards a decline in ΔΨm and mitochondrial mass was noted in the healthy fibroblasts when treated with IL-17 (Fig. 4.2.1.1A&B). The occurrence of these hallmark features indicated that an IL-17 rich microenvironment renders the healthy fibroblasts vulnerable to mitochondrial malfunction and intensifies the pre-existing mitochondrial dysfunction in S-As fibroblasts. Our findings suggest that S-As fibroblasts show greater susceptibility to IL-17-mediated damage.

IL-17 induced reduction in mitochondrial mass implies enhanced mitochondrial degradation through mitophagy. As expected, IL-17 increased the expression of autophagy-related genes (Fig. 4.2.1.2A), LC3B lipidation and protein levels of p62 (Fig. 4.2.1.2B), more significantly in S-As fibroblasts than in healthy. Interestingly, IL-17 treatment induced an increase in mitophagy in the healthy, while a declining trend was observed in the S-As fibroblasts (Fig. 4.2.1.2C). The associated decline in mitochondrial biogenesis in both group of fibroblasts (Fig. 4.2.1.2D) reflect an impairment in the mitochondrial QC machinery as a result of prolonged exposure to IL-17. This supports the notion that due to the innate phenotypic differences between non-asthmatic and S-As fibroblasts, they display unique responses to IL-17 stimulation.

Dysregulation of mitochondrial QC is involved in the pathogenesis of age-related lung diseases, such as COPD and IPF (298). Further, impaired mitochondrial homeostasis has been increasingly linked to lung fibrosis. Perturbation of mitochondrial homeostasis was recently reported in alveolar macrophages from IPF patients (299). These macrophages displayed swollen and dysmorphic mitochondria which accumulated as a result of significant reduction in the mitochondrial QC regulators, PINK1, PRKN and NRF1. The dysregulation of mitochondrial QC mechanisms thus, leads to the accumulation of damaged mitochondria (298). Insufficient PINK1/Parkin-mediated mitophagy was also shown to be a potent underlying mechanism for myofibroblast differentiation and proliferation of lung fibroblasts in the pathogenesis of IPF (178). Likewise, reduced autophagy flux, mitophagy and functional mitochondrial defects characterized myofibroblast differentiation in pulmonary fibrosis (300).

Autophagy has emerged as a key player of cell survival in asthma (301). Increased LC3B expression exerted a cytoprotective role and inhibited hypoxia-induced epithelial apoptosis in lung epithelial cells (302). In addition to increasing autophagy but disabling the mitochondrial QC machinery, IL-17 inhibited apoptosis by decreasing Annexin V staining (Fig. 4.2.1.1C) and increasing the expression of anti-apoptotic protein, Survivin (Fig. 4.2.1.1D) in both non-asthmatic and S-As fibroblasts. IL-17 was previously reported to impair apoptosis in rheumatoid arthritis synovial fibroblasts through the activation of autophagy (256) and our findings are in accordance with this study.

We speculated that as a result of IL-17 induced mitochondrial damage, the healthy and S-As fibroblasts endured this damage by initiating autophagy. In the presence of IL-17, the declining $\Delta\Psi m$ in the otherwise healthy mitochondria in non-asthmatic fibroblasts trigger a corresponding increase in mitophagy to mitigate the damage. However, the increased mitophagy is not

paralleled by an increase in biogenesis resulting in a decrease in mitochondrial mass in healthy fibroblasts. On the contrary, the continuous dissipation of mitochondrial ΔΨm as a result of IL-17 disables the mitophagy and biogenesis machinery in S-As fibroblasts. Nevertheless, the decreased mitochondrial mass in these fibroblasts suggests the recruitment of alternative mitochondrial degradation mechanisms, including proteasomes, intramitochondrial proteolytic systems and vacuole/lysosome-mediated pathway (303). Mitochondrial QC was shown to be regulated by a vesicular trafficking pathway distinct from the canonical autophagy and mitophagy pathways involving mitochondria-derived vesicles targeted to lysosomes for degradation (304). These mechanisms may contribute to IL-17 induced increased persistence of the healthy and S-As fibroblasts despite their mitochondrial dysfunction.

The observation of increased autophagy and mitochondrial dysfunction brought about by IL-17 in S-As fibroblasts led us to hypothesize that autophagy facilitates IL-17 induced mitochondrial dysfunction as well as promotes the fibrotic phenotype of these diseased fibroblasts. Therefore, we pre-treated the bronchial fibroblasts with Baf-A1 to study the effects of autophagy blockade on these fibroblasts. Accordingly, inhibition of autophagy using Baf-A1 reversed the IL-17 mediated increase in *PINK1* and *PRKN* gene expression in S-As fibroblasts (Fig. 4.2.1.3C&D). Co-incubation with IL-17 and Baf-A1 also brought about a significant reduction in *PINK1* and *PRKN* gene expression in the healthy fibroblasts when compared to their untreated controls (Fig. 4.2.1.3C&D). Since increased *PINK1* and *PRKN* gene expression is induced upon mitochondrial damage, their decreased gene expression may imply a reduction in mitochondrial dysfunction. These findings highlight the importance of autophagy in driving IL-17 induced mitochondrial dysfunction in these bronchial fibroblasts.

We, along with many others, have previously reported that subepithelial fibrosis in asthmatic airways is characterized by increased deposition of collagens, specifically collagen types I, III and V, and fibronectin (82, 102, 260, 305) as well as increased myofibroblast accumulation (261). More importantly, we have showed the association between increased levels of IL-17 and collagen types I and III in severe asthmatic bronchial tissues (102). In a study of orbital fibroblasts in thyroid-associated ophthalmopathy, IL-17 promoted the gene expression of collagen types I and III, and *ACTA2* (306). In line with these previous studies, IL-17 augmented the gene expression of *COL1A1*, *COL3A1*, *COL5A1* and *FNI* to a greater extent in S-As fibroblasts than their healthy counterparts (Fig. 4.2.1.4A).

A recent study demonstrated selective activation of autophagy in a cell context-dependent manner in asthma (164). In this study, autophagy was found to be critical in the development of airway remodeling with multiple autophagy markers showing positive staining in tissue sections of asthmatic airways. We have also previously reported that dysregulation of autophagy is associated with subepithelial fibrosis in the airways of refractory asthmatics (166). In this study, *ATG5* gene expression positively correlated with *COL5A1* expression in bronchial biopsies from refractory asthmatics. Interestingly, co-incubation of bronchial fibroblasts with Baf-A1 significantly reduced *COL1A1*, *COL3A1*, *FN1* and *ACTA2* gene expression in both non-asthmatic and severe asthmatic fibroblasts (Fig. 4.2.1.4B-F). Additionally, inhibition of autophagy also blocked the IL-17 mediated increase in pro-fibrotic gene signature in both groups of fibroblasts.

Our findings are in line with previous studies which have showed that autophagy represents a plausible therapeutic target in alleviating the pathology associated with asthma. Inhibition of autophagy using 3-MA treatment or *Atg5* knockdown in severe allergic asthmatic mice was

found to significantly attenuate AHR, eosinophilic inflammation and IL-5 levels in bronchoalveolar lavage fluid in addition to reducing histological lung inflammation (175). Furthermore, TGF-β1-induced fibrotic responses in ASM cells was mediated by autophagy where both pharmacological inhibition using 3-MA and Baf-A1 as well as silencing of key autophagy genes *Atg5* and Atg7 impeded the fibrotic response in these airway structural cells (165). The importance of autophagy in both airway inflammation and airway remodeling (307) makes it an ideal target to impact both pathophysiological processes in asthma.

In severe asthma, the airway fibroblasts are under chronic exposure to various pro-inflammatory and pro-fibrotic cytokines, including but not limited to IL-17, TGF-β1 and IL-13. IL-17 has been shown to induce mitochondrial dysfunction in various disease models including rheumatoid arthritis (256) and vitiligo (308), and interestingly enough, IL-17 induced mitochondrial dysfunction was associated with the activation of autophagy. In renal fibrosis, TGF-β1 induced fibrotic response was accompanied by mitochondrial dysfunction (262). IL-13 is another important inducer of mitochondrial dysfunction in the lung (309). In agreement, we showed the ability of IL-17, TGF-β1 and IL-13 in inducing mitochondrial dysfunction in both healthy and S-As fibroblasts by depolarizing their mitochondrial membrane potential (Fig. 4.2.2A). The observation that these cytokines concomitantly reduced the ROS levels and improved cell viability (Fig. 4.2.2B-C) further emphasizes on the pleiotropic role of these cytokines in maintaining ROS at optimal levels to boost redox signaling and thus, improve cell viability. The bronchial fibroblasts, thus, exhibited bioenergetic plasticity that enabled them to acclimatize to their ever-changing environment.

As a further validation to our findings so far, we also investigated PINK1 expression as well as distribution in bronchial biopsy tissues from non-asthmatics and severe asthmatics. PINK1

accumulation is a characteristic of mitochondrial damage and intense PINK1 immunoreactivity was observed in S-As airway biopsies (Fig. 4.2.3A), which reinforced increased mitochondrial damage in S-As airways than in healthy airways.

Peripheral blood cells from patients with severe asthma demonstrated significantly increased autophagy levels when compared to non-severe asthma and healthy controls (174). Therefore, we asked ourselves if the characteristic autophagy and mitochondrial profiles observed in severe asthmatic fibroblasts were reflected in peripheral blood cells as well. Surprisingly, we detected a mild increase in the expression of autophagy, mitophagy and mitochondrial biogenesis markers in non-severe asthma but a significant drop in their expression was noted in patients with severe asthma when compared to non-severe asthma and healthy controls (Fig. 4.2.3B). Autophagy and mitochondrial QC profiles in the lung is thus, distinct from the blood, emphasizing the cell-specific behavior of autophagy and mitochondrial pathways depending on the varying cellular contribution to airway structure and function.

In summary, we show that asthma-related cytokines, IL-17, TGF-β1 and IL-13 induce mitochondrial dysfunction in both non-asthmatic and severe asthmatic fibroblasts, with a more profound effect on the diseased fibroblasts. IL-17, in particular, was found to promote mitochondrial dysfunction and pro-fibrotic phenotype in these fibroblasts through the parallel induction of autophagy. The pre-existing mitochondrial damage and fibrotic phenotype in S-As fibroblasts was thus, amplified by IL-17.

5.3 Over expression of Bcl10 in severe asthmatic fibroblasts

Human studies as well as *in vivo* animal models have reported increased activation of the classical and alternative NF-κB pathways in asthmatic airway tissues as well as in inflammatory cells (266, 310). NF-κB activation in the airway epithelium is also known to play an important role in regulating peribronchial fibrosis (92). Bcl10 being a critical mediator of NF-κB signaling prompted us to explore its role in fibrotic remodeling in bronchial fibroblasts from severe asthma as an alternative mechanism to mitochondrial dysfunction that contributes to subepithelial fibrosis in severe asthma. This is the first report providing evidence of elevated protein expression of Bcl10 in the pathogenesis of severe asthma. Additionally, we are also the first to identify the participation of Bcl10-mediated NF-κB pathway in the LPS-induced activation of IL-8 in bronchial fibroblasts.

Overexpression of Bcl10 is an indicator of constitutive NF-κB activation in tumors including MALT lymphoma (217, 311). At baseline, the S-As fibroblasts demonstrated differential gene expression of various components of the NF-κB pathway when compared to their healthy counterparts, supporting the notion of constitutive activation of NF-κB in severe asthma (Fig. 4.3.1C). This was further confirmed by the increased protein expression of Bcl10 as well as phospho-IKBα at basal levels in S-As fibroblasts (Fig. 4.3.1A&B). The overexpression of Bcl10 in S-As fibroblasts was close to statistical significance, reflecting the need for a larger sample size. Nevertheless, the increase of Bcl10 expression in S-As fibroblasts appears to signify the constitutive activation of the Bcl10-mediated NF-κB pathway in severe asthma. The observation that complete Bcl10 deficiency severely impaired fibroblast function in an immunodeficient individual (274) is testament to its importance in fibroblast response.

The subcellular localization pattern of Bcl10 and IKBα was different between the bronchial fibroblasts and epithelial cells, indicating cell-dependent functional role of Bcl10 and IKBα. In bronchial epithelial cells, Bcl10 was primarily cytoplasmic in the healthy and asthmatic (Fig. 4.3.2B), while in bronchial fibroblasts, Bcl10 expression was below detection levels in the healthy and was detected in the cytoplasm and membrane/organelle compartments of S-As fibroblasts (Fig. 4.3.2A). Here, it is interesting to note that the NF-κB-independent functions of Bcl10 include actin remodeling. For instance, Bcl10 regulates TCR-induced actin polymerization and cell spreading in T cells, and FcγR-induced actin polymerization and phagocytosis in monocytes/macrophages (312). Subsequently, the role of Bcl10 in actin dynamics, cytoskeletal and membrane remodeling in macrophages was found to entail phagosome formation (313). This may perhaps explain the expression of Bcl10 in the membrane compartment of S-As fibroblasts indicating Bcl10-dependent actin polymerization. Actin dynamics and polymerization is key to the contractile property of fibroblasts (314). Thus, the presence of Bcl10 in the membrane compartment of S-As fibroblasts may signify its role in regulating actin dynamics and contraction of bronchial fibroblasts and by this means, contributing to airway hyperresponsiveness in severe asthma. However, further studies are required to completely understand the physiological relevance of this subcellular localization.

In this study, IKBα was detected in the cytoplasm and membrane/organelle fractions of bronchial epithelial cells, and in all three fractions of bronchial fibroblasts (Fig. 4.3.2B&A). Interestingly, IKBα existed in two different molecular weights. Although primarily a cytosolic protein, there are reports of IκBα localizing to the OMM to inhibit apoptosis, particularly in tumor cells with constitutively active NF-κB (271). This protection of mitochondrial integrity by IκBα thus guarded the cell against the mitochondrial pathway for apoptosis. Moreover, this

protective effect was more prominent in tumor cells with constitutively active NF-κB where IκBα accumulation was observed at the mitochondria. There are however, contradicting reports on the relevance of nuclear localization of IκBα where it has been shown to both inhibit NF-κB binding to the DNA (315) as well as exercise no effect on NF-κB binding to the DNA (316). Therefore, these baseline alterations in subcellular localization of Bcl10 and IKBα observed in bronchial fibroblasts would be more meaningful under stimulation.

Bcl10 was found to be differentially expressed in the sub-epithelium among the varying severities of asthma, ranging from weak expression in control biopsies to moderate expression in mild-to-moderate asthma and strong expression in severe asthma (Fig. 4.3.3). Just as in the case of MALT lymphoma, high Bcl10 expression in fibrotic airway tissues is paradoxical, considering that Bcl10 is a pro-apoptotic CARD-containing adaptor molecule (317). However, certain cellular contexts *in vivo* may influence Bcl10 to behave as an anti-apoptotic molecule. For instance, overexpression of Bcl10 conferred a survival advantage to activated primary B cells even after withdrawal of the activating stimuli (318). Alternately, the subcellular localization of Bcl10 may be a pre-determining factor in explaining this paradox. Although predominantly expressed in the cytoplasm of subepithelial fibroblasts irrespective of the disease severity (Fig. 4.3.3), subcellular fractionation indicated strong expression of Bcl10 also in the organelle/membrane compartment of S-As fibroblasts (Fig. 4.3.2A). However, Bcl10 nuclear expression was detected in the bronchial epithelium of non-asthmatic and asthmatic individuals (Fig. 4.3.3). This altered subcellular localization may confer a pathogenic potential to Bcl10.

Toll-like receptors (TLR), such as TLR4 and TLR2, are important for the adaptive Th2-cytokine-driven inflammatory response in asthma (319, 320). Engagement of the TLR receptor initiates the recruitment and activation of several adaptor molecules resulting in the activation

of multiple signaling cascades, including NF-κB. TLR activation of NF-κB pathway regulates the expression of immunomodulatory and inflammatory mediators. However, the signal transduction of the TLR4-Bcl10-NF-κB axis in asthmatic fibroblasts is far from understood and the role of Bcl10 in TLR4-mediated fibroblast function is largely unknown. Since CARMA1 is exclusive to the immune system, CARMA3/ CARD10 was considered in our study due to its wide pattern of tissue distribution, including fibroblasts (321, 322). As the basal levels of *TLR4*, *CARMA3*, *BCL10* and *MALT1* were upregulated in DHBF when compared to NHBF (Fig. 4.3.1C), we speculated that the TLR4-CBM-3-NF-κB inflammatory axis responds to LPS stimulation in bronchial fibroblasts and stays upregulated in S-As fibroblasts contributing to the constitutive activation of NF-κB in these cells. Here, we show that Bcl10 is a mediator of LPS-induced IL-8 expression (Fig. 4.3.4). LPS stimulation boosted the expression of all three components of the CBM-3 signalosome indicating increased complex formation upon LPS exposure in bronchial fibroblasts. The evidence compiled in our study also indicates a direct link between LPS exposure and expression of components of the CBM-3 complex as well as its downstream targets, including RELA and IL-8, in bronchial fibroblasts.

Severe asthma is characterized by elevated IL-8 levels and associated neutrophilia (104, 323). The S-As fibroblasts used in our study also demonstrated an upregulation of *IL-8* expression at basal levels when compared to non-asthmatic fibroblasts (Fig. 4.1.5C). The ability of these fibroblasts to produce increased levels of ECM proteins as well as pro-inflammatory cytokines have implicated them in remodeling and inflammation, two key processes involved in the pathogenesis of asthma. IL-8 is known to contribute to the pathogenesis of severe asthma by facilitating various features of airway remodeling, including neutrophil recruitment, epithelial-to-mesenchymal transition (324), angiogenesis (325), and proliferation and migration of ASM

cell (326). Here, we showed that Bcl10 mediated the LPS-induced IL-8 expression in bronchial fibroblasts, with considerably higher *IL-8* mRNA transcript levels in S-As fibroblasts, highlighting the pathogenic role of Bcl10-mediated signaling in promoting airway remodeling in severe asthma.

Although extensively studied in immune cells, Bcl10-mediated NF-κB activation is emerging as an important pathway in non-immune cells as well. Angiotensin II promotes liver fibrosis by the activation of CBM-3-dependent NF-κB pathway in hepatocytes (234). Lysophosphatidic acid-induced NF-κB activation and IL-6 production in murine embryonic fibroblasts involves signaling through adapter proteins Bcl10 and Malt1 (327). In one study, Bcl10 was found to be an essential component of TLR4 response in human primary fibroblasts (274) and Bcl10 deficiency was found to abolish TLR4 signaling in response to LPS stimuli and subsequent production of IL-6 and IL-8. Our results are consistent with the observations made in this study.

Numerous lymphoid malignancies are characterized by the constitutive aberrant activation of the NF-κB pro-inflammatory pathway. Here, we demonstrated a similar pattern of constitutive Bcl10-mediated NF-κB activation in airway structural fibroblasts. To further assess whether Bcl10 expression levels in PBMCs correlate to the development of asthma, we studied the gene expression of *BCL10* in PBMCs from healthy donors and asthmatics of varying severities. Interestingly, the pattern of Bcl10 expression in PBMCs was contrary to that in fibroblasts from severe asthma (Fig. 4.3.5A), indicating that the portrayal of lung inflammation by Bcl10 is distinct from its portrayal of systemic inflammation. This stresses the importance of cell-dependent behavior of the Bcl10 pathway in asthma. When compared to healthy subjects, *BCL10* expression showed a mild increase in non-severe asthmatics but significantly declined in severe asthmatics. *BCL10* levels also positively correlated with FEV1/FVC ratio and

negatively correlated with blood serum IgE levels in both asthmatics and severe asthmatics (Fig. 4.3.5B-C). Thus, the Bcl10 profile in blood may help distinguish non-severe asthmatics from the severe asthmatics and thus, may prove beneficial in phenotyping asthma severity and staging.

In summary, the Bcl10 protein was identified to be differentially expressed in the S-As fibroblasts in comparison to non-asthmatic fibroblasts. Furthermore, the differential expression of Bcl10 in the sub-epithelium of airway tissues of varying severities, indicated its importance in the severity of asthma. Overexpression of Bcl10 may confer a survival advantage to the diseased fibroblasts under certain circumstances, pre-disposing them to fibrotic remodeling associated with severe asthma. The CBM-3 complex appears responsible for signal transduction from TLR4 to NF-κB culminating in IL-8 secretion in bronchial fibroblasts, as proposed in Fig. 5.2. The activation of CARMA3/Bcl10/MALT1 signaling in bronchial fibroblasts also stresses their fibrotic potential. This is a reasonable speculation as LPS is known to play an important role in hepatic/liver fibrosis (328, 329). Bronchial fibroblast response to bacterial stimuli is thus, significantly enhanced in severe asthma.

Some limitations of our study include difference in the number of fibroblasts used in each experiment. We were restricted by the number of cells required for the experiment and cells going into senescence after a couple of passages. Diversity in the total cell count obtainable from each donor fibroblast was another factor. The low sample size of patient-derived cells used in our study may not represent the widely heterogenous population of severe asthmatics, considering their individual genetic variations and environmental factors. However, we included fibroblasts from non-smokers alone to reduce the confounding variables. Furthermore, fibroblasts from only severe asthma patients were intentionally included in our study since they

represent a separate phenotype refractory to current medications and in dire need of new therapeutic interventions.

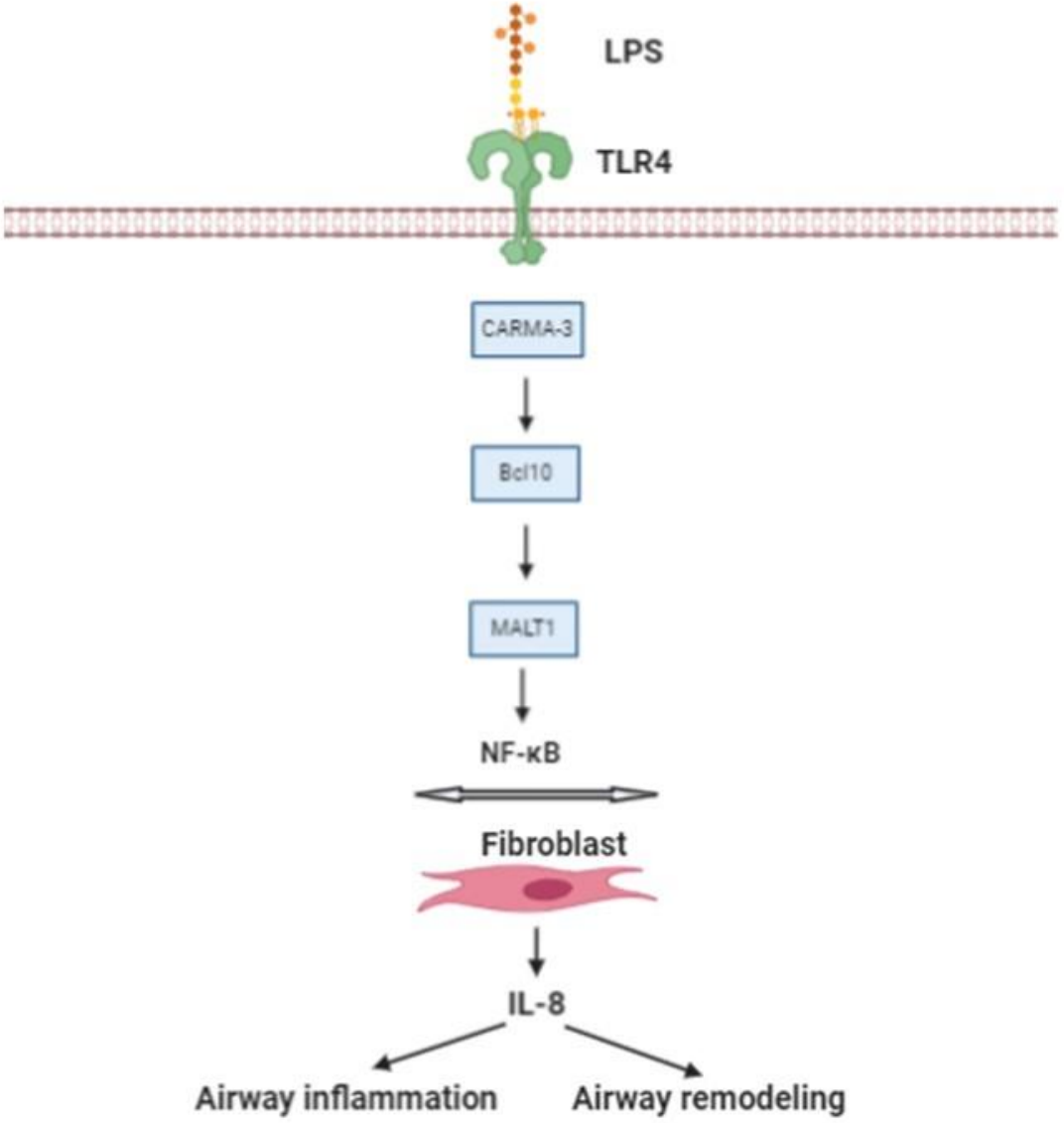

Figure 5.2 Proposed model of CBM-3 signaling in bronchial fibroblasts.

The CARMA3/Bcl10/MALT1 (CBM-3) complex mediates NF-κB activation in response to LPS-TLR4 cross-linking in bronchial fibroblasts. In the airways, LPS stimulation of TLR4 receptor activates the CBM-3 complex which leads to NF-κB activation which has downstream consequences on airway inflammation and remodeling.

5.4 Perspectives and future directions

Interestingly, our study reveals new important findings regarding mitochondrial phenotype in bronchial fibroblasts from patients with severe asthma. Our results demonstrated the presence of mitochondrial damage at baseline in bronchial fibroblasts from severe asthmatics, and manifestation of mitochondrial dysfunction in these cells in the presence of asthma-related cytokines IL-17, TGF-β and IL-13. Mitochondrial structural and functional abnormalities can pave way to airway tissue damage by rendering the fibroblasts more susceptible to the diseased asthma phenotype. Further studies are necessary to elucidate the molecular events driven by mitochondrial dysfunction in severe asthmatic fibroblasts that leads to their persistent activation and fibrotic behavior.

To date, there are no reports on metabolic profiling of asthmatic airway fibroblasts. Generally, cells rely on the highly efficient mitochondrial oxidative phosphorylation (OXPHOS) as the primary source of cellular energy. However, human cancer cells switch the core cellular energy source from mitochondrial OXPHOS to aerobic glycolysis, a phenomenon termed Warburg effect (330). A metabolic shift to aerobic glycolysis was shown to predispose fibroblasts to a pro-fibrotic phenotype (331, 332). TGF-β1-induced mitochondrial biogenesis and aerobic glycolysis that in turn regulated myofibroblast contractility and differentiation (331). Likewise, glycolytic reprogramming contributed to the pathogenesis of lung fibrosis by promoting myofibroblast differentiation (332). We, therefore, speculate that the dysfunctional mitochondria in bronchial fibroblasts induce metabolic reprogramming in severe asthmatics by switching the core cellular energy source from oxidative phosphorylation to glycolysis. It would, therefore, be interesting to compare the glycolytic potential and oxidative phosphorylation capacity in these severe asthmatic fibroblasts in future studies. It would also be

of interest to compare the expression of OXPHOS genes in non-asthmatic and S-As fibroblasts to detect defects in mitochondrial respiration.

Mitochondria being a ubiquitous cellular element may play differential roles in the airway resident cells, namely the fibroblasts, epithelium and smooth muscles, considering their varying contribution to airway structure and function. Therefore, it is essential to study the mitochondrial behavior in each of these resident structural cells separately and to understand their close-knit interactions that lead to the progression of asthma.

We also identified Bcl10-mediated NF-κB pathway as a mechanism contributing to fibrotic remodeling and inflammation in severe asthma. Further studies are, however, essential to delineate the molecular interactions of Bcl10 to develop a more complete understanding to explain the signal transduction in bronchial fibroblasts. We noticed alterations in the subcellular localization of Bcl10 and IκBα in S-As bronchial fibroblasts. However, further studies using different stimuli such as LPS, are required to understand the physiological relevance of their subcellular localizations. Another exciting option is to explore the kinetics of CBM-3 formation in S-As fibroblasts taking into account the constitutive activation of Bcl10-mediated NF-κB pathway in these fibroblasts. Furthermore, the Bcl10 expression profile in blood raises its potential as a biomarker to characterize asthma patient phenotype and severity. The relevance of Bcl10 as a biomarker will be investigated in future studies.

The work presented in this thesis aids us in better understanding of the potential players in the intricate development of airway remodeling in severe asthma. With future experimental work, we hope for the potential development of novel therapeutic strategies with plausible targets of mitochondrial dysfunction, autophagy and Bcl10, all of which have been shown to contribute to asthma pathology.

5.5 Conclusions

Fibrosis is a challenging pathophysiological condition to treat in asthmatics. The inability of current asthma drugs to reverse fibrosis adds to the burden in asthmatic patients (333). To the best of our knowledge, this is the first study to demonstrate perturbations in mitochondrial function in severe asthmatic fibroblasts. We have demonstrated a role for autophagy in the pathogenesis of severe asthma where bronchial fibroblasts expanded from endobronchial biopsies of severe asthmatic patients displayed increased mitophagy flux, reduced mitochondrial membrane potential and increased activation of the AMPKα and mitochondrial biogenesis pathways. Mitochondrial quality control mechanisms may thus, contribute to airway remodeling in severe asthma by promoting the persistence of fibroblasts.

Chronic exposure to asthma-related cytokines, IL-17, TGF-β1 and IL-13, may lead to accumulative mitochondrial damage resulting in mitochondrial dysfunction in bronchial fibroblasts. IL-17 induced mitochondrial abnormalities in bronchial fibroblasts, including lowered $\Delta\Psi m$, increased autophagy, impaired mitochondrial quality control, resulted in increased persistence of these fibroblasts. In summary, our data suggest that IL-17 plays a direct role in modulating mitochondrial homeostasis. TGF-β1 and IL-13 also altered mitochondrial bioenergetics in bronchial fibroblasts reinforcing the pathological behavior of these cytokines in the pathogenesis of severe asthma. Furthermore, IL-17 induced mitochondrial dysfunction and fibrotic signature through the activation of autophagy in bronchial fibroblasts. This provides insights into a potential pathway that contributes to fibrosis in severe asthmatic airways revealing the therapeutic potential of autophagy in ameliorating fibrosis, particularly in severe asthmatic individuals.

The presence of damaged mitochondria in severe asthmatic fibroblasts at baseline and induction of mitochondrial dysfunction in both healthy and severe asthmatic fibroblasts with exposure to asthma-related cytokines have important implications in understanding the mitochondrial contribution to airway remodeling in severe asthma. Restoring mitochondrial integrity may thus, help maintain a normal fibroblast phenotype and thus, attenuate the development of sub-epithelial fibrosis in severe asthmatic patients.

Although NF-κB signaling is a well-characterized pathway in airway inflammation, we for the first time show constitutive activation of Bcl10-mediated NF-κB pathway in severe asthmatic fibroblasts. Furthermore, Bcl10 immunoreactivity in the subepithelium of airway tissues varied in intensity and distribution with increasing severity of asthma relaying its importance in asthma severity. We further identified the CBM-3 complex as a mediator of signal transduction from TLR4 to NF-κB activation of IL-8 gene expression in bronchial fibroblasts, which provides us with insights into the mechanisms of airway inflammation and remodeling associated with these fibroblasts and also with the opportunity of selectively targeting this complex to impede its pathological signaling in severe asthma.

6. Summary

Subepithelial fibrosis is a characteristic feature of airway remodeling in asthma which correlates with disease severity. The accumulation of fibroblasts, their synthesis of extracellular matrix proteins and their innate resistance to apoptosis are characteristics of subepithelial fibrosis observed in severe asthma. Current asthma medications are ineffective in treating airway fibrosis necessitating a deeper understanding of the mechanism of fibrosis in asthma, particularly in the severe phenotype that represents a distinct phenotype with their mixed pattern of neutrophilic-eosinophilic inflammation and glucocorticoid insensitivity making them refractory to currently available therapies. Disrupted mitochondrial quality control mechanisms and mitochondrial dysfunction have been extensively studied in the pathogenesis of other chronic lung diseases, including chronic obstructive pulmonary disease and idiopathic pulmonary fibrosis, but less explored in asthma and severe asthma *per se*.

In this study, we aimed to investigate mitochondrial health in bronchial fibroblasts isolated from airway biopsies of non-asthmatic and severe asthmatic subjects by examining their mitochondrial quality control machinery as a mechanism contributing to fibroblast persistence and thereby, fibrosis in severe asthma. We hypothesized that severe asthmatic fibroblasts exhibit mitochondrial damage resulting in their aberrant pro-fibrotic phenotype. Firstly, we provide evidence of increased activation of mitophagy and mitochondrial biogenesis in severe asthmatic fibroblasts as a result of significantly reduced mitochondrial membrane potential at baseline compared to non-asthmatic controls. Interestingly, these fibroblasts displayed neither an apoptotic nor senescent phenotype, but an adaptive survival mechanism triggered by increased AMPKα phosphorylation.

Cytokines, such as IL-17A, TGF-β1 and IL-13 are enriched in severe asthmatic airways and are important regulators of airway remodeling in asthma. However, their regulation of mitochondrial function and pro-fibrotic phenotype in severe asthmatic fibroblasts is not well characterized. We hypothesized that these asthma-related cytokines impair mitochondrial function in severe asthmatic fibroblasts contributing to the development of fibrosis. To our knowledge, this is the first study to demonstrate that IL-17, TGF-β and IL-13 accelerated mitochondrial dysfunction in bronchial fibroblasts, but to a greater extent in severe asthmatic fibroblasts when compared to non-asthmatic controls. IL-17, in particular, intensified the mitochondrial dysfunction but impaired the mitochondrial quality control machinery in the non-asthmatic and severe asthmatic fibroblasts. Moreover, IL-17 augmented a pro-fibrotic and anti-apoptotic response in both group of fibroblasts. Inhibition of autophagy using bafilomycin-A1 appeared to reduce the need for mitophagy and restored the IL-17 mediated changes in these markers to their basal levels. Bafilomycin-A1 also reversed the IL-17 associated fibrotic response in these fibroblasts, suggesting a role for autophagy in the induction of fibrosis by IL-17 in bronchial fibroblasts. Our findings thus, suggest that IL-17 induced autophagy promotes mitochondrial dysfunction and fibrosis in bronchial fibroblasts from both non-asthmatic and severe asthmatic subjects.

Additionally, we also studied Bcl10-mediated NF-κB activation as a potential pathway regulating fibrotic signaling in severe asthmatic fibroblasts. This is the first report providing evidence of elevated protein expression of Bcl10 in the pathogenesis of severe asthma. Additionally, we also identified the participation of Bcl10-mediated NF-κB pathway in the LPS-induced activation of IL-8 in bronchial fibroblasts, where an exaggerated response was noted in severe asthmatic fibroblasts when compared to controls.

This work finds its importance in describing the role of mitochondria and autophagy in the development of subepithelial fibrosis in severe asthma. Our results demonstrate that the enhanced turnover of mitochondria in bronchial fibroblasts may contribute to their increased survival and pro-fibrotic phenotype observed in severe asthma. Interestingly, the cytokine-mediated induction of mitochondrial dysfunction appears to be associated with the activation of autophagy highlighting the pathological role of autophagy in severe asthma. Our study also provides insights into a potential pathological pathway involving Bcl10 that contributes to the fibrotic signaling in severe asthmatic airways revealing the therapeutic potential of targeting autophagy and Bcl10 signaling in ameliorating fibrosis, particularly in severe asthmatic individuals.

7. Zusammenfassung

Subepitheliale Fibrose ist ein charakteristisches Merkmal der Atemwegsmodellierung bei Asthma, das mit der Schwere der Erkrankung korreliert. Die Anhäufung von Fibroblasten, ihre Synthese von extrazellulären Matrixproteinen und ihre angeborene Resistenz gegen Apoptose sind Merkmale der subepithelialen Fibrose, die bei schwerem Asthma beobachtet wird. Die derzeitigen Asthmamedikamente sind bei der Behandlung von Atemwegsfibrosen unwirksam, was ein tieferes Verständnis des Mechanismus der Fibrose bei Asthma erfordert, insbesondere bei dem schweren Phänotyp, der mit seinem gemischten Muster aus neutrophil-eosinophiler Entzündung und Glukokortikoid-Unempfindlichkeit, das sie für die derzeit verfügbaren Therapien refraktär macht, einen eigenen Phänotyp darstellt. Gestörte mitochondriale Qualitätskontrollmechanismen und mitochondriale Dysfunktion sind in der Pathogenese anderer chronischer Lungenerkrankungen, einschließlich der chronisch obstruktiven Lungenerkrankung und der idiopathischen Lungenfibrose, umfassend untersucht worden, aber bei Asthma und schwerem Asthma an sich weniger erforscht.

In dieser Studie wollten wir den mitochondrialen Gesundheitszustand von Bronchialfibroblasten untersuchen, die aus Atemwegsbiopsien von nicht-asthmatischen und schwer asthmatischen Personen isoliert wurden, indem wir ihre mitochondriale Qualitätskontrollmaschinerie als einen Mechanismus untersuchten, der zur Fibroblastenpersistenz und damit zur Fibrose bei schwerem Asthma beiträgt. Wir stellten die Hypothese auf, dass schwere asthmatische Fibroblasten einen mitochondrialen Schaden aufweisen, der zu ihrem aberranten pro-fibrotischen Phänotyp führt. Erstens liefern wir Hinweise auf eine erhöhte Aktivierung der Mitophagie und der mitochondrialen Biogenese bei schweren asthmatischen Fibroblasten als Folge eines signifikant reduzierten mitochondrialen

Membranpotenzials zu Beginn der Erkrankung im Vergleich zu nicht-asthmatischen Kontrollen. Interessanterweise zeigten diese Fibroblasten weder einen apoptotischen noch einen seneszenten Phänotyp, sondern einen adaptiven Überlebensmechanismus, der durch eine erhöhte AMPK-α-Phosphorylierung ausgelöst wurde.

Zytokine wie IL-17A, TGF-β1 und IL-13 sind in schweren asthmatischen Atemwegen angereichert und wichtige Regulatoren der Atemwegsmodellierung bei Asthma. Ihre Regulation der mitochondrialen Funktion und des pro-fibrotischen Phänotyps bei schweren asthmatischen Fibroblasten ist jedoch nicht gut charakterisiert. Wir stellten die Hypothese auf, dass diese asthmabedingten Zytokine die mitochondriale Funktion in schweren asthmatischen Fibroblasten, die zur Entwicklung einer Fibrose beitragen, beeinträchtigen. Nach unserem Wissen ist dies die erste Studie, die zeigt, dass IL-17, TGF-β und IL-13 die mitochondriale Dysfunktion bei Bronchialfibroblasten, aber in größerem Umfang bei schweren asthmatischen Fibroblasten im Vergleich zu nichtasthmatischen Kontrollen beschleunigte. Insbesondere IL-17 intensivierte die mitochondriale Dysfunktion, beeinträchtigte jedoch die mitochondriale Qualitätskontrollmaschinerie bei den nichtasthmatischen und schweren asthmatischen Fibroblasten. Darüber hinaus verstärkte IL-17 eine pro-fibrotische und anti-apoptotische Reaktion in beiden Gruppen von Fibroblasten. Die Hemmung der Autophagie mit Bafilomycin-A1 schien die Notwendigkeit einer Mitophagie zu reduzieren und stellte die IL-17-vermittelten Veränderungen dieser Marker auf ihre basalen Werte zurück. Bafilomycin-A1 kehrte auch die IL-17-assoziierte fibrotische Reaktion in diesen Fibroblasten um, was auf eine Rolle der Autophagie bei der Induktion einer Fibrose durch IL-17 in Bronchialfibroblasten hindeutet. Unsere Ergebnisse deuten daher darauf hin, dass die durch IL-17 induzierte Autophagie die

mitochondriale Dysfunktion und Fibrose in Bronchialfibroblasten sowohl bei nicht-asthmatischen als auch bei schweren Asthmatikern fördert.

Darüber hinaus untersuchten wir auch die Bcl10-vermittelte NF-κB-Aktivierung als potenziellen Weg zur Regulierung der fibrotischen Signalübertragung bei schweren asthmatischen Fibroblasten. Dies ist der erste Bericht, der Hinweise auf eine erhöhte Proteinexpression von Bcl10 in der Pathogenese von schwerem Asthma liefert. Darüber hinaus identifizierten wir auch die Beteiligung des Bcl10-vermittelten NF-κB-Signalwegs an der LPS-induzierten Aktivierung von IL-8 in Bronchialfibroblasten, wobei bei schweren asthmatischen Fibroblasten im Vergleich zu Kontrollen eine übertriebene Reaktion festgestellt wurde.

Diese Arbeit findet ihre Bedeutung bei der Beschreibung der Rolle der Mitochondrien und der Autophagie bei der Entwicklung einer subepithelialen Fibrose bei schwerem Asthma. Unsere Ergebnisse zeigen, dass der erhöhte Umsatz von Mitochondrien in Bronchialfibroblasten zu deren erhöhter Überlebensrate und dem pro-fibrotischen Phänotyp, der bei schwerem Asthma beobachtet wird, beitragen kann. Interessanterweise scheint die zytokinvermittelte Induktion einer mitochondrialen Dysfunktion mit der Aktivierung der Autophagie in Verbindung zu stehen, was die pathologische Rolle der Autophagie bei schwerem Asthma unterstreicht. Unsere Studie gibt auch Einblicke in einen potenziellen pathologischen Pfad, der Bcl10 einschliesst und zur fibrotischen Signalgebung in den schweren asthmatischen Atemwegen beiträgt, und zeigt das therapeutische Potenzial, die Autophagie und die Bcl10-Signalgebung bei der Verbesserung der Fibrose, insbesondere bei schweren Asthmatikern, zu beeinflussen.

8. Bibliography

1. Network GA. The Global Asthma Report 2018 Auckland, New Zealand2018 [03-04-2020]. Available from: http://globalasthmareport.org/Global%20Asthma%20Report%202018.pdf.
2. Saunders KB. Origin of the word "asthma". Thorax. 1993;48(6):647-.
3. Network GA. About Asthma [03-04-2020]. Available from: http://www.globalasthmanetwork.org/patients/asthma.php.
4. Gerritsen J. Airway responsiveness in teenagers is becoming sexier. American journal of respiratory and critical care medicine. 2008;178(4):321-2.
5. Holgate ST. A brief history of asthma and its mechanisms to modern concepts of disease pathogenesis. Allergy, asthma & immunology research. 2010;2(3):165-71.
6. International consensus report on diagnosis and treatment of asthma. National Heart, Lung, and Blood Institute, National Institutes of Health. Bethesda, Maryland 20892. Publication no. 92-3091, March 1992. The European respiratory journal. 1992;5(5):601-41.
7. Asthma GIf. Global Strategy for Asthma Management and Prevention 2019 [03-04-2020]. Available from: https://ginasthma.org/wp-content/uploads/2019/06/GINA-2019-main-report-June-2019-wms.pdf.
8. Prevention CfDCa. CDC - Asthma 2019 [03-04-2020]. Available from: https://www.cdc.gov/asthma/default.htm.
9. Mallol J, Crane J, von Mutius E, Odhiambo J, Keil U, Stewart A. The International Study of Asthma and Allergies in Childhood (ISAAC) Phase Three: a global synthesis. Allergologia et immunopathologia. 2013;41(2):73-85.
10. To T, Stanojevic S, Moores G, Gershon AS, Bateman ED, Cruz AA, et al. Global asthma prevalence in adults: findings from the cross-sectional world health survey. BMC public health. 2012;12:204.
11. Dharmage SC, Perret JL, Custovic A. Epidemiology of Asthma in Children and Adults. Frontiers in pediatrics. 2019;7:246.
12. Fuhlbrigge AL, Jackson B, Wright RJ. Gender and asthma. Immunology and Allergy Clinics. 2002;22(4):753-89.
13. al-Maskari F, Bener A, al-Kaabi A, al-Suwaidi N, Norman N, Brebner J. Asthma and respiratory symptoms among school children in United Arab Emirates. Allergie et immunologie. 2000;32(4):159-63.
14. Mahboub BH, Al-Hammadi S, Rafique M, Sulaiman N, Pawankar R, Al Redha AI, et al. Population prevalence of asthma and its determinants based on European Community Respiratory Health Survey in the United Arab Emirates. BMC pulmonary medicine. 2012;12:4.
15. Skloot GS. Asthma phenotypes and endotypes: a personalized approach to treatment. Current opinion in pulmonary medicine. 2016;22(1):3-9.
16. Lin TY, Poon AH, Hamid Q. Asthma phenotypes and endotypes. Current opinion in pulmonary medicine. 2013;19(1):18-23.

17. National Asthma Education and Prevention Program. Expert Panel Report: Guidelines for the Diagnosis and Management of Asthma Update on Selected Topics--2002. The Journal of allergy and clinical immunology. 2002;110(5 Suppl):S141-219.
18. Bateman ED, Hurd SS, Barnes PJ, Bousquet J, Drazen JM, FitzGerald JM, et al. Global strategy for asthma management and prevention: GINA executive summary. The European respiratory journal. 2008;31(1):143-78.
19. Chung KF, Wenzel SE, Brozek JL, Bush A, Castro M, Sterk PJ, et al. International ERS/ATS guidelines on definition, evaluation and treatment of severe asthma. The European respiratory journal. 2014;43(2):343-73.
20. Lommatzsch M, Virchow JC. Severe asthma: definition, diagnosis and treatment. Deutsches Arzteblatt international. 2014;111(50):847-55.
21. Awadh N, Muller NL, Park CS, Abboud RT, FitzGerald JM. Airway wall thickness in patients with near fatal asthma and control groups: assessment with high resolution computed tomographic scanning. Thorax. 1998;53(4):248-53.
22. Carroll N, Elliot J, Morton A, James A. The structure of large and small airways in nonfatal and fatal asthma. The American review of respiratory disease. 1993;147(2):405-10.
23. Laitinen LA, Heino M, Laitinen A, Kava T, Haahtela T. Damage of the airway epithelium and bronchial reactivity in patients with asthma. The American review of respiratory disease. 1985;131(4):599-606.
24. Vrugt B, Wilson S, Bron A, Holgate ST, Djukanovic R, Aalbers R. Bronchial angiogenesis in severe glucocorticoid-dependent asthma. The European respiratory journal. 2000;15(6):1014-21.
25. Elliot JG, Jones RL, Abramson MJ, Green FH, Mauad T, McKay KO, et al. Distribution of airway smooth muscle remodelling in asthma: relation to airway inflammation. Respirology (Carlton, Vic). 2015;20(1):66-72.
26. Lutchen KR, Gillis H. Relationship between heterogeneous changes in airway morphometry and lung resistance and elastance. Journal of applied physiology (Bethesda, Md : 1985). 1997;83(4):1192-201.
27. Araujo BB, Dolhnikoff M, Silva LF, Elliot J, Lindeman JH, Ferreira DS, et al. Extracellular matrix components and regulators in the airway smooth muscle in asthma. The European respiratory journal. 2008;32(1):61-9.
28. King GG, James A, Harkness L, Wark PAB. Pathophysiology of severe asthma: We've only just started. Respirology (Carlton, Vic). 2018;23(3):262-71.
29. Murphy DM, O'Byrne PM. Recent advances in the pathophysiology of asthma. Chest. 2010;137(6):1417-26.
30. Holloway JW, Yang IA, Holgate ST. Genetics of allergic disease. The Journal of allergy and clinical immunology. 2010;125(2 Suppl 2):S81-94.
31. Martinez FD. Genes, environments, development and asthma: a reappraisal. The European respiratory journal. 2007;29(1):179-84.
32. Mukherjee AB, Zhang Z. Allergic asthma: influence of genetic and environmental factors. The Journal of biological chemistry. 2011;286(38):32883-9.
33. Vercelli D. Discovering susceptibility genes for asthma and allergy. Nature reviews Immunology. 2008;8(3):169-82.

34. Vercelli D. Genetics and biology of asthma 2010: La' ci darem la mano. The Journal of allergy and clinical immunology. 2010;125(2):347-8.
35. Woodruff PG, Modrek B, Choy DF, Jia G, Abbas AR, Ellwanger A, et al. T-helper type 2-driven inflammation defines major subphenotypes of asthma. American journal of respiratory and critical care medicine. 2009;180(5):388-95.
36. Haldar P, Brightling CE, Singapuri A, Hargadon B, Gupta S, Monteiro W, et al. Outcomes after cessation of mepolizumab therapy in severe eosinophilic asthma: a 12-month follow-up analysis. The Journal of allergy and clinical immunology. 2014;133(3):921-3.
37. Ortega H, Chupp G, Bardin P, Bourdin A, Garcia G, Hartley B, et al. The role of mepolizumab in atopic and nonatopic severe asthma with persistent eosinophilia. The European respiratory journal. 2014;44(1):239-41.
38. De Boever EH, Ashman C, Cahn AP, Locantore NW, Overend P, Pouliquen IJ, et al. Efficacy and safety of an anti-IL-13 mAb in patients with severe asthma: a randomized trial. The Journal of allergy and clinical immunology. 2014;133(4):989-96.
39. Al-Ramli W, Prefontaine D, Chouiali F, Martin JG, Olivenstein R, Lemiere C, et al. T(H)17-associated cytokines (IL-17A and IL-17F) in severe asthma. The Journal of allergy and clinical immunology. 2009;123(5):1185-7.
40. Bullens DM, Truyen E, Coteur L, Dilissen E, Hellings PW, Dupont LJ, et al. IL-17 mRNA in sputum of asthmatic patients: linking T cell driven inflammation and granulocytic influx? Respiratory research. 2006;7:135.
41. Arron JR, Scheerens H, Matthews JG. Redefining approaches to asthma: developing targeted biologic therapies. Advances in pharmacology (San Diego, Calif). 2013;66:1-49.
42. Postma DS, Kerstjens HA. Characteristics of airway hyperresponsiveness in asthma and chronic obstructive pulmonary disease. American journal of respiratory and critical care medicine. 1998;158(5 Pt 3):S187-92.
43. Fowler SJ, Dempsey OJ, Sims EJ, Lipworth BJ. Screening for bronchial hyperresponsiveness using methacholine and adenosine monophosphate. Relationship to asthma severity and beta(2)-receptor genotype. American journal of respiratory and critical care medicine. 2000;162(4 Pt 1):1318-22.
44. Sont JK, Willems LN, Bel EH, van Krieken JH, Vandenbroucke JP, Sterk PJ. Clinical control and histopathologic outcome of asthma when using airway hyperresponsiveness as an additional guide to long-term treatment. The AMPUL Study Group. American journal of respiratory and critical care medicine. 1999;159(4 Pt 1):1043-51.
45. Brutsche MH, Downs SH, Schindler C, Gerbase MW, Schwartz J, Frey M, et al. Bronchial hyperresponsiveness and the development of asthma and COPD in asymptomatic individuals: SAPALDIA cohort study. Thorax. 2006;61(8):671-7.
46. Leuppi JD, Salome CM, Jenkins CR, Anderson SD, Xuan W, Marks GB, et al. Predictive markers of asthma exacerbation during stepwise dose reduction of inhaled corticosteroids. American journal of respiratory and critical care medicine. 2001;163(2):406-12.

47. Yan K, Salome C, Woolcock AJ. Rapid method for measurement of bronchial responsiveness. Thorax. 1983;38(10):760-5.
48. Cockcroft DW, Killian DN, Mellon JJ, Hargreave FE. Bronchial reactivity to inhaled histamine: a method and clinical survey. Clinical allergy. 1977;7(3):235-43.
49. Chapman DG, Irvin CG. Mechanisms of airway hyper-responsiveness in asthma: the past, present and yet to come. Clinical and experimental allergy : journal of the British Society for Allergy and Clinical Immunology. 2015;45(4):706-19.
50. Bumbacea D, Campbell D, Nguyen L, Carr D, Barnes PJ, Robinson D, et al. Parameters associated with persistent airflow obstruction in chronic severe asthma. The European respiratory journal. 2004;24(1):122-8.
51. Cutz E, Levison H, Cooper DM. Ultrastructure of airways in children with asthma. Histopathology. 1978;2(6):407-21.
52. Sumi Y, Hamid Q. Airway remodeling in asthma. Allergology international : official journal of the Japanese Society of Allergology. 2007;56(4):341-8.
53. Huber HL, Koessler KK. THE PATHOLOGY OF BRONCHIAL ASTHMA. Archives of Internal Medicine. 1922;30(6):689-760.
54. Bergeron C, Tulic MK, Hamid Q. Airway remodelling in asthma: from benchside to clinical practice. Canadian respiratory journal. 2010;17(4):e85-93.
55. Little SA, Sproule MW, Cowan MD, Macleod KJ, Robertson M, Love JG, et al. High resolution computed tomographic assessment of airway wall thickness in chronic asthma: reproducibility and relationship with lung function and severity. Thorax. 2002;57(3):247-53.
56. Wadsworth S, Sin D, Dorscheid D. Clinical update on the use of biomarkers of airway inflammation in the management of asthma. Journal of asthma and allergy. 2011;4:77-86.
57. Fahy JV. Type 2 inflammation in asthma--present in most, absent in many. Nature reviews Immunology. 2015;15(1):57-65.
58. Elias JA, Zhu Z, Chupp G, Homer RJ. Airway remodeling in asthma. The Journal of clinical investigation. 1999;104(8):1001-6.
59. Boulet LP, Laviolette M, Turcotte H, Cartier A, Dugas M, Malo JL, et al. Bronchial subepithelial fibrosis correlates with airway responsiveness to methacholine. Chest. 1997;112(1):45-52.
60. Payne DN, Rogers AV, Adelroth E, Bandi V, Guntupalli KK, Bush A, et al. Early thickening of the reticular basement membrane in children with difficult asthma. American journal of respiratory and critical care medicine. 2003;167(1):78-82.
61. Jenkins HA, Cool C, Szefler SJ, Covar R, Brugman S, Gelfand EW, et al. Histopathology of severe childhood asthma: a case series. Chest. 2003;124(1):32-41.
62. Westergren-Thorsson G, Larsen K, Nihlberg K, Andersson-Sjoland A, Hallgren O, Marko-Varga G, et al. Pathological airway remodelling in inflammation. The clinical respiratory journal. 2010;4 Suppl 1:1-8.
63. Alkhouri H, Poppinga WJ, Tania NP, Ammit A, Schuliga M. Regulation of pulmonary inflammation by mesenchymal cells. Pulmonary pharmacology & therapeutics. 2014;29(2):156-65.

64. Postma DS, Timens W. Remodeling in asthma and chronic obstructive pulmonary disease. Proceedings of the American Thoracic Society. 2006;3(5):434-9.
65. Erle DJ, Pytela R. How do integrins integrate? The role of cell adhesion receptors in differentiation and development. American journal of respiratory cell and molecular biology. 1992;6(5):459-60.
66. Johnson PR. Role of human airway smooth muscle in altered extracellular matrix production in asthma. Clinical and experimental pharmacology & physiology. 2001;28(3):233-6.
67. Roberts CR, Burke AK. Remodelling of the extracellular matrix in asthma: proteoglycan synthesis and degradation. Canadian respiratory journal. 1998;5(1):48-50.
68. Bergeron C, Page N, Joubert P, Barbeau B, Hamid Q, Chakir J. Regulation of procollagen I (alpha1) by interleukin-4 in human bronchial fibroblasts: a possible role in airway remodelling in asthma. Clinical and experimental allergy : journal of the British Society for Allergy and Clinical Immunology. 2003;33(10):1389-97.
69. Benayoun L, Druilhe A, Dombret MC, Aubier M, Pretolani M. Airway structural alterations selectively associated with severe asthma. American journal of respiratory and critical care medicine. 2003;167(10):1360-8.
70. Weitoft M, Andersson C, Andersson-Sjoland A, Tufvesson E, Bjermer L, Erjefalt J, et al. Controlled and uncontrolled asthma display distinct alveolar tissue matrix compositions. Respiratory research. 2014;15:67.
71. Boser SR, Mauad T, Araujo-Paulino BB, Mitchell I, Shrestha G, Chiu A, et al. Myofibroblasts are increased in the lung parenchyma in asthma. PloS one. 2017;12(8):e0182378.
72. Kis K, Liu X, Hagood JS. Myofibroblast differentiation and survival in fibrotic disease. Expert reviews in molecular medicine. 2011;13:e27.
73. Chetta A, Foresi A, Del Donno M, Bertorelli G, Pesci A, Olivieri D. Airways remodeling is a distinctive feature of asthma and is related to severity of disease. Chest. 1997;111(4):852-7.
74. Hoshino M, Nakamura Y, Sim JJ. Expression of growth factors and remodelling of the airway wall in bronchial asthma. Thorax. 1998;53(1):21-7.
75. Huang J, Olivenstein R, Taha R, Hamid Q, Ludwig M. Enhanced proteoglycan deposition in the airway wall of atopic asthmatics. American journal of respiratory and critical care medicine. 1999;160(2):725-9.
76. Wenzel SE, Balzar S, Cundall M, Chu HW. Subepithelial basement membrane immunoreactivity for matrix metalloproteinase 9: association with asthma severity, neutrophilic inflammation, and wound repair. The Journal of allergy and clinical immunology. 2003;111(6):1345-52.
77. Johnson C, Galis ZS. Matrix metalloproteinase-2 and -9 differentially regulate smooth muscle cell migration and cell-mediated collagen organization. Arteriosclerosis, thrombosis, and vascular biology. 2004;24(1):54-60.
78. Johnson C, Sung HJ, Lessner SM, Fini ME, Galis ZS. Matrix metalloproteinase-9 is required for adequate angiogenic revascularization of ischemic tissues: potential role in capillary branching. Circulation research. 2004;94(2):262-8.

79. Vignola AM, Riccobono L, Mirabella A, Profita M, Chanez P, Bellia V, et al. Sputum metalloproteinase-9/tissue inhibitor of metalloproteinase-1 ratio correlates with airflow obstruction in asthma and chronic bronchitis. American journal of respiratory and critical care medicine. 1998;158(6):1945-50.
80. Suzuki R, Kato T, Miyazaki Y, Iwata M, Noda Y, Takagi K, et al. Matrix metalloproteinases and tissue inhibitors of matrix metalloproteinases in sputum from patients with bronchial asthma. The Journal of asthma : official journal of the Association for the Care of Asthma. 2001;38(6):477-84.
81. Roche WR, Beasley R, Williams JH, Holgate ST. Subepithelial fibrosis in the bronchi of asthmatics. Lancet (London, England). 1989;1(8637):520-4.
82. Wilson JW, Li X. The measurement of reticular basement membrane and submucosal collagen in the asthmatic airway. Clinical and experimental allergy : journal of the British Society for Allergy and Clinical Immunology. 1997;27(4):363-71.
83. Munakata M. Airway remodeling and airway smooth muscle in asthma. Allergology international : official journal of the Japanese Society of Allergology. 2006;55(3):235-43.
84. Joubert P, Lajoie-Kadoch S, Labonte I, Gounni AS, Maghni K, Wellemans V, et al. CCR3 expression and function in asthmatic airway smooth muscle cells. Journal of immunology (Baltimore, Md : 1950). 2005;175(4):2702-8.
85. Hirst SJ, Martin JG, Bonacci JV, Chan V, Fixman ED, Hamid QA, et al. Proliferative aspects of airway smooth muscle. The Journal of allergy and clinical immunology. 2004;114(2 Suppl):S2-17.
86. Panettieri RA, Jr. Airway smooth muscle: an immunomodulatory cell. The Journal of allergy and clinical immunology. 2002;110(6 Suppl):S269-74.
87. Montefort S, Roberts JA, Beasley R, Holgate ST, Roche WR. The site of disruption of the bronchial epithelium in asthmatic and non-asthmatic subjects. Thorax. 1992;47(7):499-503.
88. Hackett TL, Knight DA. The role of epithelial injury and repair in the origins of asthma. Current opinion in allergy and clinical immunology. 2007;7(1):63-8.
89. Holgate ST. The airway epithelium is central to the pathogenesis of asthma. Allergology international : official journal of the Japanese Society of Allergology. 2008;57(1):1-10.
90. Davies DE. The role of the epithelium in airway remodeling in asthma. Proceedings of the American Thoracic Society. 2009;6(8):678-82.
91. Schleimer RP, Kato A, Kern R, Kuperman D, Avila PC. Epithelium: at the interface of innate and adaptive immune responses. The Journal of allergy and clinical immunology. 2007;120(6):1279-84.
92. Broide DH, Lawrence T, Doherty T, Cho JY, Miller M, McElwain K, et al. Allergen-induced peribronchial fibrosis and mucus production mediated by IkappaB kinase beta-dependent genes in airway epithelium. Proceedings of the National Academy of Sciences of the United States of America. 2005;102(49):17723-8.
93. Mullings RE, Wilson SJ, Puddicombe SM, Lordan JL, Bucchieri F, Djukanovic R, et al. Signal transducer and activator of transcription 6 (STAT-6)

expression and function in asthmatic bronchial epithelium. The Journal of allergy and clinical immunology. 2001;108(5):832-8.
94. Takeda N, Sumi Y, Prefontaine D, Al Abri J, Al Heialy N, Al-Ramli W, et al. Epithelium-derived chemokines induce airway smooth muscle cell migration. Clinical and experimental allergy : journal of the British Society for Allergy and Clinical Immunology. 2009;39(7):1018-26.
95. Jeffery PK, Wardlaw AJ, Nelson FC, Collins JV, Kay AB. Bronchial biopsies in asthma. An ultrastructural, quantitative study and correlation with hyperreactivity. The American review of respiratory disease. 1989;140(6):1745-53.
96. Aikawa T, Shimura S, Sasaki H, Ebina M, Takishima T. Marked goblet cell hyperplasia with mucus accumulation in the airways of patients who died of severe acute asthma attack. Chest. 1992;101(4):916-21.
97. Shale DJ, Ionescu AA. Mucus hypersecretion: a common symptom, a common mechanism? The European respiratory journal. 2004;23(6):797-8.
98. Li X, Wilson JW. Increased vascularity of the bronchial mucosa in mild asthma. American journal of respiratory and critical care medicine. 1997;156(1):229-33.
99. Tanaka H, Yamada G, Saikai T, Hashimoto M, Tanaka S, Suzuki K, et al. Increased airway vascularity in newly diagnosed asthma using a high-magnification bronchovideoscope. American journal of respiratory and critical care medicine. 2003;168(12):1495-9.
100. Hoshino M, Takahashi M, Aoike N. Expression of vascular endothelial growth factor, basic fibroblast growth factor, and angiogenin immunoreactivity in asthmatic airways and its relationship to angiogenesis. The Journal of allergy and clinical immunology. 2001;107(2):295-301.
101. Minshall E, Chakir J, Laviolette M, Molet S, Zhu Z, Olivenstein R, et al. IL-11 expression is increased in severe asthma: association with epithelial cells and eosinophils. The Journal of allergy and clinical immunology. 2000;105(2 Pt 1):232-8.
102. Chakir J, Shannon J, Molet S, Fukakusa M, Elias J, Laviolette M, et al. Airway remodeling-associated mediators in moderate to severe asthma: effect of steroids on TGF-beta, IL-11, IL-17, and type I and type III collagen expression. The Journal of allergy and clinical immunology. 2003;111(6):1293-8.
103. Ramakrishnan RK, Al Heialy S, Hamid Q. Role of IL-17 in asthma pathogenesis and its implications for the clinic. Expert review of respiratory medicine. 2019;13(11):1057-68.
104. Shannon J, Ernst P, Yamauchi Y, Olivenstein R, Lemiere C, Foley S, et al. Differences in airway cytokine profile in severe asthma compared to moderate asthma. Chest. 2008;133(2):420-6.
105. Molet S, Hamid Q, Davoine F, Nutku E, Taha R, Page N, et al. IL-17 is increased in asthmatic airways and induces human bronchial fibroblasts to produce cytokines. The Journal of allergy and clinical immunology. 2001;108(3):430-8.
106. Loubaki L, Hadj-Salem I, Fakhfakh R, Jacques E, Plante S, Boisvert M, et al. Co-culture of human bronchial fibroblasts and CD4+ T cells increases Th17 cytokine signature. PloS one. 2013;8(12):e81983.

107. Camargo LDN, Righetti RF, Aristoteles L, Dos Santos TM, de Souza FCR, Fukuzaki S, et al. Effects of Anti-IL-17 on Inflammation, Remodeling, and Oxidative Stress in an Experimental Model of Asthma Exacerbated by LPS. Frontiers in immunology. 2017;8:1835.
108. Yang YC, Zhang N, Van Crombruggen K, Hu GH, Hong SL, Bachert C. Transforming growth factor-beta1 in inflammatory airway disease: a key for understanding inflammation and remodeling. Allergy. 2012;67(10):1193-202.
109. Undevia NS, Dorscheid DR, Marroquin BA, Gugliotta WL, Tse R, White SR. Smad and p38-MAPK signaling mediates apoptotic effects of transforming growth factor-beta1 in human airway epithelial cells. American journal of physiology Lung cellular and molecular physiology. 2004;287(3):L515-24.
110. Chu HW, Balzar S, Seedorf GJ, Westcott JY, Trudeau JB, Silkoff P, et al. Transforming growth factor-beta2 induces bronchial epithelial mucin expression in asthma. The American journal of pathology. 2004;165(4):1097-106.
111. Michalik M, Pierzchalska M, Legutko A, Ura M, Ostaszewska A, Soja J, et al. Asthmatic bronchial fibroblasts demonstrate enhanced potential to differentiate into myofibroblasts in culture. Medical science monitor : international medical journal of experimental and clinical research. 2009;15(7):Br194-201.
112. Khalil N, Xu YD, O'Connor R, Duronio V. Proliferation of pulmonary interstitial fibroblasts is mediated by transforming growth factor-beta1-induced release of extracellular fibroblast growth factor-2 and phosphorylation of p38 MAPK and JNK. The Journal of biological chemistry. 2005;280(52):43000-9.
113. Leivonen SK, Hakkinen L, Liu D, Kahari VM. Smad3 and extracellular signal-regulated kinase 1/2 coordinately mediate transforming growth factor-beta-induced expression of connective tissue growth factor in human fibroblasts. The Journal of investigative dermatology. 2005;124(6):1162-9.
114. Chen G, Khalil N. TGF-beta1 increases proliferation of airway smooth muscle cells by phosphorylation of map kinases. Respiratory research. 2006;7:2.
115. Ito I, Fixman ED, Asai K, Yoshida M, Gounni AS, Martin JG, et al. Platelet-derived growth factor and transforming growth factor-beta modulate the expression of matrix metalloproteinases and migratory function of human airway smooth muscle cells. Clinical and experimental allergy : journal of the British Society for Allergy and Clinical Immunology. 2009;39(9):1370-80.
116. Kobayashi T, Liu X, Wen FQ, Fang Q, Abe S, Wang XQ, et al. Smad3 mediates TGF-beta1 induction of VEGF production in lung fibroblasts. Biochemical and biophysical research communications. 2005;327(2):393-8.
117. Ingram JL, Huggins MJ, Church TD, Li Y, Francisco DC, Degan S, et al. Airway fibroblasts in asthma manifest an invasive phenotype. American journal of respiratory and critical care medicine. 2011;183(12):1625-32.
118. Firszt R, Francisco D, Church TD, Thomas JM, Ingram JL, Kraft M. Interleukin-13 induces collagen type-1 expression through matrix metalloproteinase-2 and transforming growth factor-beta1 in airway fibroblasts in asthma. The European respiratory journal. 2014;43(2):464-73.
119. Booth BW, Adler KB, Bonner JC, Tournier F, Martin LD. Interleukin-13 induces proliferation of human airway epithelial cells in vitro via a mechanism

mediated by transforming growth factor-alpha. American journal of respiratory cell and molecular biology. 2001;25(6):739-43.
120. Wills-Karp M, Luyimbazi J, Xu X, Schofield B, Neben TY, Karp CL, et al. Interleukin-13: central mediator of allergic asthma. Science (New York, NY). 1998;282(5397):2258-61.
121. Grunig G, Warnock M, Wakil AE, Venkayya R, Brombacher F, Rennick DM, et al. Requirement for IL-13 independently of IL-4 in experimental asthma. Science (New York, NY). 1998;282(5397):2261-3.
122. Perkins C, Wills-Karp M, Finkelman FD. IL-4 induces IL-13-independent allergic airway inflammation. The Journal of allergy and clinical immunology. 2006;118(2):410-9.
123. Erle DJ, Sheppard D. The cell biology of asthma. The Journal of cell biology. 2014;205(5):621-31.
124. Hoshino M, Nakamura Y, Hamid QA. Gene expression of vascular endothelial growth factor and its receptors and angiogenesis in bronchial asthma. The Journal of allergy and clinical immunology. 2001;107(6):1034-8.
125. Lee CG, Link H, Baluk P, Homer RJ, Chapoval S, Bhandari V, et al. Vascular endothelial growth factor (VEGF) induces remodeling and enhances TH2-mediated sensitization and inflammation in the lung. Nature medicine. 2004;10(10):1095-103.
126. Focusing on autophagy. Nature cell biology. 2010;12(9):813.
127. Levine B, Klionsky DJ. Development by self-digestion: molecular mechanisms and biological functions of autophagy. Developmental cell. 2004;6(4):463-77.
128. Levine B, Kroemer G. Autophagy in the pathogenesis of disease. Cell. 2008;132(1):27-42.
129. Shintani T, Klionsky DJ. Autophagy in health and disease: a double-edged sword. Science (New York, NY). 2004;306(5698):990-5.
130. Russell RC, Tian Y, Yuan H, Park HW, Chang YY, Kim J, et al. ULK1 induces autophagy by phosphorylating Beclin-1 and activating VPS34 lipid kinase. Nature cell biology. 2013;15(7):741-50.
131. Dooley HC, Razi M, Polson HE, Girardin SE, Wilson MI, Tooze SA. WIPI2 links LC3 conjugation with PI3P, autophagosome formation, and pathogen clearance by recruiting Atg12-5-16L1. Molecular cell. 2014;55(2):238-52.
132. Aggarwal S, Mannam P, Zhang J. Differential regulation of autophagy and mitophagy in pulmonary diseases. American journal of physiology Lung cellular and molecular physiology. 2016;311(2):L433-52.
133. Klionsky DJ, Abdelmohsen K, Abe A, Abedin MJ, Abeliovich H, Acevedo Arozena A, et al. Guidelines for the use and interpretation of assays for monitoring autophagy (3rd edition). Autophagy. 2016;12(1):1-222.
134. Mathew R, Karantza-Wadsworth V, White E. Role of autophagy in cancer. Nature reviews Cancer. 2007;7(12):961-7.
135. Kuma A, Hatano M, Matsui M, Yamamoto A, Nakaya H, Yoshimori T, et al. The role of autophagy during the early neonatal starvation period. Nature. 2004;432(7020):1032-6.

136. Lum JJ, Bauer DE, Kong M, Harris MH, Li C, Lindsten T, et al. Growth factor regulation of autophagy and cell survival in the absence of apoptosis. Cell. 2005;120(2):237-48.
137. Yu L, Alva A, Su H, Dutt P, Freundt E, Welsh S, et al. Regulation of an ATG7-beclin 1 program of autophagic cell death by caspase-8. Science (New York, NY). 2004;304(5676):1500-2.
138. Yousefi S, Perozzo R, Schmid I, Ziemiecki A, Schaffner T, Scapozza L, et al. Calpain-mediated cleavage of Atg5 switches autophagy to apoptosis. Nature cell biology. 2006;8(10):1124-32.
139. Maiuri MC, Zalckvar E, Kimchi A, Kroemer G. Self-eating and self-killing: crosstalk between autophagy and apoptosis. Nature reviews Molecular cell biology. 2007;8(9):741-52.
140. He C, Klionsky DJ. Regulation mechanisms and signaling pathways of autophagy. Annual review of genetics. 2009;43:67-93.
141. Klionsky DJ, Abdalla FC, Abeliovich H, Abraham RT, Acevedo-Arozena A, Adeli K, et al. Guidelines for the use and interpretation of assays for monitoring autophagy. Autophagy. 2012;8(4):445-544.
142. Kirisako T, Baba M, Ishihara N, Miyazawa K, Ohsumi M, Yoshimori T, et al. Formation process of autophagosome is traced with Apg8/Aut7p in yeast. The Journal of cell biology. 1999;147(2):435-46.
143. Chu CT. Autophagic stress in neuronal injury and disease. Journal of neuropathology and experimental neurology. 2006;65(5):423-32.
144. Saftig P, Klumperman J. Lysosome biogenesis and lysosomal membrane proteins: trafficking meets function. Nature reviews Molecular cell biology. 2009;10(9):623-35.
145. Luzio JP, Pryor PR, Bright NA. Lysosomes: fusion and function. Nature reviews Molecular cell biology. 2007;8(8):622-32.
146. Zeki AA, Yeganeh B, Kenyon NJ, Post M, Ghavami S. Autophagy in airway diseases: a new frontier in human asthma? Allergy. 2016;71(1):5-14.
147. Yang YP, Hu LF, Zheng HF, Mao CJ, Hu WD, Xiong KP, et al. Application and interpretation of current autophagy inhibitors and activators. Acta pharmacologica Sinica. 2013;34(5):625-35.
148. Kim DH, Sarbassov DD, Ali SM, King JE, Latek RR, Erdjument-Bromage H, et al. mTOR interacts with raptor to form a nutrient-sensitive complex that signals to the cell growth machinery. Cell. 2002;110(2):163-75.
149. Tanemura M, Ohmura Y, Deguchi T, Machida T, Tsukamoto R, Wada H, et al. Rapamycin causes upregulation of autophagy and impairs islets function both in vitro and in vivo. American journal of transplantation : official journal of the American Society of Transplantation and the American Society of Transplant Surgeons. 2012;12(1):102-14.
150. Yamamoto A, Tagawa Y, Yoshimori T, Moriyama Y, Masaki R, Tashiro Y. Bafilomycin A1 prevents maturation of autophagic vacuoles by inhibiting fusion between autophagosomes and lysosomes in rat hepatoma cell line, H-4-II-E cells. Cell structure and function. 1998;23(1):33-42.

151. Takatsuka C, Inoue Y, Matsuoka K, Moriyasu Y. 3-methyladenine inhibits autophagy in tobacco culture cells under sucrose starvation conditions. Plant & cell physiology. 2004;45(3):265-74.
152. Seglen PO, Gordon PB. 3-Methyladenine: specific inhibitor of autophagic/lysosomal protein degradation in isolated rat hepatocytes. Proceedings of the National Academy of Sciences of the United States of America. 1982;79(6):1889-92.
153. Poon AH, Chouiali F, Tse SM, Litonjua AA, Hussain SN, Baglole CJ, et al. Genetic and histologic evidence for autophagy in asthma pathogenesis. The Journal of allergy and clinical immunology. 2012;129(2):569-71.
154. Martin LJ, Gupta J, Jyothula SS, Butsch Kovacic M, Biagini Myers JM, Patterson TL, et al. Functional variant in the autophagy-related 5 gene promotor is associated with childhood asthma. PloS one. 2012;7(4):e33454.
155. Nimmerjahn F, Milosevic S, Behrends U, Jaffee EM, Pardoll DM, Bornkamm GW, et al. Major histocompatibility complex class II-restricted presentation of a cytosolic antigen by autophagy. European journal of immunology. 2003;33(5):1250-9.
156. Dorfel D, Appel S, Grunebach F, Weck MM, Muller MR, Heine A, et al. Processing and presentation of HLA class I and II epitopes by dendritic cells after transfection with in vitro-transcribed MUC1 RNA. Blood. 2005;105(8):3199-205.
157. Paludan C, Schmid D, Landthaler M, Vockerodt M, Kube D, Tuschl T, et al. Endogenous MHC class II processing of a viral nuclear antigen after autophagy. Science (New York, NY). 2005;307(5709):593-6.
158. Pua HH, Dzhagalov I, Chuck M, Mizushima N, He YW. A critical role for the autophagy gene Atg5 in T cell survival and proliferation. The Journal of experimental medicine. 2007;204(1):25-31.
159. Pua HH, Guo J, Komatsu M, He YW. Autophagy is essential for mitochondrial clearance in mature T lymphocytes. Journal of immunology (Baltimore, Md : 1950). 2009;182(7):4046-55.
160. Paul S, Kashyap AK, Jia W, He YW, Schaefer BC. Selective autophagy of the adaptor protein Bcl10 modulates T cell receptor activation of NF-kappaB. Immunity. 2012;36(6):947-58.
161. Wei J, Long L, Yang K, Guy C, Shrestha S, Chen Z, et al. Autophagy enforces functional integrity of regulatory T cells by coupling environmental cues and metabolic homeostasis. Nature immunology. 2016;17(3):277-85.
162. Miller BC, Zhao Z, Stephenson LM, Cadwell K, Pua HH, Lee HK, et al. The autophagy gene ATG5 plays an essential role in B lymphocyte development. Autophagy. 2008;4(3):309-14.
163. Xia F, Deng C, Jiang Y, Qu Y, Deng J, Cai Z, et al. IL4 (interleukin 4) induces autophagy in B cells leading to exacerbated asthma. Autophagy. 2018;14(3):450-64.
164. McAlinden KD, Deshpande DA, Ghavami S, Xenaki D, Sohal SS, Oliver BG, et al. Autophagy Activation in Asthma Airways Remodeling. American journal of respiratory cell and molecular biology. 2019;60(5):541-53.

165. Ghavami S, Yeganeh B, Serebrin A, Mutawe MM, Sharma P, McNeill KD, et al. Autophagy Regulates Tgf-Beta1 Induced Fibrosis In Human Airway Smooth Muscle Cells. A67 SURVIVOR-RCMB: AUTOPHAGY, SENESCENCE, AND SURVIVAL. American Thoracic Society International Conference Abstracts: American Thoracic Society; 2011. p. A2110-A.
166. Poon AH, Choy DF, Chouiali F, Ramakrishnan RK, Mahboub B, Audusseau S, et al. Increased Autophagy-Related 5 Gene Expression Is Associated with Collagen Expression in the Airways of Refractory Asthmatics. Frontiers in immunology. 2017;8:355.
167. Dickinson JD, Alevy Y, Malvin NP, Patel KK, Gunsten SP, Holtzman MJ, et al. IL13 activates autophagy to regulate secretion in airway epithelial cells. Autophagy. 2016;12(2):397-409.
168. Fang C, Gu L, Smerin D, Mao S, Xiong X. The Interrelation between Reactive Oxygen Species and Autophagy in Neurological Disorders. Oxidative medicine and cellular longevity. 2017;2017:8495160.
169. Zhou Z, Jiang X, Liu D, Fan Z, Hu X, Yan J, et al. Autophagy is involved in influenza A virus replication. Autophagy. 2009;5(3):321-8.
170. Li M, Li J, Zeng R, Yang J, Liu J, Zhang Z, et al. Respiratory Syncytial Virus Replication Is Promoted by Autophagy-Mediated Inhibition of Apoptosis. Journal of virology. 2018;92(8).
171. Abdoli A, Alirezaei M, Mehrbod P, Forouzanfar F. Autophagy: The multi-purpose bridge in viral infections and host cells. Reviews in medical virology. 2018;28(4):e1973.
172. Gannage M, Dormann D, Albrecht R, Dengjel J, Torossi T, Ramer PC, et al. Matrix protein 2 of influenza A virus blocks autophagosome fusion with lysosomes. Cell host & microbe. 2009;6(4):367-80.
173. Cottam EM, Whelband MC, Wileman T. Coronavirus NSP6 restricts autophagosome expansion. Autophagy. 2014;10(8):1426-41.
174. Ban GY, Pham DL, Trinh TH, Lee SI, Suh DH, Yang EM, et al. Autophagy mechanisms in sputum and peripheral blood cells of patients with severe asthma: a new therapeutic target. Clinical and experimental allergy : journal of the British Society for Allergy and Clinical Immunology. 2016;46(1):48-59.
175. Liu JN, Suh DH, Trinh HK, Chwae YJ, Park HS, Shin YS. The role of autophagy in allergic inflammation: a new target for severe asthma. Experimental & molecular medicine. 2016;48(7):e243.
176. Pham DL, Ban GY, Kim SH, Shin YS, Ye YM, Chwae YJ, et al. Neutrophil autophagy and extracellular DNA traps contribute to airway inflammation in severe asthma. Clinical and experimental allergy : journal of the British Society for Allergy and Clinical Immunology. 2017;47(1):57-70.
177. Tsubouchi K, Araya J, Kuwano K. PINK1-PARK2-mediated mitophagy in COPD and IPF pathogeneses. Inflammation and regeneration. 2018;38:18.
178. Kobayashi K, Araya J, Minagawa S, Hara H, Saito N, Kadota T, et al. Involvement of PARK2-Mediated Mitophagy in Idiopathic Pulmonary Fibrosis Pathogenesis. Journal of immunology (Baltimore, Md : 1950). 2016;197(2):504-16.

179. Lee HC, Wei YH. Mitochondrial role in life and death of the cell. Journal of biomedical science. 2000;7(1):2-15.
180. Smeitink J, van den Heuvel L, DiMauro S. The genetics and pathology of oxidative phosphorylation. Nature reviews Genetics. 2001;2(5):342-52.
181. Nunnari J, Suomalainen A. Mitochondria: in sickness and in health. Cell. 2012;148(6):1145-59.
182. Marchi S, Giorgi C, Suski JM, Agnoletto C, Bononi A, Bonora M, et al. Mitochondria-ros crosstalk in the control of cell death and aging. Journal of signal transduction. 2012;2012:329635.
183. Li X, Fang P, Mai J, Choi ET, Wang H, Yang XF. Targeting mitochondrial reactive oxygen species as novel therapy for inflammatory diseases and cancers. Journal of hematology & oncology. 2013;6:19.
184. Rehman J. Empowering self-renewal and differentiation: the role of mitochondria in stem cells. Journal of molecular medicine (Berlin, Germany). 2010;88(10):981-6.
185. Sena LA, Chandel NS. Physiological roles of mitochondrial reactive oxygen species. Molecular cell. 2012;48(2):158-67.
186. Wood LG, Gibson PG, Garg ML. Biomarkers of lipid peroxidation, airway inflammation and asthma. The European respiratory journal. 2003;21(1):177-86.
187. Servais S, Boussouar A, Molnar A, Douki T, Pequignot JM, Favier R. Age-related sensitivity to lung oxidative stress during ozone exposure. Free radical research. 2005;39(3):305-16.
188. Prakash YS, Pabelick CM, Sieck GC. Mitochondrial Dysfunction in Airway Disease. Chest. 2017;152(3):618-26.
189. Pickles S, Vigie P, Youle RJ. Mitophagy and Quality Control Mechanisms in Mitochondrial Maintenance. Current biology : CB. 2018;28(4):R170-r85.
190. Narendra D, Tanaka A, Suen DF, Youle RJ. Parkin is recruited selectively to impaired mitochondria and promotes their autophagy. The Journal of cell biology. 2008;183(5):795-803.
191. Lin W, Kang UJ. Characterization of PINK1 processing, stability, and subcellular localization. Journal of neurochemistry. 2008;106(1):464-74.
192. Matsuda N, Sato S, Shiba K, Okatsu K, Saisho K, Gautier CA, et al. PINK1 stabilized by mitochondrial depolarization recruits Parkin to damaged mitochondria and activates latent Parkin for mitophagy. The Journal of cell biology. 2010;189(2):211-21.
193. Gegg ME, Cooper JM, Chau KY, Rojo M, Schapira AH, Taanman JW. Mitofusin 1 and mitofusin 2 are ubiquitinated in a PINK1/parkin-dependent manner upon induction of mitophagy. Human molecular genetics. 2010;19(24):4861-70.
194. Wang X, Winter D, Ashrafi G, Schlehe J, Wong YL, Selkoe D, et al. PINK1 and Parkin target Miro for phosphorylation and degradation to arrest mitochondrial motility. Cell. 2011;147(4):893-906.
195. Kubli DA, Gustafsson AB. Mitochondria and mitophagy: the yin and yang of cell death control. Circulation research. 2012;111(9):1208-21.

196. Canto C, Jiang LQ, Deshmukh AS, Mataki C, Coste A, Lagouge M, et al. Interdependence of AMPK and SIRT1 for metabolic adaptation to fasting and exercise in skeletal muscle. Cell metabolism. 2010;11(3):213-9.
197. Jeninga EH, Schoonjans K, Auwerx J. Reversible acetylation of PGC-1: connecting energy sensors and effectors to guarantee metabolic flexibility. Oncogene. 2010;29(33):4617-24.
198. Sureshbabu A, Bhandari V. Targeting mitochondrial dysfunction in lung diseases: emphasis on mitophagy. Frontiers in physiology. 2013;4:384.
199. Westermann B. Mitochondrial fusion and fission in cell life and death. Nature reviews Molecular cell biology. 2010;11(12):872-84.
200. Hoppins S, Lackner L, Nunnari J. The machines that divide and fuse mitochondria. Annual review of biochemistry. 2007;76:751-80.
201. Berman SB, Pineda FJ, Hardwick JM. Mitochondrial fission and fusion dynamics: the long and short of it. Cell death and differentiation. 2008;15(7):1147-52.
202. Twig G, Shirihai OS. The interplay between mitochondrial dynamics and mitophagy. Antioxidants & redox signaling. 2011;14(10):1939-51.
203. Choi AM, Ryter SW, Levine B. Autophagy in human health and disease. The New England journal of medicine. 2013;368(19):1845-6.
204. Ryter SW, Choi AM. Autophagy in lung disease pathogenesis and therapeutics. Redox biology. 2015;4:215-25.
205. Ryter SW, Rosas IO, Owen CA, Martinez FJ, Choi ME, Lee CG, et al. Mitochondrial Dysfunction as a Pathogenic Mediator of Chronic Obstructive Pulmonary Disease and Idiopathic Pulmonary Fibrosis. Annals of the American Thoracic Society. 2018;15(Suppl 4):S266-s72.
206. Rangarajan S, Bernard K, Thannickal VJ. Mitochondrial Dysfunction in Pulmonary Fibrosis. Annals of the American Thoracic Society. 2017;14(Supplement_5):S383-s8.
207. Malsin ES, Kamp DW. The mitochondria in lung fibrosis: friend or foe? Translational research : the journal of laboratory and clinical medicine. 2018;202:1-23.
208. Heinzmann A, Thoma C, Dietrich H, Deichmann KA. Identification of common polymorphisms in the mitochondrial genome. Allergy. 2003;58(8):830-1.
209. Mabalirajan U, Dinda AK, Kumar S, Roshan R, Gupta P, Sharma SK, et al. Mitochondrial structural changes and dysfunction are associated with experimental allergic asthma. Journal of immunology (Baltimore, Md : 1950). 2008;181(5):3540-8.
210. Aguilera-Aguirre L, Bacsi A, Saavedra-Molina A, Kurosky A, Sur S, Boldogh I. Mitochondrial dysfunction increases allergic airway inflammation. Journal of immunology (Baltimore, Md : 1950). 2009;183(8):5379-87.
211. Konradova V, Copova C, Sukova B, Houstek J. Ultrastructure of the bronchial epithelium in three children with asthma. Pediatric pulmonology. 1985;1(4):182-7.

212. Comhair SA, Bhathena PR, Dweik RA, Kavuru M, Erzurum SC. Rapid loss of superoxide dismutase activity during antigen-induced asthmatic response. Lancet (London, England). 2000;355(9204):624.
213. Fitzpatrick AM, Teague WG, Holguin F, Yeh M, Brown LA. Airway glutathione homeostasis is altered in children with severe asthma: evidence for oxidant stress. The Journal of allergy and clinical immunology. 2009;123(1):146-52.e8.
214. Jones M, Mitchell P, Wang JJ, Sue C. MELAS A3243G mitochondrial DNA mutation and age related maculopathy. American journal of ophthalmology. 2004;138(6):1051-3.
215. Raby BA, Klanderman B, Murphy A, Mazza S, Camargo CA, Jr., Silverman EK, et al. A common mitochondrial haplogroup is associated with elevated total serum IgE levels. The Journal of allergy and clinical immunology. 2007;120(2):351-8.
216. Schuliga M. NF-kappaB Signaling in Chronic Inflammatory Airway Disease. Biomolecules. 2015;5(3):1266-83.
217. Willis TG, Jadayel DM, Du MQ, Peng H, Perry AR, Abdul-Rauf M, et al. Bcl10 is involved in t(1;14)(p22;q32) of MALT B cell lymphoma and mutated in multiple tumor types. Cell. 1999;96(1):35-45.
218. Ye H, Dogan A, Karran L, Willis TG, Chen L, Wlodarska I, et al. BCL10 expression in normal and neoplastic lymphoid tissue. Nuclear localization in MALT lymphoma. The American journal of pathology. 2000;157(4):1147-54.
219. Lucas PC, Yonezumi M, Inohara N, McAllister-Lucas LM, Abazeed ME, Chen FF, et al. Bcl10 and MALT1, independent targets of chromosomal translocation in malt lymphoma, cooperate in a novel NF-kappa B signaling pathway. The Journal of biological chemistry. 2001;276(22):19012-9.
220. Gaide O, Martinon F, Micheau O, Bonnet D, Thome M, Tschopp J. Carma1, a CARD-containing binding partner of Bcl10, induces Bcl10 phosphorylation and NF-kappaB activation. FEBS letters. 2001;496(2-3):121-7.
221. Ruland J, Hartjes L. CARD-BCL-10-MALT1 signalling in protective and pathological immunity. Nature reviews Immunology. 2019;19(2):118-34.
222. Oeckinghaus A, Wegener E, Welteke V, Ferch U, Arslan SC, Ruland J, et al. Malt1 ubiquitination triggers NF-kappaB signaling upon T-cell activation. The EMBO journal. 2007;26(22):4634-45.
223. Wu CJ, Ashwell JD. NEMO recognition of ubiquitinated Bcl10 is required for T cell receptor-mediated NF-kappaB activation. Proceedings of the National Academy of Sciences of the United States of America. 2008;105(8):3023-8.
224. Zhou H, Wertz I, O'Rourke K, Ultsch M, Seshagiri S, Eby M, et al. Bcl10 activates the NF-kappaB pathway through ubiquitination of NEMO. Nature. 2004;427(6970):167-71.
225. Blonska M, Pappu BP, Matsumoto R, Li H, Su B, Wang D, et al. The CARMA1-Bcl10 signaling complex selectively regulates JNK2 kinase in the T cell receptor-signaling pathway. Immunity. 2007;26(1):55-66.
226. Bhatt D, Ghosh S. Regulation of the NF-kappaB-Mediated Transcription of Inflammatory Genes. Frontiers in immunology. 2014;5:71.

227. Turvey SE, Durandy A, Fischer A, Fung SY, Geha RS, Gewies A, et al. The CARD11-BCL10-MALT1 (CBM) signalosome complex: Stepping into the limelight of human primary immunodeficiency. The Journal of allergy and clinical immunology. 2014;134(2):276-84.
228. Gehring T, Seeholzer T, Krappmann D. BCL10 - Bridging CARDs to Immune Activation. Frontiers in immunology. 2018;9:1539.
229. Schmidt-Supprian M, Tian J, Grant EP, Pasparakis M, Maehr R, Ovaa H, et al. Differential dependence of CD4+CD25+ regulatory and natural killer-like T cells on signals leading to NF-kappaB activation. Proceedings of the National Academy of Sciences of the United States of America. 2004;101(13):4566-71.
230. Xue L, Morris SW, Orihuela C, Tuomanen E, Cui X, Wen R, et al. Defective development and function of Bcl10-deficient follicular, marginal zone and B1 B cells. Nature immunology. 2003;4(9):857-65.
231. Chen Y, Pappu BP, Zeng H, Xue L, Morris SW, Lin X, et al. B cell lymphoma 10 is essential for FcepsilonR-mediated degranulation and IL-6 production in mast cells. Journal of immunology (Baltimore, Md : 1950). 2007;178(1):49-57.
232. Klemm S, Gutermuth J, Hultner L, Sparwasser T, Behrendt H, Peschel C, et al. The Bcl10-Malt1 complex segregates Fc epsilon RI-mediated nuclear factor kappa B activation and cytokine production from mast cell degranulation. The Journal of experimental medicine. 2006;203(2):337-47.
233. Wang D, You Y, Lin PC, Xue L, Morris SW, Zeng H, et al. Bcl10 plays a critical role in NF-kappaB activation induced by G protein-coupled receptors. Proceedings of the National Academy of Sciences of the United States of America. 2007;104(1):145-50.
234. McAllister-Lucas LM, Ruland J, Siu K, Jin X, Gu S, Kim DS, et al. CARMA3/Bcl10/MALT1-dependent NF-kappaB activation mediates angiotensin II-responsive inflammatory signaling in nonimmune cells. Proceedings of the National Academy of Sciences of the United States of America. 2007;104(1):139-44.
235. Marko L, Henke N, Park JK, Spallek B, Qadri F, Balogh A, et al. Bcl10 mediates angiotensin II-induced cardiac damage and electrical remodeling. Hypertension (Dallas, Tex : 1979). 2014;64(5):1032-9.
236. Bhattacharyya S, Borthakur A, Pant N, Dudeja PK, Tobacman JK. Bcl10 mediates LPS-induced activation of NF-kappaB and IL-8 in human intestinal epithelial cells. American journal of physiology Gastrointestinal and liver physiology. 2007;293(2):G429-37.
237. Scharschmidt E, Wegener E, Heissmeyer V, Rao A, Krappmann D. Degradation of Bcl10 induced by T-cell activation negatively regulates NF-kappa B signaling. Molecular and cellular biology. 2004;24(9):3860-73.
238. Lobry C, Lopez T, Israel A, Weil R. Negative feedback loop in T cell activation through IkappaB kinase-induced phosphorylation and degradation of Bcl10. Proceedings of the National Academy of Sciences of the United States of America. 2007;104(3):908-13.
239. Panariti A, Baglole CJ, Sanchez V, Eidelman DH, Hussain S, Olivenstein R, et al. Interleukin-17A and vascular remodelling in severe asthma; lack of evidence

for a direct role. Clinical and experimental allergy : journal of the British Society for Allergy and Clinical Immunology. 2018;48(4):365-78.
240. Wiegman CH, Michaeloudes C, Haji G, Narang P, Clarke CJ, Russell KE, et al. Oxidative stress-induced mitochondrial dysfunction drives inflammation and airway smooth muscle remodeling in patients with chronic obstructive pulmonary disease. The Journal of allergy and clinical immunology. 2015;136(3):769-80.
241. Ichikawa T, Panariti A, Audusseau S, Mogas AK, Olivenstein R, Chakir J, et al. Effect of bronchial thermoplasty on structural changes and inflammatory mediators in the airways of subjects with severe asthma. Respiratory medicine. 2019;150:165-72.
242. Tanida I, Minematsu-Ikeguchi N, Ueno T, Kominami E. Lysosomal turnover, but not a cellular level, of endogenous LC3 is a marker for autophagy. Autophagy. 2005;1(2):84-91.
243. Ordureau A, Sarraf SA, Duda DM, Heo JM, Jedrychowski MP, Sviderskiy VO, et al. Quantitative proteomics reveal a feedforward mechanism for mitochondrial PARKIN translocation and ubiquitin chain synthesis. Molecular cell. 2014;56(3):360-75.
244. Okatsu K, Koyano F, Kimura M, Kosako H, Saeki Y, Tanaka K, et al. Phosphorylated ubiquitin chain is the genuine Parkin receptor. The Journal of cell biology. 2015;209(1):111-28.
245. Stolz A, Ernst A, Dikic I. Cargo recognition and trafficking in selective autophagy. Nature cell biology. 2014;16(6):495-501.
246. Mosmann T. Rapid colorimetric assay for cellular growth and survival: application to proliferation and cytotoxicity assays. Journal of immunological methods. 1983;65(1-2):55-63.
247. van Meerloo J, Kaspers GJ, Cloos J. Cell sensitivity assays: the MTT assay. Methods in molecular biology (Clifton, NJ). 2011;731:237-45.
248. Herzig S, Shaw RJ. AMPK: guardian of metabolism and mitochondrial homeostasis. Nature reviews Molecular cell biology. 2018;19(2):121-35.
249. Canto C, Gerhart-Hines Z, Feige JN, Lagouge M, Noriega L, Milne JC, et al. AMPK regulates energy expenditure by modulating NAD+ metabolism and SIRT1 activity. Nature. 2009;458(7241):1056-60.
250. Benard G, Trian T, Bellance N, Berger P, Lavie J, Espil-Taris C, et al. Adaptative capacity of mitochondrial biogenesis and of mitochondrial dynamics in response to pathogenic respiratory chain dysfunction. Antioxidants & redox signaling. 2013;19(4):350-65.
251. Stotland A, Gottlieb RA. Mitochondrial quality control: Easy come, easy go. Biochimica et biophysica acta. 2015;1853(10 Pt B):2802-11.
252. Doherty T, Broide D. Cytokines and growth factors in airway remodeling in asthma. Current opinion in immunology. 2007;19(6):676-80.
253. Minshall EM, Leung DY, Martin RJ, Song YL, Cameron L, Ernst P, et al. Eosinophil-associated TGF-beta1 mRNA expression and airways fibrosis in bronchial asthma. American journal of respiratory cell and molecular biology. 1997;17(3):326-33.

254. Fulkerson PC, Fischetti CA, Hassman LM, Nikolaidis NM, Rothenberg ME. Persistent effects induced by IL-13 in the lung. American journal of respiratory cell and molecular biology. 2006;35(3):337-46.
255. Dessalle K, Narayanan V, Kyoh S, Mogas A, Halayko AJ, Nair P, et al. Human bronchial and parenchymal fibroblasts display differences in basal inflammatory phenotype and response to IL-17A. Clinical and experimental allergy : journal of the British Society for Allergy and Clinical Immunology. 2016;46(7):945-56.
256. Kim EK, Kwon JE, Lee SY, Lee EJ, Kim DS, Moon SJ, et al. IL-17-mediated mitochondrial dysfunction impairs apoptosis in rheumatoid arthritis synovial fibroblasts through activation of autophagy. Cell death & disease. 2017;8(1):e2565.
257. Wang C, Youle RJ. The role of mitochondria in apoptosis*. Annual review of genetics. 2009;43:95-118.
258. Marino G, Niso-Santano M, Baehrecke EH, Kroemer G. Self-consumption: the interplay of autophagy and apoptosis. Nature reviews Molecular cell biology. 2014;15(2):81-94.
259. Berezhnov AV, Soutar MP, Fedotova EI, Frolova MS, Plun-Favreau H, Zinchenko VP, et al. Intracellular pH Modulates Autophagy and Mitophagy. The Journal of biological chemistry. 2016;291(16):8701-8.
260. Ignotz RA, Massague J. Transforming growth factor-beta stimulates the expression of fibronectin and collagen and their incorporation into the extracellular matrix. The Journal of biological chemistry. 1986;261(9):4337-45.
261. Brewster CE, Howarth PH, Djukanovic R, Wilson J, Holgate ST, Roche WR. Myofibroblasts and subepithelial fibrosis in bronchial asthma. American journal of respiratory cell and molecular biology. 1990;3(5):507-11.
262. Yu J, Mao S, Zhang Y, Gong W, Jia Z, Huang S, et al. MnTBAP Therapy Attenuates Renal Fibrosis in Mice with 5/6 Nephrectomy. Oxidative medicine and cellular longevity. 2016;2016:7496930.
263. Suzuki-Karasaki M, Ochiai T, Suzuki-Karasaki Y. Crosstalk between mitochondrial ROS and depolarization in the potentiation of TRAIL-induced apoptosis in human tumor cells. International journal of oncology. 2014;44(2):616-28.
264. Redza-Dutordoir M, Averill-Bates DA. Activation of apoptosis signalling pathways by reactive oxygen species. Biochimica et biophysica acta. 2016;1863(12):2977-92.
265. Pickrell AM, Youle RJ. The roles of PINK1, parkin, and mitochondrial fidelity in Parkinson's disease. Neuron. 2015;85(2):257-73.
266. Gagliardo R, Chanez P, Mathieu M, Bruno A, Costanzo G, Gougat C, et al. Persistent activation of nuclear factor-kappaB signaling pathway in severe uncontrolled asthma. American journal of respiratory and critical care medicine. 2003;168(10):1190-8.
267. Shembade N, Harhaj EW. Regulation of NF-kappaB signaling by the A20 deubiquitinase. Cellular & molecular immunology. 2012;9(2):123-30.

268. Crews CM, Alessandrini A, Erikson RL. The primary structure of MEK, a protein kinase that phosphorylates the ERK gene product. Science (New York, NY). 1992;258(5081):478-80.
269. Lipton SA, Bossy-Wetzel E. Dueling activities of AIF in cell death versus survival: DNA binding and redox activity. Cell. 2002;111(2):147-50.
270. Workman JL, Kingston RE. Alteration of nucleosome structure as a mechanism of transcriptional regulation. Annual review of biochemistry. 1998;67:545-79.
271. Pazarentzos E, Mahul-Mellier AL, Datler C, Chaisaklert W, Hwang MS, Kroon J, et al. IkappaBetaalpha inhibits apoptosis at the outer mitochondrial membrane independently of NF-kappaB retention. The EMBO journal. 2014;33(23):2814-28.
272. Coiras M, López-Huertas MR, Rullas J, Mittelbrunn M, Alcamí J. Basal shuttle of NF-κB/IκBα in resting T lymphocytes regulates HIV-1 LTR dependent expression. Retrovirology. 2007;4(1):56.
273. Bhattacharyya S, Dudeja PK, Tobacman JK. Lipopolysaccharide activates NF-kappaB by TLR4-Bcl10-dependent and independent pathways in colonic epithelial cells. American journal of physiology Gastrointestinal and liver physiology. 2008;295(4):G784-90.
274. Torres JM, Martinez-Barricarte R, Garcia-Gomez S, Mazariegos MS, Itan Y, Boisson B, et al. Inherited BCL10 deficiency impairs hematopoietic and nonhematopoietic immunity. The Journal of clinical investigation. 2014;124(12):5239-48.
275. Cho JS, Kang JH, Um JY, Han IH, Park IH, Lee HM. Lipopolysaccharide induces pro-inflammatory cytokines and MMP production via TLR4 in nasal polyp-derived fibroblast and organ culture. PloS one. 2014;9(11):e90683.
276. Poon A, Eidelman D, Laprise C, Hamid Q. ATG5, autophagy and lung function in asthma. Autophagy. 2012;8(4):694-5.
277. Gottlieb RA, Andres AM, Sin J, Taylor DP. Untangling autophagy measurements: all fluxed up. Circulation research. 2015;116(3):504-14.
278. Tanaka Y, Guhde G, Suter A, Eskelinen EL, Hartmann D, Lullmann-Rauch R, et al. Accumulation of autophagic vacuoles and cardiomyopathy in LAMP-2-deficient mice. Nature. 2000;406(6798):902-6.
279. Colosetti P, Puissant A, Robert G, Luciano F, Jacquel A, Gounon P, et al. Autophagy is an important event for megakaryocytic differentiation of the chronic myelogenous leukemia K562 cell line. Autophagy. 2009;5(8):1092-8.
280. Toepfer N, Childress C, Parikh A, Rukstalis D, Yang W. Atorvastatin induces autophagy in prostate cancer PC3 cells through activation of LC3 transcription. Cancer biology & therapy. 2011;12(8):691-9.
281. Zheng Q, Su H, Ranek MJ, Wang X. Autophagy and p62 in cardiac proteinopathy. Circulation research. 2011;109(3):296-308.
282. Berridge MV, Tan AS. Characterization of the cellular reduction of 3-(4,5-dimethylthiazol-2-yl)-2,5-diphenyltetrazolium bromide (MTT): subcellular localization, substrate dependence, and involvement of mitochondrial electron

transport in MTT reduction. Archives of biochemistry and biophysics. 1993;303(2):474-82.
283. Dagda RK, Cherra SJ, 3rd, Kulich SM, Tandon A, Park D, Chu CT. Loss of PINK1 function promotes mitophagy through effects on oxidative stress and mitochondrial fission. The Journal of biological chemistry. 2009;284(20):13843-55.
284. Bewley MA, Preston JA, Mohasin M, Marriott HM, Budd RC, Swales J, et al. Impaired Mitochondrial Microbicidal Responses in Chronic Obstructive Pulmonary Disease Macrophages. American journal of respiratory and critical care medicine. 2017;196(7):845-55.
285. Ashmore R, Durham A, Michaeloudes C, Rossios C, Adcock I. Investigating mitochondrial dysfunction in asthma. European Respiratory Journal. 2015;46(suppl 59):OA1775.
286. Trian T, Benard G, Begueret H, Rossignol R, Girodet PO, Ghosh D, et al. Bronchial smooth muscle remodeling involves calcium-dependent enhanced mitochondrial biogenesis in asthma. The Journal of experimental medicine. 2007;204(13):3173-81.
287. Mizumura K, Cloonan SM, Nakahira K, Bhashyam AR, Cervo M, Kitada T, et al. Mitophagy-dependent necroptosis contributes to the pathogenesis of COPD. The Journal of clinical investigation. 2014;124(9):3987-4003.
288. Hoffmann RF, Zarrintan S, Brandenburg SM, Kol A, de Bruin HG, Jafari S, et al. Prolonged cigarette smoke exposure alters mitochondrial structure and function in airway epithelial cells. Respiratory research. 2013;14:97.
289. Bueno M, Lai YC, Romero Y, Brands J, St Croix CM, Kamga C, et al. PINK1 deficiency impairs mitochondrial homeostasis and promotes lung fibrosis. The Journal of clinical investigation. 2015;125(2):521-38.
290. Mihaylova MM, Shaw RJ. The AMPK signalling pathway coordinates cell growth, autophagy and metabolism. Nature cell biology. 2011;13(9):1016-23.
291. Distelmaier F, Valsecchi F, Liemburg-Apers DC, Lebiedzinska M, Rodenburg RJ, Heil S, et al. Mitochondrial dysfunction in primary human fibroblasts triggers an adaptive cell survival program that requires AMPK-alpha. Biochimica et biophysica acta. 2015;1852(3):529-40.
292. Jin M, Liu X, Klionsky DJ. SnapShot: Selective autophagy. Cell. 2013;152(1-2):368-.e2.
293. Koopman WJ, Nijtmans LG, Dieteren CE, Roestenberg P, Valsecchi F, Smeitink JA, et al. Mammalian mitochondrial complex I: biogenesis, regulation, and reactive oxygen species generation. Antioxidants & redox signaling. 2010;12(12):1431-70.
294. Larson-Casey JL, Deshane JS, Ryan AJ, Thannickal VJ, Carter AB. Macrophage Akt1 Kinase-Mediated Mitophagy Modulates Apoptosis Resistance and Pulmonary Fibrosis. Immunity. 2016;44(3):582-96.
295. Bishopp A, Sathyamurthy R, Manney S, Webbster C, Krishna MT, Mansur AH. Biomarkers of oxidative stress and antioxidants in severe asthma: A Prospective Case-Control Study. Annals of allergy, asthma & immunology : official publication of the American College of Allergy, Asthma, & Immunology. 2017;118(4):445-51.

296. Reddy PH. Mitochondrial Dysfunction and Oxidative Stress in Asthma: Implications for Mitochondria-Targeted Antioxidant Therapeutics. Pharmaceuticals (Basel, Switzerland). 2011;4(3):429-56.
297. Sahiner UM, Birben E, Erzurum S, Sackesen C, Kalayci O. Oxidative stress in asthma. The World Allergy Organization journal. 2011;4(10):151-8.
298. Hara H, Kuwano K, Araya J. Mitochondrial Quality Control in COPD and IPF. Cells. 2018;7(8).
299. Tsitoura E, Vasarmidi E, Bibaki E, Trachalaki A, Koutoulaki C, Papastratigakis G, et al. Accumulation of damaged mitochondria in alveolar macrophages with reduced OXPHOS related gene expression in IPF. Respiratory research. 2019;20(1):264.
300. Sosulski ML, Gongora R, Danchuk S, Dong C, Luo F, Sanchez CG. Deregulation of selective autophagy during aging and pulmonary fibrosis: the role of TGFbeta1. Aging cell. 2015;14(5):774-83.
301. Jyothula SS, Eissa NT. Autophagy and role in asthma. Current opinion in pulmonary medicine. 2013;19(1):30-5.
302. Tanaka A, Jin Y, Lee SJ, Zhang M, Kim HP, Stolz DB, et al. Hyperoxia-induced LC3B interacts with the Fas apoptotic pathway in epithelial cell death. American journal of respiratory cell and molecular biology. 2012;46(4):507-14.
303. Mijaljica D, Prescott M, Devenish RJ. Different fates of mitochondria: alternative ways for degradation? Autophagy. 2007;3(1):4-9.
304. McLelland GL, Soubannier V, Chen CX, McBride HM, Fon EA. Parkin and PINK1 function in a vesicular trafficking pathway regulating mitochondrial quality control. The EMBO journal. 2014;33(4):282-95.
305. Hoshino M, Nakamura Y, Sim J, Shimojo J, Isogai S. Bronchial subepithelial fibrosis and expression of matrix metalloproteinase-9 in asthmatic airway inflammation. The Journal of allergy and clinical immunology. 1998;102(5):783-8.
306. Fang S, Huang Y, Wang S, Zhang Y, Luo X, Liu L, et al. IL-17A Exacerbates Fibrosis by Promoting the Proinflammatory and Profibrotic Function of Orbital Fibroblasts in TAO. The Journal of clinical endocrinology and metabolism. 2016;101(8):2955-65.
307. Lee J, Kim HS. The Role of Autophagy in Eosinophilic Airway Inflammation. Immune network. 2019;19(1):e5.
308. Zhou J, An X, Dong J, Wang Y, Zhong H, Duan L, et al. IL-17 induces cellular stress microenvironment of melanocytes to promote autophagic cell apoptosis in vitiligo. FASEB journal : official publication of the Federation of American Societies for Experimental Biology. 2018;32(9):4899-916.
309. Mabalirajan U, Ahmad T, Rehman R, Leishangthem GD, Dinda AK, Agrawal A, et al. Baicalein reduces airway injury in allergen and IL-13 induced airway inflammation. PloS one. 2013;8(4):e62916.
310. Tully JE, Hoffman SM, Lahue KG, Nolin JD, Anathy V, Lundblad LK, et al. Epithelial NF-kappaB orchestrates house dust mite-induced airway inflammation, hyperresponsiveness, and fibrotic remodeling. Journal of immunology (Baltimore, Md : 1950). 2013;191(12):5811-21.

311. Zhang Q, Siebert R, Yan M, Hinzmann B, Cui X, Xue L, et al. Inactivating mutations and overexpression of BCL10, a caspase recruitment domain-containing gene, in MALT lymphoma with t(1;14)(p22;q32). Nature genetics. 1999;22(1):63-8.
312. Rueda D, Gaide O, Ho L, Lewkowicz E, Niedergang F, Hailfinger S, et al. Bcl10 controls TCR- and FcgammaR-induced actin polymerization. Journal of immunology (Baltimore, Md : 1950). 2007;178(7):4373-84.
313. Marion S, Mazzolini J, Herit F, Bourdoncle P, Kambou-Pene N, Hailfinger S, et al. The NF-kappaB signaling protein Bcl10 regulates actin dynamics by controlling AP1 and OCRL-bearing vesicles. Developmental cell. 2012;23(5):954-67.
314. Symons MH, Mitchison TJ. Control of actin polymerization in live and permeabilized fibroblasts. The Journal of cell biology. 1991;114(3):503-13.
315. Arenzana-Seisdedos F, Turpin P, Rodriguez M, Thomas D, Hay RT, Virelizier JL, et al. Nuclear localization of I kappa B alpha promotes active transport of NF-kappa B from the nucleus to the cytoplasm. Journal of cell science. 1997;110 (Pt 3):369-78.
316. Lain de Lera T, Folgueira L, Martin AG, Dargemont C, Pedraza MA, Bermejo M, et al. Expression of IkappaBalpha in the nucleus of human peripheral blood T lymphocytes. Oncogene. 1999;18(8):1581-8.
317. Yan M, Lee J, Schilbach S, Goddard A, Dixit V. mE10, a novel caspase recruitment domain-containing proapoptotic molecule. The Journal of biological chemistry. 1999;274(15):10287-92.
318. Tian MT, Gonzalez G, Scheer B, DeFranco AL. Bcl10 can promote survival of antigen-stimulated B lymphocytes. Blood. 2005;106(6):2105-12.
319. Lam D, Ng N, Lee S, Batzer G, Horner AA. Airway house dust extract exposures modify allergen-induced airway hypersensitivity responses by TLR4-dependent and independent pathways. Journal of immunology (Baltimore, Md : 1950). 2008;181(4):2925-32.
320. Li X, Chen Q, Chu C, You H, Jin M, Zhao X, et al. Ovalbumin-induced experimental allergic asthma is Toll-like receptor 2 dependent. Allergy and asthma proceedings. 2014;35(2):e15-20.
321. Wang L, Guo Y, Huang WJ, Ke X, Poyet JL, Manji GA, et al. Card10 is a novel caspase recruitment domain/membrane-associated guanylate kinase family member that interacts with BCL10 and activates NF-kappa B. The Journal of biological chemistry. 2001;276(24):21405-9.
322. Stilo R, Varricchio E, Liguoro D, Leonardi A, Vito P. A20 is a negative regulator of BCL10- and CARMA3-mediated activation of NF-kappaB. Journal of cell science. 2008;121(Pt 8):1165-71.
323. Ordonez CL, Shaughnessy TE, Matthay MA, Fahy JV. Increased neutrophil numbers and IL-8 levels in airway secretions in acute severe asthma: Clinical and biologic significance. American journal of respiratory and critical care medicine. 2000;161(4 Pt 1):1185-90.
324. Fernando RI, Castillo MD, Litzinger M, Hamilton DH, Palena C. IL-8 signaling plays a critical role in the epithelial-mesenchymal transition of human carcinoma cells. Cancer research. 2011;71(15):5296-306.

325. Kristan SS, Marc MM, Kern I, Flezar M, Suskovic S, Kosnik M, et al. Airway angiogenesis in stable and exacerbated chronic obstructive pulmonary disease. Scandinavian journal of immunology. 2012;75(1):109-14.
326. Kuo PL, Hsu YL, Huang MS, Chiang SL, Ko YC. Bronchial epithelium-derived IL-8 and RANTES increased bronchial smooth muscle cell migration and proliferation by Kruppel-like factor 5 in areca nut-mediated airway remodeling. Toxicological sciences : an official journal of the Society of Toxicology. 2011;121(1):177-90.
327. Klemm S, Zimmermann S, Peschel C, Mak TW, Ruland J. Bcl10 and Malt1 control lysophosphatidic acid-induced NF-kappaB activation and cytokine production. Proceedings of the National Academy of Sciences of the United States of America. 2007;104(1):134-8.
328. Ceccarelli S, Panera N, Mina M, Gnani D, De Stefanis C, Crudele A, et al. LPS-induced TNF-alpha factor mediates pro-inflammatory and pro-fibrogenic pattern in non-alcoholic fatty liver disease. Oncotarget. 2015;6(39):41434-52.
329. Chen M, Liu J, Yang W, Ling W. Lipopolysaccharide mediates hepatic stellate cell activation by regulating autophagy and retinoic acid signaling. Autophagy. 2017;13(11):1813-27.
330. Vander Heiden MG, Cantley LC, Thompson CB. Understanding the Warburg effect: the metabolic requirements of cell proliferation. Science (New York, NY). 2009;324(5930):1029-33.
331. Bernard K, Logsdon NJ, Ravi S, Xie N, Persons BP, Rangarajan S, et al. Metabolic Reprogramming Is Required for Myofibroblast Contractility and Differentiation. The Journal of biological chemistry. 2015;290(42):25427-38.
332. Xie N, Tan Z, Banerjee S, Cui H, Ge J, Liu RM, et al. Glycolytic Reprogramming in Myofibroblast Differentiation and Lung Fibrosis. American journal of respiratory and critical care medicine. 2015;192(12):1462-74.
333. Durrani SR, Viswanathan RK, Busse WW. What effect does asthma treatment have on airway remodeling? Current perspectives. The Journal of allergy and clinical immunology. 2011;128(3):439-48; quiz 49-50.

9. Attachments

9.1 List of abbreviations

GINA: Global Initiative for Asthma

Th2: T-helper type 2

SNP: Single nucleotide polymorphism

AHR: Airway hyperresponsiveness

ASM: Airway smooth muscle

COPD: Chronic obstructive pulmonary disease

IPF: Idiopathic pulmonary fibrosis

ECM: Extracellular matrix

MMP: Matrix metalloproteinases

TIMP: Tissue inhibitor of metalloproteinases

FEV1: Forced expiratory volume in 1 second

TGF-β: Transforming growth factor beta

VEGF: Vascular endothelial growth factor

NF-κB: Nuclear factor-kappa B

LPS: Lipopolysaccharide

PI3K: Phosphoinositide 3-kinase

LC3B: Microtubule-associated protein 1 light chain 3B

LAMP2: Lysosomal-associated membrane protein 2

3-MA: 3-methyladenine

Baf-A1: Bafilomycin-A1

ROS: Reactive oxygen species

ATG5: Autophagy related 5

OXPHOS: Oxidative phosphorylation

$\Delta\Psi m$: Mitochondrial membrane potential

H_2O_2: Hydrogen peroxide

PINK1: PTEN-induced putative kinase 1

SIRT1: Sirtuin 1

PGC1α: Peroxisome proliferator-activated receptor gamma coactivator 1 alpha

AMPK: AMP-activated protein kinase

DRP1: Dynamin-related protein 1

MFF: Mitochondrial fission factor

MFN: Mitofusin

OPA1: Optic atrophy type 1

QC: Quality control

AEC: Alveolar epithelial cells

Bcl10: B-cell lymphoma/leukemia 10

MALT: Mucosa-associated lymphoid tissue

TCR and BCR: T and B cell receptors

IκBα: inhibitor of nuclear factor κB

DMEM: Dulbecco's Modified Eagle's Medium

FBS: Fetal bovine serum

FCCP: Carbonyl cyanide-4-(trifluoromethoxy) phenylhydrazone

PBMCs: Peripheral blood mononuclear cells

RT: Room temperature

PBS: Phosphate-buffered saline

qRT-PCR: Quantitative Real Time-Polymerase Chain Reaction

BSA: Bovine serum albumin

NHBF: Normal human bronchial fibroblasts

DHBF: Diseased human bronchial fibroblasts

S-As: Severe asthmatic

SQSTM1/p62: Sequestosome-1

PRKN: Parkin

COL1A1: Collagen, type I, alpha 1

COL3A1: Collagen, type III, alpha 1

COL5A1: Collagen, type V, alpha 1

FN1: Fibronectin

BECN1: Beclin 1

9.2 List of tables

9.3 List of figures

9.4 Appendix

9.4.1 Proliferation of bronchial fibroblasts

In order to determine if the asthma status influences the proliferative response of bronchial fibroblasts, we analyzed the proliferation and cell cycle progression of bronchial fibroblasts from non-asthmatic (NHBF) and S-As (DHBF) subjects. Proliferation was measured by cell counting using trypan blue and cell cycle analysis was measured using propidium iodide (PI). The cells were seeded into 100mm petri-dishes and serum-starved for 24 hours upon reaching ~80% confluency. The cells were then cultured in DMEM complete medium for 72 hours. The cell count was noted at the time of seeding and harvesting, and the total number of hours in culture was noted to calculate the proliferation rate for each passage using the formula:

$$\text{Proliferation rate} = \frac{(\text{Cell count at harvesting}/\text{Cell count at seeding}) \times 100}{\text{Total number of hours in culture}}$$

For cell cycle staining, the cell pellet was resuspended in 1ml ice-cold PBS and fixed using 2ml ice-cold 100% ethanol. The fixed cells were stored at -20ºC until analysis. The cells were then centrifuged and washed twice with PBS before staining with PI staining buffer containing PBS, PI, RNase A and Triton X-100. The cells were stained at RT for 20 minutes in the dark. The distribution of the cell cycle phases with different DNA content was analyzed using flow cytometry. Analysis of cell cycle distribution and percentage of cells in G0/G1, S and G2/M phases of cell cycle was determined using the cell cycle platform of FlowJo software.

Across the tested NHBF and DHBF, the proliferation rate declined with advancement in passage number (Fig. 8.4.1A). Under matched culture conditions, the proliferative response of fibroblasts from non-asthmatics and severe asthmatics was not significantly different.

In order to extend these findings, cell cycle progression analysis was performed, and these findings were re-iterated. A greater proportion of the cells was observed in the G0/G1 phase and fewer cells in the G2/M phase with advancement in the passage number across all the fibroblasts (Fig. 8.4.1B). No characteristic difference in cell cycle progression was observed between the severe asthmatic and healthy fibroblasts. Taken together, these findings suggest that basal proliferation is not increased in bronchial fibroblasts from severe asthma patients *in vitro*.

Since subepithelial fibrosis increases with asthma severity and severely thickened airway walls with increased number of myofibroblasts are observed in severe asthma, a possible explanation for our findings could be that *in vitro,* the fibroblasts are maintained in culture conditions distinct from the asthmatic microenvironment in the airway wall and its associated cell interactions and inflammatory and remodeling mediators in the milieu. This could perhaps result in a less apparent change in asthma-related proliferation.

A

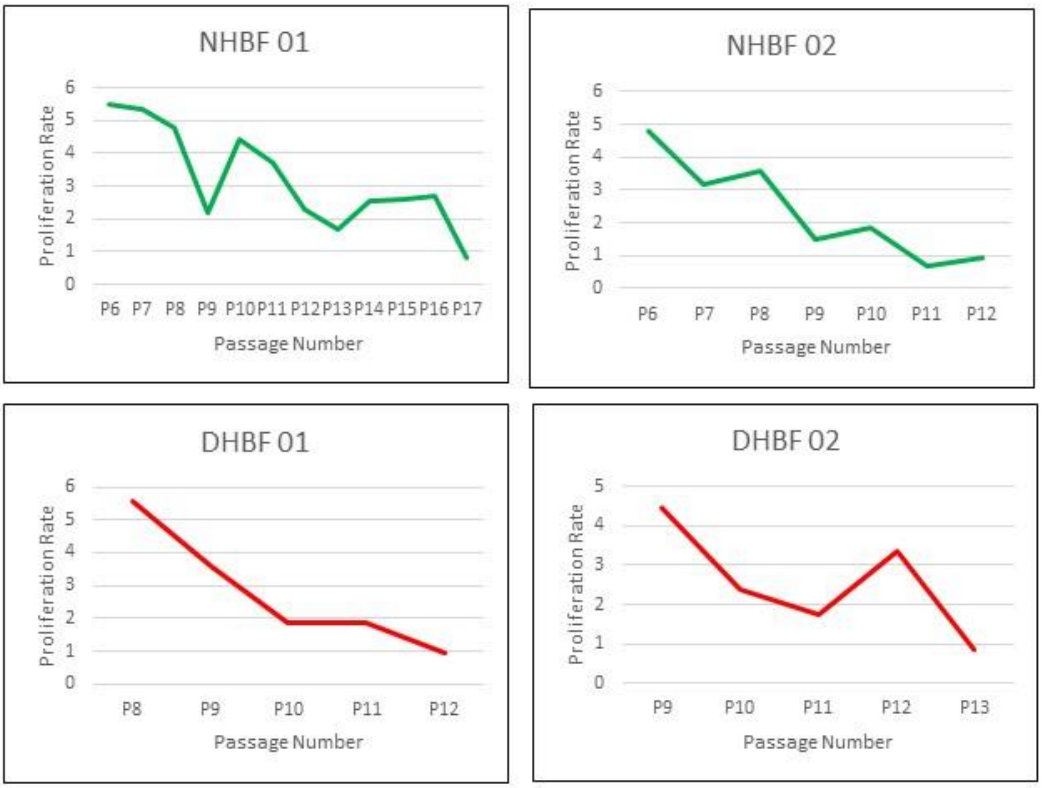
NHBF 01
Proliferation Rate
0 1 2 3 4 5 6
P6 P7 P8 P9 P10 P11 P12 P13 P14 P15 P16 P17
Passage Number
NHBF 02
Proliferation Rate
0 1 2 3 4 5 6
P6 P7 P8 P9 P10 P11 P12
Passage Number
DHBF 01
Proliferation Rate
0 1 2 3 4 5 6
P8 P9 P10 P11 P12
Passage Number
DHBF 02
Proliferation Rate
0 1 2 3 4 5
P9 P10 P11 P12 P13
Passage Number

B

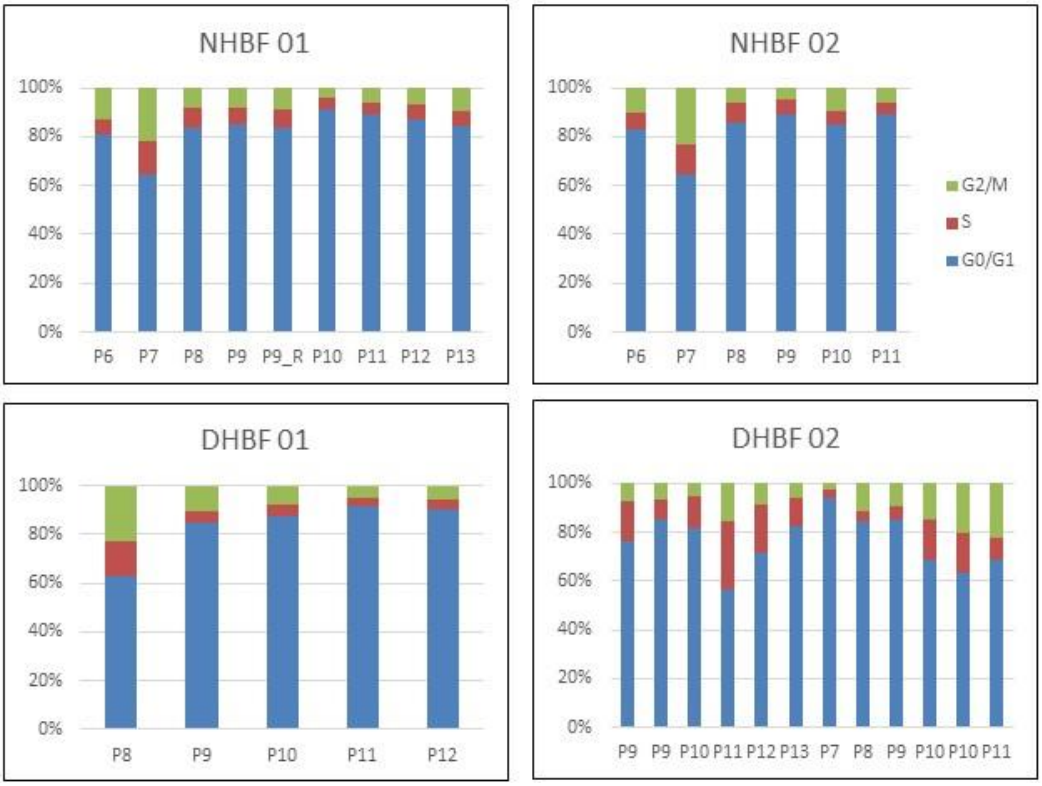
NHBF 01
100% 80% 60% 40% 20% 0%
P6 P7 P8 P9 P9_R P10 P11 P12 P13
NHBF 02
100% 80% 60% 40% 20% 0%
P6 P7 P8 P9 P10 P11
G2/M
S
G0/G1
DHBF 01
100% 80% 60% 40% 20% 0%
P8 P9 P10 P11 P12
DHBF 02
100% 80% 60% 40% 20% 0%
P9 P9 P10 P11 P12 P13 P7 P8 P9 P10 P10 P11

Appendix 9.4.1. Proliferation of bronchial fibroblasts. NHBF and DHBF were serum-starved for 24 hours and thereafter, cultured in DMEM complete medium for 72 hours across each of the tested passages. The fibroblasts were then harvested. **(A)** The cell count was noted at the time of seeding and harvesting, and the total number of hours in culture was noted to calculate the proliferation rate for each passage. The graph denotes the variation in proliferation rate with passage number across NHBF and DHBF. **(B)** The cells were then stained with propidium iodide (PI) for cell cycle analysis and analyzed using flow cytometry. Bar graph showing percentage of cells in G0/G1, S, G2/M phases of cell cycle, was determined using the cell cycle platform of FlowJo software.

9.4.2 Mitochondrial dynamics in bronchial fibroblasts

Mitochondrial dynamics is another critical element of the mitochondrial QC machinery, where the mitochondria dynamically change its shape through processes of mitochondrial fission and fusion. Changes in mitochondrial dynamics are regulated by mitochondrial dynamin-related GTPases, including dynamin-related protein 1 (DRP1), mitofusin-1 (Mfn1), mitofusin-2 (Mfn2), and optic atrophy protein 1 (OPA1). Moreover, fibroblasts with mitochondrial defects are known to adapt to metabolic stress by altering their mitochondrial dynamics and biogenesis. Since the S-As fibroblasts exhibited mitochondrial defects and associated changes in mitophagy and biogenesis, we, therefore, investigated the expression of various fission and fusion proteins involved in mitochondrial dynamics signaling. We used the Mitochondrial Dynamics Antibody Sampler Kit (Cell Signaling Technology, Cat. No. 48799T) to determine the expression of fission-related proteins, mitochondrial fission factor (MFF) and DRP1, and fusion-related proteins, OPA1, Mfn1 and Mfn2, by western blot. The mitochondrial dynamics markers showed no remarkable differences between NHBF and DHBF (Fig. 8.4.2A-B). Mitochondrial fission proteins, MFF and DRP1, showed an increased trend in DHBF compared to NHBF; however,

it did not reach statistical significance (Fig. 8.4.2A). Similarly, the expression of fusion proteins, OPA1, Mfn1 and Mfn2, also demonstrated a tendency to increase in DHBF, but without statistical significance (Fig. 8.4.2B). Therefore, it can be summarized that the mitochondrial dynamics are not significantly altered in S-As fibroblasts at baseline when compared to their healthy counterparts.

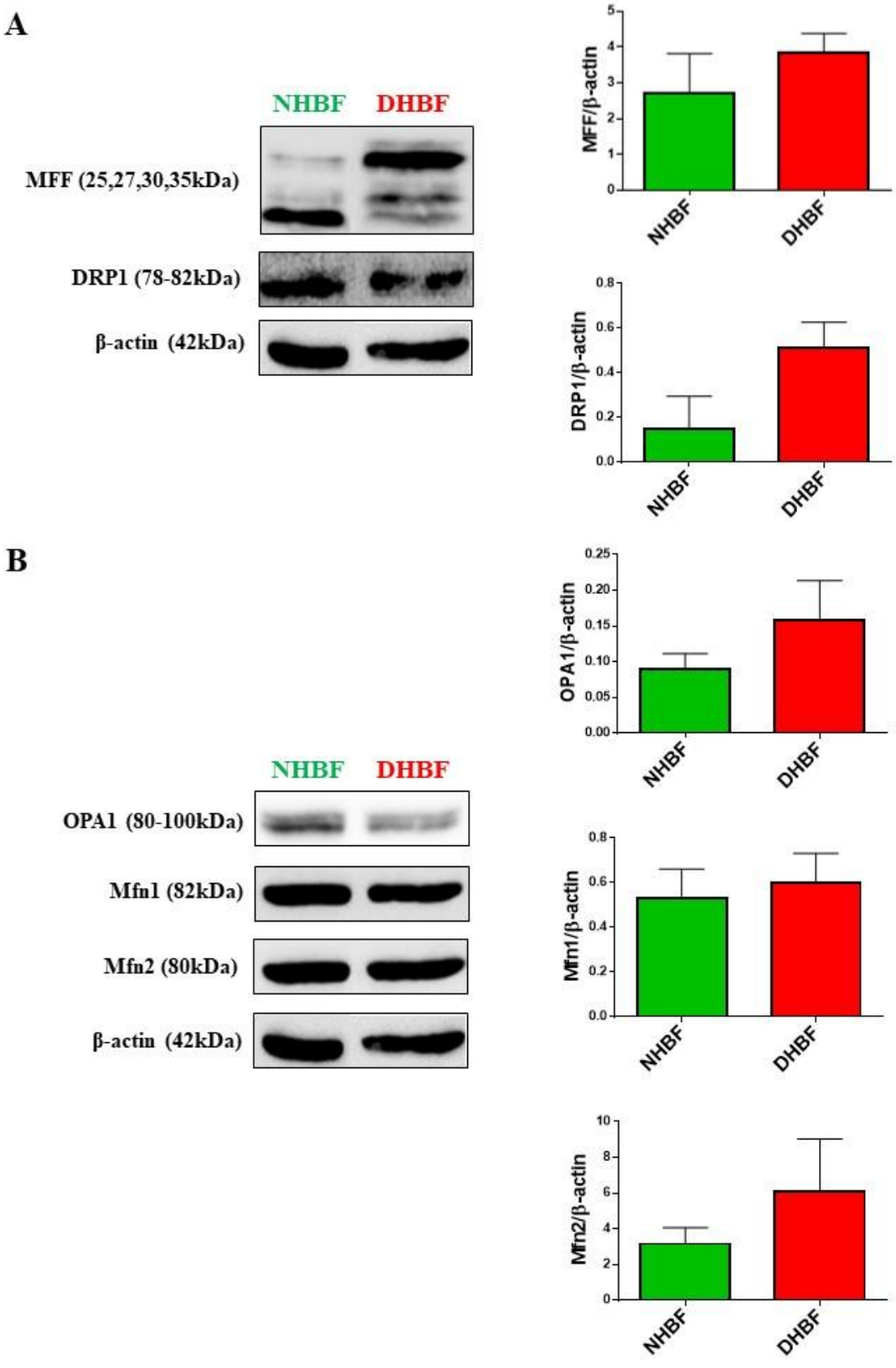
A
NHBF
DHBF
MFF (25,27,30,35kDa)
DRP1 (78-82kDa)
β-actin (42kDa)
MFF/β-actin
DRP1/β-actin
B
NHBF
DHBF
OPA1 (80-100kDa)
Mfn1 (82kDa)
Mfn2 (80kDa)
β-actin (42kDa)
OPA1/β-actin
Mfn1/β-actin
Mfn2/β-actin

Appendix 9.4.2 Mitochondrial dynamics in bronchial fibroblasts. NHBF and DHBF were serum-starved for 24 hours and thereafter, cultured in DMEM complete medium for 4 hours. The mitochondrial dynamics at baseline was measured in these fibroblasts using western blotting. **(A)** Representative blots showing the levels of mitochondrial fission proteins, MFF and DRP1, in NHBF and DHBF (left panel). Quantitative analysis of relative expression of MFF and DRP1 in NHBF and DHBF (right panel). **(B)** Representative blots showing the levels of mitochondrial fusion proteins, OPA1, Mfn1 and Mfn2, in NHBF and DHBF (left panel). Quantitative analysis of relative expression of OPA1, Mfn1 and Mfn2 in NHBF and DHBF (right panel). Graphical data are represented as mean ± SEM from at least 3 unique donors in each group.

9.4.3 Effect of autophagy regulators on bronchial fibroblasts

Since autophagy was demonstrated to be a critical regulator of mitochondrial dysfunction and pro-fibrotic signaling in bronchial fibroblasts, we targeted autophagy using multiple pharmacological agents, including rapamycin to induce autophagy and 3-MA to block autophagosomal formation, in addition to Baf-A1.

NHBF and DHBF were pre-treated with 1000nM rapamycin (Santa Cruz, Cat. No. sc-3504) or 1mM 3-methyl adenine (3-MA) (R&D Systems, Cat. No. 3977) for 4 hours prior to their stimulation with 25ng/ml of IL-17 for 48 hours. Treatment with 1mM of 3-MA severely affected the cell viability of these fibroblasts. This could be explained by the limitations posed by 3-MA. For instance, 3-MA is a general PI3K inhibitor, which in turn inhibits various other cellular processes. Furthermore, due to its weak pharmacological potency, it is generally used in millimolar concentrations at which it has been reported to exhibit additional effects, including JNK and p38 kinase inhibition, leading to stress-induced cell death.

Stimulation with 1000nM rapamycin did not lead to the induction of *BECN1* gene expression as expected in NHBF (Fig. 8.4.3A). However, the assayed concentration was found to be effective in DHBF but in the absence of IL-17 stimulation. On the other hand, 3-MA was found to effectively suppress *BECN1* gene expression in both NHBF and DHBF and was more effective in autophagy suppression when compared to Baf-A1. Furthermore, the IL-17 induced induction in *BECN1*, was also reversed with 3-MA treatment.

While rapamycin did not have an effect on *PINK1* gene expression, it did lead to elevated *PRKN* gene expression in both NHBF and DHBF (Fig. 8.4.3B-C). 3-MA treatment led to a remarkable decline in *PINK1* and *PRKN* expression in both group of fibroblasts. In addition, it also withdrew the effect of IL-17 on *PINK1* and *PRKN* in these fibroblasts. The effects of 3-MA on *PINK1* and *PRKN* gene expression further strengthens our findings with Baf-A1 confirming that IL-17 induced mitochondrial dysfunction in S-As fibroblasts is regulated by autophagy and blocking autophagy may result in an improvement in mitochondrial health.

Similar to our findings with Baf-A1, treatment with 3-MA effectively suppressed *COL1A1, COL3A1, COL5A1, FN1* and *ACTA2* gene expression in both group of fibroblasts (Fig. 8.4.3D-H). 3-MA also successfully reversed the IL-17 induced increase in fibrotic signature highlighting the role of autophagy in the induction of pro-fibrotic signaling in bronchial fibroblasts. Thus, our findings highlight autophagy as a potentially targetable pathway to ameliorate fibrotic signaling in severe asthmatic fibroblasts.

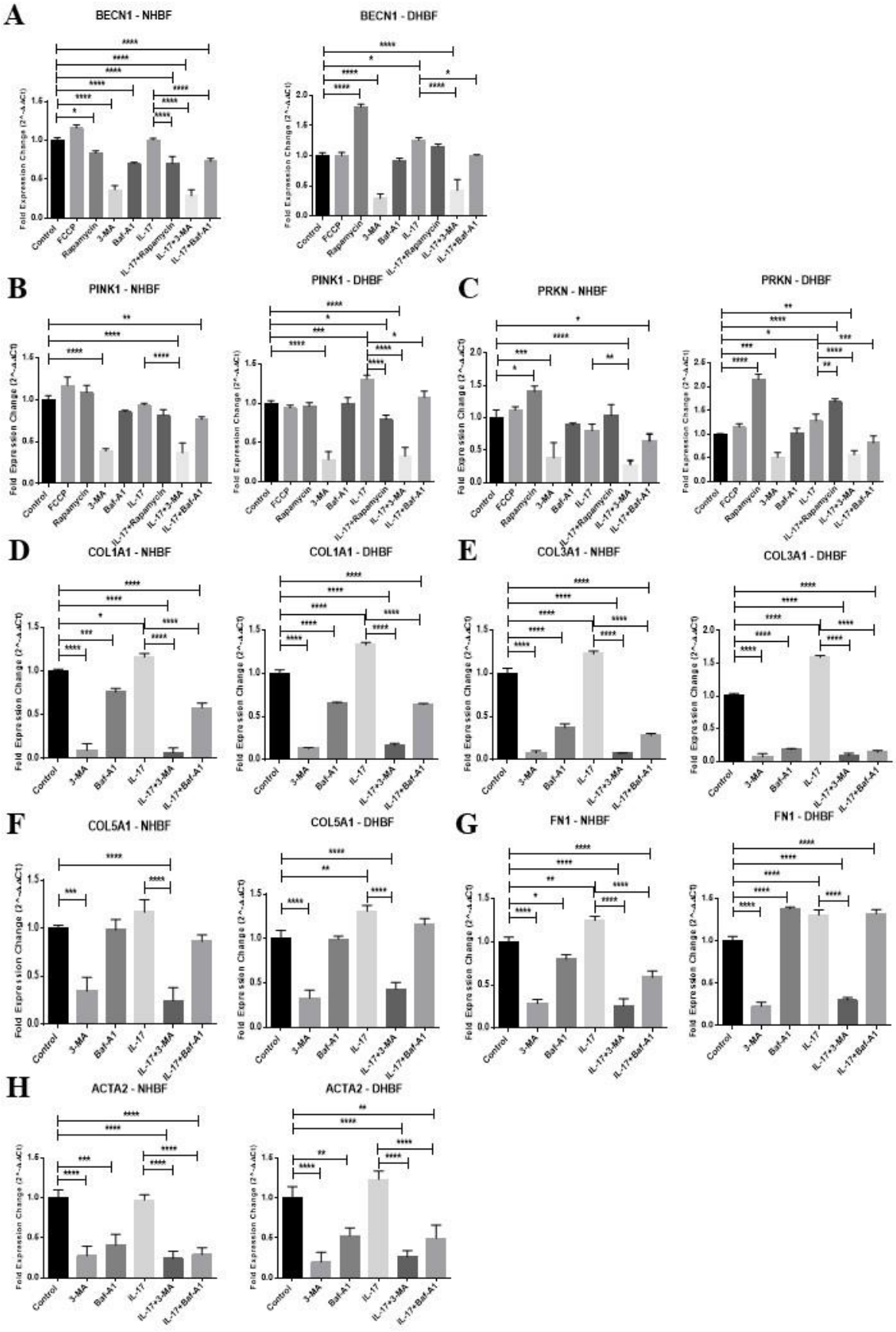
A
BECN1 - NHBF
BECN1 - DHBF
B
PINK1 - NHBF
PINK1 - DHBF
C
PRKN - NHBF
PRKN - DHBF
D
COL1A1 - NHBF
COL1A1 - DHBF
E
COL3A1 - NHBF
COL3A1 - DHBF
F
COL5A1 - NHBF
COL5A1 - DHBF
G
FN1 - NHBF
FN1 - DHBF
H
ACTA2 - NHBF
ACTA2 - DHBF
Fold Expression Change (2^-ΔΔCt)
Control
FCCP
Rapamycin
3-MA
Baf-A1
IL-17
IL-17+Rapamycin
IL-17+3-MA
IL-17+Baf-A1

Appendix 9.4.3 Effect of autophagy regulators on bronchial fibroblasts. NHBF and DHBF were serum-starved for 24 hours, pre-treated with Rapamycin (1000nM), 3-MA (1mM), or Bafilomycin-A1 (Baf-A1) (10nM) for 4 hours and thereafter, cultured in DMEM complete medium without or with IL-17 (25ng/ml) for 48 hours for mRNA analysis. The cells were co-incubated with FCCP (10μM) in the final 2 hours of treatment. mRNA expression of **(A)** autophagy gene, BECN1, mitophagy genes, **(B)** PINK1 and **(C**) Parkin, fibrotic genes, **(D)** COL1A1, **(E)** COL3A1, **(F)** COL5A1, **(G)** FN1, and **(H)** ACTA2 in NHBF (left panel) and DHBF (right panel) in response to Rapamycin, 3-MA, Baf-A1 and IL-17 was analyzed by qPCR and expressed as fold expression change relative to the untreated control post normalization to housekeeping gene 18s rRNA. Data presented as mean ± SEM after normalization to untreated control. Data representative of n=3 replicates. * $p<0.05$, ** $p<0.01$, *** $p<0.001$, **** $p<0.0001$, statistical significance assessed by 1-way ANOVA with Tukey's multiple comparison tests.

9.4.4 Effect of TGF-β1 on mitophagy in bronchial fibroblasts

Exposure to TGF-β1 resulted in mitochondrial depolarization and regulated the mitochondrial bioenergetics in bronchial fibroblasts, with a more profound effect on S-As fibroblasts. We, therefore, treated NHBF and DHBF with 10ng/ml of TGF-β1 for upto 24 hours and examined their effect of PINK1 and LC3B expression using western blotting.

As expected, accumulation of predominantly the FL isoform of PINK1 was observed in DHBF while all 3 isoforms were seen in the case of NHBF (Fig. 8.4.4, left panel). Interestingly, TGF-β1 led to a reduction in PINK1 expression in NHBF and strengthened the expression of FL PINK1 in DHBF. TGF-β1 further contributed to increased LC3B lipidation in DHBF compared to NHBF. LC3B existed predominantly as LC3BII in DHBF upon TGF-β1 treatment. Since mitochondrial integrity is critical in PINK1 processing, stabilization of FL PINK1 and LC3BII accumulation with TGF-β1 treatment indicates increased dissipation of $\Delta\Psi m$ leading to

increased mitophagy in S-As fibroblasts. These results confirm the induction of mitochondrial dysfunction by TGF-β1, especially in severe asthmatic fibroblasts.

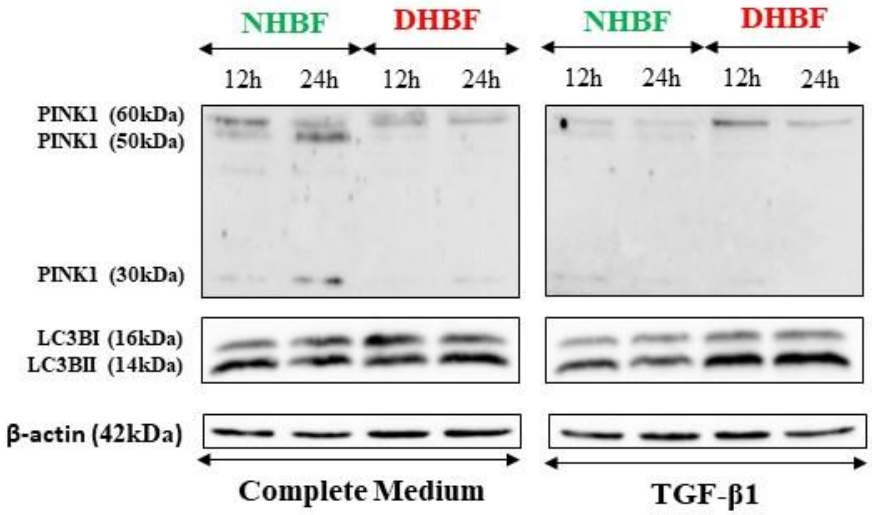

Appendix 9.4.4 Effect of TGF-β1 on mitophagy in bronchial fibroblasts. NHBF and DHBF were cultured in DMEM complete medium for the indicated time points without or with TGF-β1 (10ng/ml) post serum-starvation. Whole cell lysates were then subjected to immunoblot analysis of PINK1 and LC3B proteins. β-actin was used as loading control. Data is from one representative experiment out of at three repeats.

10. Acknowledgements

My PhD journey has truly been an enlightening experience, thanks to the support and guidance of many, close and far. Firstly, I would like to start by expressing my love and gratitude to my husband, Neeraj, who motivated me to pursue my PhD and encouraged me all through the way. It has indeed been a long journey, but I could not have made it through without him by my side. Next, I would like to share my love and tight hugs to my little car-crazy nephew, Winnie, for being my ray of sunshine amidst my hardest lab and writing days. One look at his cherubic face would brighten the darkest of my days. Next, I would like to thank my family and my in-laws for their immense patience, and always trusting and supporting my decisions. I would also like to give a shout out to my friends for being very understanding and supportive. Love you guys to the moon and back!

I would like to share my sincerest appreciation and respect to Prof. Qutayba Hamid for taking me under his umbrella. Besides being an eminent scientist himself, Prof. has been a huge inspiration and indeed a great man. He always encouraged me to pursue my own ideas, learn from my mistakes and never failed to support my endeavors. Above all, he entrusted his lab onto me which I can now proudly say I helped build. Having him as my supervisor helped me grow both as a scientist and as a person. Thank you, Prof., for trusting in me.

I would like to share my sincere gratitude to my supervisor at Lübeck Prof. Saleh Ibrahim. I am really thankful for the opportunity to work in his lab at Lübeck, and above all, our scientific discussions have helped shape me into a better scientist.

Next, I would like to thank my mentor, Prof. Rabih Halwani, who I frankly wish I had met much earlier in my PhD. I am truly indebted to him for making time to meet with me and guiding me through some of the most challenging phases of my PhD. Thank you for providing me with

biological insights, moral support and reviewing my manuscripts. I would also like to thank Dr. Bassam Mahboub for believing in me and always extending a helping hand. I would also like to appreciate Dr. Rifat Hamoudi for his support and guidance.

I would like to express my gratitude to Dr. Taleb Al Tal, Director of the Sharjah Institute for Medical Research (SIMR), for overseeing an excellent research facility, which I am glad to call my second home, and also ensuring its smooth running so that our experiments go unimpeded. Thanks to all SIMR staff for their technical support as well. I would also like to acknowledge my office buddies and fellow PhD colleagues, in particular Noha Elemam, Hayat Al Jaibeji, Mahmood Hachim, Dana Zaher and Wafa Ramadan, for their amazing company and support throughout my PhD journey. A huge thanks to my team, Asthma Research Group, for their support, constructive criticisms and motivation all through the way. A special note to Dr. Khuloud Bajbouj and Dr. Saba Al Heialy for being my two pillars in this journey, who I could turn to for advice day or night. I am really thankful to them for their constant support and guidance.

Last but not the least, I would like to acknowledge His Highness, Sheikh Sultan bin Muhammad Al-Qasimi, for supporting my PhD journey through his generous funding.

11. Curriculum vitae

Rakhee K. Ramakrishnan

Address : C/o Neeraj P. Raveendran
C/o Nielsen, Level 3, Al Reem Plaza,
Buheirah Al Corniche, Al Majaz,
Sharjah, U.A.E
Contact No. : +971568204008/ +97165312338
Email : rakhee.kr.22@gmail.com
LinkedIn : https://ae.linkedin.com/pub/rakhee-k-ramakrishnan/52/241/9b5

Education

- **Master of Biotechnology (Advanced)**
  The University of Queensland, Brisbane, Australia / *2012 – 2014*
  CGPA – **6.94/7**
- **Bachelor of Biotechnology and Biochemical Engineering**
  University of Kerala, Kerala, India */ 2006 – 2010*
  CGPA – **8.42/10**
- **All India Senior School Certificate Examination (AISSCE)**
  IES Public School, Kerala, India / 2006
  Aggregate - **88.4%**
- **All India Secondary School Examination (AISSE)**
  Sharjah Indian School, Sharjah, United Arab Emirates / 2004
  Aggregate - **89.6%**

Scholarships and Awards

- **CHEST Foundation Diversity Travel Grant 2019**, CHEST Foundation, United States of America
- **University of Sharjah PhD Scholarship 2016**, University of Sharjah, United Arab Emirates
- **John Kapeleris Medal for Biotechnology 2014**, The University of Queensland, Australia
- **Dean's Commendation for Academic Excellence** (Semester 1, 2014 and Semester 1, 2013), The University of Queensland, Australia
- **Dean's Commendation for High Achievement** (Semester 2, 2012), The University of Queensland, Australia
- **UQ Summer Research Scholarship 2012**, The University of Queensland, Australia
- **School of Chemistry and Molecular Biosciences Indian Scholarship 2012**, The University of Queensland, Australia
- **University of Kerala Second Rank Holder** in Bachelor of Biotechnology and Biochemical Engineering, 2010, University of Kerala, India

Work Experience

- **Sharjah Institute for Medical Research, Sharjah, United Arab Emirates [2016-Present]**
  - Designation : PhD Fellow and Graduate Research Assistant

- **Institute of Nutrition Medicine, University of Lübeck, Lübeck, Germany [2018]**
  - Designation : Exchange Student

- **Mater Research, Translational Research Institute, Brisbane, Australia [2013 – 2015]**
  - Designation : Research Assistant, Stem Cells and Cancer Group [February – April, 2015]
    Research Assistant, Inflammation and Cancer Therapeutics Group [June – December, 2014]
    Masters Research Student, Inflammation and Cancer Therapeutics Group [July, 2013 – June, 2014]

- **Australian Institute for Bioengineering and Nanotechnology, Brisbane, Australia [2012 – 2013]**
  - Designation : Summer Research Scholar, Delivery of Drugs and Genes Group

Publication Profile

- **Ramakrishnan RK**, Bajbouj K, Al Hiealy S, Mahboub B, Ansari AW, Hachim IY, Rawat S, Salameh L, Hachim MY, Olivenstein R, Halwani R, Hamoudi R, Hamid Q. IL-17 induced autophagy regulates mitochondrial dysfunction and fibrosis in severe asthmatic bronchial fibroblasts. This work has been submitted to the Frontiers in Immunology.
- **Ramakrishnan RK**, Bajbouj K, Hachim MY, Mogas A, Mahboub B, Olivenstein R, Hamoudi R, Halwani R, Hamid Q. Enhanced mitophagy in bronchial fibroblasts from severe asthmatic patients. This work has been submitted to the Journal of Asthma and Allergy.
- Hachim MY, Elemam NM, **Ramakrishnan RK**, Hachim IY, Salameh L, Mahboub B, Al Heialy S, Halwani R, Hamoudi R, Hamid Q. (2019) Confounding Patient Factors Affecting the Proper Interpretation of the Periostin Level as a Biomarker in Asthma Development. doi: 10.2147/JAA.S230892
- **Ramakrishnan RK**, Al Heialy S, Hamid Q. (2019) Role of IL-17 in asthma pathogenesis and its implications for the clinic. Expert Review of Respiratory Medicine. doi: 10.1080/17476348.2019.1666002
- **Ramakrishnan RK**, Mahboub B, Hamid Q. (2018) Asthma-chronic obstructive pulmonary disease overlap: A distinct pathophysiological and clinical entity. In: Asthma, COPD, and Overlap: A Case-Based Overview of Similarities and Differences, 1st Edition, edited by Bernstein J, Boulet LP, Wechsler M. Boca Raton: CRC Press. Chapter 4
- Poon AH, Choy DF, Chouiali F, **Ramakrishnan RK**, Mahboub B, Audusseau S, Mogas A, Harris JM, Arron JR, Laprise C, Hamid Q. (2017) Increased Autophagy-Related 5 Gene Expression is Associated with Collagen Expression in the Airways of Refractory Asthmatics. Frontiers in Immunology. doi: 10.3389/fimmu.2017.00355.